



University of  
Stavanger

**Faculty of Science and Technology**

## **MASTER'S THESIS**

Study program/ Specialization:

Mechanical and Structural Engineering/  
Offshore Construction

Spring semester, 2013

Open

Author:

Tor Edvard Søfteland

.....  
(Signature author)

Faculty supervisor:

Daniel Karunakaran

External supervisor:

Odd Vegard Skrunes

Title of thesis:

Lifting analysis of integrated spool cover

Credits (ECTS): 30

Key words:

- Static lifting analysis
- Dynamic lifting analysis
- Framework structure
- Spools
- Dynamic amplification factor
- Hydrodynamic coefficients in splash zone

Pages: 112

+ Appendix: 72

Stavanger, 17/06/2013



## **PREFACE**

This thesis concludes my master degree in Mechanical and Structural Engineering with specialization in Offshore Construction at the University of Stavanger. The subject was proposed by the Structural Department of Subsea 7. By combining topics related to structural engineering and marine dynamics this thesis represents a natural closure to my degree.

I would like to thank Håkon Thingstad for offering me this challenge and providing me with office space, computer and additional software that was necessary to finalize this thesis. Thanks to my supervisor, Odd Vegard Skrunes for good feedbacks and giving me confidence to write about something that first was unknown to me. Thanks to my professor and supervisor Daniel Karunakaran for giving me motivation and “pushing me to the limit” at the late phases of my thesis. Thanks to my fellow student Ingvild Lodden for good discussions and advice during this thesis. I would also like to thank professor Ove Tobias Gudmestad, though he hasn’t helped me directly in this thesis, he provided me with knowledge, motivations and encouragement through his courses in marine technology and marine operations.

Stavanger, June 2013.

Tor Edvard Søfteland.



## ABSTRACT

Large competition in the offshore industry requires innovative solutions to satisfy the demand. A new concept of spool installations is considered where three large spools are lifted in an integrated protection structure designed to support the spools during the lift and protect them from impact loads associated with fishing activities and dropped objects after installation. By integrating the spool and protection structure, the time needed for the installation will be significantly reduced. Installation of subsea structures and equipment involves a lifting operation where the object is exposed to large hydrodynamic forces when entering the oscillating sea-surface. The largest load during the structures lifetime may occur during the installation and could be snap forces after slack, or overload due to dynamic forces when the structure is lifted from the vessel and into the water, which is why the lifting analysis is considered in this thesis.

The purpose of this report is to verify the structural integrity of the new concept, designed as a complex framework structure and determine the maximum allowable sea state in which the structure can be installed safely. A static analysis is performed where all structural parts are checked according to Eurocode 3 ensuring that no parts of the framework (or spools) are overloaded during the lift. The dynamic forces associated with the lift was accounted for using a dynamic amplification factor to magnify the static force and represent loads occurring during lift off from deck until the structure is fully submerged. From the static analysis, the assumed dynamic forces in slings and crane wire are obtained and compared to associated forces from the dynamic analysis.

A dynamic analysis is performed by creating a simplified model in a marine dynamics program where the structure was analyzed in different sea states characterized by the JONSWAP spectra. The tension in slings and crane wire are considered to make sure that they are not subjected to slack or larger forces than the structure can withstand which is represented by the dynamic amplification factor defined in the static analysis. Time domain analysis is performed comparing deterministic (extreme) and stochastic (most probable) values to obtain the limiting sea state for different wave headings, wave periods and significant wave heights which characterize the sea state in which the structure will be installed. The forces on the “real structure” can be obtained with a scale factor that is obtained assuming that the hydrodynamic forces are proportional to the largest relative increase in mass or solid projected area with respect to the simplified model. The assumption is appropriate since the simplified model has the same structural properties as the “real structure” with less structural members.

According to the dynamic analysis, the structure could be installed in irregular waves characterized by the JONSWAP spectra with significant wave heights equal or less than 2.5 meter (not including uncertainties in weather forecast). The associated max utilized member with respect to design loads had a utilization ratio of 80% (no 100% utilized members) to account for uncertainties in the structural design that must be finalized before the installation of the spools is performed.



# NUMENCLATURE

## Latin characters

A	Area, $[m^2]$
$A_{33}$	Added mass, $[kg]$
$A_p$	Projected area, $[m^2]$
$B_{33}$	Linear damping coefficient, $[kg/s]$
$C_A$	Added mass coefficient, $[-]$
$C_D$	Drag coefficient, $[-]$
$C_M$	Inertia coefficient, $[-]$
$C_S$	Slamming coefficient, $[-]$
D	Diameter, $[m]$
$D_C$	Characteristic diameter, $[m]$
E	E-modulus, $[N/mm^2]$
$F_B$	Buoyancy force, $[N]$
$F_D$	Drag force, $[N]$
$F_{Dist.}$	Disturbance force, $[N]$
$F_{dyn.}$	Dynamic force, $[N]$
$F_{ext.}$	External wave forces, $[N]$
$F_{FK}$	Froude-Kriloff force, $[N]$
$F_I$	Inertia force, $[N]$
$F_{max}$	Maximum total force, $[N]$
$F_{min}$	Minimum total force, $[N]$
$F_S$	Slam force, $[N]$
$F_{static}$	Static force, $[N]$
$F_{total}$	Combined stat. and dyn. force, $[N]$
g	Gravity acceleration constant, $[m/s^2]$
H	Regular wave height, $[m]$
$H_{max}$	Maximum wave height, $[m]$
$H_S$	Significant wave height, $[m]$
h	Distance, SWL to cylinder center, $[m]$
$h_s$	Distance, surface to cylinder center, $[m]$
I	Moment of inertia, $[mm^4]$
k	Wave number, $[1/m]$
$k_{y/z}$	Reduction factor for buckling, $[-]$
K	Stiffness in hoist line, $[N/m]$
$K_C$	Keulegan Carpenter number, $[-]$
L	Length of cylinder, $[m]$
$L_{eff.}$	Effective buckling length, $[m]$
M	Structural mass, $[kg]$
$N_{Cr}$	Euler buckling load, $[N]$
$p_D$	Dynamic wave pressure, $[N/mm^2]$
$Re$	Reynolds number, $[-]$
$R_{max}$	Rayleigh distributed dynamic loads, $[N]$
r	Radius of cylinder, $[m]$
s	Distance surface to cylinder bottom $[m]$
T	Regular wave period, $[s]$
$T_p$	Peak wave period, $[s]$

$T_Z$	Zero up-crossing period, $[s]$
t	Time, $[s]$
V	Volume, $[m^3]$
$V_S$	Submerged volume, $[m^3]$
$v_3$	Vertical water particle velocity, $[m/s]$
$\dot{v}_3$	Vertical particle acceleration, $[m/s^2]$
$v_m$	Maximum particle velocity, $[m/s]$
W	Weight, $[kg]$
$z_{ct}$	Vertical motion of crane tip, $[m]$
$\alpha$	Angle for illustration, $[deg]$
$\beta$	Wave direction, $[deg]$
$Z_0$	Wave amplitude, $[m]$

## Greek characters

$\zeta$	Vertical velocity of sea surface, $[m/s]$
$\lambda$	Wave length, $[m]$
$\eta$	Vertical motion, lifted object, $[m]$
$\dot{\eta}$	Vertical velocity, lifted object, $[m/s]$
$\ddot{\eta}$	Vertical acc., lifted object, $[m/s^2]$
$\theta$	Polar coordinate, $[rad]$
$\rho$	Density of sea water, $[kg/m^3]$
$\omega$	Wave frequency, $[1/s]$
$\gamma$	Peak shape parameter, $[-]$
$\gamma_c$	Consequence factor, $[-]$
$\gamma_{COG}$	COG inaccuracy factor, $[-]$
$\gamma_f$	Load inaccuracy factor, $[-]$
$\gamma_{weig.}$	Weight inaccuracy factor, $[-]$
$\sigma_a$	Spectral width parameter a, $[-]$
$\sigma_b$	Spectral width parameter b, $[-]$
$\sigma_r$	Standard deviation, dyn. loads, $[N]$
$\sigma_v$	Standard deviation, fluid velocity, $[N]$

## Abbreviations

DAF	Dynamic amplification factor
MBL	Minimum breaking load
MWL	Mean water level
SLF	Skew load factor
SWL	Still water level
RAO	Response amplitude operator
ROV	Remotely operated vehicle





# CONTENTS

- 1 INTRODUCTION.....1**
- 1.1 THESIS BACKGROUND..... 1
- 1.2 GOAL AND SCOPE OF WORK..... 2
- 2 THEORY .....3**
- 2.1 DYNAMIC LIFTING ANALYSIS ..... 3
  - 2.1.1 Equation of motion..... 4
  - 2.1.2 Equation of vertical motion for lifted objects ..... 5
- 2.2 EXTERNAL WAVE FORCES ON RIGID HORIZONTAL CYLINDERS ..... 6
  - 2.2.1 Buoyancy force ..... 6
  - 2.2.2 Inertia force ..... 7
  - 2.2.3 Drag force ..... 9
  - 2.2.4 Slam force ..... 11
  - 2.2.5 External force on rigid horizontal cylinders..... 12
- 2.3 HYDRODYNAMIC COEFFICIENTS ..... 13
  - 2.3.1 Inertia coefficient ..... 13
  - 2.3.2 Drag coefficient ..... 18
  - 2.3.3 Slam coefficient ..... 20
- 2.4 HYDRODYNAMIC FORCES ON LIFTED OBJECTS..... 22
  - 2.4.1 Equation of vertical motion for lifted objects ..... 22
- 2.5 DYNAMIC AMPLIFICATION FACTOR ..... 23
  - 2.5.1 Solutions of equation of motion..... 23
  - 2.5.2 Dynamic amplification factor ..... 24
- 3 DESIGN OF INTEGRATED SPOOL COVER .....25**
- 3.1 DESIGN BASIS ..... 25
  - 3.1.1 Field layout ..... 25
  - 3.1.2 Spool installation ..... 26
  - 3.1.3 Technical data..... 27
- 3.2 DESIGN LOADS FOR STATIC LIFTING ANALYSIS..... 29
  - 3.2.1 Inaccuracy factors..... 30
  - 3.2.2 Skew load factor, SKL..... 31
  - 3.2.3 Dynamic amplification factor, DAF ..... 31
  - 3.2.4 Design factors for slings..... 32
  - 3.2.5 Code check ..... 33
  - 3.2.6 Load cases..... 34
- 3.3 DESIGN CONCEPT ..... 35

<b>4</b>	<b>STATIC LIFTING ANALYSIS</b> .....	<b>37</b>
4.1	STATIC ANALYSIS, PREPROCESSING .....	37
4.1.1	Structure geometry .....	38
4.1.2	Define material and sectional properties.....	39
4.1.3	Define support conditions and member release.....	40
4.1.4	Define load conditions.....	41
4.1.5	Obtaining center of gravity.....	44
4.1.6	Define code, material factor and yield stress.....	44
4.1.7	Define buckling lengths .....	45
4.2	STATIC RESULTS (GENERAL STRUCTURAL VERIFICATION).....	48
4.2.1	Summary of results.....	49
4.2.2	Sensitivity analysis and hook positioning.....	51
4.2.3	Buckling of main members .....	56
4.2.4	Max utilized member .....	58
4.3	GLOBAL BUCKLING.....	59
4.4	SUMMARY, STATIC ANALYSIS.....	61
4.4.1	Further work:.....	62
<b>5</b>	<b>DYNAMIC LIFTING ANALYSIS</b> .....	<b>63</b>
5.1	DESIGN CRITERIA .....	63
5.1.1	Acceptance criteria, DNV.....	63
5.1.2	Time domain analysis .....	64
5.2	DYNAMIC ANALYSIS, PREPROCESSING .....	65
5.2.1	Main assumptions .....	66
5.2.2	Simplified model.....	68
5.2.3	Static analysis .....	70
5.2.4	Vessel properties .....	72
5.2.5	Environmental data .....	73
5.2.6	Simplified time domain analysis.....	74
5.3	HYDRODYNAMIC PROPERTIES.....	76
5.3.1	Keulegan-Carpenter and Reynolds number .....	76
5.3.2	Inertia coefficient .....	79
5.3.3	Drag and slam coefficient.....	80
5.4	DYNAMIC RESULTS.....	81
5.4.1	Dynamic loads in different wave direction.....	81
5.4.2	Dynamic loads in different level of submergence .....	82
5.4.3	Dynamic loads in different sea states.....	85
5.4.4	Limiting sea state using stochastic approaches.....	87
5.5	SUMMARY, DYNAMIC ANALYSIS.....	91
5.5.1	Further work.....	92
<b>6</b>	<b>CONCLUSION</b> .....	<b>93</b>
<b>7</b>	<b>REFERENCES</b> .....	<b>94</b>

# APPENDIX

- APPENDIX A. WEIGHT CALCULATIONS ..... 97
- APPENDIX B. SENSITIVITY ANALYSIS, SKL-FACTOR: ..... 103
- APPENDIX C. BUCKLING LENGTHS: ..... 109
- APPENDIX D. GLOBAL BUCKLING ..... 113
- APPENDIX E. ILLUSTRATION FROM STAAD.PRO ..... 135
- APPENDIX F. DOMINATING WAVE FORCE REGIMES ..... 137
- APPENDIX G. SOLID HORIZONTAL PROJECTED AREA ..... 139
- APPENDIX H. HYDRODYNAMIC COEFFICIENTS ..... 141
- APPENDIX I. ORCAFLEX RESULTS ..... 145
- APPENDIX J. OUTPUT FILE STAAD.PRO ..... 151



# LIST OF FIGURES

Figure 2.1: Lifted object in splash zone. .... 4

Figure 2.2: Definition sketch for cylinders in splash zone..... 6

Figure 2.3: Cylinder in constant, non-viscous flow, (Journée (2001) 3.23). .... 9

Figure 2.4: Cylinder in constant viscous flow, (Journée (2001) 3.23). .... 9

Figure 2.5: Theoretical  $C_A$  values for partly submerged cylinders, applicable for  $-1 < h_g/r < 0$  ..... 15

Figure 2.6: Vertical added mass coefficient for cylinders at different distances from the free surface..... 16

Figure 2.7: Vertical added mass coefficient for cylinders with small diameters..... 16

Figure 2.8:  $C_M$  versus Reynolds number for different values of  $K_C$ , (Sarpkaya (2010) figure 3.24)). .... 17

Figure 2.9: Drag coefficient for fixed cylinders for steady flow for various roughnesses. .... 18

Figure 2.10:  $C_D$  versus Reynolds number for different values of  $K_C$ , (Sarpkaya (2010) figure 3.23)). .... 19

Figure 2.11: Combined slam and drag coefficient versus relative submergence level..... 21

Figure 3.1: Field layout..... 25

Figure 3.2: Typical spoolbank..... 26

Figure 3.3: Gooseneck detail..... 27

Figure 3.4: Forces in crane wire during submergence of lifted objects, (Hosaas (2009)). .... 34

Figure 3.5, Illustration of load combinations. .... 34

Figure 3.6: Proposed design for integrated protection cover..... 35

Figure 3.7: Main dimensions of integrated spool cover, all values in meter with dimensions from c/c. .... 36

Figure 3.8: Cross sectional properties for the framework. .... 36

Figure 4.1: Illustration of load combinations. .... 42

Figure 4.2. Deflected column with pinned ends, due to applied compressive load P, Li (2012). .... 45

Figure 4.3. Forces in one section of the column, Li (2012). .... 45

Figure 4.4. Buckling lengths and Euler buckling load for different support conditions, (Lovett (2008)). .... 45

Figure 4.5: Main members subjected to buckling. .... 46

Figure 4.6: Hook position envelope. .... 52

Figure 4.7. Change in utilization ratios due to movement of hook-position in “direction 1” and “direction 6”. 53

Figure 4.8. Lift in water when hook is placed above  $COG_{100, \text{ lift in air}}$ ..... 54

Figure 4.9. Lift in air when hook is placed above  $COG_{101, \text{ lift in water}}$ ..... 54

Figure 4.10: Bending moment diagrams, “BEAM 3”, in both y and z axis. .... 57

Figure 4.11: Eurocode 3 check. Utilization ratios  $>0.8$  are red, utilization ratios  $>0.7$  are blue. .... 58

Figure 4.12: Simplified cross section of global beam. .... 59

Figure 4.13: Staad.Pro model of simplified load case on global beams..... 59

Figure 5.1: Connection with defined end orientation for members.....	69
Figure 5.2: Connection with default end orientation for members.....	69
Figure 5.3: Framework model made in OrcaFlex. ....	69
Figure 5.4: Framework model with defined end orientation for each member. ....	69
Figure 5.5: Spools, yx-plane. ....	69
Figure 5.6: Spools, zx-plane.....	69
Figure 5.7: Staad.Pro model of structure.....	71
Figure 5.8: OrcaFlex model of structure. ....	71
Figure 5.9: Crane tip position and wave headings. ....	72
Figure 5.10: Skandi Acergy, (Subsea 7 (2012))......	72
Figure 5.11: Critical wave profile for $H_S=2.0\text{m}$ , $T_Z=6.0\text{s}$ , Wave search duration=3h. ....	75
Figure 5.12: $K_C$ versus level of submergence for 12'' spools (cylinders with $D=0.434\text{m}$ )......	77
Figure 5.13: $R_c$ versus level of submergence for 12'' spools (cylinders with $D=0.434\text{m}$ ). ....	78
Figure 5.14: $C_A$ versus submergence level, $h$ for 5 different sized cylinders.....	79
Figure 5.15: $C_S+C_D$ versus submergence level, $h$ for 5 different sized cylinders.....	80
Figure 5.16: Crane wire tension versus heading angle, $\beta$ for $H_S=2.0\text{m}$ , $T_Z=6.0\text{s}$ , $h_B=1.0\text{m}$ .....	81
Figure 5.17: Illustration of the lifted structure position relevant to the still water level. ....	83
Figure 5.18: Crane wire tension versus level of submergence for $H_S=2.0\text{m}$ , $T_Z=6.0\text{s}$ , $\beta=195^\circ$ . ....	83
Figure 5.19: Crane wire tension versus zero up crossing period for $H_S=1.5\text{m}$ , $h_B=1.0\text{m}$ and $\beta=195^\circ$ . ....	85
Figure 5.20: Crane wire tension versus zero up crossing period for $H_S=2.0\text{m}$ , $h_B=1.0\text{m}$ and $\beta=195^\circ$ . ....	85
Figure 5.21: Crane wire tension versus zero up crossing period for $H_S=2.5\text{m}$ , $h_B=1.0\text{m}$ and $\beta=195^\circ$ . ....	85
Figure 5.22: Characteristic dimension of the structure relevant to the wave direction, $\beta$ . ....	86
Figure 5.23: Structure (with characteristic dimension) in regular waves with wave length, $\lambda$ .....	86
Figure 5.24: Crane wire tension versus significant wave height, for $T_Z=6.0\text{m}$ , $h_B=1.8\text{m}$ and $\beta=195^\circ$ . ....	87
Figure 5.25: Crane wire tension versus significant wave height for $T_Z=6.0\text{m}$ , $h_B=0\text{m}$ and $\beta=195^\circ$ . ....	88
Figure 5.26: Crane wire tension versus storm duration following the Weibull distribution at $H_S=2.0\text{m}$ . ....	89
Figure 5.27: Crane wire tension versus storm duration following Generalized Pareto distribution at $H_S=2.0\text{m}$ . .	89
Figure 5.28: Crane wire tension versus time (30min), $H_S=2.5\text{m}$ , $T_Z=6.0\text{m}$ , $h_B=0\text{m}$ and $\beta=195^\circ$ . ....	89
Figure 5.29: Max crane wire tension versus significant wave height for $T_Z=6.0\text{m}$ , $h_B=0\text{m}$ and $\beta=195^\circ$ . ....	90

# LIST OF TABLES

Table 3.1: Spool size data for spool #1,#2,#3, (figure 3.2). ..... 27

Table 3.2: Gooseneck properties for spool #1,#2,#3, (figure 3.2)..... 27

Table 3.3, Material properties ..... 28

Table 3.4: Spool weight data: Uniform weight of spools and content. .... 28

Table 3.5: Spool weight data: Total weight of spools and content..... 28

Table 3.6: Material factors for design of steel structures, (Eurocode 3 and NORSOK N-004). ..... 33

Table 4.1: Primary load cases for static analysis in Staad.Pro, (Subsea 7 (2011) 3.2.5). ..... 41

Table 4.2: Relevant load combinations for static analysis in Staad.Pro,(Subsea 7 (2011) 3.2.5)..... 42

Table 4.3: Load factors from DNV (1996) for each primary load case,(Subsea 7 (2011) 3.2.5). ..... 43

Table 4.4: Weight summary, values obtained from Staad.Pro model. .... 49

Table 4.5: Summary of main results. .... 50

Table 4.6:Sling loads..... 50

Table 4.7: Effective buckling lengths of main members versus utilization ratio for beams. .... 57

Table 4.8: Global capacities of the structure..... 60

Table 5.1: Sling wire and crane wire stiffness, (Redaelli tecna (2012))..... 70

Table 5.2: Deviation in static load in OrcaFlex and Staad.Pro model..... 71

Table 5.3: Wave properties with relevant references, applied in OrcaFlex..... 73





# Chapter 1

## INTRODUCTION

Over the last decade there has been a huge increase in subsea development requiring innovative solutions to satisfy the demand in the offshore industry. Different types of subsea structures are installed to process and transport the recovered hydrocarbons to nearby process plants through subsea pipelines. The installation of subsea structures and equipment involves a lifting operation where the object is exposed to large hydrodynamic forces when entering the oscillating sea-surface. In this thesis, the lifting analysis of a complex framework is considered. The framework is designed to support three spools to reduce the overall time associated with the installation.

### 1.1 Thesis Background

Three spools will be installed connecting a subsea template to a gas-transporting pipeline. The installation of the spools involves a production stop at the currently operating field where the installation is considered a bottleneck in the operation.

Spoolpieces are short sections of pipeline that provide an interface between the pipeline end and associated facility or between subsea templates. They are designed as flexible element to ensure sealed connections that dissipate/reduce the expansion forces associated with pressure and temperature changes during the transportation of hydrocarbons. Spools are characterized as long slender objects where the shape is mainly decided by the field layout.

Spools are normally installed using spreaderbars or framework structures that are connected to the spools at selected positions, ensuring that the slender pipe-pieces don't collapse when they are lifted through the waterline. Spools normally vary in shape and size, requiring uniquely designed spreader-structure for each installation. When the spools are safely lifted in position, the spreader is disconnected and retrieved. Due to fishing activities and possibilities of dropped object, separate protection covers must be installed on top of the spools where the covers are characterized as light structures requiring additional rock dumping to ensure that they are stabilized on the sea bottom.

To save time and reducing number of lifts required for the marine operation, the possibility of installing the spools and protection structure in one lift is considered. By designing an integrated spool cover where the spools and protection structure are integrated in the fabrication phase, there will be no need for spreaderbars and the spools are protected from trawlers and impact from dropped objects after the installation. The structure will be designed as a framework structure in steel covered with GRP grating (Glass reinforced polyethylene) designed to withstand impact loads from trawlers and dropped objects.

After the spools are installed and have been operating some years, the operator wish to be able to replace the spools individually making it necessary to design the integrated spool cover to support the possibility of replacing one of the three spools. If the integrated spool cover is designed as an enclosed structure, all three spools must be removed from the field when one of them is replaced. To satisfy the

operators requirements, an open structure with locking mechanisms where GRP covers are connected to the structure as lids that are opened or closed by ROV's (Remotely operated vehicle) is considered. The cross sectional strength of the structure will be compromised when the structure is regarded as open which is the basis for this thesis.

## 1.2 Goal and scope of work

The goal of this thesis is to verify if the complex framework structure described in the "thesis background" can withstand the hydrodynamic forces associated with the subsea installation. This research should represent subsea lifting analysis in general, with focus on large framework structures composed of slender elements. The following tasks are associated with the analysis:

- Study of standards and papers with respect to the considered issue.
- Study of hydrodynamic forces on objects in the splash zone (close to oscillating sea-surface) where the "vertical equation of motion" for lifted objects, "hydrodynamic coefficient" and the "dynamic amplification factor" are in focus. The theory is used to estimate hydrodynamic coefficient applicable for structures lifted in splash zone.
- Designing an integrated spool cover that support the given features explained in the "thesis background". The structure will be based on an earlier study of the spool installation where the spool cover is designed as an enclosed structure.
- Perform a static lifting analysis of the considered structure in a finite element program (Staad.Pro) where the hydrodynamic forces are taken into account by using a factor (DAF) to quantify the dynamic loads. The structural integrity of the structure is verified according to Eurocode 3.
- Perform a dynamic lifting analysis of the considered structure in a marine dynamics program (OrcaFlex) where the "true" dynamic loads are obtained and compared to the loads obtained in the static analysis. The maximum sea state that the structure can withstand without compromising the structural integrity is obtained using both deterministic and stochastic approaches.
- Discuss and evaluate results where necessary assumptions and simplifications are highlighted.

The largest forces that the integrated spool cover is subjected to in its lifetime are assumed to be the forces during the deployment of the structure. Relevant forces during transportation and after the structure are installed is not considered (loads associated with seafastening and impact load from trawlers or dropped object). The Practical issues regarding soil conditions, locking mechanism, tie-in, disconnecting and replacement of spools are mentioned, but not discussed further in this thesis.

## Chapter 2

### THEORY

When performing subsea lifting analysis it is of great importance to understand how the lifted objects are affected by hydrodynamic forces which are present during the lift. When the structure enters the oscillating sea-surface the structure and waves interact creating vortices in all directions with large circulations, trying to push and twist each and every element of the structure. The complex turbulent effects cannot be described analytically, forcing engineers to make idealizations based on experience and simplifications to describe the occurring forces, (Sarpkaya (2010) p.123).

In this chapter the dynamic motion of lifted objects is considered using the equation of motion which is used to describe the behavior of physical systems in terms of motion as a function of time, (Lerner (1991)). From the equation of motion, the dynamic amplification factor (DAF) can be obtained. The factor is used to connect the static and dynamic loads where the maximum dynamic force of objects can be by obtained by multiplying DAF with the static force affecting the object.

The hydrodynamic forces on structures in water are obtained using coefficients to represent force contributions from inertia, drag and slam that occurs when objects are located close to the surface of oscillating water. The forces will be described and appropriate assumptions will be made to obtain force coefficients for horizontal cylinders close to the surface. These force coefficients will be applied in the dynamic lifting analysis to obtain hydrodynamic forces on the considered framework structure composed of tubular elements.

#### 2.1 Dynamic lifting analysis

When performing subsea lifting operations, the lifted object will be lifted from the vessel, into the sea and lowered down to the sea bottom. During the operation the lifted structure will be affected by the irregular motion of the waves and the vertical motion of the crane tip as a result of the vessel motion.

The total force on the structure will be represented by the sling and crane wire forces connecting the object to the crane tip where the hydrodynamic forces are obtained by performing a dynamic analysis in a marine dynamics program like SIMO or OrcaFlex.

The behavior of the lifted structure can be described using the equation of motion, which is the basis for calculating forces on moving objects where contributions from the systems inertia, damping, stiffness and external loads are taken into account by different coefficients.

*Figure 2.1* illustrates the elements of motions that need to be considered when performing a dynamic lifting analysis. The vertical displacement of the crane tip and the motions (position, velocity and acceleration) of both lifted structure and waves must be taken into account when estimating the forces on lifted object and crane wire included in the equation of motion presented in *section 2.1.2*.

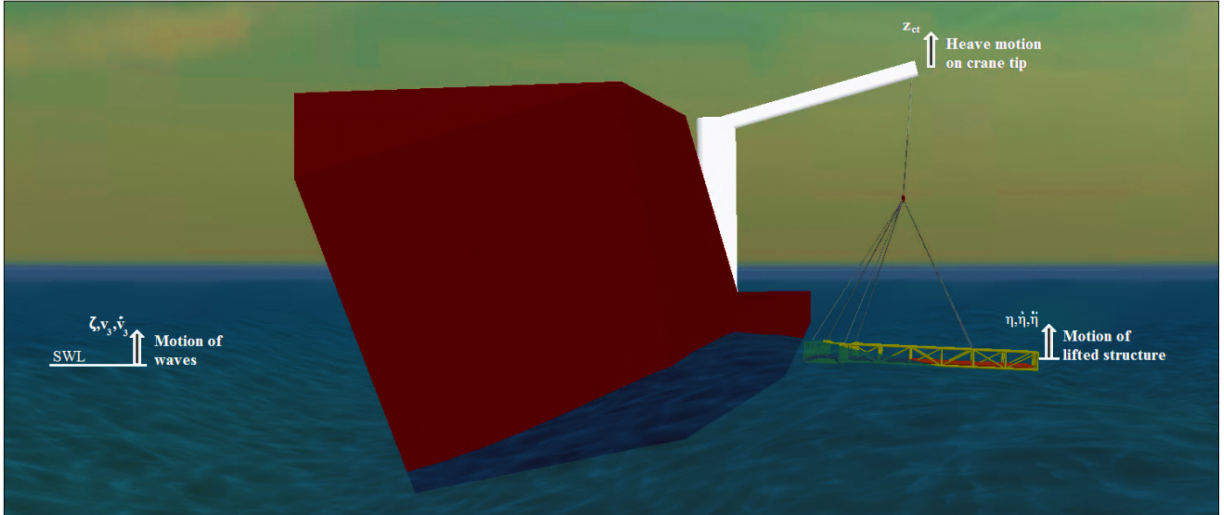


Figure 2.1: Lifted object in splash zone.

### 2.1.1 Equation of motion

The equation of motion is a product of Newton's second law of motion which states that the product of an object's mass and acceleration equals the sum of forces acting on the object. In case of floating objects affected by oscillating fluids, the applied forces are the external (wave) forces, radiation forces and hydrostatic forces as shown in eq. (2.1).

$$F = F_R + F_S + F_{external} \quad (2.1)$$

The force  $F$  is the product of the object's mass and acceleration. The radiation forces ( $F_R = -A\ddot{z} - B\dot{z}$ ) are the hydromechanical forces from added mass and damping related to motions of the object pointing in the opposite direction of the movement. The hydrostatic restoring forces ( $F_S = -Cz$ ) are also called the stiffness of the motion which is the buoyancy force acting on the object. The external forces ( $F_{external} = F_I + F_B + F_D + F_S$ ) are the applied environmental forces from inertia, drag and slam which will be discussed further in section 2.2. The forces affecting the object in vertical direction can be written as the general equation of motion shown in eq. (2.2).

$$(M + A_{33})\ddot{\eta} + B_{33}\dot{\eta} + C_{33}\eta = F_{external} \quad (2.2)$$

Where  $M$  is the mass of the body,  $A_{33}$  is the added mass related to the vertical motion,  $B_{33}$  is the damping,  $C_{33}$  is the restoring force,  $F_{external}$  is the exciting force and  $\eta, \dot{\eta}, \ddot{\eta}$  represents the position, velocity and acceleration of the object respectively. The equation of motion has the same form for movement in all directions (linear and rotational movement), but the vertical motion is of main interest when considering lifting operations.

## 2.1.2 Equation of vertical motion for lifted objects

The general equation of motion presented in *eq. (2.2)* can be used to describe most kinds of oscillating movement depending on how the coefficients for damping, stiffness and external force are defined. *Eq. (2.3)* illustrates the general expression for the equation of motion for lifted objects lowered into the wave zone combining contributions from, inertia, buoyancy, drag and slam forces (DNV-RP-H103 (2012) 3.2.10). The equation describes the behavior of the object as well as all relevant forces affecting the structure.

$$(M + A_{33})\ddot{\eta} + B_{33}(\dot{\eta} - v_3) + K(\eta - z_{ct}) = (V_S \rho + A_{33})\dot{v}_3 + \frac{1}{2} \rho A_p C_D (v_3 - \dot{\eta})|v_3 - \dot{\eta}| + \frac{1}{2} \rho A_p C_S (\dot{\zeta} - \dot{\eta})^2 \quad (2.3)$$

Where the different terms are listed below and terms describing motion, velocity and acceleration are shown in *figure 2.1*.

$A_{33}$	= Added mass due to acceleration in vertical direction	[kg]
$A_p$	= Projected area for slam and drag	[m <sup>2</sup> ]
$B_{33}$	= Linear damping coefficient	[kg/s]
$C_D$	= Drag coefficient	[-]
$C_S$	= Slam coefficient	[-]
$K$	= Stiffness of hoist line	[N/m]
$M$	= Structural mass	[kg]
$v_3$	= Water particle velocity	[m/s]
$\dot{v}_3$	= Water particle acceleration	[m/s <sup>2</sup> ]
$V_S$	= Submerged volume	[m <sup>3</sup> ]
$z_{ct}$	= Vertical motion of crane tip	[m]
$\dot{\zeta}$	= Vertical velocity of sea-surface	[m/s]
$\eta$	= Vertical motion of lifted object	[m]
$\dot{\eta}$	= Vertical velocity of lifted object	[m/s]
$\ddot{\eta}$	= Vertical acceleration of lifted object	[m/s <sup>2</sup> ]
$\rho$	= Density of sea water	[kg/m <sup>3</sup> ]

This few next sections describes the relevant force contributions in *eq. (2.3)* and proposes solutions for the added mass ( $A_{33}$ ), drag ( $C_D$ ) and slam ( $C_S$ ) coefficients that will be used in the dynamic analysis presented in *chapter 5*.

## 2.2 External wave forces on rigid horizontal cylinders

To understand the forces which are present when lifting objects is lowered through the splash zone, the vertical forces on a rigid horizontal pipe are considered. The main difference between the external forces affecting rigid and moving bodies is that the external forces is proportional to the relative movement between still water level and center of gravity of the object which is constant in case of rigid bodies. The forces for both cases can be described as the sum of four force contributions; buoyancy force  $F_B$ , inertia force  $F_I$ , drag force  $F_D$  and slam force  $F_S$  as shown in *eq. (2.4)*.

$$F_{external} = F_B + F_I + F_D + F_S \quad (2.4)$$

By making proper assumptions for the different force contributions, the total wave force,  $F_{external}$  can represent the real forces affecting the considered object.

### 2.2.1 Buoyancy force

The varying buoyancy force,  $F_B$  on a rigid horizontal cylinder is related to the physical geometry of the waves. The force is dependent on how many percent of the objects volume is submerged at a given time as shown in *eq. (2.5)*. In the splash zone, the buoyancy force will vary depending on the water surface elevation.

$$F_B = \rho g V_s \quad (2.5)$$

Where  $V_s$  is the submerged volume of the object,  $g$  is the gravity acceleration and  $\rho$  is the density of sea water. For cylinders, the submerged volume can be described as in *eq. (2.6)*, (Prasad (1994) p.16).

$$V_s = \frac{1}{2} L r^2 (\alpha - \sin \alpha) \quad (2.6)$$

$$\alpha = 2 \cos^{-1} \left( -\frac{h_s}{r} \right) \quad \text{for } -1 \leq \left( \frac{h_s}{r} \right) \leq 1 \quad (2.7)$$

Where  $r$  is the radius of the cylinder,  $L$  is the length of the cylinder,  $\alpha$  represent the angle shown in *figure 2.2* and  $h_s$  is the distance from the oscillating sea to the center of the cylinder with positive direction downwards. When the cylinder is fully submerged (at  $h_s/r=1$ ) the submerged volume equals the cylinder volume,  $\pi L r^2$ .

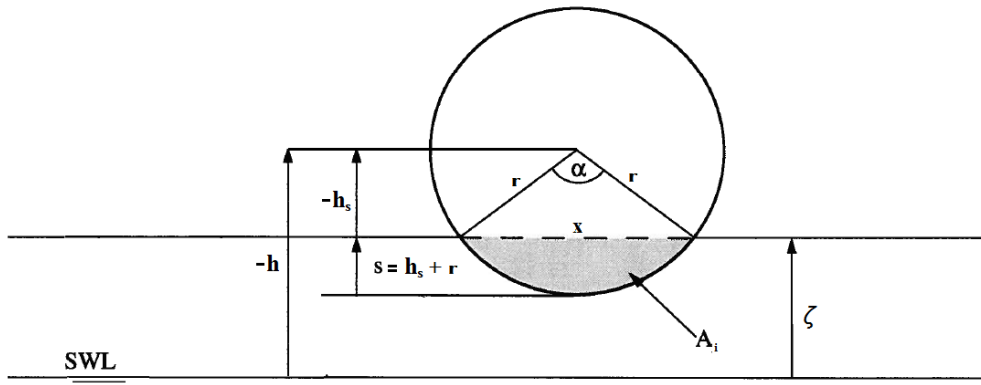


Figure 2.2: Definition sketch for cylinders in splash zone. Be aware of the difference between  $h_s$  and  $h$  where  $h_s$  is distance from the varying sea-surface while  $h$  is the distance from still water level to the center of the cylinder both with positive direction pointing downward, (Sarpkaya (2010) p.168).

## 2.2.2 Inertia force

The inertia force,  $F_I$  is related to the displaced mass of water when an object is present in waves. The inertia force is the part of the wave exciting force which is in phase with the vertical fluid acceleration  $\dot{v}_3$ . This force can be represented by two components; the Froude-Kriloff force,  $F_{FK}$  and disturbance force,  $F_{disturbance}$ . The total inertia force can be expressed as the total mass of displaced water (included added mass) multiplied by the relevant water particle acceleration (eq. (2.18)).

$$F_I = F_{FK} + F_{disturbance} \quad (2.8)$$

### Froude-Kriloff force

The Froude-Kriloff force is the wave force which would be present at the location of the observed cylinder if the cylinder were absent, in other words the undisturbed pressure field. The total wave force is found by integrating the undisturbed pressure over the area of the located object as in eq. (2.9), (Faltinsen (1990) p.59).

$$F_{FK} = \iint_S p_D ds \quad (2.9)$$

The forces are obtained by considering wave forces on a rigid body at sea using linear wave theory where the dynamic wave pressure for deepwater is given as  $p_D$  in eq. (2.10), (DNV-RP-C205 (2010) Table 3-1) and eq. (2.11).

$$p_D = \rho g \zeta_0 e^{kz} \sin(\omega t - kx) \quad (2.10)$$

Where  $\rho$  and  $g$  is the density of seawater and the gravity constant,  $\zeta_0$  is the wave amplitude,  $\omega$  is the wave frequency,  $t$  is the time,  $k$  is the wave number,  $z$  is the distance from still water level and  $x$  is the position relative to center of gravity of the object. The equation for dynamic wave pressure in sinusoidal waves is converted to polar coordinates in eq. (2.11), ( $x=r \cdot \cos\theta$ ).

$$p_D = \rho g \zeta_0 e^{k(-h)} \sin(\omega t - k \cdot r \cos \theta) \quad (2.11)$$

Where  $r$  is the radius and  $\theta$  is the angle that defines the integral of the circle. The cylinder diameter is assumed small so that the pressure is assumed constant at a distance  $-h$  from still water level to the center of the cylinder.

$$F_{FK} = \int_L \rho g \zeta_0 e^{k(-h)} dy \cdot r \int_0^{2\pi} \sin(\omega t - k \cdot r \cos \theta) \cos \theta \cdot d\theta \quad (2.12)$$

By assuming that the wavelength is much larger than the radius,  $r$  so that the values of  $k \cdot r$  is small eq. (2.12) is modified to eq. (2.13).

$$\begin{aligned} F_{FK} &= L \rho g \zeta_0 e^{k(-h)} r \left[ \int_0^{2\pi} (\sin(\omega t) \cdot \cos \theta - k \cdot r \cdot \cos(\omega t) \cdot \cos^2 \theta) d\theta \right] \\ &= L \rho g \zeta_0 e^{k(-h)} r [-\pi \cdot r \cdot \cos(\omega t)] \\ &= (\pi r^2 L) \rho \cdot (-g \zeta_0 e^{k(-h)} \cos(\omega t)) \end{aligned} \quad (2.13)$$

Where  $-g\zeta_0 e^{k(-h)} \cos(\omega t)$  is the vertical fluid acceleration for deep water (DNV-RP-C205 (2010) Table 3-1),  $\pi^2 L$  is the submerged volume and  $\rho$  is the fluid density. Eq. (2.13) states that the Froude-Kriloff force is described as the mass of the displaced water multiplied by the vertical fluid acceleration;  $\dot{v}_3$  at  $x=0$  at a constant depth;  $-h$  as expressed in eq. (2.14) (Faltinsen (1990) p.60).

$$F_{FK} = V_S \rho \dot{v}_3 \quad (2.14)$$

Where  $V_S$  is the submerged volume of the object,  $\rho$  is the density of sea water and  $\dot{v}_3$  is the vertical fluid acceleration.

### Disturbance force

The Froude-Kriloff force is the force that would act on the object if it were transparent to the wave motion, but since the water don't pass through the structure, the pressure field around the object will change and affect the force on the structure. The disturbance force is the sum of inertia, drag and slam force in when considering objects in the splash zone. The inertia-part of the disturbance force is discussed in this section.

In case of bodies with small breadth (diameter in case of a cylinder) compared to the wave length (wave length/diameter,  $\lambda/D > 5$ ), the Morrison equation can be applied. The Morrison equation is a numerical model for estimating fluid forces on a fixed body in an unsteady flow and states that the total force on cylinders is the sum of an inertia load (proportional to the fluid acceleration) and drag (proportional to the fluid velocity squared). The formula estimates the magnitude of these force components by using drag and inertia coefficients that are determined by semi empirical formulas depending on many parameters like Reynolds number, Keulegan-Carpenter number and surface roughness ratio (Prasad (1994) p.6).

The Morrison equation stated in eq. (2.15) is applicable for rigid submerged objects that are not affected by varying buoyancy or slam force with small characteristic dimension relative to the wave length ( $D < \lambda/5$ ).

$$\begin{aligned} F_{Morrison} &= F_I + F_D \\ &= V_S \rho C_M \dot{v}_3 + \frac{\rho}{2} C_D A_p |v_3| v_3 \end{aligned} \quad (2.15)$$

Where  $F_I$  is the inertia force proportional to fluid acceleration,  $\dot{v}_3$  and  $F_D$  is the drag force proportional to fluid velocity squared.  $V_S$ , is the submerged volume of the body,  $C_M$  is the inertia coefficient,  $C_D$  is the drag coefficient and  $A_p$  is the projected area. If the concerned object is located in the splash zone subjected to varying impact loads from the oscillating surface or if the object in is oscillating the Morrison equation should be modified to include associated added mass.

$$F_{Morrison} = V_S \rho \dot{v}_3 + A_{33} \dot{v}_3 + \frac{\rho}{2} C_D A_p |v_3| v_3 \quad (2.16)$$

The first term ( $V_S \rho \dot{v}_3$ ) is the Froude-Kriloff force, and the second term ( $A_{33} \dot{v}_3$ ) can be called the added mass force. The added mass represents the mass of fluid that is displaced due to movement of the object relevant to the fluid. The added mass should not be considered as a physical mass, but rather as a hydrodynamic force that is represented by a mass force in phase with the relative acceleration between object and fluid. If the object was moving in still water (with no boundaries), additional fluid would be accelerated by the moving body creating a field of fluid moving along with the object. The



resultant force created from the water particles will be in phase with the acceleration of the body and is represented by added mass equivalent to mass of accelerated fluid, (Faltinsen (1990) p.61).

The total inertia load is the force component that is proportional to the vertical acceleration of the fluid and is according to the Morison equation the sum of displaced and added mass as result of the presence of the object. The part of the disturbance force related to inertia is therefore the added mass force which is the equivalent added mass multiplied by vertical fluid velocity as shown in eq. (2.17).

$$F_{disturbance} = A_{33}\dot{v}_3 = V\rho C_A \dot{v}_3 \tag{2.17}$$

Where the added mass coefficient,  $C_A$  should be determined experimentally for unsteady flow and  $V$  is the volume of the object, (the added mass coefficient must be determined according to chosen reference volume,  $V$ ).

**Total inertia load**

By substituting the equations for Froude Kriloff force and added mass force into eq. (2.8) the inertia load for rigid objects in oscillating fluid is presented in eq. (2.18)

$$F_I = (V_S\rho + A_{33})\dot{v}_3 \tag{2.18}$$

Where  $V_S$  is the submerged volume,  $\rho$  is the density of sea water,  $A_{33}$  is the added mass described in section 2.3.1 and  $\dot{v}_3$  is the vertical acceleration of the fluid.

**2.2.3 Drag force**

When a cylinder is affected by a constant flow there will be a pressure difference up and down stream of the cylinder due to friction between water particles and the cylinder. If there were no friction between the water particles and the cylinder, the cylinder is subjected to potential flow as shown in figure 2.3. In a potential flow there would be no drag force, but since the relative friction between the water particles is causing rotational properties in the flow, eddy currents is created downstream of the cylinder. When the flow is separated there will be pressure differences, inducing drag forces on the cylinder, (Journée (2001) p.4-2).

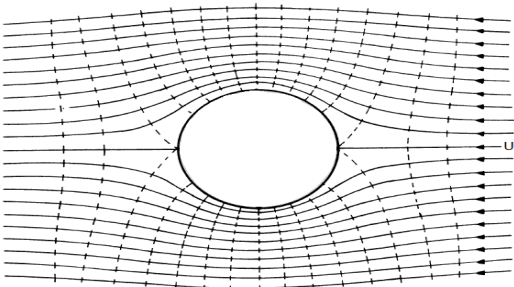


Figure 2.3: Cylinder in constant, non-viscous flow, (Journée (2001) 3.23).

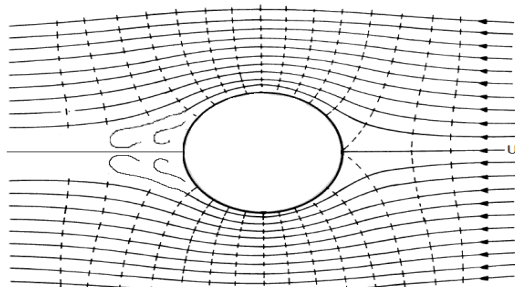


Figure 2.4: Cylinder in constant viscous flow, (Journée (2001) 3.23).

## Morison equation

The Morison equation is based on the assumption that forces on objects can be determined by a linear superposition of the drag force proportional to the velocity squared and the inertia force proportional to the acceleration of the fluid, (Prasad (1994) p.6). The Morison equation is applicable for both constant and oscillating flow depending on how the inertia and drag coefficients ( $C_M$  and  $C_D$ ) are determined. Note that the forces are 90 degrees out of phase since inertia and drag are dependent on the acceleration and velocity respectively.

$$F_{Morison} = V\rho C_M \dot{v}_3 + \frac{\rho}{2} C_D A_p |v_3| v_3 \quad (2.19)$$

Where  $V$  is the volume,  $\rho$  is the density of seawater,  $C_M$  is the inertia coefficient,  $C_D$  is the drag coefficient,  $A_p$  is the projected area,  $\dot{v}_3$  is the fluid acceleration and  $v_3$  is the fluid velocity acting on the object.

Since the inertia force is proportional with fluid acceleration while the drag is proportional to fluid velocity squared (the velocity has its maximum value while the acceleration is zero and vice versa), the force is normally either inertia or drag dominated. The relevant wave force regimes are dependent on the Keulegan-Carpenter number ( $K_C$  number, see *section 2.3.1*) where large  $K_C$  number indicates drag dominated force (small diameter compared to wave length) and low  $K_C$  number (large diameter compared to wave length) indicates inertia dominated force. The different wave force regimes are illustrated in *APPENDIX F* as a relation between wave length,  $\lambda$ , wave height,  $H$  and characteristic diameter,  $D_C$ .

## Drag force in splash zone

Objects affected by waves in the splash zone will not experience a flow (constant or oscillating) passing by the structure which is a basic assumption for the Morison equation. During the early stages of impact the drag force due to flow separation will vary from zero to the force relation given in the Morison equation (*eq. (2.16)*) when the object is fully submerged. The drag coefficients for partly submerged objects are not available due to inconsistent experimental values and must be determined based on further assumptions, (Prasad (1994) p.26).

When the object is fully submerged the drag force is given by *eq. (2.20)* where the drag coefficient is determined based on Reynolds number, Keulegan- Carpenter number and surface roughness ratio.

$$F_D = 0.5\rho C_D A_p v_3 |v_3| \quad (2.20)$$

Where  $A_p$  is the projected area and  $v_3$  is the vertical fluid velocity. The equation is applicable for both constant and oscillating flow depending on how the drag coefficient  $C_D$  is determined.

To determine the total force acting on rigid objects in the splash zone, the additional impact force from the waves must be taken into account. The impact load is represented by a slam force that is proportional to the squared surface velocity (similar to the drag force). The combined contribution from slam force and drag force should be considered where the combined force equal the slam force at early stages of impact and drag force when the object is fully submerged, (Prasad (1994) p.26).

## 2.2.4 Slam force

The force on a rigid object subjected to impact from a rising surface can be described as the sum of the varying buoyancy force, the Froude-Kriloff force and impact force which is the time rate of change in momentum as shown in *eq. (2.21)*. The slam load are calculated based on incompressible potential-flow (ideal fluid, frictionless flow) theory and zero drag force, (Sarpkaya (2010) p.168).

$$\begin{aligned} F_{external*} &= F_B + F_{FK} + F_{impact} \\ &= \rho g V_S + V_S \rho \dot{v}_3 + \frac{\partial}{\partial t} (A_{33} \dot{\zeta}_3) \end{aligned} \quad (2.21)$$

Where  $F_{external*}$  is the external force due to a rising surface,  $\rho$  is density of seawater,  $g$  is the gravitation constant,  $V_S$  is the submerged volume,  $\dot{v}_3$  is the vertical fluid acceleration,  $A_{33}$  is the added mass,  $v_3$  is the vertical fluid velocity and  $\dot{\zeta}_3$  is the vertical velocity of the sea-surface. Be aware of the difference between the vertical velocity of the fluid and the surface,  $\dot{v}_3$  and  $\dot{\zeta}_3$  respectively which is discussed in *section 2.3.3*.

By performing the partial derivative of the momentum, the equation is modified:

$$\begin{aligned} F_{external*} &= \rho g V_S + V_S \rho \dot{v}_3 + \left( A_{33} \frac{\partial v_3}{\partial t} + \dot{\zeta}_3 \frac{\partial A_{33}}{\partial t} \right) \\ &= \rho g V_S + V_S \rho \dot{v}_3 + \left( A_{33} \dot{v}_3 + \dot{\zeta}_3 \frac{\partial s}{\partial t} \frac{\partial A_{33}}{\partial s} \right) \\ &= \rho g V_S + V_S \rho \dot{v}_3 + \left( A_{33} \dot{v}_3 + \dot{\zeta}_3^2 \frac{\partial A_{33}}{\partial s} \right) \\ &= \rho g V_S + (V_S \rho + A_{33}) \dot{v}_3 + \frac{\partial A_{33}}{\partial s} \dot{\zeta}_3^2 \end{aligned} \quad (2.22)$$

Where  $s$  is the distance from the oscillating sea-surface to the bottom of the cylinder as shown in *figure 2.2*. The first and second terms are the varying buoyancy (*eq. (2.5)*) and inertia (*eq. (2.18)*) force respectively and the third term is the one of interest, the slam force. The slam force,  $F_S$  is proportional to the squared surface velocity and can be presented in a similar form as the drag force with positive direction pointing upwards as in *eq. (2.23)*.

$$F_S = 0.5 \rho C_S A_p \dot{\zeta}_3^2 \quad (2.23)$$

Where the slam coefficient,  $C_S$  is expressed as *eq. (2.24)* to satisfy the relation given in *eq. (2.21)*.

$$C_S = \frac{2}{\rho A_p} \frac{\partial A_{33}}{\partial s} \quad (2.24)$$

The slam force is only relevant during the early stages of submergence and goes to zero when the object is fully submerged.

### 2.2.5 External force on rigid horizontal cylinders

By combining the force contribution from buoyancy (eq. (2.5)), inertia (eq. (2.18)), drag (eq. (2.20)) and slam (eq. (2.23)) the equation for the total external force on rigid horizontal cylinders are obtained:

$$F_{external} = \rho g V_S + (A_{33} + V_S \rho) \dot{v}_3 + 0.5 \rho C_D A_p v_3 |v_3| + 0.5 \rho C_S A_p v_3^2 \quad (2.25)$$

Where  $F_{external}$  is the hydrodynamic force acting on the cylinder,  $\rho$  the fluid density,  $V_S$  is the submerged volume,  $\dot{v}_3$  is the vertical fluid acceleration,  $v_3$  is the vertical fluid velocity,  $A_p$  is the projected area normal to the flow direction,  $A_{33}$  is the added mass,  $C_D$  is the drag coefficient described and  $C_S$  is the slam coefficient described in *section 2.3*.

## 2.3 Hydrodynamic coefficients

The hydrodynamic forces acting on objects subjected to oscillating flow is determined by combining contributions from inertia, drag and slam forces. The force contributions are dependent on non-linear effects due to turbulence, separation and viscosity and cannot be determined by analytical equations alone. The forces are determined by semi-empirical formulations based on experiments for similar objects in flow characterized by parameters like Reynolds number, Keulegan-Carpenter number and surface roughness ratio, (Sarpkaya (2010) p.69).

This section describe the hydrodynamic coefficients needed to calculate forces on objects in oscillating flow and provides suggestions for coefficient values for partly and fully submerged cylinders.

In case of complex subsea structures, the hydrodynamic coefficients should be determined by model tests where the considered structure is subjected to “forced oscillations” or “free motion in oscillating flow” where the structural forces are collected and the hydrodynamic coefficients are based on the obtained experimental data. In case of open structures, the hydrodynamic coefficients can be calculated as the sum of contributions from individual structural members with known coefficients, (DNV-RP-H103 (2012) 3.3.3).

### 2.3.1 Inertia coefficient

The inertia force is the force that occurs due to movement of mass and is proportional to the acceleration of displaced mass. This relates both to the self-weight of a moved body and the weight of displaced fluid associated with an oscillating flow (see *section 2.4*). The inertia coefficient is a measure of the total mass effect relevant to the self-weight of the displaced mass. The applied inertia force for horizontal cylinders subjected to vertical flow is calculated as the sum of added mass and weight of displaced water as shown in *eq. (2.26)*.

$$\begin{aligned} F_I &= (V_S \rho + A_{33}) \dot{v}_3 \\ &= C_M V_S \rho \dot{v}_3 \\ &= V_S \rho \dot{v}_3 + C_A V \rho \dot{v}_3 \end{aligned} \tag{2.26}$$

Where  $C_M$  is the inertia coefficient,  $C_A$  is the added mass coefficient,  $V_S$  is the submerged volume,  $V$  is the total volume,  $\rho$  is the density of sea water and  $\dot{v}_3$  is the vertical fluid velocity. The added mass coefficient,  $C_A$  can be determined as for two-dimensional bodies if the object is considered as long cylinders with constant cross section.

## Added mass

When an object is affected by fluid in velocity, it will interact and displace the fluid close to the object. When the object is moving, the approaching fluid will be accelerated by the moving body. The affected water particles will affect other water particles creating a field of fluid moving along with the object. If the fluid has enough space to be accelerated freely, (in case of deep water) the resultant force created from the water particles will be in phase with the acceleration of the cylinder. (Cormick et al. (2002) p. 13)

The added mass is often associated with a physical mass (which is wrong), but is in truth a hydrodynamic force proportional to the relative acceleration of the fluid and body. Since the added mass force is in phase with the relative acceleration between the cylinder and waves, the force is taken into account by finding an equivalent mass to the added mass force. The added mass can then be considered as some additional fluid with a given mass moving along with the cylinder.

The added mass depends on a cylinders ability to move additional fluid. The fluid is displaced both because of the fact that the physical body is displacing water, but the viscosity, separation and interaction between fluid and object plays a part in how much fluid that is affected by the object

Unlike the mass of the system, the added mass will change when the force frequency of the system is changing. In case of zero relative motion of a body and waves, the additional added mass will be zero, proving that the added mass is dependent on frequency.

## Ideal values of added mass

By considering a oscillating body with a constant cross sections in still water (e.g. cylinder), the added mass can be calculated (according to experiments) as the mass of half a circle with the waters density and diameter equal to the characteristic diameter of the object. The ideal values for added mass are only applicable when the object is located in infinite fluid (far from boundaries) and does not account for separation and viscous effects that change the added mass in viscous fluids, (Sarpkaya (2010) p.23).

The analytical added masses are found in DNV (DNV-RP-H103 (2012) Appendix A) for various two-dimensional shapes where the added mass of cylinders is given as:

$$\begin{aligned}\frac{A_{33}}{L} &= \rho C_A \pi r^2 \\ \Rightarrow A_{33} &= \rho C_A V\end{aligned}\tag{2.27}$$

Where  $A_{33}/L$  is the added mass per unit length,  $\rho$  is the density of the fluid,  $V$  is the volume of the object and  $C_A$  is the analytical added mass coefficient equals 1.0 for cylinders, (DNV-RP-H103 (2012) Appendix A).

### Added mass of partly submerged cylinders

By assuming that the added mass of a partly submerged cylinder can be calculated as an ideal value where viscous effects take no part, the added mass is calculated as given by Taylor (1930). The added mass per unit length is calculated as the mass of water in half a circle with diameter equal the submerged breadth ( $x$  in *figure 2.2*) according to *eq. (2.27)*, (Sarpkaya (2010) p. 166).

$$\frac{A_{33}}{L} = 0.5\rho r^2 \left[ \frac{2\pi^3}{3} \frac{(1 - \cos \alpha)}{(2\pi - \alpha)^2} + \frac{\pi}{3} (1 - \cos \alpha) + (\sin \alpha - \alpha) \right] \quad (2.28)$$

Where  $\rho$  is the fluid density,  $r$  is the circle radius and  $\alpha$  is illustrated in *figure 2.2*. This geometrical relation is applicable in the range  $-1 < h_s/r < 0$ . A formula for the added mass is obtained by substituting *eq. (2.28)* into *eq. (2.26)* and is given in *eq. (2.29)* and plotted in *figure 2.5*.

$$C_A = \frac{0.5}{\pi} \left[ \frac{2\pi^3}{3} \frac{(1 - \cos \alpha)}{(2\pi - \alpha)^2} + \frac{\pi}{3} (1 - \cos \alpha) + (\sin \alpha - \alpha) \right] \quad (2.29)$$

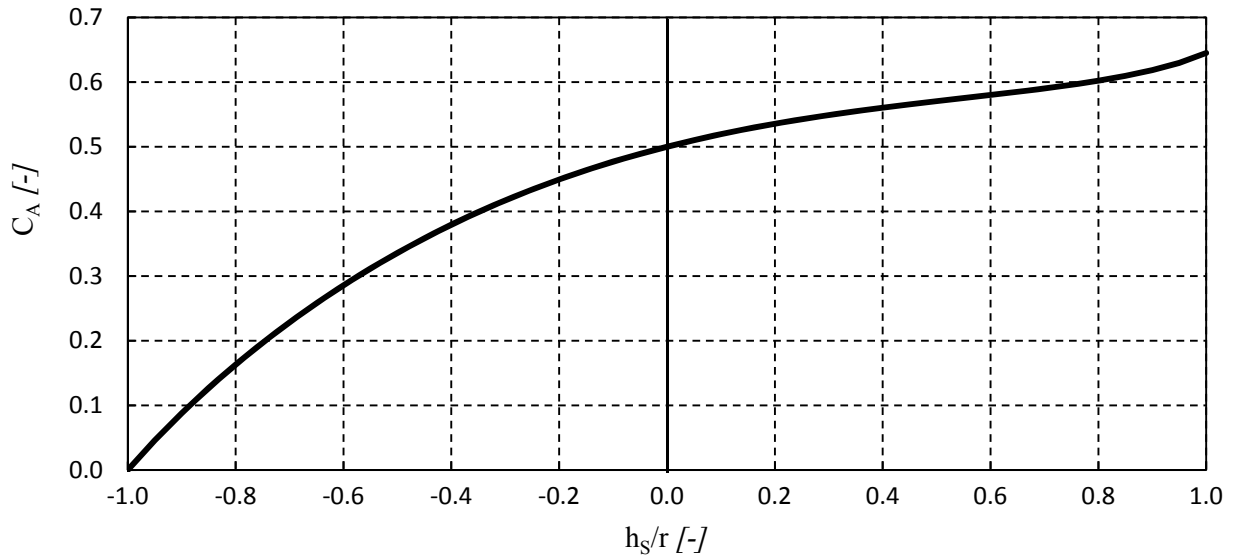


Figure 2.5: Theoretical  $C_A$  values for partly submerged cylinders, applicable for  $-1 < h_s/r < 0$

When the cylinder is exactly halfway submerged ( $h_s/r=0$ ) the  $C_A$  coefficient is 0.5 which is half of the theoretical added mass value for fully submerged cylinders indicating that the cylinder is able to displace half the amount of water as the fully submerged cylinder. This value would only be a good estimate in case of no non-linear effects due to turbulence, separation and viscosity where the fluid attracted to the upper half of the cylinder is neglected. This model will be used to estimate the slam coefficient in *section 2.3.3*.

### Added mass of submerged cylinders close to surface

When the oscillating cylinder is fully submerged the added mass is strongly dependent on the wave frequency and position relative to the free surface,  $h_s$  (illustrated in *figure 2.2*) due to viscous and separating effects, (DNV-RP-C205 (2010) 6.9.3). The added mass coefficient,  $C_A$  is given for various level of submergence as proposed by Greenhow & Ahn (1988) in *figure 2.6*.

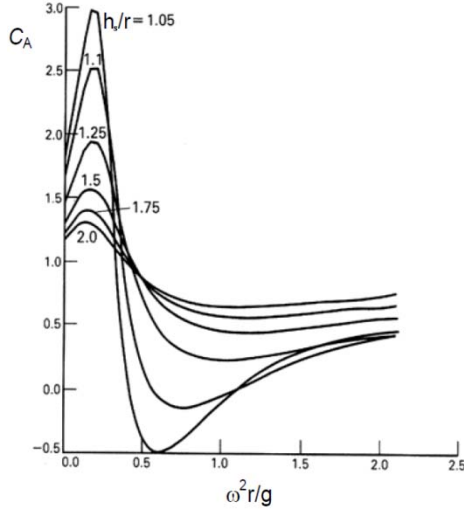


Figure 2.6: Vertical added mass coefficient for cylinders at different distances from the free surface, (DNV-RP-C205 (2010) figure 6-10).

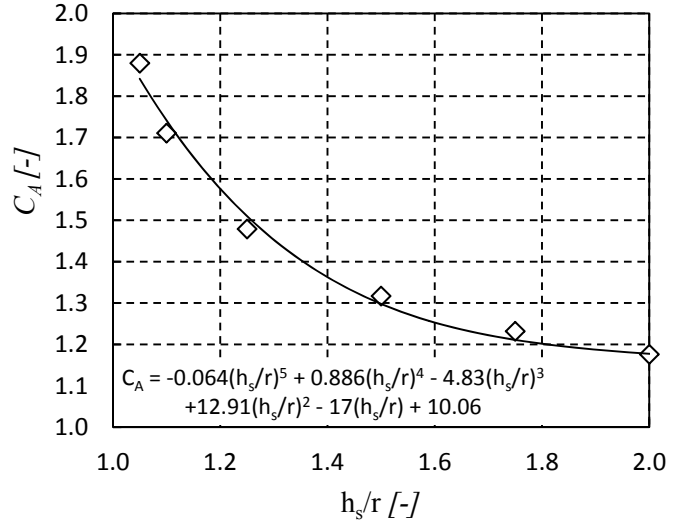


Figure 2.7: Vertical added mass coefficient for cylinders with small diameters relevant to wave period at different distances from the free surface.

In case of cylinders with small radius ( $\omega^2 r/g \approx 0$ ), the vertical added mass coefficients can be determined based on fifth grade polynomial equation given in *figure 2.7*. The equation is simply a result of plotting the values for  $C_A$  at  $\omega^2 r/g = 0$  from *figure 2.6* and finding the best fitting line for the values, which is applicable for small cylinders relative to the wave period,  $T$  ( $\omega = 2\pi / T$ ). The added mass coefficient is gradually reduced towards the ideal values for added mass when the distance between the free surface and the cylinder increase.

### Inertia coefficients for submerged cylinders

As mentioned earlier, the inertia of objects subjected to oscillating flow is dependent on non-linear effects due to turbulence, separation and viscosity. To obtain realistic values for inertia and added mass, the coefficients should be obtained based on experimental data for similar objects and flow.

The Keulegan-Carpenter number,  $K_C$  and Reynolds number,  $R_e$  is used to characterize oscillating flow and interaction between flow and structures. They are given in *eq. (2.30)* and *eq. (2.31)* respectively for unsteady flow for linear waves (DNV-RP-H103 (2012) 3.3.1.1).

$$K_C = \frac{v_m T}{D} \quad (2.30)$$

The dimensionless Keulegan- Carpenter number,  $K_C$  describe the water displacement amplitude relevant to the diameter,  $D$  where  $v_m$  is the maximum orbital particle velocity and  $T$  is the wave period. A large  $K_C$  indicates that the drag force is large compared to the inertia force since the diameter,  $D$  is small compared to the wave height  $H_s$ . A small  $K_C$  indicates a larger inertia force due to a large diameter compared to wave height which is supported by the experimental values illustrated *figure 2.8* and *figure 2.10* where one can see that the inertia coefficient tend to increases with reduced  $K_C$  and drag is increased with increased  $K_C$ .



The dimensionless Reynolds number,  $R_e$  describes the separation and viscous properties of the flow relative to diameter and total flow velocity which is the maximum orbital particle velocity close to the surface (small wave current contribution). The inertia coefficient increases with  $R_e$  since the viscous contribution get smaller compared to the product of the diameter and fluid particle velocity.

$$R_e = \frac{v_m D}{\nu} \quad (2.31)$$

Where  $v_m$  is the maximum orbital particle velocity,  $D$  is the diameter and  $\nu$  is the viscosity of the fluid.

After countless experiments on cylinders with diameter  $D$ , Sarpkaya (2010) has obtained inertia coefficients for flows depending on  $K_C$  and  $R_e$  number for cylinders as illustrated in *figure 2.8*.

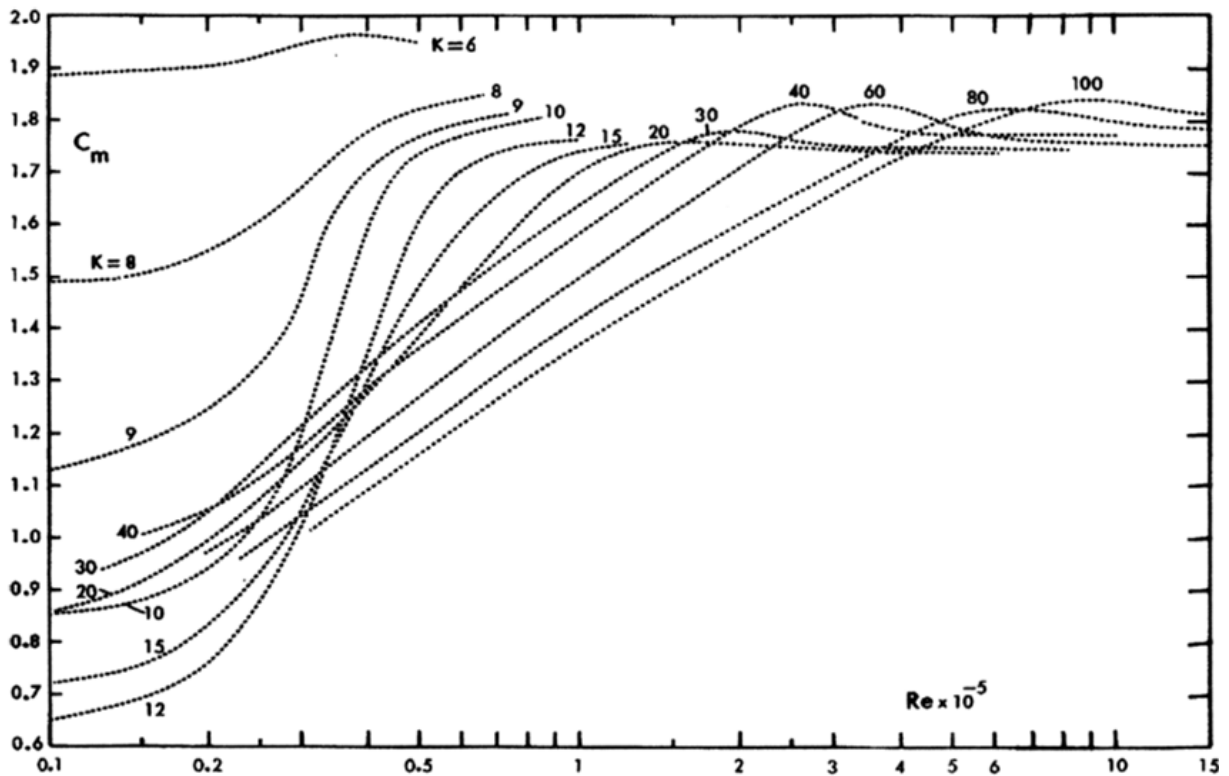


Figure 2.8:  $C_M$  versus Reynolds number for different values of  $K_C$ , (Sarpkaya (2010) figure 3.24)).

The inertia (and added mass) coefficient should be based on the combination of Keulegan- Carpenter and Reynolds number as in *figure 2.8*. When the inertia coefficient are determined based on a combination of  $R_e$  and  $K_C$  numbers the relevant changes in flow properties for various wave height, wave velocities, wave periods and diameters should be accounted for.

### 2.3.2 Drag coefficient

As described in *section 2.2.3* the drag force is the force that arises when the flow around a body is disturbed by inconstant flow due to separation and viscous effects creating a pressure difference on the downstream and upstream side of the body. In case of partly submerged cylinders there is no clear downstream path and there are no available values for drag coefficient for partly submerged cylinders.

#### Drag coefficients for partly submerged cylinders in oscillating flow

Since both drag and slam force can be described as forces proportional to the squared flow (or surface) velocity, they can be regarded as one combined effect with a coefficient  $C_D+C_S$  as described in *section 2.3.3*. The combined effect is simpler to handle and more convenient since the drag and slam is related when the considered structure is in the early stages of submergence. During the early stages of impact the slam coefficient will have its largest value while the drag coefficient is zero, and when the structure is fully submerged the slam coefficient is zero while the drag is large.

#### Drag coefficients for cylinders in steady flow

A lot of experiments have been conducted for cylinders in steady flow with large distance from boundaries showing consistent values for drag coefficients for various surface roughnesses. Drag coefficients for cylinder in steady flow for low Keulegan-Carpenter numbers ( $K_C$  numbers get low at increased depth due to reduced flow velocity) depending on Reynolds number are plotted in *figure 2.9*.

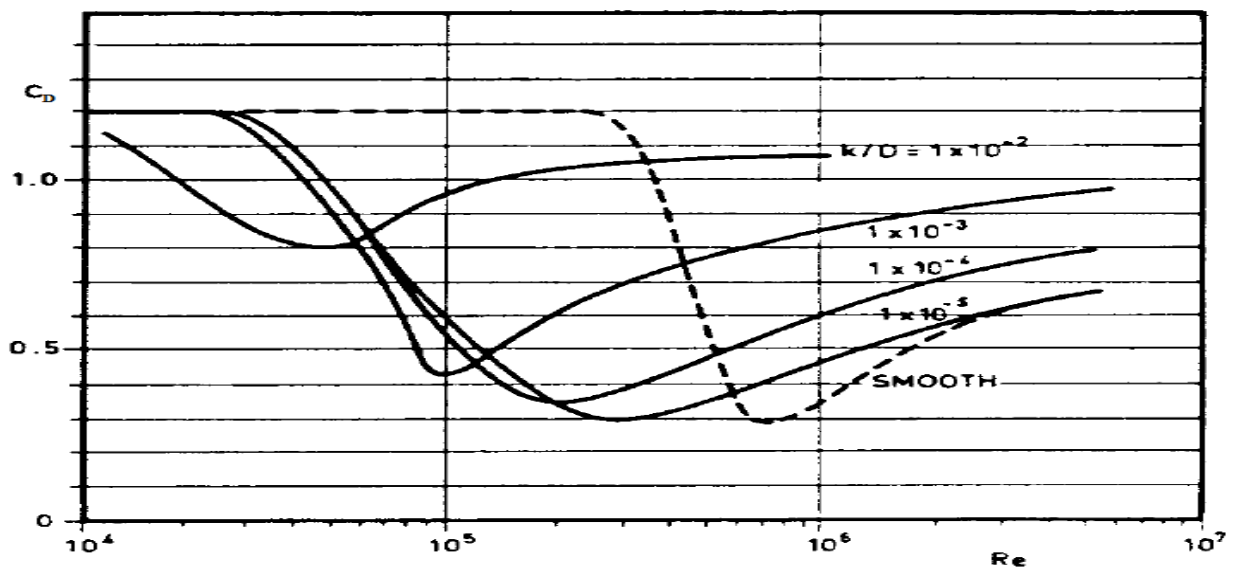


Figure 2.9: Drag coefficient for fixed cylinders for steady flow for various roughnesses, (DNV-RP-C205 (2010) figure 6-6).

The real drag coefficient in oscillating flow is highly dependent on  $K_C$  number and is typically two to three times larger than the drag coefficient for steady flow. If no further analysis has been performed, the drag coefficient is recommended to be larger than 2.5 times the drag coefficient for steady flow, (DNV-RP-H103 (2012) 4.6.2.4).

## Drag coefficients for submerged cylinders

As mentioned earlier, the drag force on objects subjected to oscillating flow is dependent on non-linear effects due to turbulence, separation and viscosity. To obtain realistic values for drag, the coefficients should be obtained based on experimental data for similar objects and flow.

In oscillating flow, the drag coefficient is dependent on both  $K_C$  and  $R_e$  number. Similar to the determination of inertia coefficients, countless of experiments has been performed and Sarpkaya has obtained drag coefficients for flows depending on  $K_C$  and  $R_e$  number as illustrated in *figure 2.10*.

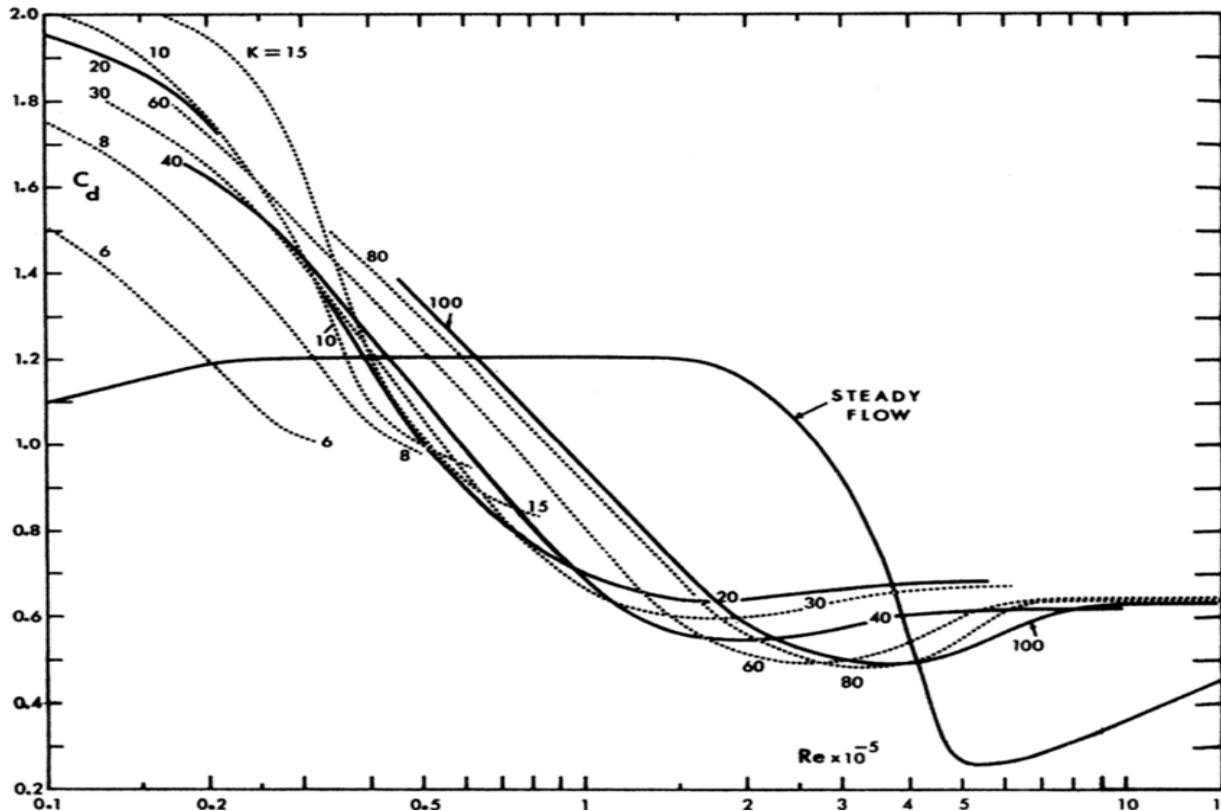


Figure 2.10:  $C_D$  versus Reynolds number for different values of  $K_C$ , (Sarpkaya (2010) figure 3.23)).

The drag coefficient can be obtained for different Keulegan- Carpenter and Reynolds number from *figure 2.10*. When the drag coefficient are determined based on a combination of  $R_e$  and  $K_C$  numbers the relevant changes in flow properties for various wave height, wave velocities, wave periods and diameters should be accounted for. Since the drag force is a result of separation of water and viscous effects, the drag force tends to be lower at increased  $R_e$ , (*eq. 2.31*) since the viscous contribution get smaller compared to the product of the diameter and fluid particle velocity.

### 2.3.3 Slam coefficient

During the early stages of impact, the waves are hitting the structure and large volumes of water are decelerated in the process causing forces on the structure. The slam contribution is largest at first contact with the rising water and is reduced to zero when the structure is fully submerged.

#### Slam coefficient

Based on the formulas derived in *section 2.2.4* the slam coefficient can be expressed as:

$$C_s = \frac{2}{\rho A_p} \frac{\partial A_{33}}{\partial s} \quad (2.32)$$

Where  $A_p$  is the projected area,  $A_{33}$  is the added mass and  $s$  is the distance from the sea-surface to the bottom of the structure (see *figure (2.2)*).

By substituting the theoretical added mass relation given by Taylor (1930) (*eq. (2.28)*), with values of  $\alpha$  as in *eq. (2.34)* (see *figure 2.2* for illustration), the slam coefficient can be described as *eq. (2.33)*, (Prasad (1994) p. 22) for cylinders.

$$C_s = \frac{1}{\sin(0.5\alpha)} \left[ \frac{2\pi^3}{3} \left( \frac{(\sin \alpha)}{(2\pi - \alpha)^2} + \frac{2(1 - \cos \alpha)}{(2\pi - \alpha)^3} \right) + \frac{\pi}{3} \sin \alpha + \cos \alpha - 1 \right] \quad (2.33)$$

Where:

$$\alpha = 2 \cos^{-1} \left( 1 - \frac{s}{r} \right) \quad \text{for } 0 \leq \left( \frac{s}{r} \right) \leq 2 \quad (2.34)$$

Here the drag coefficient is treated as a theoretical value based on the relative submergence level of the object. At first impact, the slam coefficient,  $C_s$  equals the value of 3.14 ( $\pi$ ) corresponding to experimental values for slam force on cylinders (Sarpkaya (2010) p. 169). The value of  $C_s$  is steadily decreasing to a value of 2/3 at the point where the cylinder is halfway submerged (*figure 2.11*). The formula is applicable in the range  $0 \leq s/r \leq 1$  (or  $-1 \leq h_s/r \leq 0$ ).

Another model for slam coefficients based on experimental values from Campbell & Weinberg is expressed in *eq. (2.35)* and should be compared to the values obtained analytically, (DNV-RP-H103 (2012) 3.2.13.10).

$$C_s = 5.15 \left[ \frac{D}{D+19s} + \frac{0.107s}{D} \right] \quad (2.35)$$

#### Idealized slam force

As stated earlier, the slam and drag effect can be looked at as a combined effect since both forces are proportional to the squared velocity where the combination of slam and drag presented in this report is based on the work of Prasad, (Prasad (1994)).

In order to combine the drag and slam force, the “slam velocity” and “drag velocity” is assumed to be equal based on the simple substitution given in *eq. (2.36)* and *eq. (2.37)* where the relation between the sea-surface velocity,  $\zeta$  and vertical particle velocity,  $\dot{v}_3$  is considered using linear theory (formulas from Faltinsen (1999) Table 2.1).

$$\begin{aligned}\dot{\zeta} &= \frac{d\zeta}{dt} = \frac{d}{dt}(\zeta_0 \sin(\omega t - kx)) \\ &= \omega \zeta_0 \cos(\omega t - kx)\end{aligned}\quad (2.36)$$

$$\begin{aligned}\dot{v}_3 &= \omega \zeta_0 e^{kz} \cos(\omega t - kx) \\ &= \dot{\zeta} \cdot e^{kz}\end{aligned}\quad (2.37)$$

Where  $\omega$  is the wave frequency,  $\zeta_0$  is the wave amplitude,  $k$  is the wave number ( $2\pi/\text{wave length}$ ),  $z$  is the vertical position relative to still water level,  $t$  is the time and  $x$  represents the horizontal position. From eq. (2.36) and eq. (2.37) the relations between the sea-surface velocity,  $\dot{\zeta}$  and vertical particle velocity,  $\dot{v}_3$  for small values of  $k \cdot z$  (large wave lengths,  $\lambda$  or  $z \approx 0$ ) makes them equal. If the slam force are determined based on the vertical particle velocity,  $\dot{v}_3$  rather than sea-surface velocity,  $\dot{\zeta}$  slightly more conservative values are obtained when the object is located above the still water level.

The equation for combined drag and slam force (given in section 2.2.3 and section 2.2.4 respectively) by assuming that both forces are in phase with the vertical fluid velocity squared is given in eq. (2.38).

$$\begin{aligned}F_S + F_D &= 0.5\rho C_S A_p \dot{\zeta}^2 + 0.5\rho C_D A_p \dot{v}_3 |\dot{v}_3| \\ &\approx 0.5\rho (C_D + C_S) A_p \dot{v}_3 |\dot{v}_3|\end{aligned}\quad (2.38)$$

### Idealized slam coefficient

From the first phases of impact until fully submergence the combined force contribution from drag and slam is changing from only slam force at first impact to only drag at fully submergence. Based on the drag coefficients given in figure 2.10 a minimum factor has been chosen for  $C_D$  equal 0.8 which is applicable for flow with  $K_C < 40$  and  $Re > 0.8 \cdot 10^{-5}$  (or  $K_C < 100$  and  $Re > 1.2 \cdot 10^{-5}$  indicated in figure 2.10).

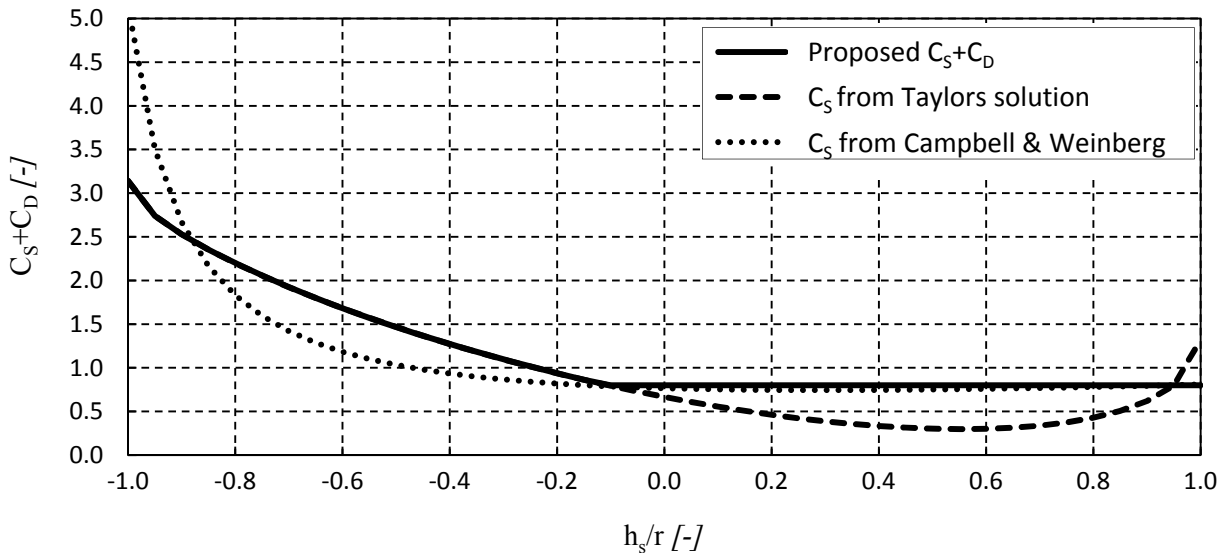


Figure 2.11: Combined slam and drag coefficient versus relative submergence level. Minimum value for  $C_S + C_D$  is set to 0.8.

## 2.4 Hydrodynamic forces on lifted objects

In *section 2.2* the hydrodynamic forces applied on a rigid horizontal cylinder in splash zone were discussed. When performing lifting operations, the vertical motion of the object (motion in heave) can be considered as a single degree of freedom system with a position, velocity and acceleration relative to the still water level. In this chapter the forces discussed in *section 2.2* is applied on elastically supported objects.

The main difference between rigid and elastic supported cylinders oscillating in water is that the fluid motions (displacement, velocity and acceleration) are replaced with the relative motion between the structure and fluid. The structural motions have oscillating behavior making the equation of motion applicable for describing structural forces.

### 2.4.1 Equation of vertical motion for lifted objects

The damping ( $B_{33}$ ) in an oscillating system tells how much energy that is dissipating while the system moves. By looking at a system induced with an initial force where no other external forces is working on the system, the response and displacement of the system will gradually decrease due to the reduction in energy. The damping term tells how much energy that is dissipated in the process, (Rao (2011) p.160). When the structure is moving relevant to the sea-surface, the linear damping term should be proportional to the difference between structural motion and wave particle motion,  $(\dot{\eta} - \dot{v}_3)$ .

In case of oscillating floating bodies, the restoring force is defined as the system's ability to restore itself to its original position. During subsea lifting operation the structure are designed to sink, and the restoring force which is a function of the waterline area are very small compared to the stiffness in the crane wire and slings connecting the lifted object to the crane tip. The structural restoring force should be represented by the combined wire stiffness,  $K$  (slings and crane wire) proportional to the elongation of the wire  $(\eta - z_{ct})$ .

The mass contribution proportional to the acceleration of the body is the sum of structural weight and added mass. The modified equation of motion can be described as:

$$(M + A_{33})\ddot{\eta} + B_{33}(\dot{\eta} - v_3) + K(\eta - z_{ct}) = F_{external} \quad (2.39)$$

Where  $M$  is the mass of the body,  $A_{33}$  is the added mass related to the vertical motion,  $B_{33}$  is the damping,  $C_{33}$  is the restoring force,  $F_{external}$  is the exciting force and  $\eta, \dot{\eta}, \ddot{\eta}$  represents the position, velocity and acceleration of the object in the vertical direction respectively. The equation of motion has the same form for movement in all directions (linear and rotational movement), but the vertical motion is of main interest when considering lifting operations.

To account for the relative motion between fluid and body, the equation for vertical external force on rigid cylinders (*eq. (2.25)*) can be modified to:

$$F_{external} = (V_S \rho + A_{33})\dot{v}_3 + 0.5\rho C_D A_p (v_3 - \dot{\eta})|v_3 - \dot{\eta}| + 0.5\rho C_S A_p (\zeta - \dot{\eta})^2 \quad (2.40)$$

Where  $F_{external}$  is the hydrodynamic force acting on the cylinder,  $\rho$  the fluid density,  $V_S$  is the submerged volume,  $\dot{v}_3$  is the vertical fluid acceleration,  $v_3$  is the vertical fluid velocity,  $\dot{\eta}$  is the vertical velocity of the object,  $A_p$  is the projected area normal to the flow direction,  $A_{33}$  is the added mass,  $C_D$  is the drag coefficient described and  $C_S$  is the slam coefficient.

## 2.5 Dynamic amplification factor

To understand the meaning of the dynamic amplification factor (DAF), the equation of motion will be solved which requires certain steps as defined in this section. The equation of motion in its general form can be given as the following equation:

$$M \ddot{z} + B\dot{z} + Cz = F_z(t) \quad (2.41)$$

### 2.5.1 Solutions of equation of motion

The equation of motion must be solved as a differential equation. When solving a differential equation, two solution must be considered; the homogeneous solution  $z_h(t)$ , and the particular solution  $z_p(t)$ . The total solution is  $z(t)=z_h(t)+z_p(t)$ . (Rao (2011) p.261)

The particular solution  $z_p(t)$  and homogeneous solution  $z_h(t)$  are given in *eq. (2.42)* and *eq. (2.43)* respectively.

$$M \ddot{z} + B\dot{z} + Cz = F_z(t) \quad (2.42)$$

$$M \ddot{z} + B\dot{z} + Cz = 0 \quad (2.43)$$

#### Particular solution

Let's consider *eq. (2.42)* as a general differential equation, where the equation equals a harmonic force with a frequency  $\omega$ , so that;  $F_z(t) = F_0 \sin(\omega t)$ . The systems mass is  $M$ , the damping is  $B$ , and the stiffness is  $C$ .

The equation can be solved as response of a damped system under harmonic force. The following calculations are also illustrated in Rao. (RAO (2011) p.271)

$$M \frac{d^2 z_p}{dt^2} + B \frac{dz_p}{dt} + Cz = F_0 \sin(\omega t) \quad (2.44)$$

Since the force is harmonic, the solution of *eq. (2.42)*,  $z_p(t)$  is also assumed harmonic with a phase difference,  $\varepsilon_z$  between the exciting force and the motion.

$$z_p = Z \sin(\omega t + \varepsilon_z), \frac{dz_p}{dt} = Z\omega \cos(\omega t + \varepsilon_z), \frac{d^2 z_p}{dt^2} = -Z\omega^2 \sin(\omega t + \varepsilon_z) \quad (2.45)$$

By substituting *eq. (2.45)* into *eq. (2.42)*, *eq. (2.46)* is obtained:

$$Z[(C - M\omega^2) \sin(\omega t + \varepsilon_z) + B\omega \cos(\omega t + \varepsilon_z)] = F_0 \sin(\omega t) \quad (2.46)$$

By using the following trigonometric relations:

$$\begin{aligned} \sin(\omega t + \varepsilon) &= \sin \omega t \cos \varepsilon + \cos \omega t \sin \varepsilon \\ \cos(\omega t + \varepsilon) &= \cos \omega t \cos \varepsilon - \sin \omega t \sin \varepsilon \end{aligned} \quad (2.47)$$

Eq. (2.48) is obtained using the trigonometric relation in eq. (2.47) on eq. (2.46).

$$Z[(C - M\omega^2)\cos(\varepsilon_z) + B\omega_e \sin(\varepsilon_z)]\sin(\omega t) = F_0 \sin(\omega t) \quad (2.48)$$

The amplitude Z can then be given as:

$$Z = \frac{F_0}{\sqrt{(C - M\omega^2)^2 + (B\omega)^2}} \quad (2.49)$$

## 2.5.2 Dynamic amplification factor

The total load acting on objects can be given as the combined structural stiffness multiplied by displacement:

$$F_{total} = Z \cdot C \quad (2.50)$$

To obtain this relation, the numerator and denominator in eq. (2.49) are divided with the stiffness coefficient, C.

$$Z = \frac{\frac{F_0}{C}}{\sqrt{\left(\frac{C}{C} - \frac{M}{C}\omega^2\right)^2 + \left(\frac{B\omega}{C}\right)^2}} \quad (2.51)$$

The following relations for natural frequency,  $\omega_n$  damping ratio,  $\lambda$  and frequency ratio, r are given in eq. (2.52) and substituted into eq. (2.51) to obtain eq. (2.53).

$$\omega_n = \sqrt{\frac{C}{M}}, \quad \lambda = \frac{B}{2M\omega_n}, \quad r = \frac{\omega}{\omega_n} \quad (2.52)$$

$$DAF = \frac{ZC}{F_0} = \frac{1}{\sqrt{(1 - r^2)^2 + (2\lambda r)^2}} \quad (2.53)$$

This relation will be the same for all single degree of freedom systems oscillating in harmonic motions. By substituting eq. (2.53) into eq. (2.50), eq. (2.54) is obtained.

$$F_{total} = F_0 \cdot DAF \quad (2.54)$$

Where  $F_{total}$  is the total force in the system including the dynamic force,  $F_0$  is the static force and DAF is the dynamic amplification factor. This proves that the total load in any system, described using the equation of motion can be obtained by multiplying the static load with the DAF.



## Chapter 3

# DESIGN OF INTEGRATED SPOOL COVER

The design of the integrated spool cover is based on the field data and technical specifications for the spools given in this chapter. The chapter includes a description of the field data, description of necessary design loads for the static analysis and a presentation of the proposed design for the integrated spool cover.

### 3.1 Design basis

The first part of any project consists of information gathering where main issues and concerns should be discovered in early phases of the project. The specific information regarding the spool layouts and sizes is found from a “Feed study” performed by Kongsberg gruppen.

#### 3.1.1 Field layout

The concerned project is a subsea compression project where the subsea field is modified by installing a wet gas compressor placed close to template M and template L located 15 km south of the platform C as illustrated in *figure 3.1*. The goal of the project is to increase the production rate and recoverable reserves from the reservoir by providing additional compression power. The project is one of the first of its kind and is considered a milestone as an important advance in subsea technology, (Statoil (2012)).

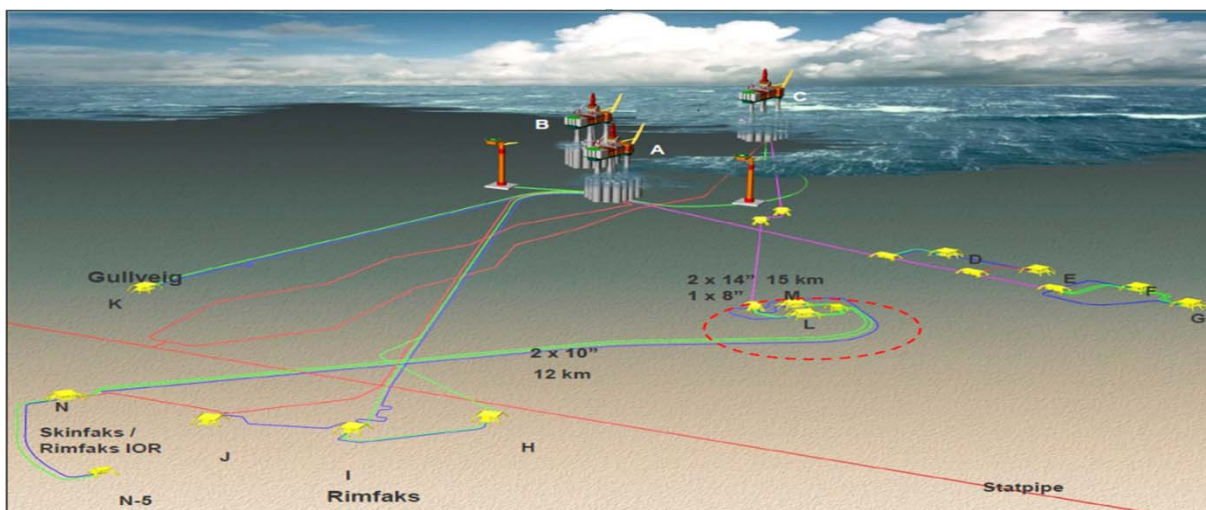


Figure 3.1: Field layout, (Statoil (2009)).

As part of modifying the satellite field, spools must be installed connecting the wet gas compressor (WGC) to the subsea templates and the wet gas compressor to the main pipelines indicated as towhead (C4) in *figure 3.2*. In this master thesis the analysis concerning the three omega shaped spools connecting the wet gas compressor to the main pipeline are considered.

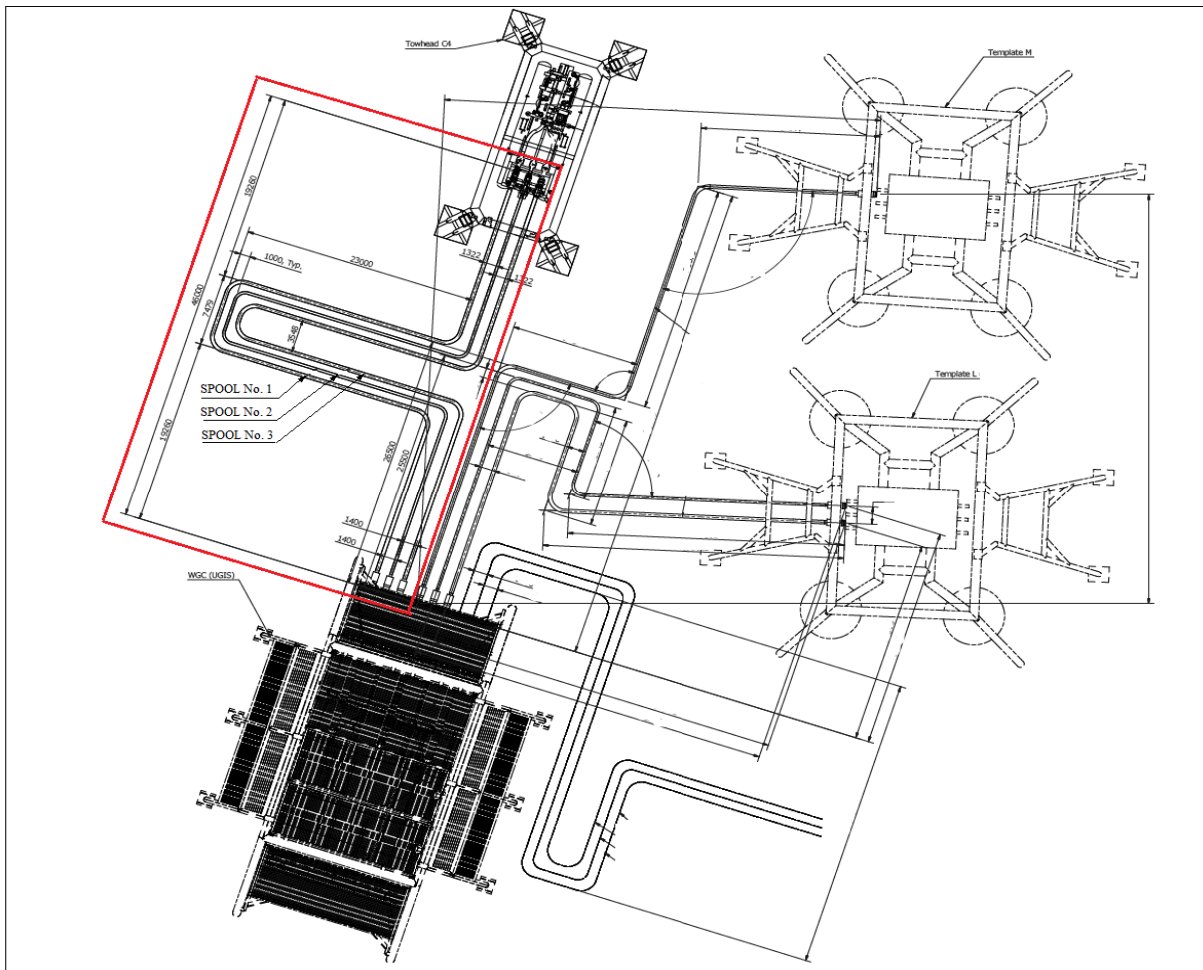


Figure 3.2: Typical spoolbank, (Kongsberg gruppen (2011)).

### 3.1.2 Spool installation

To modify the satellite field, the production must be shut down while the compressor is installed and connected to the main pipeline and subsea templates. Normally the spools would be installed using spreaderbars or framework structures supporting the spools during the lift through the waterline area and down to the sea bottom where the spools are disconnected from the spreader. The spools would then be connected (tied-in) to the wet gas compressor and pipeline towhead using a hydraulic tie in device ensuring tight connections. After the spools are connected to each unit, additional protection covers (normally GRP covers) are lifted in position above the spools to protect them from dropped objects and fishing trawlers.

The installation of the three “omega ( $\Omega$ )” shaped spools are considered the most critical of the spool lifts due to weight ( $\approx 90\text{Te}$ ) and large size ( $\approx 46 \times 26\text{m}$ ) and is analyzed in this thesis. In order to reduce downtime, the three spools of concern will be installed in one lift where the structure (spreader) supporting the spools during the lift also function as a protection cover able to withstand loads from dropped objects and trawlers after the installation is finished.

After the spools have been operating for some years, the operator would like to replace some of the spools individually. If the three omega spools are installed in a closed protection cover, all three spools must be removed in order to replace one of the spools. Due to the operator’s requirements, the protection cover (spreader structure) will be designed with a locking mechanism making it possible to open the spool cover and replace the spools one at a time.

### 3.1.3 Technical data

#### Cross sectional properties

Table 3.1: Spool size data for spool #1,#2,#3, (figure 3.2).

Spool size	OD [mm]	wt <sub>spool</sub> [mm]	ID [mm]	ct <sub>spool</sub> [mm]
12" spool (#1 and #3)	323.8	23.8	276.2	55.0
8" spool (#2)	219.1	15.9	187.3	40.0

#### Gooseneck

The connection points of spools are normally placed above seabed and the spool ends must therefore be designed with a geometric change as illustrated in *figure 3.3* referred to as the “gooseneck”. This shape is necessary to provide easy installation when the spools are lifted in place and the termination heads (*figure 3.3*) are connected (tied-in) to the subsea structure. The tie-in is performed by a hydraulic device pulling the termination heads 460mm and 800mm to the main pipeline and WGC respectively, (Kongsberg gruppen (2011)). The termination heads are located at each side of the spool and are necessary to ensure a tight connection between spool pipes and respective subsea units.

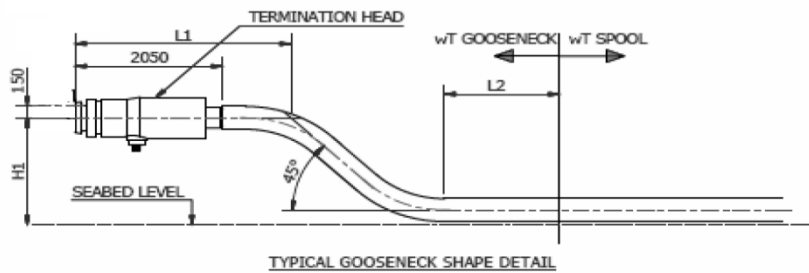


Figure 3.3: Gooseneck detail, (Kongsberg gruppen (2011)).

Large forces in the gooseneck both due to the massive weight of the termination head and axial strain that occurs during the tie-in, makes it necessary to increase wall thickness in the goosenecks to account for increased stresses during lifting and tie in of the spools.

Table 3.2: Gooseneck properties for spool #1,#2,#3, (figure 3.2).

Spool (number)	L1 [m]	L2 [m]	H1 [m]	wt <sub>spool</sub> [mm]	wt <sub>goose</sub> [mm]
12" spool (#1, #3)	3.0	2.0	1.8	23.8	31.0
8" spool (#2)	3.0	2.0	1.8	15.9	15.9

## Material properties

The spools are designed with Super duplex 25% Cr duplex steel which is characterized as a hard, corrosion resistant alloy. The spools will be filled with MEG (Ethylene glycol) during the installation. This will increase the weight of the structure, but is necessary to protect the spools from corrosion.

Table 3.3: Material properties

Mechanical characteristics	Coefficient	Value	Unit
Min. yield strength, 25%Cr duplex steel ( <i>spool</i> )	SMYS <sub>25%Cr</sub>	550	Mpa
Min. yield strength, steel at 20°C ( <i>cover</i> )	SMYS <sub>spreader</sub>	355	Mpa
Density, 25%Cr duplex steel	$\rho_{25\%Cr.Steel}$	7820	kg/m <sup>3</sup>
Density, regular steel	$\rho_{steel}$	7850	kg/m <sup>3</sup>
Density, concrete coating	$\rho_{coating}$	1300	kg/m <sup>3</sup>
Density, MEG at 20°C	$\rho_{MEG}$	1115	kg/m <sup>3</sup>
Density, salt water	$\rho$	1025	kg/m <sup>3</sup>
Young's Modulus, steel	E	$2.07 \cdot 10^5$	Mpa
Poisson ratio, steel	$\nu$	0.3	-

## Spool weight data

Based on cross sectional data given in *table 3.1* to *table 3.3*, the distributed weight of the spools are obtained. *Table 3.4* illustrates the weight contributions from the spool pipe, coating, content and displaced water. The calculated weight in air and submerged weight will be used as input in a finite element program (Staad.Pro) to calculate forces on the structure supporting the spools. More detailed weight calculations are shown in *APPENDIX A*.

Table 3.4: Spool weight data: Uniform weight of spools and content.

Spool ( <i>number</i> )	Spool pipe [kN/m]	Coating [kN/m]	MEG [kN/m]	Displaced water [kN/m]	Weight in air [kN/m]	Submerged weight [kN/m]
12" spool (#1, #3)	1.73	0.83	0.66	1.49	3.22	1.73
12" gooseneck (#1, #3)	2.21	0.83	0.59	1.49	3.63	2.15
8" spool (#2)	0.78	0.42	0.30	0.71	1.50	0.79
8" gooseneck (#2)	0.78	0.42	0.30	0.71	1.50	0.79

The total weight of the spools includes the weight of the spool pipe (steel walls), the coating, the MEG and the termination heads which weigh 1.7Te in air and 1.5Te in water located at each spool ends as shown in *figure 3.3*. The total weight of the spools are calculated by modeling the spools in a finite element program or by multiplying uniform weights with relevant length of spools and are given in *table 3.5*.

Table 3.5: Spool weight data: Total weight of spools and content.

Spool ( <i>number</i> )	Total weight in air [Te]	Total submerged weight [Te]
12" spool (#1)	34.7	20.1
8" spool (#2)	17.8	10.6
12" spool (#3)	35.2	20.3
<b>Total weight</b>	<b>87.7</b>	<b>51.0</b>

## 3.2 Design loads for static lifting analysis

During subsea lifting operations, the full force of the structure must be carried by the “main hook” that is connected to the crane by the crane wire. The lifted object is connected to the main hook by several slings attached to the structure at carefully decided lifting points to optimize the force distribution in the structure. In a static analysis, only the self-weight of the structure (including attached items) is applied where environmental loads is taken into account by a dynamic amplification factor as discussed in this chapter.

The goal of the static analysis is to verify the integrity of the structure and all applied loads must be taken into account in the analysis. In subsea lifting operations the following loads should be considered:

- Hydrodynamic forces from waves and current.
- Inertia force due to acceleration of the crane tip.
- Static force due to the self-weight of the structure.

As proven in *section 2.5* the total force in the crane wire during the dynamic lifting operation is represented by the stiffness of the wire, “K” multiplied by the varying elongation of the wire:

$$K(\eta - z_{ct}) = DAF \cdot F_{Static} \quad (3.1)$$

Where  $(\eta - z_{ct})$  is the relative displacement between lifted object and crane wire,  $F_{static}$  is the total self-weight of the structure and DAF is the dynamic amplification factor. It is therefore a reasonable assumption that the total force including hydrodynamic and inertia forces in the structure is represented as the weight of the structure multiplied by the DAF.

$$F_{Total} = F_{Static} + F_{Dynamic} = F_{static} \cdot DAF \quad (3.2)$$

The static loads are vertical loads pointing downwards meaning that the dynamic forces will be applied in the same direction. The horizontal forces on the structure (mainly environmental) are very small compared to the vertical forces and are not included in the static analysis.

In this chapter design loads for the static lifting analysis is discussed, where the total structural load are accounted for by using uncertainty factors, skew load factor and dynamic amplification factor that are multiplied with the self-weight of the structure to account for total loads and uncertainties during the lifting operation.

### 3.2.1 Inaccuracy factors

The structure is verified using a LRFD (load and resistance factor design) approach where the applied loads multiplied by relevant load factors must be less than the design resistance of the structure (eq. 3.6). The design load,  $F_{static}$  is given as:

$$F_{Static} = W \cdot \gamma_{weight} \cdot \gamma_{COG} \cdot \gamma_f \cdot \gamma_c \quad (3.3)$$

Where  $W$  is the self-weight of the structure and the inaccuracy factors,  $\gamma_n$  are described in this section.

#### **Weight inaccuracy, $\gamma_{weight}$**

The weight of the structure is found by accurate estimates during the structural analysis performed in Staad.Pro. The structure will be test lifted before the installation in order to verify the true weight of the structure before deployment. Due to fabrication tolerances inaccuracy in relevant mass calculations, DNV (DNV (1996) Pt.1, Ch.3, section 3.5.2) recommends a minimum weight contingency factor which is chosen 1.05 in the structural analysis. The weight test is conducted under safe conditions where the true and estimated weight should have a deviation less than 5 %. If larger deviations are observed, the structure is tested analytically for the increased weight, or enhanced measures are applied to ensure the integrity of the structure.

#### **Center of gravity, $\gamma_{COG}$**

When doing lifting operation, the hook is placed above the objects center of gravity so that the sum of vertical forces (static self-weight) is below the hook preventing the structure from tilting when the structure is in air. Due to inaccuracies in weight and estimated center of gravity, a COG factor is applied. The inaccuracy factor can be obtained using a COG envelope where the sensitivities in the structural integrity due to change in COG is checked by testing how the structure react when the COG is changed. If there is a linear relation between shifts in COG and resulting load effects while the structure shows little sensitivity to changes, the value for COG inaccuracy should not be less than 1.05 according to DNV (DNV (1996) Pt.1, Ch.3, section 3.5.3). The COG is obtained by accurate estimates during the structural analysis performed in Staad.Pro with high weight control where all weight components are included in the model. The structure will be test-lifted before the installation, and if the structure doesn't tilt in any direction the estimated center of gravity is the same as the real one.

#### **Load factor, $\gamma_f$**

The uncertainty in the load is represented by a load factor. The relevant load factor for all parts of the lifted object should be 1.3, (DNV (1996) Pt.2, Ch.5, table .4.1).

#### **Consequence factor, $\gamma_c$**

The consequence factor is applied to account for severe consequences of single element failure. If members in the lifting equipment such as critical spreader member, slings and crane wire would fail, the whole lift would fail making it necessary to use a higher consequence factor for critical members than other members which don't support the lift. According to (DNV (1996) (Table 4.1)) the consequence factors are chosen according to redundancy so that the lifting equipment has high consequence factors (1.3), the main elements supporting the lifting point should have medium consequence factors (1.15). For parts of the structure that doesn't support the lift, no consequence factor is necessary (1.0).

### 3.2.2 Skew load factor, SKL

The skew load factor is used to account for extra loading due to sling length miss matches due to equipment and fabrication tolerances in lifts. In case of statically indeterminate 4 point lifts with sling length tolerances less than 0.15% a skew load factor (SKL) equal 1.25 should be applied according to DNV (1996) (Sec.2.3).

The skew load factor should reflect the structures ability to adjust itself to relevant fabrication and equipment inaccuracies and resulting tilt due to change in center of gravity. The skew load factor can be found by specifying change in the sling lengths by changing lengths of each sling and finding the worst combination of sling elongation and compression. To make sure that the skew load factor for 4 point lifts is applicable for the considered structure, a sensitivity study is performed in *APPENDIX B* and presented in *section 4.2.2*.

### 3.2.3 Dynamic amplification factor, DAF

The sum of dynamic and static loading can be found by taking the product of the dynamic amplification (DAF) and the static loading as shown in *eq. (3.2)*. By using this method, the structural loads are easily obtained using one variable for the whole structure to account for dynamic forces during the lift.

The DAF must be larger than 1.0 representing lifts with no dynamic loads, and smaller than 2.0 where the hydrodynamic forces are equal the static weight of the structure resulting in a resultant vertical force upwards and slack crane wire which is unacceptable.

During a subsea lift, three phases are considered: When the structure is in air, when it is partly submerged (in the splash zone) and when it's fully submerged. When the object is in air (deck handling), the dynamic forces occur due to vessel motions resulting in increased inertia force on the structure. The DAF is chosen 1.2 according to DNV's minimum requirements in case of offshore lifts (in air) heavier than 100 tones (DNV (1996) table 2.1). When the structure is crossing the waterline and is subjected to hydrodynamic loads, the dynamic loads are increased which is represented by a larger DAF chosen to 1.6 for the structural design.

A dynamic lifting analysis in a marine dynamics program like SIMO or OrcaFlex should be performed to check if the real hydrodynamic loads are larger than applied loads in the static analysis. The following requirement must be satisfied for the structure at all times during the analysis:

$$DAF_{static} \geq DAF_{dynamic} \quad (3.4)$$

Where  $DAF_{static}$  is the applied dynamic amplification factor in the static analysis and  $DAF_{dynamic}$  is the associated factor found from the dynamic analysis.

### 3.2.4 Design factors for slings

Lifting equipment like slings and crane wire must be designed with more conservative design factors than the structure itself because the consequence of collapse of slings, hooks or crane wire are much more severe than collapse of individual members in the redundant framework structure.

#### Design sling load

The total nominal safety factors for the slings are obtained by multiplying all relevant factors given in DNV (DNV (1996) PT.2, CH.5, Section 3.1)

Load factor:	$\gamma_f = 1.30$	
Consequence factor:	$\gamma_c = 1.30$	
Reduction factor:	$\gamma_r = 1.33$	
Bending factor:	$\gamma_b = 1.00$	(hard eyes on both ends)
Wear factor:	$\gamma_w = 1.00$	(single application purpose)
Material factor:	$\gamma_m = 1.35$	(certified new steel wire rope sling)
<hr/>		
Total safety factor:	$\gamma_{sf} = 3.03$	(minimum 3.0)

The minimum breaking limit (MBL) of the wire sling is given by eq. (3.4).

$$F_{sling} \leq \frac{MBL_{sling}}{\gamma_{sf}} \quad (3.5)$$

Where  $F_{sling}$  is the dynamic sling load obtained in the static analysis.



### 3.2.5 Code check

All members are controlled according to Eurocode 3 in Staad.Pro. The purpose of the design check is to control the utilization ratios of each member according to the selected code and ensure that they don't exceed the requirements given by the selected limit state. (DNV-C101-2010 Sec.2 D200)

$$S_d \leq R_d$$

$$S_d = \sum_{i=1}^n \gamma_{fi} \cdot S_{ki} , R_d = \frac{R_k}{\gamma_M} \quad (3.6)$$

Where  $S_d$  is the design load effect (sum of all loads), defined as all characteristic loads,  $S_{ki}$  multiplied with relevant load factor,  $\gamma_{fi}$ , and the design resistance,  $R_d$  is defined as the characteristic resistance,  $R_k$  divided by the material factor,  $\gamma_M$ . This is called the Load and Resistance Factor Design (LRFD) approach, where the equation:  $S_d=R_d$  defines the limit state.

#### Material factor

The LRFD approach requires a material factor,  $\gamma_M$  for the design. This is needed to account for uncertainty related to the material capacity. According to Eurocode 3 and the Norwegian national appendix (NS1993-1-1-2005 NA.6.1) the material factors are given in *table 3.6* obtained from Eurocode 3 and NORSOK (NORSOK N-004 (2004)). The NORSOK gives the appropriate material factors for tubular cross sections according to DNV, (DNV-OS-C101 Sec.5 D.100).

Table 3.6: Material factors for design of steel structures, (Eurocode 3 and NORSOK N-004).

Description	Eurocode 3 1993-1-1-2005		NORSOK N-004
	EC3 6.1	EC3 NA.6.1	Chapter 6.3
$\gamma_0$ Capacity for all cross section classes	1.00	1.05	1.15
$\gamma_1$ Capacity for instability in trusses	1.00	1.05	1.15
$\gamma_2$ Axial tensile capacity	1.25	1.25	1.30

#### Eurocode 3 vs. NORSOK N-004

According to DNV (DNV-C101-2010 Sec.5. D.100) all tubular steel members and joints should be designed according to NORSOK N-004, while NON-tubular steel members should be designed according to Eurocode 3 (with materialfactor,  $\gamma_M=1.15$ ). The structure consist of mainly tubular sections making NORSOK N-004 the relevant standard. The main reason why NORSOK should be the relevant standard for offshore structures with tubular members is because the hollow sections can be subjected to buckling due to hydrostatic pressure differences. The considered structure are located close to the mean water level and the tubular sections are perforated (so they are easily flooded during submergence) making the pressure difference negligible. The basic formulas for steel design is the same for both standards (except the interaction formulas for buckling) making Eurocode 3 applicable for the tubular sections in the considered structure when it is lifted through the splash zone.

### 3.2.6 Load cases

During subsea installations, lifted objects are exposed to different phases with respect to location of the object relevant to mean water level. Before the structure touches the water it is subjected to inertia forces due to motions of the vessel. At first impact with the oscillating sea-surface, the structure will be subjected to impact forces combined with small contributions from added mass, drag and varying buoyancy that are steadily increasing with level of submergence while the slam contributions get reduced to zero when the object is fully submerged. The largest hydrodynamic force would normally occur at the exact point of fully submergence where the drag and inertia force is largest due to large fluid particle velocity which is steadily decreasing with level of submergence. From *figure 3.4* one can see that the hydrodynamic forces have a nonlinear variation during the deployment while the static forces have a close to linear relation as observed in *figure 3.4*.

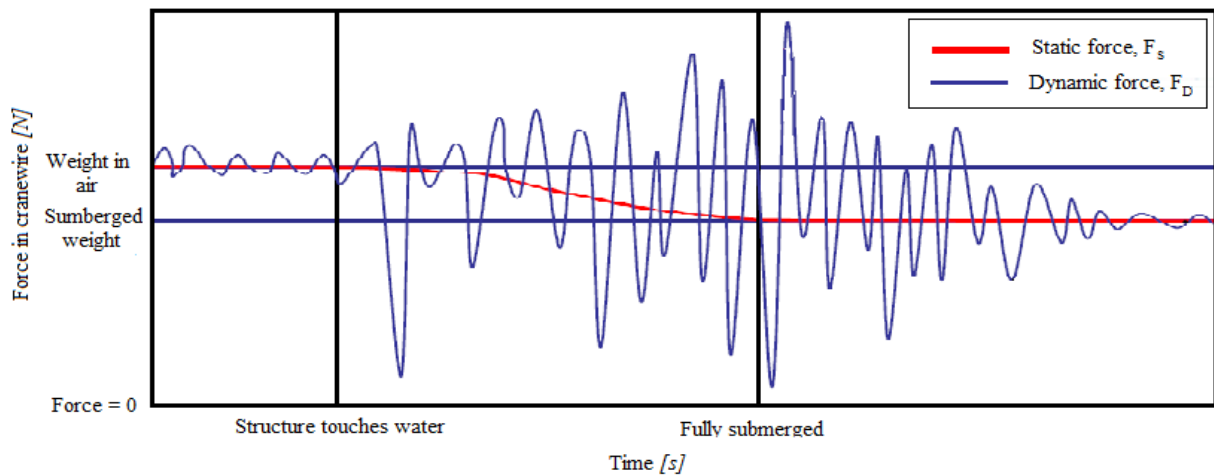


Figure 3.4: Forces in crane wire during submergence of lifted objects, (Hosaas (2009)).

Structural design loads are found by considering three main phases of the lift. The three cases are lift in air, partly submerged and lift in water as illustrated in *figure 3.5*. Each of the three load cases will be considered and the appropriate design factors will be applied according to the discussion in *section 3.2*.

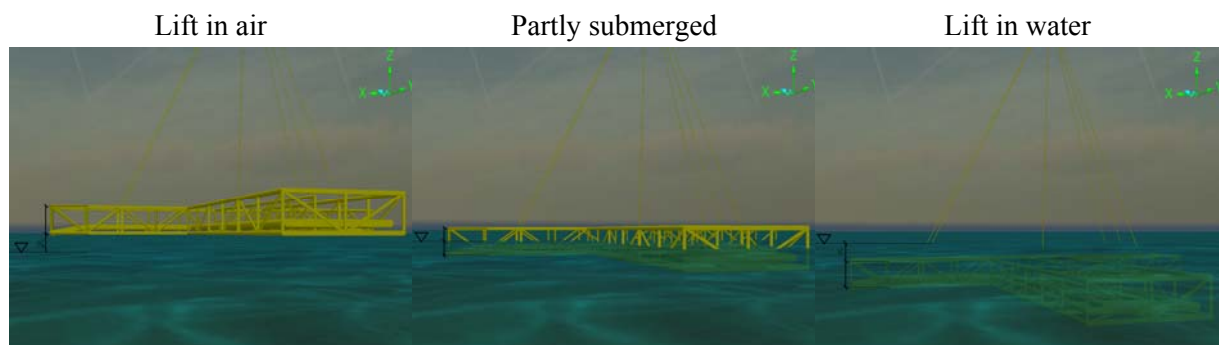


Figure 3.5: Illustration of load combinations.

### 3.3 Design concept

The integrated spool cover must be designed to tolerate all relevant forces that the structure is subjected to during its lifetime. This includes forces during transportation, installation and while the spools are operating. The largest load during the structures lifetime may occur during the installation which is the structural integrity should be verified by controlling forces associated with the lift of the structure.

The spool cover must be design with the possibility of replacing one spool at a time after the system is installed. This issue is solved by designing it as an open structure with eight transverse beams (indicated with blue in *figure 3.1*) to provide lateral strength during the lift. The eight beams are connected to the top members of the structure designed to be removed after the installation by ROV's either by cutting or providing some sort of locking mechanism between the lateral beams and the framework structure. The temporary members should be designed as rigid connections to the main beams ensuring that they are capable of absorbing bending moments to increase structural stability. Creating a temporary and rigid connection is rather difficult, and either the rigidness or detachability will be compromised which should be considered with care.

In order to protect the spools from dropped objects, the structure will be covered with GRP grating. The GRP grating will be designed as lids that are hinged along the top side of the structure, (see *figure A.2*). The hinged lids will not cover the spools during the lift, but rather hanging down from the sides in order to reduce hydrodynamic loading during the lift. GRP grating will also be fastened at the trawlbords, (see *figure A.1*)

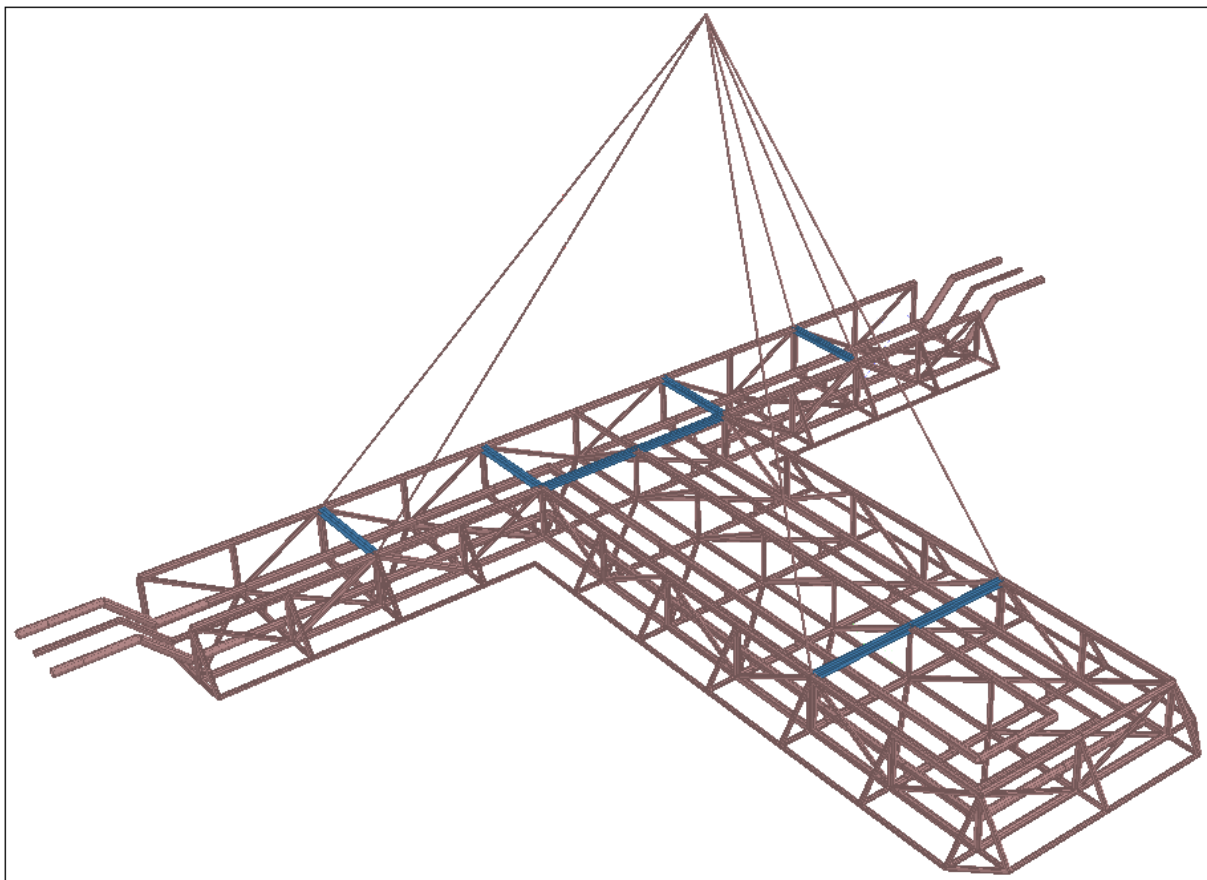


Figure 3.6: Proposed design for integrated protection cover.

The dimensions of the spool cover are displayed in *figure 3.07*, where the main height of the structure is 2.1m to satisfy the joint welding requirement making sure that all braces are designed with angles larger than 30 degrees (Eurocode 3 (2005 1-8)). The trawl board breadth of 1.32 m gives a trawlboard angle of 58 degrees which is the minimum requirement from NORSOK, (NORSOK (2002) 5.3.4). Cross sectional properties are illustrated in *figure 3.7* and supplemented in the Staad.Pro output file, (*APPENDIX J*).

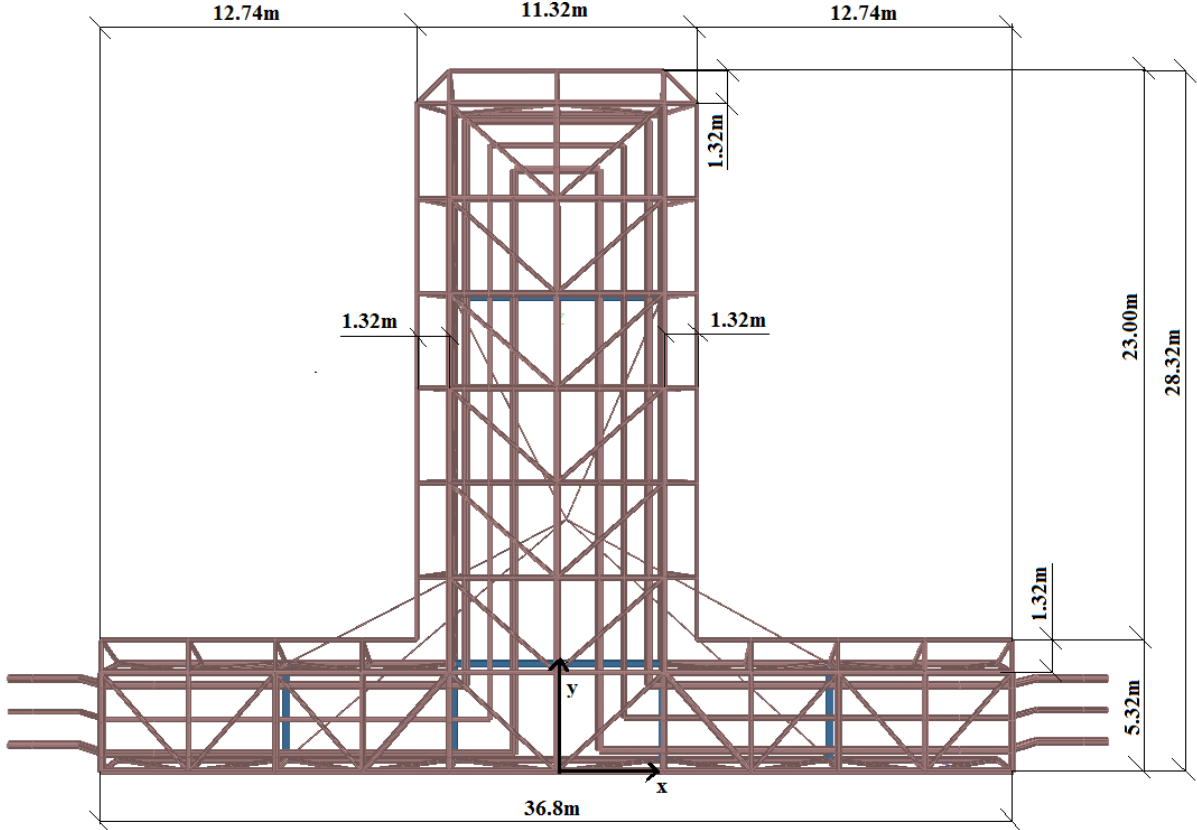


Figure 3.7: Main dimensions of integrated spool cover, all values in meter with dimensions from c/c.

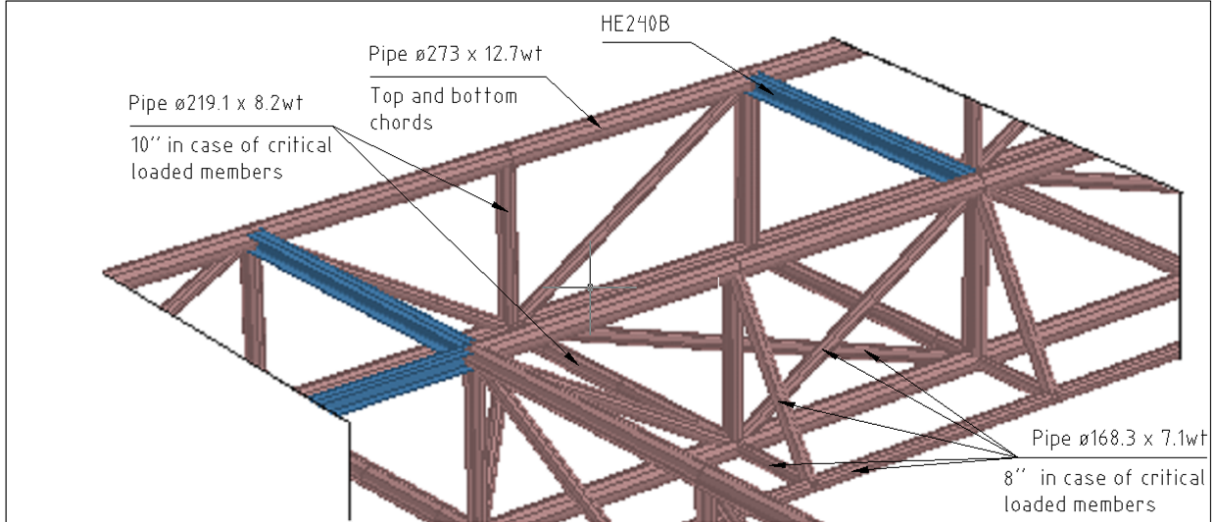


Figure 3.8: Cross sectional properties for the framework. More details are given in the Staad.Pro output file in *APPENDIX J*.

## Chapter 4

### STATIC LIFTING ANALYSIS

The purpose of this thesis is to verify the structural integrity of the integrated spool cover during the subsea lift of the structure. A design check is necessary to control the utilization ratios of each member according to the selected code and ensure that they don't exceed the requirements given by the selected limit state where all members are controlled according to Eurocode 3 in Staad.Pro.

To verify the structure, all relevant design loads during the lifetime of the structure must be considered. In its lifetime, the integrated spool cover is (assumed) subjected to the largest forces during deployment, which is why the structural integrity should be verified by the lifting analysis.

The following posts are checked and described in this chapter:

- General structural verification of all elements according to Eurocode 3.
- Perform sensitivity tests to confirm applied skew load factor.
- Global buckling check of the structure according to Eurocode 3.
- Obtain maximum forces in wires to obtain minimum breaking limit (MBL) for the wires.

#### 4.1 Static analysis, preprocessing

Staad.Pro (Structural Analysis And Design for Professionals) is a finite element software developed by Bentley. The program is capable of analyzing advanced structures and does so by calculating deformations as well as internal forces and stresses. The program is capable of checking the structure according to local codes and standards since the software supports 70 international and 20 U.S. codes (Bentley (2013)).

When performing framework analysis in Staad.Pro, the preprocessor part (everything that needs to be done before getting the results) includes the following in advised chronological order:

- Defining structure geometry: Creating nodes in all connection points and defining members between them.
- Defining section properties: Select appropriate cross sections for all members.
- Defining material properties: Selecting E-modulus, poisson ratio, density, alpha factor (in case of temperature changes) and damping coefficient for materials.
- Defining support conditions: Choose necessary supports, (pinned, fixed, and partly fixed).
- Member release: Hinges and members not able to absorb moments or forces in certain directions must be defined.
- Define structural loads: Define loads applied on nodes or members and define load cases with appropriate factors for relevant loads

- Obtaining center of gravity: and combine them separately. The “hook-node” is placed above the COG.
- Define code: Tell the program which code that should be used to check the structure.
- Define code specification: When using Eurocode 3, material factors, yield stress, buckling lengths and buckling factors should be defined manually.

The data is described by using either the user interface or the script function (editor) in Staad.Pro.

This chapter describes how the relevant Staad.pro model is obtained and gives some recommendations for how to proceed to ensure good model control.

#### 4.1.1 Structure geometry

Before the structure is modeled, the main geometry of the structure is decided based on practical requirements for the integrated spool cover and proposed design-concept. The main topics of consideration for defining the structural geometry are:

- The spool cover must be made to fit the three omega spools with shape and size given in *figure 3.2*. The spool cover should start at an appropriate distance from the termination head giving space to the tie-in tools and at the same time support the gooseneck during the lift.
- The distance between the spools and spool cover walls need to be larger than the fabrication tolerances and take into account the largest possible movement of the spools during tie-in and operation, (minimum 200mm).
- The height of the structure should be sufficient to ensure that the minimum angle of all braces is at least 30° to ensure high capacity welds, (Eurocode 3 (2005) 1-8).
- Maximum trawlboard angles to prevent that trawling equipment from getting stuck in the structure. All structural corners should have a maximum angle of 58°, (NORSOK U-001 (2002) 5.3.4).
- Properties of GRP cover for the roof related to span length.

After the main size of the integrated cover is decided, the geometry is modeled in Staad.Pro, (the model may be imported from Autocad, or designed in similar program, to model in Staad.Pro is recommended).

The structure is modeled using the general user interface in Staad.Pro. All connection points and member ends are created as nodes. Members are created as beams between the nodes. The members should be divided in different groups to provide greater structural control. The members are described in the Staad.Pro output file given in *APPENDIX J* and the model will now look like *figure E.1*.

## 4.1.2 Define material and sectional properties

### Material properties:

Material properties for all members must be defined. This includes E-modulus, Poisson ratios and density of the materials. Material properties for spool and integrated spool cover are selected from *table 3.3*. The sling wire and additional rigging must be considered individually, where the relevant forces will be obtained using Staad.Pro. Elements with different material properties should be divided in different groups, so that material properties could be selected for relevant groups rather than individual members in Staad.Pro.

### Section properties:

The first time that the section properties for each member are selected, the selection is based on a qualified guessing, experience and rough estimations. The model will be analyzed using the chosen members where Staad.Pro provides utilization ratios in each member according to the selected code. The sections for each member can be adjusted according to the utilization ratios obtained from the first results. This can be done manually or by using automatic selection functions in the software as an iteration process.

Similar members (based on member function and location) should be placed in the same groups since it is easy to change member properties for entire groups. It is therefore important to divide the members in appropriate groups making it easy to change section properties for many members at once.

The selected members are illustrated in *figure 3.7* and given in the Staad.Pro output file in *APPENDIX J*.

### 4.1.3 Define support conditions and member release

#### Support conditions:

In case of lifting operations there is only one rigid point in the structure, namely the masterhook that all slings are connected to (two hooks in case of tandem-lift). This point is defined as a pinned connection free to rotate and not capable of transferring moments.

If the only defined support is the pinned hook-node, the structure will be free to rotate around all axes and cause singularities in the structure. This occurs since the structure is exposed to abrupt changes in motion, even when subjected to negligible forces causing instabilities to the structure. This singularity is prevented by introducing very weak stiffeners at each side of the structure to make it stable.

#### Member release:

If no member release is defined, all connections are designed as fixed connections in Staad.Pro. If nothing is specified, all joints will carry moments and forces in all directions (as rigid connections). Since all member doesn't carry moments or forces in certain directions, (e.g. the slings that cannot carry moments) the release properties must be defined in Staad.Pro. All connections that are not considered rigid must be defined with member releases for relevant directions (moments and shear forces). The following connections in the integrated spool cover are not considered as rigid:

- Slings: They are connected to padeyes and hook with bending-free connections (shackles) and will not transfer moments.
- Spool connections: The spools are laid on top of the bottom transverse members and connected in a moment free connections. The spools should not be capable of absorbing forces from the structure so that only vertical forces should be translated from the spools to the structure.

In the model the beams and spools are connected with short vertical members "released" for all moments and shear forces. (except the vertical connections at the end of the structure which is necessary for the model to be stable – no singularities) This is a conservative design.

- Temporary beams: To increase the structural performance, transverse beams are needed on top of the structure to prevent the members from buckling. These members must be temporary so that the spools can be removed individually to satisfy the requirements for the design.

These beams are connected as moment free around the axis they are connected to, the local x – axis. Otherwise they are considered as fixed, see description in *section 3.3* for more details.



#### 4.1.4 Define load conditions

##### Primary load cases

Before establishing the major load combination (structure in air, partly submerged and in water), the primary load cases must be decided. The considered structure consists of three spools and the integrated cover supporting the spools. Different consequence factors are applied for the spool and the cover (since the spool is not supporting the lift and requires a lower consequence factor). When designing the structure in Staad.Pro the primary load cases is necessary to provide model control and easy access to weight summary of individual structural parts.

The primary load cases used for the structural evaluation of the model are described in *table 4.1*.

Table 4.1: Primary load cases for static analysis in Staad.Pro, (Subsea 7 (2011) 3.2.5).

Primary load case	Definition	Description
11	Weight of spool in air	Total weight of spool including steel pipe, termination heads, coating and pipe content (MEG) in air.
12	Weight of spreader in air	Weight of spreader including steel in members, GRP and additional weight to account for weight of welds, rigging, paint and polyethylene plates in air.
13	Weight of spreader partly submerged, submerged part	Weight of steel in horizontal members in bottom part of structure and additional weight to account for weight of welds, rigging, paint and polyethylene plates in water.
14	Weight of spreader partly submerged, in air part	Weight of steel members not accounted for in "load case 13" and additional weight of GRP grating in air.
15	Weight of trapped water in spool in air	Weight of trapped water in spool before submergence, <i>(no trapped water when the spool is filled with MEG)</i> .
16	Weight of trapped water in spreader in air	Weight of trapped water in spool cover before submergence, <i>(assume 50% filled spreader members)</i> .
21	Weight of spool in water	Total weight of spool including steel pipe, termination heads, coating and pipe content (MEG) in water.
22	Weight of spreader in water	Weight of spreader including members (waterfilled), GRP and additional weight to account for weight of welds, rigging, paint and polyethylene plates in water.

Before the structure enters the splash zone, the structure will be partly filled with water which is accounted for by primary load case 15 and 16 for trapped water in spool and spreader respectively. Since the spool is already filled with MEG, the trapped water in the spool is zero.

## Load combinations

Load combinations are defined according to which loads the structure will be influenced by at a certain point in time. All loads during the deployment is represented by three main phases; lift in air, partly submerged and lift in water as illustrated in *figure 4.1*. Each phase has a certain set of applied environmental load and self-weight (none is equal).

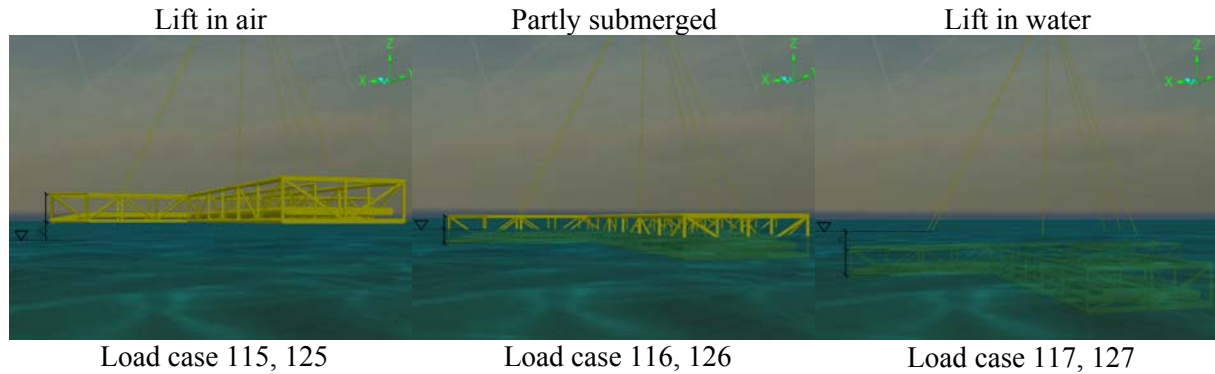


Figure 4.1: Illustration of load combinations.

Two load cases are defined for each of the three phases of the lift: One for the structural design, and one for the rigging design (slings, crane-wire, etc.) due to the difference in load factors. Two additional load combinations (static lift in air and water) are necessary to obtain the total weight of the structure and the COG for both lift in water and lift in air.

Table 4.2: Relevant load combinations for static analysis in Staad.Pro,(Subsea 7 (2011) 3.2.5).

Load combination	Primary load cases	Description	Purpose
100	11, 12	Static weight in air	COG in air, sensitivity tests
101	21, 22	Static weight in water	COG in water
115	11, 12, 15, 16	Lift in splash zone (spool and spreader in splash zone)	Structural design
116	13, 14, 21	Partly submerged (spool submerged, spreader partly submerged)	Structural design
117	21, 22	Lift in water	Structural design
125	11, 12, 15, 16, 21	Lift in splash zone (spool and spreader in splash zone)	Rigging design
126	13, 14, 21	Partly submerged (spool submerged, spreader in splash)	Rigging design
127	21, 22	Lift in water	Rigging design

The relevant load factors for the load combination and each primary load case are illustrated in *table 4.3* based on DNV (1996) and Subsea 7 (2011) for spool analysis.

Table 4.3: Load factors from DNV (1996) for each primary load case,(Subsea 7 (2011) 3.2.5).

Load combinations	Basic loads	$\gamma_f$	$\gamma_{c.spool}$	$\gamma_{c.spre.}$	$\gamma_{inac.}^{(3)}$	DAF	SKL	<b>Total factor</b>
100	11, 12	1.00	1.00	1.00	1.00	1.00	1.00	<b>1.00</b>
101	21, 22	1.00	1.00	1.00	1.00	1.00	1.00	<b>1.00</b>
115	11, 15	1.30	1.00	NA	1.10	1.20	1.25	<b>2.15</b>
	12, 16	1.30	NA	1.30	1.10	1.20	1.25	<b>2.79</b>
116	21	1.30	1.00	NA	1.10	1.60	1.25	<b>2.87</b>
	13	1.30	NA	1.30	1.10	1.60	1.25	<b>3.73</b>
	14	1.30	NA	1.30	1.10	1.20	1.25	<b>2.79</b>
117	21	1.30	1.00	NA	1.10	1.60	1.25	<b>2.87</b>
	22	1.30	NA	1.30	1.10	1.60	1.25	<b>3.73</b>
125	11, 12, 15, 16	1.00	1.00	1.00	1.10	1.20	1.25	<b>1.65</b>
126	21	1.00	1.00	1.00	1.10	1.60	1.25	<b>2.21</b>
	13	1.00	1.00	1.00	1.10	1.60	1.25	<b>2.21</b>
	14	1.00	1.00	1.00	1.10	1.20	1.25	<b>1.65</b>
127	21, 22	1.00	1.00	1.00	1.10	1.60	1.25	<b>2.21</b>

Note that the inaccuracy factor,  $\gamma_{inac.}$  is the combined factor for weight and COG inaccuracy ( $\gamma_{inac.} = \gamma_{weight} \cdot \gamma_{COG}$ )

Selected values for dynamic amplification factors must satisfy the condition given in eq. (4.1).

$$DAF_{static} \leq DAF_{dynamic} \quad (4.1)$$

Where  $DAF_{static}$  is the selected dynamic amplification factor for the static analysis in Staad.Pro and  $DAF_{dynamic}$  is the true dynamic amplification factor that occurs during deployment of the structure. The true DAF should be checked in a finite element program like OrcaFlex or SIMO which are capable of calculating dynamic loads on lifted objects.

The load combinations for rigging design does not include the consequence factor,  $\gamma_c$  or the load factor,  $\gamma_f$  since other set of safety factors are needed for the slings as described in section 3.2.4.

#### 4.1.5 Obtaining center of gravity

The center of gravity is critical in lifting operations since the hook must be placed correctly above the COG of the structure to make the lift stable. The COG is determined in Staad.Pro by applying a fixed connection in one end of the object and observing the resulting force and moment in the fixed connection which is similar to a cantilever. The center of gravity is obtained by finding the mean length from the “weighted” forces to the rigid connection as performed in *eq. (4.2)* and *eq. (4.3)*.

$$\begin{aligned}\sum F_z &= F_1 + F_2 + F_3 + \dots + F_n \\ \sum M_i &= F_1L_1 + F_2L_2 + F_3L_3 + \dots + F_nL_n\end{aligned}\tag{4.2}$$

Where  $M_i$  represent moment around the relevant horizontal axis x or y.

$$COG_i = \frac{\sum M_i}{\sum F_z} = \frac{F_1L_1 + F_2L_2 + F_3L_3 + \dots + F_nL_n}{F_1 + F_2 + F_3 + \dots + F_n}\tag{4.3}$$

The COG is double checked in the post processing phase in Staad.Pro by observing a deflection diagram that doesn't tilt in load condition 100 (lift in air) or by checking that the support forces in the weak links (see *section 4.1.3*) are negligible.

#### 4.1.6 Define code, material factor and yield stress

After the geometry, member and material properties, support condition, member release and loads are applied, the analysis can be performed according to the selected code. Staad.Pro is capable of checking the structure according to rules given in 70 international and 20 U.S. codes (Bentley (2013)). The leading regulation in Norway and other European countries is Eurocode 3 which is selected for the design. All members are controlled according to Eurocode 3 in the Staad.Pro analysis.

##### **Material factor:**

When designing structures, a material factor is needed to account for uncertainty related to material capacities. The default values for material factors in Eurocode 3 are lower than the minimum material factors given in DNV (OS-C101-2010 Sec.5 D100), and the material factors are manually chosen in Staad.Pro to be 1.15 for the design.

##### **Yield stress:**

The yield stresses for steel and super duplex steel are selected according to *section 3.1.3*.

##### **Buckling lengths:**

The buckling lengths of elements must be selected manually as described in *section 4.1.7*.

### 4.1.7 Define buckling lengths

Buckling is a failure mode that must be checked for members subjected to axial compression. When slender members are subjected to large axial compression forces it may result in elastic instability of the member which is called buckling. This is a result of axial loads that exceed the critical load (Euler buckling load) resulting in lateral deflection (large compared to axial displacement due to size) in the column. The critical load for slender columns will be much less than the necessary force to exceed the yield stress of the column (if the column is only subjected to axial force), (Li (2012)).

The buckling effect occurs due to imperfections in the column. When small lateral displacement occurs in the column, it will be subjected to eccentricities causing moments and shear forces in the column (even if the column is subjected to only axial loads). Deflection of a slender pin-ended column is illustrated in *figure 4.2*:

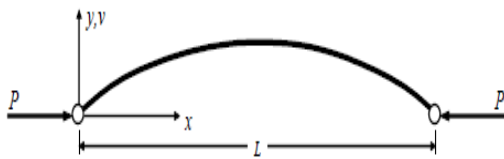


Figure 4.2. Deflected column with pinned ends, due to applied compressive load P, Li (2012).

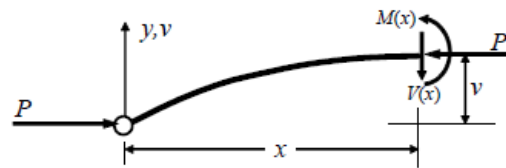


Figure 4.3. Forces in one section of the column, Li (2012).

From *figure 4.3* the occurring moment and shear in a slender column subjected to only axial load is illustrated. From regular beam theory, using kinematic boundary conditions, the critical buckling load can be derived as a function of length, L, E-modulus and moment of inertia, I as given in *figure 4.4*.

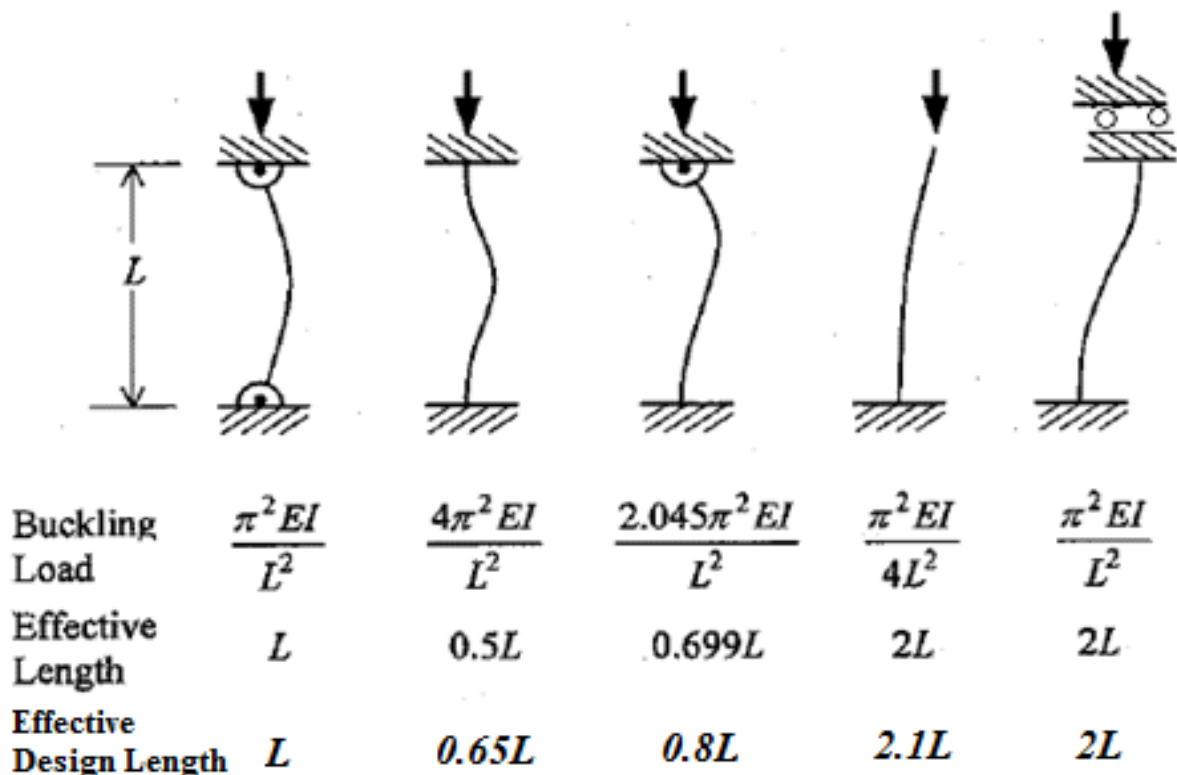


Figure 4.4. Buckling lengths and Euler buckling load for different support conditions, (Lovett (2008)).

**Effective buckling length:**

The buckling length is not necessarily the same as the columns physical length. The buckling load is derived assuming that the ends where are to rotate. If the ends have other end conditions than pinned, the effective buckling length can be defined as the distance between zero moments for members subjected to compressive force representing the equivalent length with the same strength as for pinned members. Buckling lengths for columns with different end conditions can be defined as in *figure 4.4*. The effective buckling length of columns,  $L_{eff}$ . can be obtained as the real length of the member,  $L$  multiplied by a factor that represents the ending condition of the column,  $k$ .

**Buckling in Staad.Pro:**

Staad.Pro will perform a buckling check on every member according to Eurocode 3, even if buckling properties are not manually defined. However the software is not capable of taking the end condition and true length of member into account. The default values of effective lengths in the software are the same as the length of individual members as they are defined in Staad.Pro (length between nodes) which are not necessary the same as the beam lengths.

For each member subjected to axial compression, the true length of the member,  $L_{y/z}$  and the reduction factor for the relevant support condition,  $k_{y/z}$  must be defined. For members where the total lengths are the same as the true length, the default values are considered conservative. This is because most members in the framework structure are welded giving fixed connections in joints that should be represented by reduction factors,  $k=0.65$  (*figure 4.4*) while the default value in Staad.Pro is  $k=1.0$ .

*Figure 4.5* illustrates the main beams that are subjected to axial compression in the considered structure. These members are compressed due to horizontal contributions from sling forces that are translated to the beams indicated in red. For these beams, lengths, end conditions and interaction between other members are taken into account by applying lengths and reduction factors for each member in Staad.Pro.

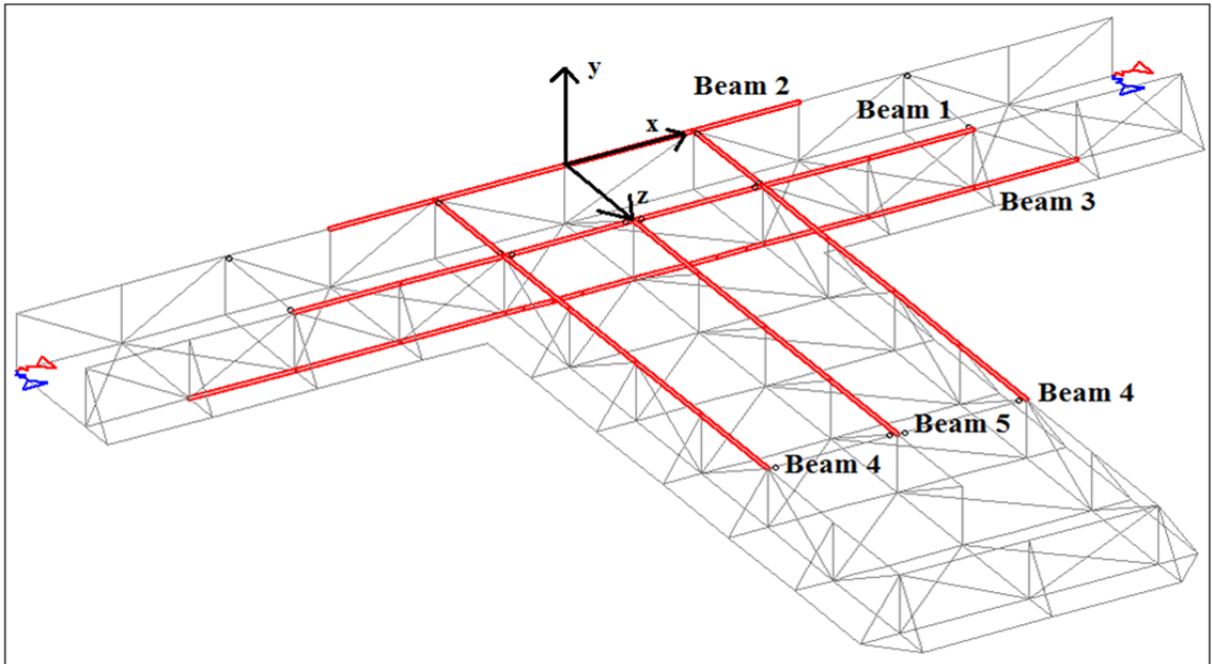


Figure 4.5: Main members subjected to buckling.

The true length of the beams,  $L$  can be defined as length of associated compressed members as illustrated in *figure 4.5*. The combined length of “BEAM 1” to “BEAM 5” is applied for all relevant members so they are considered as five beams when checked for buckling.

The buckling factor,  $k$  used to calculate the effective buckling length (different for  $y$  and  $z$  axis) are in case of columns (supported in both ends) only dependent on the end conditions. Since the considered structure consist of many transvers members (welded to the main chords) they will “disturb” the buckling effects of the columns since they are no longer free to rotate over the length. The buckling factors should not be based on the ending conditions alone which would be too conservative. The effective buckling lengths is rather obtained by performing a parametric study where the utilization ratio for each beam depending on the chosen buckling factor,  $k$  is obtained and would be evaluated using “engineering judgment”. The resulting factor that gives acceptable utilization ratio according to design limit will be discussed to see if the chosen values are acceptable. The effective buckling lengths will be compared to distance between zero-moments for each beam (*APPENDIX C*) which should represent the equivalent effective buckling length for each member. The buckling lengths and associated utilization ratios for each beam is given in *section 4.2*.

The design of a beams subjected to axial compression is checked in *APPENDIX D* (global buckling check) where all relevant formulas for calculating cross sectional capacities with respect to axial force, shear and bending as well as performing a full buckling check according to Eurocode 3 is included.

## 4.2 Static results (general structural verification)

After the Staad.Pro model is finished, the structure is analyzed by running the analysis. If no error occurs, the structure is checked according to the selected code (checked, but not yet verified).

Staad.Pro is capable of calculating stresses, forces and displacements in all sections of each member in the structure. The user is provided with critical values, graphical illustrations and utilization ratios for each member according to the selected code. This information should be used to evaluate the critical load conditions to understand and optimize the structure.

When performing lifting operations, a lot of information is needed to verify the structure and plan the lifting procedure. The following information is considered the most important output from the static lifting analysis in Staad.Pro and will be discussed in this chapter.

- The static weight of the structure and structure parts (spools, framework, etc.).
- The center of gravity (COG) of the structure in both air and water.
- Utilization ratios for members according to given design codes.
- Max dynamic hook load.
- Forces in each sling.
- Tilt of structure (global deflection).

The structure is made according to the design basis in *section 3.1* (the design is illustrated in *section 3.3*), the applied self-weights according to *APPENDIX A*, weight calculations and load combinations according to *table 4.3*. (All information is also illustrated and described in the Staad.Pro output file given in *APPENDIX J*)



### 4.2.1 Summary of results

This section provides the most important results obtained from the Staad.Pro lifting analysis.

#### Static weight of structure and structure parts:

Table 4.4 shows all weight contributions from spool and protection cover. This data should be compared with available hand calculations and expected weights for similar structures in order to verify the reliability of the Staad.Pro model. Normally the structure will be modeled in software that provides more detailed weight calculations, (e.g. CAD model). If the Staad.Pro model gives the same weight calculations as the CAD model, the structure weight is proven very accurate where low weight and COG inaccuracy factors are necessary for the structural loads.

Table 4.4: Weight summary, values obtained from Staad.Pro model.

Part	Description	Weight in air [Te]	Submerged weight [Te]
Spools	Weight of steel pipes	42.1	36.6
	Weight of coating	19.9	4.2
	Weight of content (MEG)	15.3	1.2
	Weight of termination heads	10.4	9.0
	Total weight of spools	88	51
Integrated cover	Weight of steel members	49.1	41.8
	GRP weight	11.2	3.4
	Additional weight <sup>(1)</sup>	2.2	2.0
	Additional weight <sup>(2)</sup>	5.0	4.4
	Total weight of cover	68	51
<b>Total static weight of system</b>		<b>155</b>	<b>103</b>

More details are given in *APPENDIX A*.

### Summary main results:

The main results from the static analysis are presented in this section. The hook load, center of gravity and relevant utilization ratios are illustrated for relevant load combinations in *table 4.5*. Be aware that the hook loads in this table is not the hook load that the crane wire should be designed for. The hook load represents the total force in the structure for each load case. The highest loading occurs in load case 115, dynamic lift in air which is the critical load case for the structural design. Maximum utilization ratios according to Eurocode 3 for spool and members in integrated cover are also presented in *table 4.5*, where the maximum utilized members are illustrated in *figure 4.11*.

Each load case has a different center of gravity (in y-direction) since the structural volumes are not evenly distributed resulting in changed COG due to buoyancy forces when the object enters the water. Center of gravity in x direction is always located at the lateral center due to structural symmetry (this is only true for the static loads).

Table 4.5: Summary of main results.

Load case	Description	hook load [kN]	Max utilization, spreader [-]	Max utilization, spool [-]	COG <sub>y</sub> [m]
100	Static lift in air	1523	0.32	0.37	8.84
101	Static lift in water	1014	0.20	0.29	8.64
<b>115</b>	<b>Dynamic lift in air</b>	<b>4085</b>	<b>0.82</b>	<b>0.79</b>	<b>9.03</b>
116	Dynamic lift in splash	3552	0.72	<b>0.84</b>	8.90
117	Dynamic lift submerged	3353	0.70	<b>0.84</b>	8.75

### Sling loads:

The sling loads are needed to design the wires and finding the minimum breaking load (MBL) for the wires. The load combinations are described in *section 4.1.4* where load combination 12x is the same as 11x, but without load and consequence factor since the rigging are designed with different design factors.

Load combinations 125 gives the critical values for sling and hook loads and should be used to calculate minimum breaking load (MBL) using *eq. (3.5)*. The crane wire should be determined based on the hook load divided by a skew load factor since change in distribution of sling loads does not have any impact on the crane wire tension. The limiting hook load is then 2193kN (2741kN/1.25), based on *table 4.6*.

Table 4.6: Sling loads.

Load case	hook load [kN]	Sling 900 [kN]	Sling 901 [kN]	Sling 902 [kN]	Sling 903 [kN]	Sling 904 [kN]	Sling 905 [kN]
100	1523	217	369	334	335	373	212
101	1014	147	250	216	216	252	144
115	4085	568	979	920	920	987	558
<b>125</b>	<b>2741</b>	<b>386</b>	<b>660</b>	<b>609</b>	<b>610</b>	<b>667</b>	<b>378</b>
126	2358	338	574	512	513	580	331
127	2241	325	552	478	478	558	319

## 4.2.2 Sensitivity analysis and hook positioning.

The center of gravity in the horizontal plane is the point where the weight of the structure seems to be concentrated. The hook must be placed right above the center of gravity in order to prevent the structure from tilting which happens if the vertical force due to the self-weight of the structure is located at a distance from the horizontal hook position.

As discussed in *section 4.1.5* the centers of gravity is obtained by considering the structure as a cantilever and divide the moment with the total weight of the structure for the relevant load case. The center of gravity can be confirmed in Staad.Pro by observing the deflection profile for the structure and graphically see that the structure does not tilt to either side (a small deviation in center of gravity results in significant visible tilting), or by checking the forces in the weak spring supports described in *section 4.3.1* which should be zero (or very close to zero) since they are not really a part of the structure.

In *table 4.5*, five different values for center of gravity are introduced. When the hook position is chosen, the following conditions must be satisfied:

- The utilization ratio for any structural part should not exceed the requirements given by the selected limit state (*section 3.2.5*)
- The tilt (structural displacement) must not be larger than what can be handled during all phases of the installation (lift onto deck (harbor), seafastening, lift of deck (offshore), seabed handling)

The utilization ratios for the most unwanted displacement of the hook are checked in the sensitivity analysis, and the tilt of the structure is considered for static lift in air and water.

### Sensitivity analysis:

The main reason that the center of gravity is considered important is because the hook node (where all slings are attached) will be placed at the estimated COG point. A sensitivity analysis is therefore performed to check the structural impact of a displacement in the hook position. The center of gravity is calculated with high precision with the method described in *section 4.1.5* and an inaccuracy factor for COG,  $\gamma_{COG}$  is introduced to account for uncertainties in the calculations. By assuming that the position of the center of gravity is known, the deviations obtained in the sensitivity analysis should reflect the impact of sling miss matches and fabrication tolerances which is represented by the skew load factor.

*APPENDIX B* considers hook displacement in all relevant directions in a hook-position envelope as illustrated in *figure 4.6*. The values are obtained by considering the static load case in air, (load case 100). It is found that movement towards point “1” (direction 1) gives the largest structural impact and that direction is therefore considered as a worst case approximation for the sensitivity analysis. Movement towards point “6” (direction 6) is considered to see how sensitive the structure is to different hook heights.

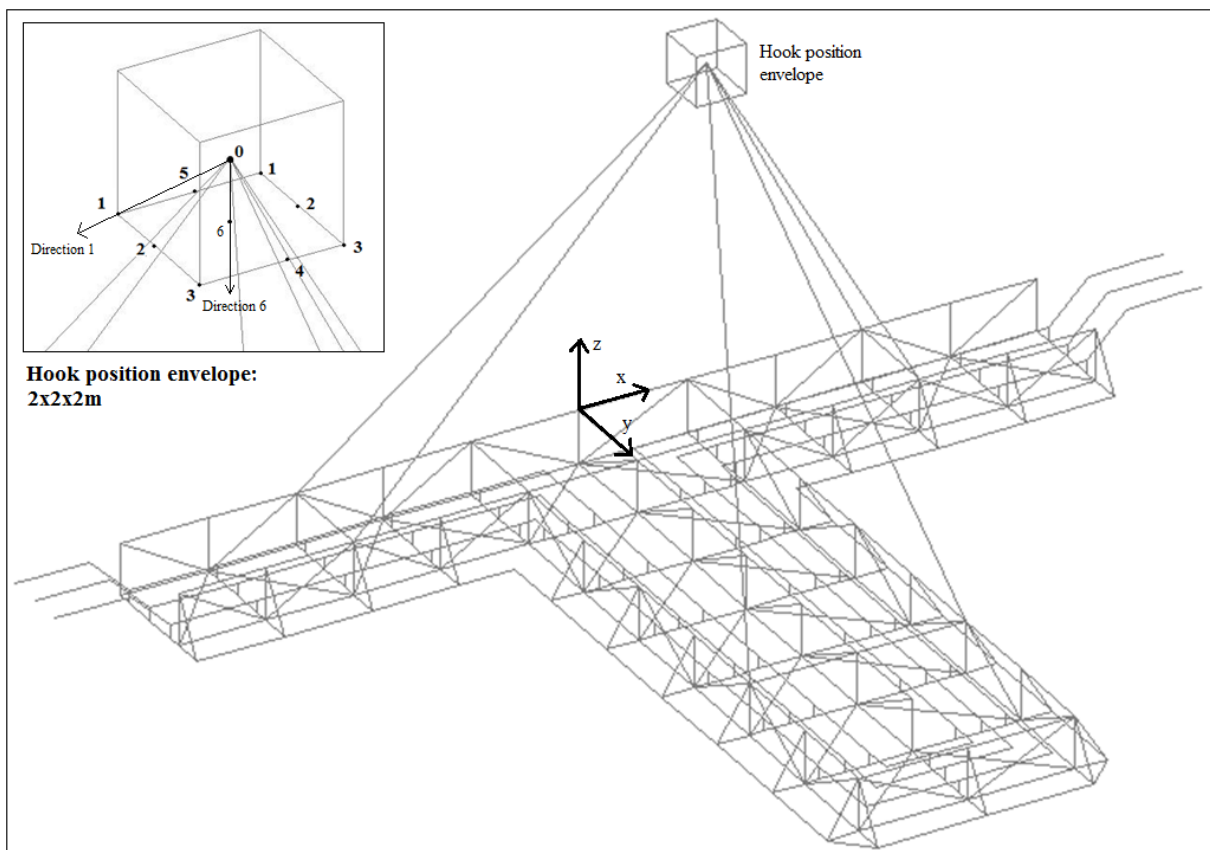


Figure 4.6: Hook position envelope.

In *APPENDIX B* the most utilized members, sling forces and sling length deviations are given for hook displacement to all (bottom) corners of the hook position envelope.

Figure 4.7 illustrates how much the utilization ratio changes for the most critical member in the structure (see APPENDIX B for more details) for hook displacement in “direction 1” and “direction 6”. The deviation reflects the relative structural impact in case of hook displacements in the chosen directions.

The skew load factor was chosen 1.25 which means that the structure is designed to tolerate a sling displacement that gives a 25% increase in utilization ratio for the structure (or structural beams). Figure 4.7 illustrates how much the hook position can be moved before the utilization is increased by 25% for relevant beams.

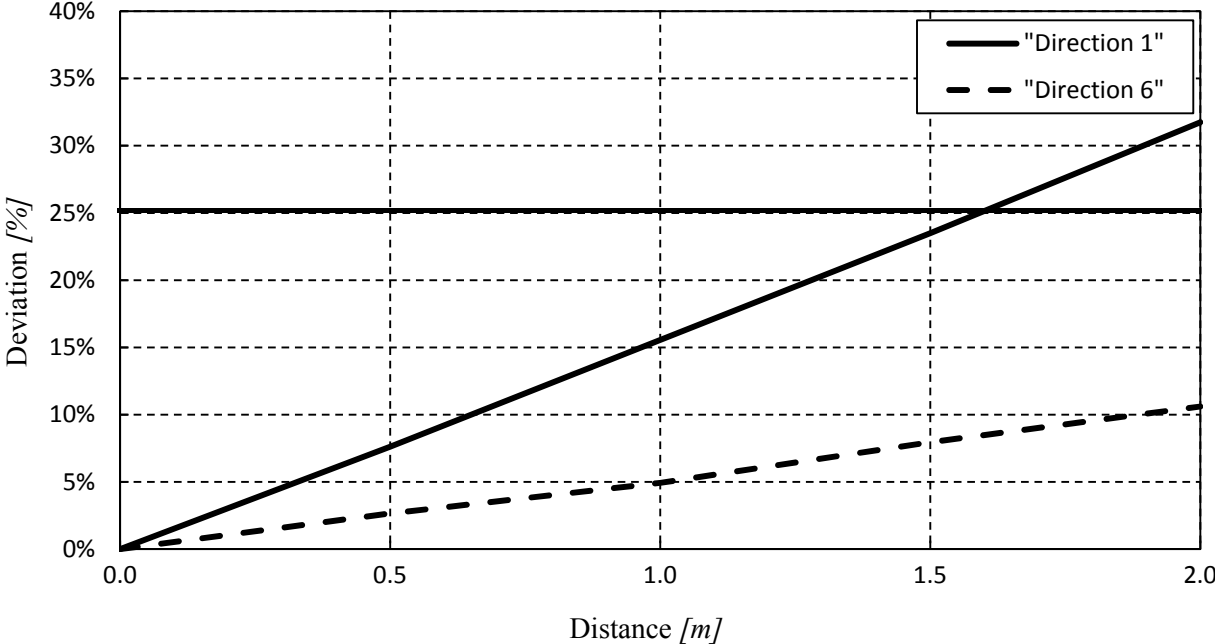


Figure 4.7. Change in utilization ratios due to movement of hook-position in “direction 1” and “direction 6”. The directions are illustrated in figure 4.5.

By observing figure 4.7, one can see that the hook can be displaced by approximately 1.7 meters without reaching the additional load that is accounted for by a skew load factor equal 1.25 for the structure in the most sensitive direction. At that point all slings are compressed between 1 % and 7%, (APPENDIX B) while the maximum tolerated sling elongation is 0.15%, (DNV (1996) 3.1.4.2). The sling displacement would never be this large making the skew load factor if 1.25 very conservative. The structural integrity of the structure is therefore verified even for large displacement of the hook position (1.7 meter) in the worst direction.

All sling lengths are elongated by more than |0.15%| at a hook displacement distance of 0.6 meter (see figure B.4) in “direction 1” (the worst direction of movement) giving a deviation in utilization ratio in max utilized member less than 10%. This means that the skew load factor can be chosen to 1.1 for the design. The structure will be designed with a skew load factor equal 1.25 for conservative design.

**Tilt of structure:**

When the hook position is located above the center of gravity, the horizontal distance between the vertical force and hook node is zero. If the hook position is moved or the center of gravity changes, the arm will differ from zero creating a momentum around the hook node causing the structure to tilt. The tilt of the structure depends on how the weight and volume is distributed over the structure. The structure will tilt as much as necessary for the new, rotated center of gravity to be exactly below the hook.

Figure 4.8 shows the relevant tilt in the y-z plane of the considered structure when the hook is placed above COG gravity in air and COG in water. The structure does not tilt in the x-z plane due to symmetry.

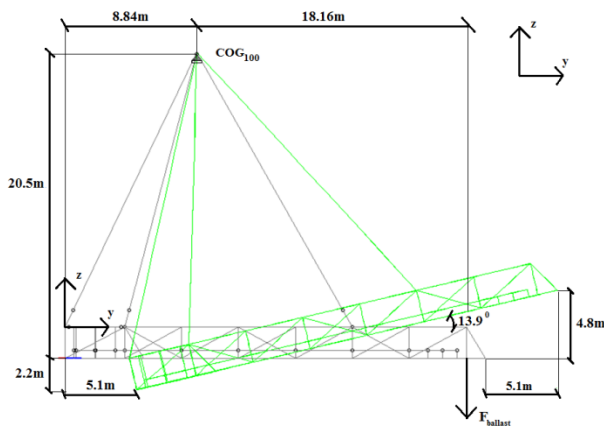


Figure 4.8. Lift in water when hook is placed above COG<sub>100</sub>, lift in air-

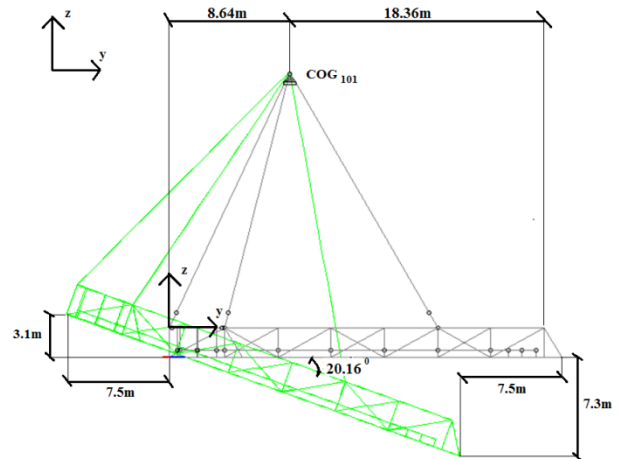


Figure 4.9. Lift in air when hook is placed above COG<sub>101</sub>, lift in water-

The utilization ratios for the structure shown in table 4.5 is calculated when the hook is placed above the center of gravity in air. When the hook node is moved above the center of gravity in water, the most utilized member shows little impact for any of the defined load cases making sure that requirement given by the selected limit state are not exceeded even when the structure experience large tilts as results of changes in the load distributions. This means that both choices of center of gravity are considered appropriate during deployment considering the structural integrity according to Staad.Pro.

Since the structural integrity for the deployment of the integrated spool cover is verified for both hook placements, other considerations are critical for determining the hook position. When the structure is lifted from harbor to the vessel in air, it's not acceptable to lift it with a vertical deflection of 7.3 meter as indicated in figure 4.9.

When the structure is fully submerged, the structure will tilt about 13.9 degrees as indicated in *figure 4.8*. This is not acceptable when the structure is placed at the sea bottom, and ballast should be attached to the structure to reduce the tilting angle. Necessary ballast can be calculated according to *eq. (4.4)*.

$$\begin{aligned}
 \sum M_{Hook} &= 0 \\
 \rightarrow F_{Hook} \cdot \Delta y_{Hook} + F_{z.ballast} \cdot \Delta y_{ballast} & \\
 \rightarrow F_{ballast} &= -F_{Hook} \cdot \frac{\Delta y_{Hook}}{\Delta y_{ballast}}
 \end{aligned} \tag{0.4}$$

Where  $F_{Hook}$  is the total hook load  $\Delta y_{hook}$  is the horizontal distance from the center of gravity to the hook,  $F_{z.ballast}$  is the weight of the needed ballast and  $\Delta y_{ballast}$  is the horizontal distance from the hook to the ballast.

$$\rightarrow F_{ballast} = -1014kN \cdot \frac{-0.2m}{18.16m} = 11.17kN = 1.14Te$$

In order to stabilize the structure in water, additional 1.14Te (submerged weight) is needed at a distance 18.16meter from the center of gravity as illustrated in *figure 4.8*.

#### **Hook position:**

The hook will be placed above the center of gravity at a height 20.5 meter above the bottom part of the structure. A low hook height gives small sling angles and larger horizontal force components in the slings resulting in larger strains in the framework structure. Since all structural loads are pointing in the vertical direction, the structure is designed to withstand mostly horizontal loading, and when larger horizontal forces are introduced, the structure will be subjected to larger axial compression and buckling effects. The maximum hook height is also limited by the crane limits and a sensitivity test is necessary to observe the structural impact of different hook heights as performed in *APPENDIX B* and is illustrated in *figure 4.7*.

As observed from *table 4.5*, the center of gravity will change in each load case and the hook position should be selected based on center of gravity in air where the COG of the object should be adjusted by adding ballast to the structure when it is submerged.

### 4.2.3 Buckling of main members

The buckling length of each member is calculated individually for local z and y axis for each member. In Staad.Pro this is done by applying the member length,  $L_{y/z}$  and  $k_{y/z}$  where the effective length is defined as  $L_{y/z} \cdot k_{y/z} = L_{y/z,eff}$ . The member lengths are chosen to be the total length of connected beams subjected to axial compression, which is the same as the distance between the sling connection points for e.g. “BEAM 1”, (see *figure 4.5*). If the reduction factor k is set to 1.0 the member and buckling lengths would be the same as for cylinders with pinned connections and no interaction effect. Since the concerned structure is a three dimensional structure with transverse members that reduces the lateral deflection of the main beams, the buckling check is performed as a parametric study where different buckling lengths are applied to obtain the largest buckling lengths that still satisfy the design criteria given by Eurocode 3. The concerned members are subjected to combined axial compression and bending force where the design criteria for the combined loading is given in Eurocode 3, ((2005) 6.3.3).

The concerned members are in general very long compared to cross sectional area (slender beams). If the beams defined in *figure 4.5* had buckling lengths equal the total compressed length while subjected to axial compression, all members would fail the design criteria in Eurocode 3 as shown in *table 4.7*. All beams connected to the considered chords in transverse direction “disturb” the bending moments reducing the distance between zero-moment points. Bending moment diagrams for each beam are given in *APPENDIX C* and should be compared to the effective buckling lengths that give acceptable utilization ratios in each beam.

From *table 4.4* applied buckling lengths and associated utilization ratios are given for “BEAM 1” to “BEAM 5” as they are illustrated in *figure 4.5*.



Table 4.7: Effective buckling lengths of main members versus utilization ratio for beams defined in *figure 4.5*.

Beam	Member length, $L_y=L_z$ [m]	Buckling factor, $k_y$ [-]	Buckling factor, $k_z$ [-]	Buckling length, $L_{y,eff}$ [m]	Buckling length, $L_{z,eff}$ [m]	Utilization ratio [-]
Beam 1	22.7	1.00	1.00	22.74	22.74	5.33
		0.90	0.90	20.47	20.47	4.38
		0.80	0.80	18.19	18.19	3.52
		0.70	0.70	15.92	15.92	2.76
		0.65	0.65	14.78	14.78	2.42
		<b>0.23</b>	<b>0.23</b>	<b>5.20</b>	<b>5.23</b>	<b>0.54</b>
Beam 2	15.7	1.00	1.00	15.71	15.71	1.09
		0.90	0.90	14.14	14.14	0.90
		<b>0.80</b>	<b>0.80</b>	<b>12.57</b>	<b>12.57</b>	<b>0.74</b>
Beam 3	29.8	1.00	1.00	29.77	29.77	10.91
		0.90	0.90	26.79	26.79	8.89
		0.80	0.80	23.82	23.82	7.07
		0.70	0.70	20.84	20.84	5.47
		0.65	0.65	19.35	19.35	4.75
		<b>0.1/0.2</b>	<b>0.2/0.3</b>	<b>3.51/7.03</b>	<b>5.21/7.81</b>	<b>0.81</b>
Beam 4	19.3	1.00	1.00	19.33	19.33	1.02
		0.90	0.90	17.40	17.40	0.85
		<b>0.80</b>	<b>0.80</b>	<b>15.46</b>	<b>15.46</b>	<b>0.70</b>
Beam 5	15.3	1.00	1.00	15.33	15.33	1.61
		0.90	0.90	13.80	13.80	1.33
		0.80	0.80	12.26	12.26	1.07
		0.70	0.70	10.73	10.73	0.84
		<b>0.65</b>	<b>0.65</b>	<b>9.96</b>	<b>9.96</b>	<b>0.74</b>

The most critical beams (“BEAM 1” and “BEAM 3”) show very large utilization ratios for effective buckling lengths larger than  $0.65L$  (applicable for fixed columns with fixed ends). To verify whether or not the beams can withstand relevant buckling loads, the largest distance between zero moments is considered as the true buckling length. This gives smaller values of buckling lengths due to the transverse beams in both vertical and lateral direction.

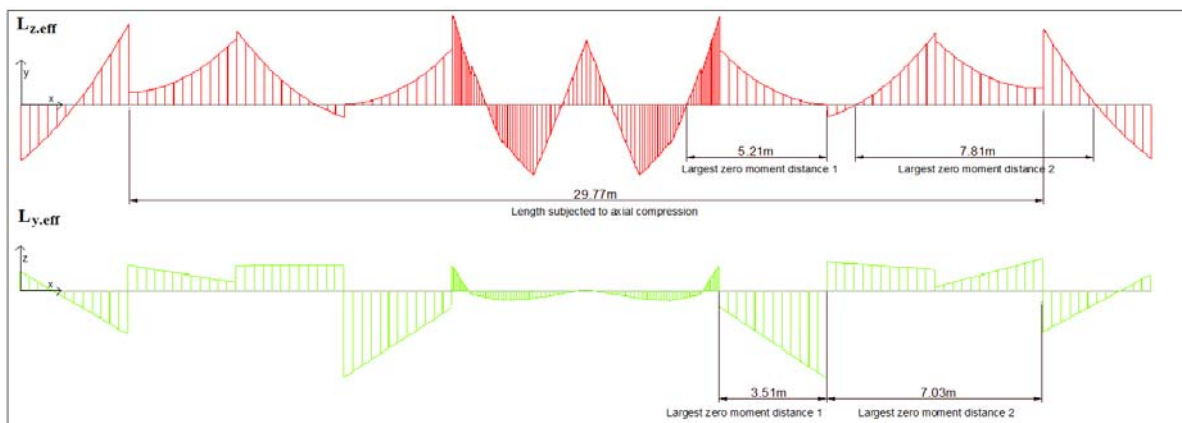


Figure 4.10: Bending moment diagrams, “BEAM 3”, in both y and z axis, (from Staad.Pro). Be aware that y is pointing upwards and z is pointing in lateral direction due to how the structure is defined in Staad.Pro.

The bending moment diagram in *figure 4.10* illustrates how the forces in the members behave when transverse members are welded to the chords. Each joint is represented by a visual “disturbance” in the moment diagrams. The bending moment diagrams shows moments around the transverse and vertical axes where the moments diagram goes from positive to negative and shows many visible peaks indicating that the equivalent effective buckling length is much less than the length of the beam. The reason why two “largest zero moment distances” were applied for “BEAM 3” (for each bending moment diagram), was because the mid-section of the beam are the most critical members in the structure (highest utilization ratio) requiring more detailed work to obtain a “realistic” rather than more conservative design. The buckling lengths of members in the mid-section are therefore chosen to be smaller than the outer part of the beam to obtain a “cheaper” design. The same procedure is applied on “BEAM 1” to reduce the buckling length to acceptable limits, (bending moment diagrams for BEAM 1 to BEAM 4 are illustrated in *APPENDIX C*).

**4.2.4 Max utilized member**

The combined results can quickly be observed in Staad.Pro using utilization ratio diagrams for members as illustrated in *figure 4.11*. The most utilized member (above chosen limits) is indicated in blue and red.

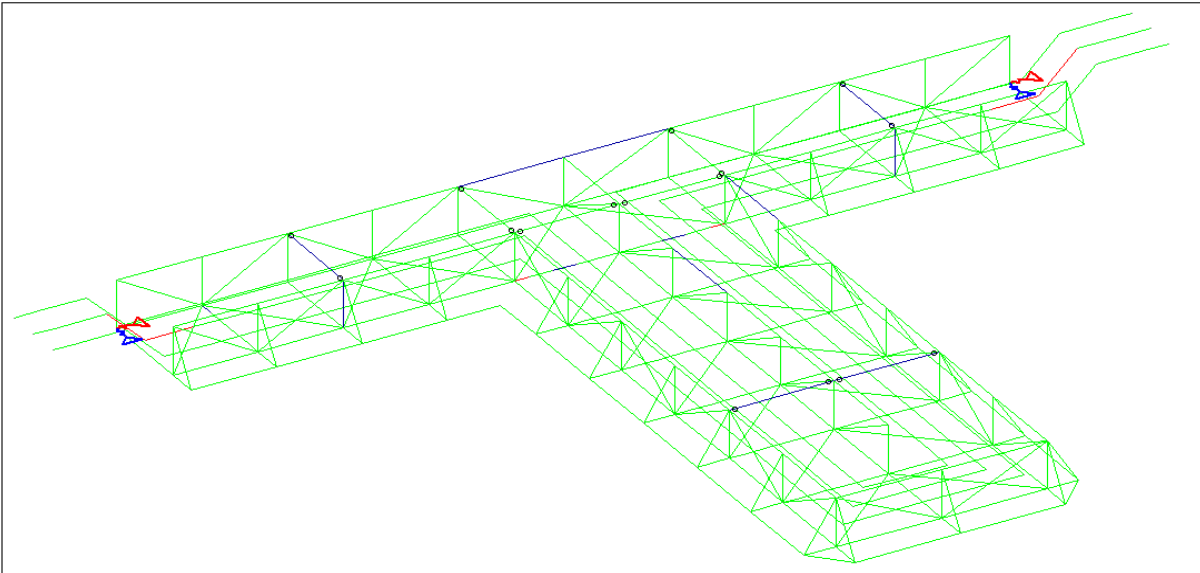


Figure 4.11: Eurocode 3 check. Utilization ratios > 0.8 are red, utilization ratios > 0.7 are blue. The red members represent the most utilized beams.

The most utilized member in the framework (indicated in red) is part of the earlier defined “BEAM 3” where the critical load is a result of combined case of bending and axial compression, (critical equation: Eurocode 3 (2005) 6.3.3). When the structure is checked according to Eurocode 3, each member is checked against all relevant formulas for the relevant load condition. A general approach that shows how steel members are designed according to Eurocode 3 is given in *APPENDIX D* where the structure is checked for global buckling and global yield.

The most utilized framework member has a utilization ratio of 81% due to buckling of members, and the most utilized spool has a utilization ratio of 84% due to the large weight of the termination heads. The design should be optimized with supports for the termination heads to reduce forces on the 8” goosenecks. The perforations of members are neglected in the analysis and the max utilization ratio should not be as large as 100%. Mark that only members with low utilization ratio should be perforated.

### 4.3 Global buckling

The structural integrity of the spool cover is checked according to Eurocode 3 for all load combinations in Staad.Pro as described in the previous sections. The software is capable of correctly distribute the loads over the structure and calculating local stresses in each member considering 13 sections along the beams and perform design checks on each of them. However, the software is not capable of controlling the global performance of the structure and the global buckling capacity of the structure need to be verified. The global performance is considered by observing the integrated spool cover as two structural beams.

The longest beam illustrated in *figure 4.13* will be checked for buckling using all necessary design checks according to Eurocode 3 in *APPENDIX D*. The “global beam” is considered as one beam with an equivalent cross section (*figure 4.12*) with equivalent loads (including inaccuracy, SKL factors and DAF from load case 115) as the structure is designed for.

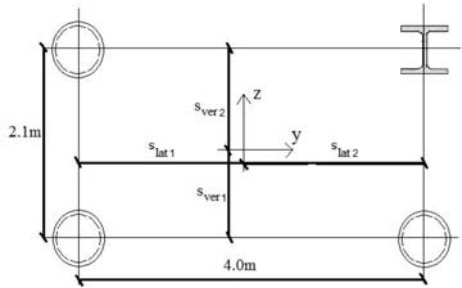


Figure 4.12: Simplified cross section of global beam. Conservatively, all transverse and vertical beams are not accounted for when obtaining equivalent cross-sectional properties.

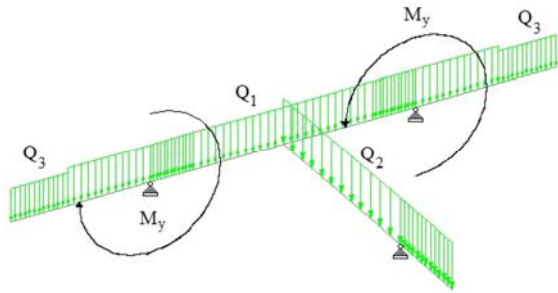


Figure 4.13: Staad.Pro model of simplified load case on global beams. This is necessary to obtain equivalent moment and shear force diagrams.

A lot of tasks are necessary to perform a global buckling check. The full procedure is performed and described in *APPENDIX D* with references to Eurocode 3. The following tasks need to be considered:

- Calculate equivalent cross sectional properties for the global beam. This includes area, area center, second moment of area and sectional modulus.
- Obtain global load picture on equivalent beam. This including uniform distributed weight of structure, eccentricity moments from sling loads and loads from “cantilever”. The loads are obtained by hand calculations or Staad.Pro.
- Find max bending moment and shear load by exposing the global beam to the obtained global load picture.
- Perform a global buckling check using Eurocode 3.
- Control general capacities of beam regarding axial, shear and bending force according to Eurocode 3.

Main results from the global buckling check from *APPENDIX D* are given in *table 4.8* represented by utilization ratios for each capacity check.

Table 4.8: Global capacities of the structure, (from *APPENDIX D*).

Description	Capacity	Utilization ratio
Beam capacity	Axial force capacity	0.042
	Shear force capacity	0.117
	Bending force capacity	0.173
	Bending and axial force capacity	0.278
Buckling capacity	Axial buckling capacity	0.042
	Bending and compression capacity	0.305
<b>Max utilization ratio</b>		<b>0.305</b>

When the structure is considered as a single beam with cross sectional properties as given in *figure 4.12*, the capacity of the structure was verified according to Eurocode 3 and the global buckling is not considered critical for the design. This is due to the relative large cross sectional size compared to the length of the structure (width=4.0m, height=2.1m, Length≈23m). Even if the 10'' tubular sections make a small total area, A, the moment of inertia, I, is considered large resulting in a large Euler buckling load (*figure 4.4*) representing the buckling capacity of the beam:

$$N_{Cr} = \frac{\pi^2 E \cdot I}{L_{eff}^2} \tag{4.5}$$

The equivalent beam is not considered slender and by observing the calculations in *APPENDIX D*, one can see that the utilization ratios with respect to general yield capacity and buckling capacity are within acceptable limits.

## 4.4 Summary, static analysis

The structural integrity of the integrated spool cover has been verified according to Eurocode 3 for all individual members as well as for the global structure when the structure is subjected to hydrodynamic forces represented by a dynamic amplification factor (DAF) of maximum 1.2 in air and 1.6 in water. The structure was checked using a LRFD (load and resistance factor design) approach where the design loads was obtained by multiplying static load (selfweigh) with relevant load factors, the SKF and the DAF. The design resistance where obtained by dividing with a material factor for all load cases

The applied inaccuracy factors are defined by DNV (DNV (1996) Pt.1 Ch.3 and Pt.2 Ch.5) and represents uncertainties in weight, COG, loads and consequence (based on redundancy). Additionally a skew load factor is needed to account for unwanted effects due to change in sling lengths. The factor was conservatively chosen to 1.25 as recommended by DNV (DNV (1996) Pt.2 Ch.5) for four point lifts. This factor was proven to be very conservative when performing a sensitivity analysis in *APPENDIX B*, illustrated in *section 4.2.2.1* and it was found that it can be reduced to 1.1, (the structure is conservatively designed for SKL-factor = 1.25).

Structural loads where calculated by assuming that all applied forces are evenly distributed over the mass of the structure. The self-weight of the structure is the only “physical” load applied, where all uncertainties and hydrodynamic forces is accounted for by using inaccuracy factors and DAF magnify the applied physical load to obtain the true load picture to represent the forces acting on the object when it is lowered through the splash zone. To verify that the loads can be represented by the dynamic amplification factor, a dynamic analysis is performed in *chapter 5* to confirm that the loads in any of the slings or crane wire doesn’t exceed the loads obtained from the static analysis.

Since the structure consists of slender cross sections, buckling of members has proven to be the most critical failure mode giving a utilization ratio of 0.8 for the most utilized member. The framework structure consist of main members (top and bottom chords) supported by transverse beams and braces supporting the chords. The interaction between members reduces the distance between zero moments in both top and bottom chords reducing the effective buckling length and increasing the maximum load that the structure can withstand. The eight temporary beams (as described in *section 3.3*) where therefore a necessary part of the design since they provided structural stability by reducing the effective buckling length.

During deployment, the center of gravity of the structure will change (considerably) since the volume versus mass ratio is not evenly distributed over the structure. If the structure is lifted horizontally into the water, the change in COG results in large inclination of the structure (about 4 meter) when the structure is fully submerged due to the static load condition. This is not acceptable when the structure should be placed horizontally on the seabottom and should be solved by attaching ballast to the structure after submergence.

When the structural integrity of the structure is verified, the most important data that is the sling loads and hook loads (for both static and dynamic load cases) which represent the load distributions in the structure and must be compared to the “real” loads obtained from a dynamic analysis performed in *chapter 5*.

#### 4.4.1 Further work:

The structure was designed using tubular cross sections which are characterized by low weight and high capacity with respect to compressive load and end moments. The disadvantage of using tubular members is fabrication difficulties where the ends of braces and transverse beams should be shaped to fit the circular main beams to ensure proper, fixed connection when they are welded together. If all members were rectangular hollow sections (RHS) the end fittings are only a matter of angles and could be cut straight off making it easy to handle the (~200) members that must be welded to make the complex framework structure.

Staad.Pro is capable of calculating stresses along the members (including at the end of members), but does not automatically check the joint capacities. To verify the structural integrity of the framework, a thorough joint check should be included in the full report. The most loaded symmetric and asymmetric joints must be checked according to Eurocode 3 (1-8, design of joints) ensuring that the connection between members is not overloaded. This should be done by manual hand calculations or using other finite element program like ANSYS where reported loads from Staad.Pro are applied on the considered joints. If the joints are overloaded they can be reinforced with plates or specially made supporters. It would be much easier to reinforce rectangular members rather than tubular members.

The temporary beams (described in *section 3.3*) should be connected to the main members with rigid connections and at the same time be detachable. The properties of such connections should be more thoroughly analyzed in the full structural report. The subsea lift of the integrated spool cover involves deformations in the structure that affects the opening mechanism of the GRP lids and the connections between temporary beams. These mechanisms should be studied in a finite element program like ANSYS where forces and deformations are considered with care.

## Chapter 5

### DYNAMIC LIFTING ANALYSIS

To confirm that the hydrodynamic loading doesn't exceed the applied load in the static analysis, the structure is checked in OrcaFlex where hydrodynamic loads are applied to represent the real loads that the structure is subjected to during deployment. The main goal is to find the largest waves that the structure can withstand during the deployment without being subjected to larger loads than the lifted object can withstand.

#### 5.1 Design criteria

The structural integrity has been verified in Staad.Pro using a dynamic amplification factor to account for hydrodynamic forces during the subsea lifting operation. In order to confirm that the true loads don't exceed the assumed hydrodynamic contributions, they are compared with dynamic forces obtained in OrcaFlex. The acceptance criteria is defined according to DNV (RP-H103 (2012) 4.4).

##### 5.1.1 Acceptance criteria, DNV

The main focus of the dynamic analysis in OrcaFlex is to ensure that the maximum and minimum sling and crane wire loads are within acceptable limits, (Subsea 7, (2011) 5.6). To ensure that:

- Slack doesn't occur in slings or crane wire.
- The integrated spool cover, slings, crane wire and spool is not overloaded.
- The crane capacity is not exceeded for the operating crane radius.

##### **The slack sling criterion, (DNV-RP-H103 (2012) 4.4.3):**

When the structure is lifted through the splash zone it is subjected to large hydrodynamic forces that can result in unwanted effects as slack slings or slack crane wire. If the tension in either slings or crane wire (at any given time) is zero, the lifted object will experience snap loads (impact loads) which results in local forces in critical connection point which is not covered by the static analysis in the ultimate limit state. The following criterion should be fulfilled to ensure that snap loads are avoided in slings and crane wire:

$$F_{\min} \geq 0.1F_{\text{static.min}} \quad (5.1)$$

Where  $F_{\min}$  is the minimum dynamic load in the considered wire and  $F_{\text{static.min}}$  is the force in the considered wire when the structure is submerged, but the flooding has not yet started. The "lower limit" of the loads in slings and crane wire is defined as:

$$\text{Lower limit} = 0.1F_{\text{static.min}} \quad (5.2)$$

If the total load never gets lower than this limit, the structure will not experience forces that give slack slings or crane wire.

#### Capacity check, (DNV-RP-H103 (2012) 4.4.4):

The structure is checked according to Eurocode 3 in Staad.Pro ensuring that all members can withstand the structural loads including design factors and a dynamic amplification factor. The static dynamic amplification factor in air was according to DNV (1996) 1.2. The converted dynamic amplification factor,  $DAF_{dynamic}$  (eq. (5.3)), should not exceed this value:

$$DAF_{dynamic} \leq DAF_{static} \quad (5.3)$$

The converted dynamic amplification,  $DAF_{dynamic}$  (valid for lift in air) can be described as eq. (5.4), (DNV-RP-H103 (2012) 4.4.4.3).

$$DAF_{dynamic} = \frac{F_{max}}{Mg} \quad (5.4)$$

Where  $F_{max}$  is the maximum dynamic load in the considered wire,  $M$  is the weight of the structure in air and  $g$  is the gravity constant. Based on eq. (5.3) and eq. (5.4) “the upper limit” of total loads in each sling and crane wire is defined as:

$$Upper\ limit = DAF_{static} \cdot Mg \quad (5.5)$$

If the tension in all wires never exceeds this limit, the structure will not experience forces that compromise the static design criteria based on Eurocode 3.

#### 5.1.2 Time domain analysis

The dynamic forces should be obtained using a non-linear time domain simulation when considering lifting analysis of complex structures. DNV recommends that the lifted object should be fixed in selected positions in simulations of minimum 30 minutes, (DNV-RP-H103 (2012) 3.4.3.7).

The largest and smallest loads in all slings and crane wires are stated and checked according to the design criteria. These values are considered conservative and represent the expected maximum values for the lifting operation, (DNV-RP-H103 (2012) 3.4.3.4).

Assuming that the dynamic loads can be Rayleigh distributed, the most probable maximum dynamic force in slings and crane wire,  $R_{max}$ , may be found by the following relation, (DNV-RP-H103 (2012) 3.4.3.5):

$$R_{max} = \sigma_r \sqrt{2 \ln \left( \frac{t}{T_z} \right)} \quad (5.6)$$

Where  $\sigma_r$  is the standard deviation of the dynamic load,  $t$  is the duration of the operation including contingency time (contingency time, is time due to unforeseen events) which should be minimum 30 minutes and  $T_z$  is the zero up-crossing period. The maximum and minimum dynamic loads are obtained by:

$$F_{max/min} = F_{static} + /- R_{max} \quad (5.7)$$

To obtain realistic design values for the dynamic lifting operation, the expected maximum and most probable maximum values are compared.



## 5.2 Dynamic analysis, preprocessing

OrcaFlex is a marine dynamics program developed by Orcina for static and dynamic analysis of offshore systems, including all types of marine risers, global analysis, moorings, installation and towed systems. OrcaFlex is a 3D non-linear time domain finite element program capable of dealing with large deflection and structural flexibility of structures (OrcaFlex (2012) p.11)

To perform a dynamic lifting analysis of comprehensive framework structures the following steps is necessary before obtaining the results:

- Make a simplified model of the structure with the same properties as the real structure: In this thesis, the simplification is done by creating the main substructure while excluding several members and structural details. Normally this would be done by senior engineer where the full structure is represented by a few members representing the same behavior (inertia, stiffness, etc.) as the “real structure”.
- Import vessel data: Import a vessel model with correct response data for the concerned ship.
- Defining section properties: In case of tubular sections, the inner and outer diameter is defined for each member, (designed as lines in OrcaFlex).
- Defining material properties: Selecting E-modulus, poisson ratio, density, stiffness (axial, bending and torsional) coefficient for materials.
- Define properties for slings, crane wire and hook: Weight and axial stiffness is applied.
- Environmental conditions: Define wave type (JONSWAP),  $H_s$ ,  $T_z$ , direction of wave heading and spectral parameters.
- Hydrodynamic coefficients: The added mass, inertia, drag and slam coefficients is defined for normal and axial direction. Be aware that the factors changes based on level of submergence, member size and environmental data and must be defined for each considered case.

The data is described by using the user interface in OrcaFlex.

## 5.2.1 Main assumptions

The hydrodynamic forces on the lifted object are obtained by finding the sum of contributions from individual structural members. While the structure is lifted through the splash zone, the water will be disturbed causing local disturbance in the fluid. The interaction between fluid and body is well described for simple objects (e.g. cylinders), but if the object is a complex framework structure, the flow interaction will affect the other members of the structure changing the force contribution from inertia, drag and slam (described in *chapter 2*). By calculating the hydrodynamic forces as the sum of force contributions from individual structural members, the interaction effect is neglected. This assumption is justified if the lifted object is considered an open structure where the solid projected area normal to the direction of motion is less than 50% of the silhouetted area, as is the case for the concerned structure (see *APPENDIX G*), (DNV-RP.H103 (2012) 3.3.3.3). OrcaFlex is able to handle structural deformations where the stiffness of each member is defined according to cross sectional properties.

The motion of the crane tip (the top of the crane wire) is assumed fixed relative to the vessel motion. This means that the stiffness and active heave compensating effects in the crane is neglected, resulting in increased vertical motion and dynamic forces on the lifted object. The dynamic simulations are performed when the structure is locked in specific submergence heights and the effect of the winch speed is assumed included in the crane tip motion. Any pendulum motion that the lifted object might have before or during first impact with the oscillating sea is not considered in this thesis.

Hydrodynamic loads on all members are calculated according to the modified Morison equation (*eq. (5.8)*) where the combined force is given as a linear superposition of drag and inertia force proportional to the relative acceleration and squared velocity respectively. The Morison equation is applicable for small volume structures where  $D < \lambda/5$ .

$$F_{Morison} = V_S \rho \dot{v}_3 + A_{33} (\dot{v}_3 - \ddot{\eta}) + 0.5 \rho C_D A_p (v_3 - \dot{\eta}) |v_3 - \dot{\eta}| \quad (5.8)$$

Where  $\rho$  the fluid density,  $V_S$  is the submerged volume,  $\dot{v}_3$  is the vertical fluid acceleration,  $v_3$  is the vertical fluid velocity,  $A_p$  is the projected area normal to the flow direction,  $A_{33}$  is the added mass,  $C_D$  is the drag coefficient and  $\dot{\eta}, \ddot{\eta}$  is the objects velocity and acceleration respectively, (OrcaFlex (2012) 5.10.5).

The environmental forces is represented by a sea state characterized by the JONSWAP spectra with average spectral parameters from DNV (RP-C205 (2010) 3.5.5.2) defined by a significant wave height,  $H_S$  and a zero up crossing period,  $T_Z$  in OrcaFlex.

The lifted object is modeled using the “line function” in OrcaFlex. The “lines” are mainly used for dynamic analysis of flexible risers, pipes and cables which are not exposed to slam forces since they easily penetrate the sea-surface with negligible impact force. The considered structure consists of about 100 horizontal “lines” and the slam contribution cannot be neglected when the structure is located in the splash zone. Since both slam and drag is proportional to the squared relative velocity between object and the fluid velocity (sea-surface velocity in case of slam), the combined effect of drag and slam can be included in one factor, (see the discussion in *section 2.3.3*). Slam is typically a short-duration phenomenon, sensitive to precise local condition at the time the object enters the water, (OrcaFlex (2013) 5.13.5). By assuming that the drag coefficient is increased to an idealized coefficient;  $C_S + C_D$ , the slam force will also be present when the cylinder is submerged, increasing the total force on the lifted object.

The hydrodynamic coefficients for inertia, drag and slam in the splash zone can be calculated as functions of submerged level  $h$ , where  $h$  is the distance from the still-water level to the center of the cylinders. To obtain the theoretical values for slam and experimental values for added mass in *section 2.3*, varying distance from the oscillating sea-surface to cylinder center,  $h_s$ , where needed, but the average value of  $h_s$  is  $h$  (see *figure 2.2* for illustration) justifying the decision of setting  $h=h_s$ . The hydrodynamic coefficient for inclined cylinders will be chosen as the largest value obtained with changing height (assuming they can be calculated as horizontal cylinders), and hydrodynamic coefficients for vertical cylinders will be chosen to the lowest value over the length since the force contribution from the vertical cylinders are considered smaller in lifting operations.

Force contributions in axial direction of all cylinders are mainly due to friction. Since all cylinders are newly painted and are considered as smooth, the hydrodynamic coefficient in axial direction is set to zero in OrcaFlex. The inertia coefficient is set to 1.0 in axial direction to account for motions of structural weight (no added mass).

The forces on the “real structure” is be obtained with a scale factor that is obtained assuming that the hydrodynamic forces are proportional to the largest relative increase in mass or solid projected area with respect to the simplified model. The assumption is appropriate since the simplified model has the same structural properties as the “real structure” with less structural members. The increased ratio between solid and silhouetted is 53% (*APPENDIX G*) and the increased mass is 62% and the design hydrodynamic force should therefore be 62% larger than the limiting hydrodynamic force.

## 5.2.2 Simplified model

The simplified model can be defined in various ways. An experienced engineer would have defined a simple structure consisting of a few beams (where the real framework consists of about 200 members), where the inertia, stiffness and hydrodynamic properties for the whole structure is represented by the very simplified structure. Due to lack of experience, the simplified structure is created with the same members and individual properties as the real structure, where the simplification is done by reducing number of members.

When defining the simplified structure, the similarities with real and simplified structure is limited by OrcaFlex's capabilities of iterate to obtain the static equilibrium (which is necessary to perform the dynamic analysis) of the structure and associated members. The framework's ability to converge is mainly based on the flexibility of the structure (deformation, etc.), connection properties (all are fixed connections) and number of connections, which is why the complexity of the structure is restricted by number of members.

### Creating the framework structure in OrcaFlex

The considered structure consists of mainly tubular sections so that all members are defined as lines with a given density, outer diameter, inner diameter and hydrodynamic coefficients. OrcaFlex is then capable of calculating the stiffness, mass and contact area (for hydrodynamic interaction) of each member. If other cross sectional properties is chosen, those properties can be defined manually while the members are represented by tubular sections in the model. The line types that are used in the structure (spools and different sized members) are defined before the geometry of the structure. If members with same size (e.g. top and bottom chords in the relevant structure) are located at different height, two line types should be defined for the same cross section since the hydrodynamic properties changes with depth and angle of each member. The hydrodynamic properties (drag, slam, added mass and inertia coefficient) differ for different level of submergence and are defined for each relevant line-type.

Each member is defined as a line with individual length and end orientation which are defined manually. The members are connected by creating 6D buoys with negligible properties (so that the position of each node after deformations and structural displacement are taken into account when the hydrodynamic forces are applied) where each member are connected to the associated 6D buoys. To create fixed connections, the end orientations need to be specified making sure that the local z axis is pointing along the lines which are defined individually for each member. If the default values are used, the end orientation will point in the same direction as the global axes and will be free to rotate in the xy-plane. Additionally the rotational stiffness of each end is set to infinity to simulate clamped ends, (OrcaFlex (2012) 5.12.17). This is a time consuming task and is not recommended to use when modeling complex structures such as this (talking with experience). *Figure 5.1 to figure 5.4* illustrates the process of defining end orientations and geometry, where the nodes (marked as red) are the negligible 6D buoys connecting the members.

The geometry of the spools are created the same way as the framework, but since they are placed above the bottom members of the framework they are connected to the 6D buoy nodes associated with the bottom members. From *figure 5.5* and *figure 5.6* the spools are illustrated where the spool nodes are connected to the closest associated 6D buoy at about 700 mm distance from the spools.

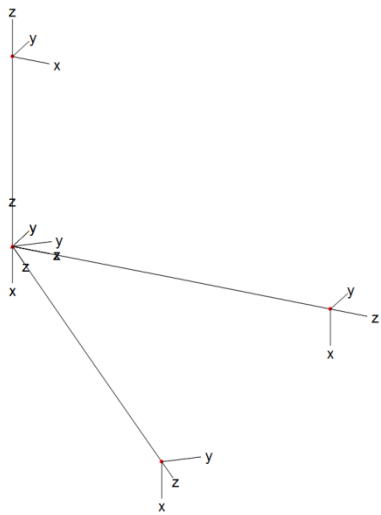


Figure 5.1: Connection with defined end orientation for members.

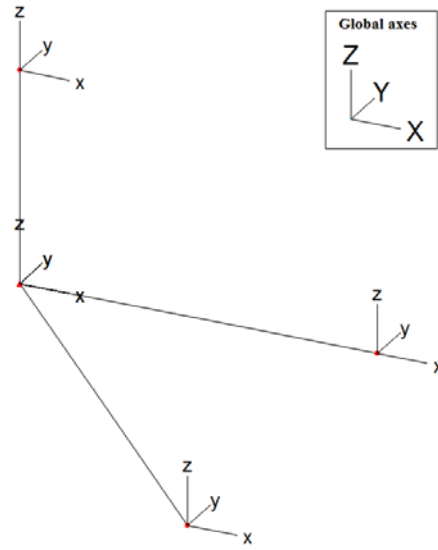


Figure 5.2: Connection with default end orientation for members.

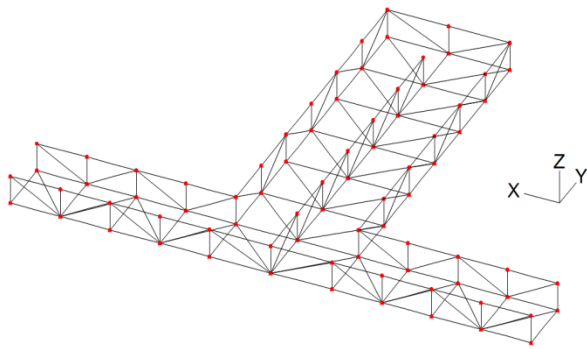


Figure 5.3: Framework model made in OrcaFlex.

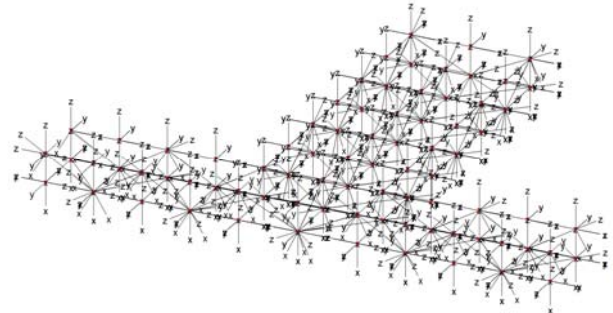


Figure 5.4: Framework model with defined end orientation for each member.

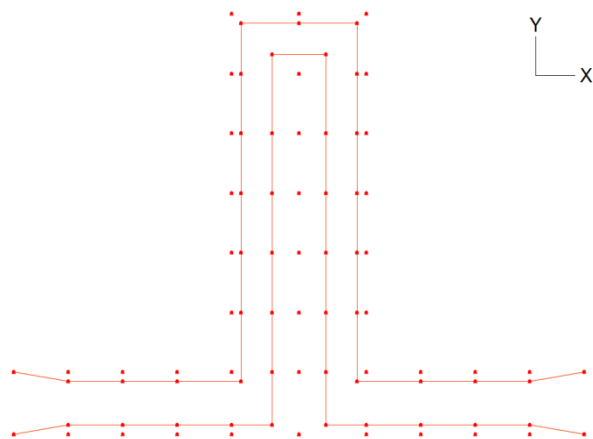


Figure 5.5: Spools, yx-plane.

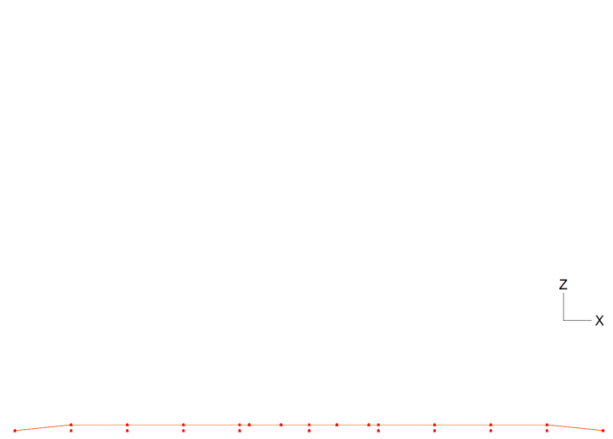


Figure 5.6: Spools, zx-plane

The slings are defined with default end orientations (made free to rotate) at the connection points defined in the static analysis. The properties of the slings and crane wire are obtained based on minimum breaking load from the static analysis (*table 4.6 in eq. (3.5)*) and are collected from Redaelli, (Redaelli tecna (2012)). The properties of the wireropes are defined in *table 5.4* and applied in OrcaFlex.

Table 5.1: Sling wire and crane wire stiffness, (Redaelli tecna (2012))

Description	Coefficient	Value	Unit
Minimum breaking load, galvanised slings	$MBL_{\text{sling}}$	2080	$kN$
Diameter, slings	$\phi_{\text{sling}}$	52	$mm$
Cross sectional area, slings	$A_{\text{sling}}$	1300	$mm^2$
Module of elasticity, slings	$E_{\text{sling}}$	110	$kN/mm^2$
Axial stiffness of slings ( $k=EA$ )	$k_{\text{sling}}$	143000	$kN$
Mass in air, slings	$W_{\text{sling}}$	11.4	$kg/m$
Minimum breaking load, crane wire	$MBL_{\text{crane wire}}$	6280	$kN$
Diameter, crane wire	$\phi_{\text{crane wire}}$	92	$mm$
Cross sectional area, slings	$A_{\text{crane wire}}$	4920	$mm^2$
Module of elasticity, slings	$E_{\text{crane wire}}$	130	$kN/mm^2$
Axial stiffness of crane wire ( $k=EA$ )	$k_{\text{crane wire}}$	639600	$kN$
Mass in air, crane wire	$W_{\text{crane wire}}$	41	$kg/m$

### 5.2.3 Static analysis

The objective of the static analysis is to determine the equilibrium configurations of the system for the given weight, buoyancy, hydrodynamic drag. The static equilibrium provides a starting configuration for dynamic simulation. (OrcaFlex (2012) 5.5).

#### Simplified model

After many tries of trial and errors, the OrcaFlex model was able to iterate, and the static analysis was successful, and the force distributions could be compared to the static analysis. To obtain the static equilibrium the model was simplified, and the following structural parts or members were not included in the model:

- Side trawlboards.
- The 8'' spool.
- Goosenecks of all spools.
- Temporary transverse beams at the top of the structure.
- Additional weight from GRP-protection cover and rigging.

The hook position relative to the object was obtained by creating a Staad.Pro model with the same geometry as the OrcaFlex model using the same procedure as described in *section 4.1.5*.

In order to verify the force distribution in the OrcaFlex model it was compared to the simplified Staad.Pro model. The force distribution in the structure is represented by the forces in each sling and the crane wire. *Figure 5.7* and *figure 5.8* shows that the simplified model in Staad.Pro and OrcaFlex have the same geometry.

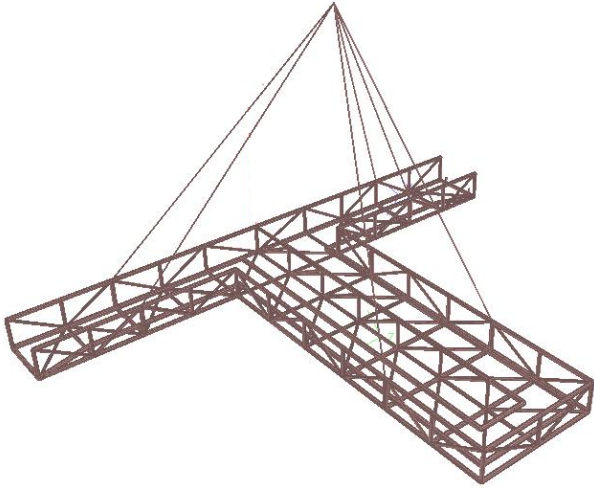


Figure 5.7: Staad.Pro model of structure.

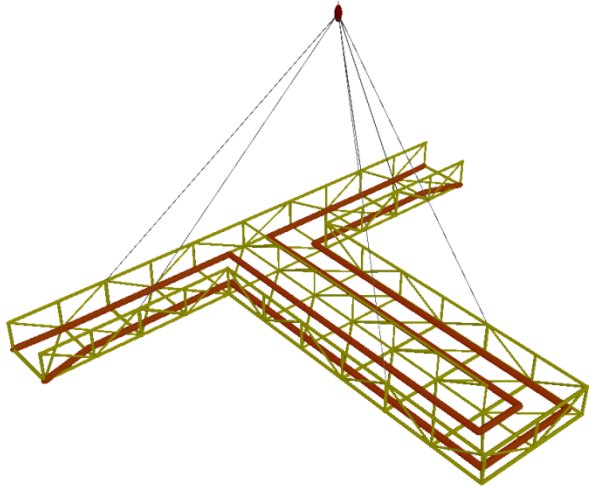


Figure 5.8: OrcaFlex model of structure.

**Verify static results**

It is important that the static results in OrcaFlex are the same as the corresponding Staad.Pro results. The force distribution in the model is checked by comparing the sling and crane wire forces in both models.

Table 5.2: Deviation in static load in OrcaFlex and Staad.Pro model.

Load case	hook load [kN]	Sling 900 [kN]	Sling 901 [kN]	Sling 902 [kN]	Sling 903 [kN]	Sling 904 [kN]	Sling 905 [kN]
100 <sub>Staad.Pro</sub>	935	152	177	236	236	177	152
100 <sub>Orcaflex</sub>	934	151	176	234	234	176	151
Deviation [%]	0.1 %	0.6 %	0.6 %	0.9 %	0.9 %	0.6 %	0.6 %
101 <sub>Staad.Pro</sub>	634	104	121	158	158	121	104
101 <sub>Orcaflex</sub>	632	102	122	156	156	122	102
Deviation [%]	0.3 %	1.8 %	-0.7 %	1.1 %	1.1 %	-0.7 %	1.8 %

When comparing the sling forces from Staad.Pro and OrcaFlex, the deviation between the sling forces in both air and water was remarkably low proving that the OrcaFlex model is applicable to obtain values for dynamic sling loads for the simplified structure. The weight of the “real structure” in air and water was obtained as 1520kN and 1005kN respectively in the static analysis, (*table 4.5*) meaning that the simplified structure weighs 60% of the real structure due to the necessary simplifications.

## 5.2.4 Vessel properties

The vessel used in the operation is Skandi Acergy (*figure 5.10*) which is a class-leading construction and flexlay vessel. The vessel has a huge deck area (2 100 m<sup>2</sup>) and a crane with a lifting capacity of 400Te and active heave compensator, (Skandi Acergy (2012)). The active heave compensator is employed to reduce the vertical motion of the lifted equipment, reducing dynamic loads in the hoisting wire system by using winches that control the payout length of the winch line, (Kim et. al (2013)).

The wave direction with respect to the vessel and the horizontal crane tip position is illustrated in *figure 5.9*. The crane tip is located at 33.9meter height above the still water level.

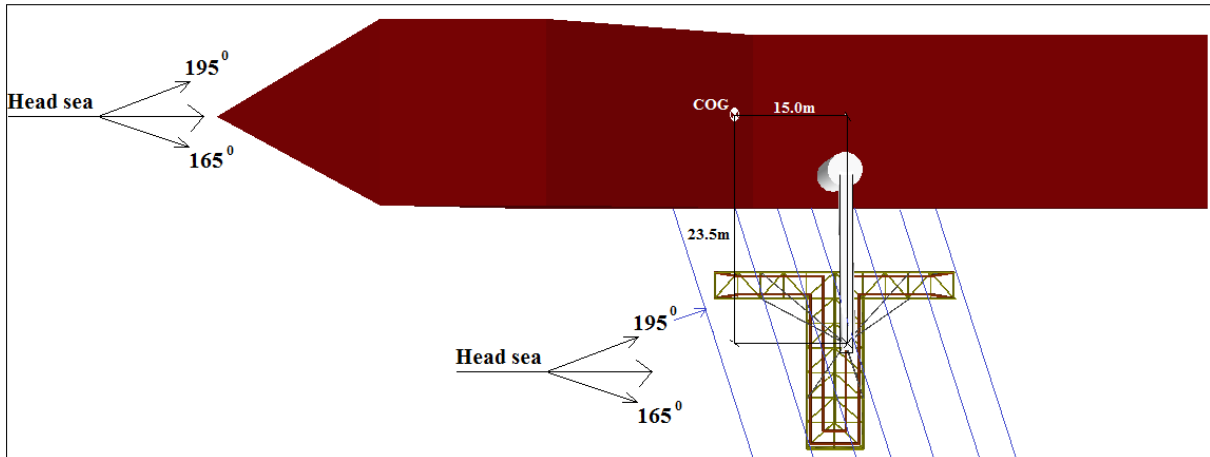


Figure 5.9: Crane tip position and wave headings.



Figure 5.10: Skandi Acergy, (Subsea 7 (2012)).



## 5.2.5 Environmental data

The hydrodynamic forces in subsea lifting operations are represented by the environmental data that is inserted in OrcaFlex. The structure will be installed in the real sea where the waves are defined as irregular and random in shape, height, length and speed. OrcaFlex is capable of creating random wave models that defines a given sea state specified by a wave frequency spectrum with a given significant wave height,  $H_s$  (mean wave height of the highest third of the waves), a peak period,  $T_p$  (defines the wave period that represent the waves with largest energy) a mean direction,  $\beta$ , and a spreading function, (DNV-RP-C205 (2010) 3.1.1). The irregular sea will be defined by the JONSWAP (Joint North Sea Wave Project) spectrum, where  $H_s$ ,  $T_p$  and additional spectral parameters are inserted in OrcaFlex to represent the real sea, (DNV-RP-C205 (2010) 3.5.5).

In the analysis the wave spreading is conservatively chosen to zero, so that all waves are approaching from the same angle,  $\beta$ . If the waves are coming from more than one direction, the waves would “neutralize” each other, reducing the impact on the lifted structure during deployment. The subsea lifting analysis will be performed for wave directions  $\pm 15^\circ$ , (DNV-RP-H103 (2012) 4.3.3.7).

Table 5.5 summarizes the properties needed to define a random wave model in OrcaFlex where the wave heights between 1.5 and 3.0 meter are considered for the analysis. Significant wave heights less than 1.5 meters are very seldom present in the North Sea and the operations are normally limited by 3.0 meter significant wave height, (Subsea 7 (2011) 5.4.1).

Table 5.3: Wave properties with relevant references, applied in OrcaFlex.

Description	Coefficient	Value	Unit	Reference
Significant wave height	$H_s$	1.5 - 3.0	<i>m</i>	
Zero up crossing period	$T_z$	3.5 - 13.0	<i>s</i>	DNV-RP-H103 (3.4.2.22)
Wave direction	$\beta$	165 - 195	<i>deg</i>	DNV-RP-H103 (4.3.3.7)
Number of wave directions		1	-	
Peak shape parameter <sup>(1)</sup>	$\gamma$	3.3	-	DNV-RP-C205 (3.5.5.2)
Spectral width parameter <sup>(1)</sup>	$\sigma_a$	0.07	-	DNV-RP-C205 (3.5.5.2)
Spectral width parameter <sup>(1)</sup>	$\sigma_b$	0.09	-	DNV-RP-C205 (3.5.5.2)
Peak period	$T_p$	4.5 - 16.7	<i>s</i>	DNV-RP-C205 (3.5.5.4)
Wave components (default)		100	-	

Note that the spectral parameters are the average values of the JONSWAP experimental data which are applicable for the North Sea environment, (Chakrabarti (2005) p. 112). The zero up-crossing period,  $T_z$  is the average time between successive crossings of mean water level in an upward direction. The zero up crossing period should be in the range of, (DNV-RP-H103 (2012)):

$$8.9\sqrt{\frac{H_s}{g}} \leq T_z \leq 13 \quad (5.9)$$

When using the JONSWAP spectrum to define the sea, the relation between the zero up-crossing period and the peak period is according to DNV (RP-C205 (2010) 3.5.5.4);

$$\frac{T_z}{T_p} = 0.6673 + 0.05037\gamma - 0.006230\gamma^2 + 0.0003341\gamma^3 \quad (5.10)$$

After the structure is analyzed and a limiting wave height is defined (the largest  $H_S$  the structure can withstand without exceeding the static loading as defined in *chapter 4*), the structure can be installed in weather forecasted significant wave heights reduced by an alpha factor as defined in DNV (OS-H101 (2011) B 700):

$$H_{S.WF} = \alpha \cdot H_{S.LIM} \quad (5.11)$$

Where  $H_{S.WF}$  is the wave height obtained from the weather forecast for the installation period.  $H_{S.LIM}$  is the limiting wave height for the marine operation and  $\alpha$  is the alpha factor defined DNV (OS-H101 (2011) B 700) to take care of uncertainties in the weather forecast. In this thesis only the  $H_{S.LIM}$  is considered and the alpha factor must be taken into account before the installation. The alpha factor is dependent on the time it takes to perform the operation where lower operation time results in higher  $H_{S.WF}$ .

### 5.2.6 Simplified time domain analysis

To perform a full dynamic analysis and verify that the lifted object can withstand the dynamic loads from a certain  $H_S$ , the dynamic simulation must be run for different level of submergence,  $h_B$ , considering different wave directions,  $\beta$  for all relevant zero up crossing periods,  $T_Z$  relevant for the given significant wave height (in case of  $H_S=1.5\text{m}$ ,  $3.5\text{s}<T_Z<13\text{s}$ ). If one were to perform a dynamic analysis for 4 different  $H_S$  (1.5, 2.0, 2.5, 3.0) considering 3 values of  $\beta$ , 3 values of  $h_B$  and 10 values of  $T_Z$  (time interval; 3, 4, ... 12, 13) one would need to perform 360 simulations, ( $4 \times 3 \times 3 \times 10$ ). DNV recommends that the structure is checked by running simulations of minimum 30 minutes, requiring a minimum 180 hours of simulation time ( $30\text{min} \cdot 360\text{simulations} / 60\text{min}$ ).

Normally the extreme values of crane wire tension in lifting analysis is obtained by considering 10 random samples of 30 minutes simulations for each sea state, taking the average of the extreme values and comparing them with the design criteria, (Sarkar (2010)), (requiring 1800 hours of total simulation time ( $180\text{h} \cdot 10\text{simulations}$ )). In this report the extreme values are obtained using a deterministic approach where the crane wire tension is obtained by exposing the structure to the largest wave in 3 hour duration.

OrcaFlex provides a wave preview function that can obtain largest rise, largest fall, highest crest and lowest trough for a sea state defined by the JONSWAP wave spectra. By defining duration of 3 hours, one can locate the time in which the most critical wave occurs and ensure that this wave is included in the dynamic simulation. The expected maximum and minimum total loads ( $F_{\max}$  and  $F_{\min}$ ) can be obtained by performing a 60 second simulation (plus a “wave build-up time” of 20s) that starts 30 seconds before the most critical event. A wave preview for  $H_S=2.0\text{m}$  and  $T_z=6.0\text{s}$  is illustrated in *figure 5.10* where the largest wave,  $H_{\max}=3.75\text{m}$ , (the largest wave  $H_{\max}$  is also defined by the storm factor in DNV (RP-H102 (2004) table 2-2) where  $H_{\max}=1.9H_S=3.8\text{m}$ ). The maximum and minimum total loads obtained using this method, will not be exceeded even if 30 minute simulations were used instead of 60 second simulations. The minimum simulation time (excluding build up time and the time needed to insert and obtain data) is now reduced to 6 hours ( $1\text{min} \cdot 360\text{simulations} / 60\text{min}$ ).

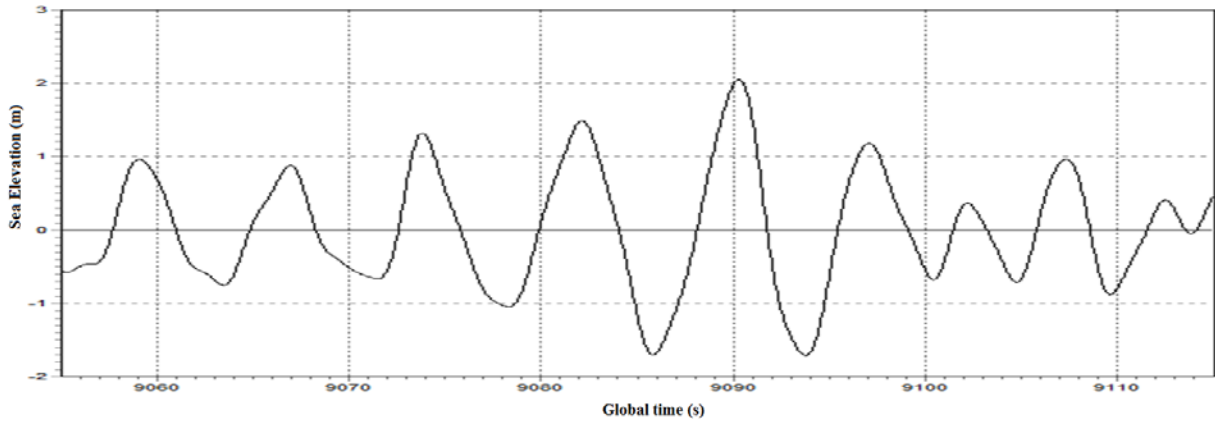


Figure 5.11: Critical wave profile for  $H_S=2.0\text{m}$ ,  $T_Z=6.0\text{s}$ , Wave search duration=3h, where largest rise, largest fall, highest crest occurs at ~9090seconds.

If the structure satisfy the accept criteria given in *section 5.1* for defined  $H_S$ ,  $T_Z$ ,  $\beta$  and  $h_B$ , the obtained  $F_{\max}$  and  $F_{\min}$ , the structural integrity is verified for all load conditions. This is a very conservative method which doesn't represent the most probable value of the maximum loading, (Subsea 7 (2011) 5.5.1).

If the structure doesn't satisfy the accept criteria given in *section 5.1*, a more thorough simulation is necessary to verify that the structure can withstand the given sea-state and load condition. 30 minutes simulations will be performed and the most probable maximum and minimum dynamic loads can be obtained by assuming that the dynamic loads can be Rayleigh distributed. The most probable largest dynamic load,  $R_{\max}$  is then found by:

$$R_{\max} = \sigma_r \sqrt{2 \ln \left( \frac{t}{T_z} \right)} \quad (5.12)$$

Where  $t$  the duration of the operation set to 30 minutes,  $T_Z$  is the zero up crossing period as defined for each sea state and  $\sigma_r$  is the standard deviation of the dynamic load obtained for each sling and crane wire in OrcaFlex.

## 5.3 Hydrodynamic properties

The integrated spool cover is designed with tubular sections making the discussion related to forces on cylinders described in *chapter 2* relevant for all structural parts. If the structural members were squared (or rectangular) with approximated equal size as the tubular cross sections, the coefficient for drag and slam should be increased due to larger contact area for impact and viscous forces, and increased wake effect around rectangle corners.

Since all members in the considered structure has tubular cross sections, the hydrodynamic coefficient can be determined based on existing experimental data for cylinders and the discussion from *section 2.3* regarding hydrodynamic coefficients for circular members. By the given assumptions, the coefficients can be calculated as functions of submerged level,  $h$  and diameter  $D$  when the cylinders are close to the still water level making it easy to obtain the factors for various diameters in different depths.

### 5.3.1 Keulegan-Carpenter and Reynolds number

To obtain hydrodynamic coefficients for structures in oscillating water, the flow and structure interaction need to be characterized by calculating Keulegan-Carpenter number,  $K_C$  and Reynolds number,  $Re$ . Both  $K_C$  and  $Re$  - number is a product of maximum orbital particle velocity,  $v_m$  which is decreasing exponentially with increased depth,  $-z$  making the numbers volatile close to the mean water level. The orbital particle velocity is according to linear theory for deep water described as in *eq. (5.13)*, (DNV-RP-C205 (2010) Table 3-1):

$$v_m = \frac{\pi H}{T} e^{kz} \quad (5.13)$$

Where  $H$  is wave height,  $T$  is wave period,  $k$  is wave number ( $2\pi/\lambda$ ) and  $z$  is the depth for the regular waves described by linear wave theory.

#### Keulegan Carpenter number

The  $K_C$  number for unsteady flow in linear waves can be calculated as shown in *eq. (5.14)*.

$$K_C = \frac{v_m T}{D} \quad (5.14)$$

Where  $v_m$  is the maximum orbital fluid velocity,  $T$  is the wave period, and  $D$  is the diameter of the cylinder. By inserting *eq. (5.4)* into *eq. (5.13)* the  $K_C$  number can be written as:

$$\begin{aligned} K_C &= \frac{\pi H}{T} e^{kz} \frac{T}{D} \\ &= \frac{\pi H}{D} e^{kz} \end{aligned} \quad (5.15)$$

Where  $H$  is wave height,  $D$  is diameter of the cylinder and  $z$  is the depth for regular waves. In case of deep water, the wave number,  $k$  can be described as:

$$k = \frac{2\pi}{\lambda} = \frac{(2\pi)^2}{gT^2} \quad (5.16)$$

Where  $\lambda$  is the wave length,  $g$  is the acceleration of gravity and  $T$  is the wave period for linear waves.

It is assumed that  $K_C$  for various depths in irregular waves can be described as for regular waves by using the significant wave height,  $H_s$  and zero up-crossing period,  $T_z$  to define the Keulegan Carpenter number and the maximum orbital velocity,  $v_m$  can be calculated as for regular waves. DNV (RP-H103 (2012) 2.4.9.2) recommend using  $v_m = \sqrt{2}\sigma_v$  and  $T=T_z$ , where  $\sigma_v$  is the standard deviation of the fluid velocity for irregular waves. The maximum orbital velocity,  $v_m$  is significantly larger than  $\sqrt{2}\sigma_v$ , (this is checked for various velocities in OrcaFlex) meaning that the assumption give larger  $K_C$  numbers in the analysis. A larger  $K_C$  number indicates a smaller relative diameter compared to wave height increasing the drag force and reducing the inertia force.

The Keulegan Carpenter number can then be calculated according to eq. (5.17). This is the same relation as for regular wave where the wave height is  $H_s$  and wave period is  $T_z$ .

$$K_C(H_s, T_z, D, h) = \frac{\pi H_s}{D} e^{\frac{(2\pi)^2}{g T_z^2} (-h)} \quad (5.17)$$

The Keulegan Carpenter number for all cylinders in the concerned structure for various depths and wave heights are given in APPENDIX H and values for the largest cylinder (12'' spools with coating) is illustrated in figure 5.12. The data will be used to compare drag and inertia coefficients obtained from Sarpkaya's coefficient diagrams (Sarpkaya (2010) p.82) with coefficients that are obtained with formulas from section 2.3.

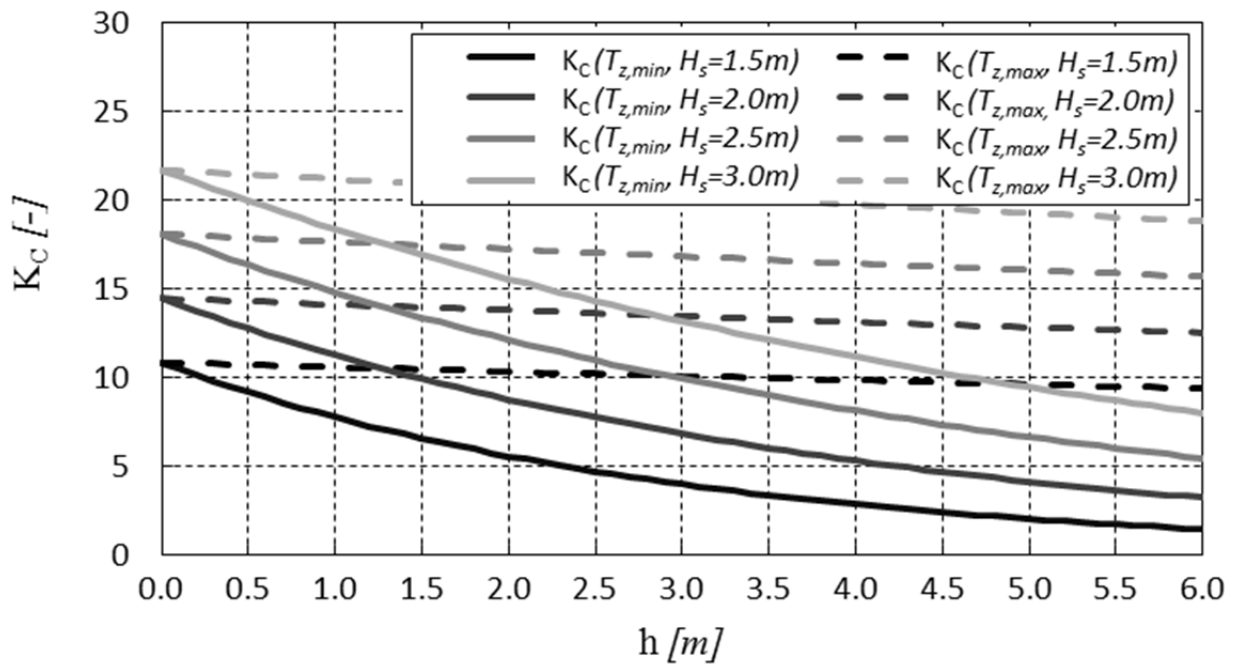


Figure 5.12:  $K_C$  versus level of submergence for 12'' spools (cylinders with  $D=0.434m$ ).

## Reynolds number, $R_e$

The  $R_e$  number for unsteady flow in linear waves can be calculated as:

$$R_e = \frac{v_m D}{\nu} \quad (5.18)$$

Where  $v_m$  is the maximum orbital fluid velocity,  $D$  is the diameter of the cylinder and  $\nu$  is the kinematic viscosity of the water. DNV (RP-H103 (2012) 2.4.9.2) recommend using  $v_m = \sqrt{2}\sigma_v$ , where  $\sigma_v$  is the standard deviation of the fluid velocity for irregular waves. The maximum orbital velocity,  $v_m$  is significantly larger than  $\sqrt{2}\sigma_v$ , (this is checked for various velocities in OrcaFlex) meaning that the assumption give larger  $R_e$  numbers in the analysis. A larger  $R_e$  indicates smaller dependency on viscosity, increasing the inertia and reducing the drag contribution (opposite of the  $K_C$  dependency on  $v_m$ ). When substituting eq. (5.13) into eq. (5.18), Reynolds number can be calculated as:

$$R_e = \frac{\pi \cdot H \cdot D}{T_z \cdot \nu} e^{k(-h)} \quad (5.19)$$

The Reynolds number for all cylinders in the concerned structure for various depths and wave heights are given in APPENDIX H and values for the largest cylinder (12'' spools with coating) is illustrated in figure 5.13. The data will be used for obtaining drag and inertia coefficients according to diagrams from Sarpkaya, (Sarpkaya (2010) p.82)

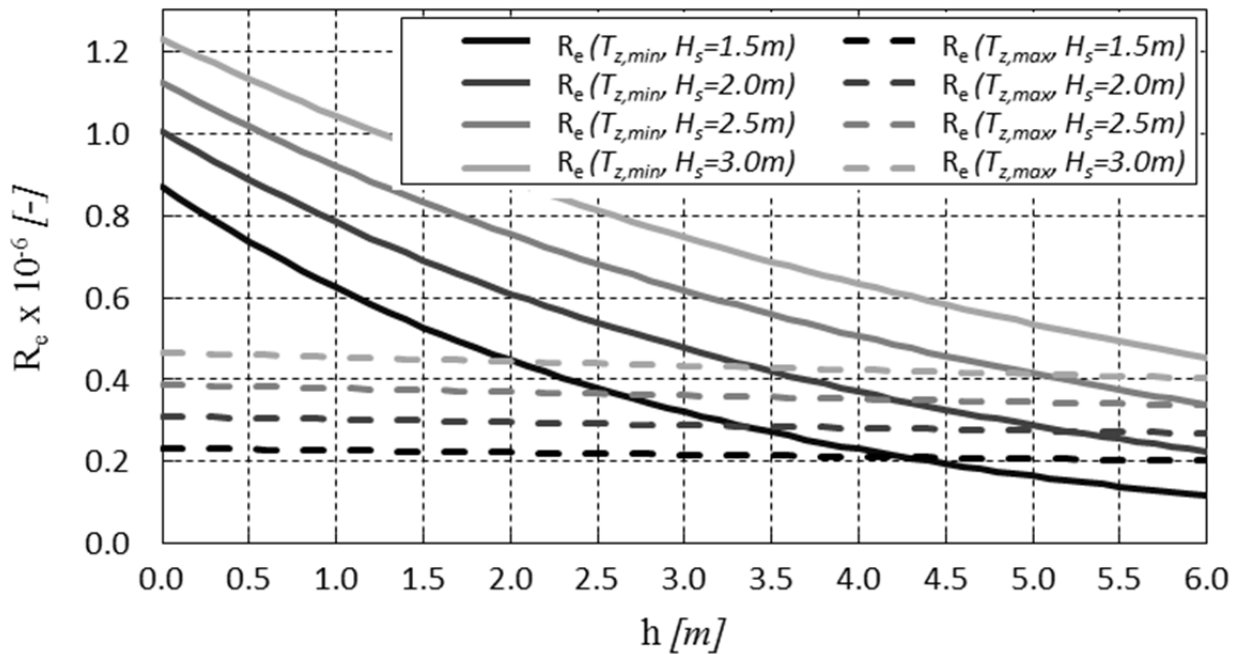


Figure 5.13:  $R_e$  versus level of submergence for 12'' spools (cylinders with  $D=0.434m$ ).

### 5.3.2 Inertia coefficient

Based on the fifth polynomial function for added mass based on experimental values from Greenhow & Ahn (DNV-RP-C205 (2010) figure 6-10) illustrated in *section 2.3.1*, the added mass of submerged cylinders close to the surface are calculated according to *eq. (5.20)*:

$$C_A = -0.064\left(\frac{h_s}{r}\right)^5 + 0.886\left(\frac{h_s}{r}\right)^4 - 4.83\left(\frac{h_s}{r}\right)^3 + 12.91\left(\frac{h_s}{r}\right)^2 - 1712.91\left(\frac{h_s}{r}\right) + 10.06 \quad (5.20)$$

Where  $h_s$  is the distance from the elevated free surface to the center of the cylinder (illustrated in *figure 2.2*) and  $r$  is the radius of the cylinder. The average value of  $h_s$  in waves is of course the distance from mean water level to the center of the cylinder  $h$ , and for the dynamic analysis of the structure in the splash zone, the coefficient will be based on  $h_s=h$ .

The estimated added mass for various members in the lifted structure at different level of submergence is illustrated in *figure 5.14*. When the cylinder is partly submerged or above the waterline, the added mass coefficient is chosen to be 2.0, (same as when the top of the cylinder is very close to surface). This is considered conservative, since less mass move with the cylinder when the top of the cylinder is above the water. The minimum value is assumed the same as the theoretical value for added mass equal 1.0.

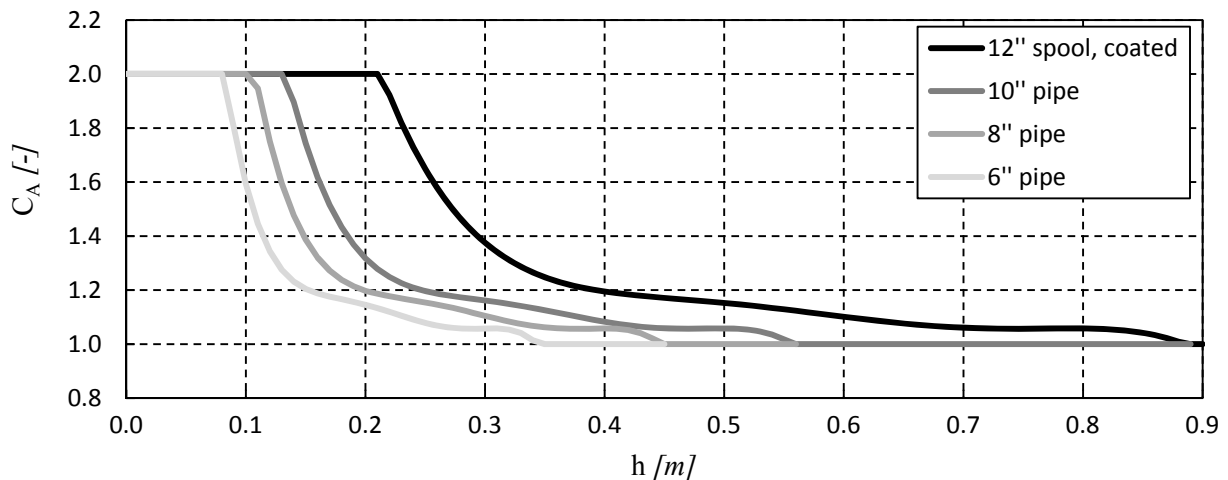


Figure 5.14:  $C_A$  versus submergence level,  $h$  for 5 different sized cylinders, based on *eq. (5.17)*, (the equation is applicable for  $1 < h/r < 2$  and it is assumed that  $1 \leq C_A \leq 2$ ).

The values given in *figure 5.14* are inserted in OrcaFlex for cylinders with different size and submergence level relevant to the still water level where the inertia coefficient,  $C_M=1+C_A$ . This is applicable for all partially submerged load cases. Hydrodynamic coefficients for all cylinders with different level of submergence are given in *APPENDIX H*.

The surface effect can be neglected when the distance from the cylinder center to the oscillating sea-surface is three to four times larger than the cylinder diameter, (Prasad (1994)), and can then be determined based on Sarpkaya's experimental values for inertia coefficients (Sarpkaya (2010) p.82).

### 5.3.3 Drag and slam coefficient

The combined drag and slam factor is calculated according to eq. (5.21) where the maximum value of idealized slam and drag coefficient is  $3.14 (\pi)$  and the minimum value is the estimated drag factor  $C_D$  based on figure 2.10, (Sarpkaya (2010)). The minimum value for partly submerged cylinder is chosen to be 0.8 according to the discussion in section 2.3.4.

$$C_s = \frac{1}{\sin(0.5\alpha)} \left[ \frac{2\pi^3}{3} \left( \frac{(\sin \alpha)}{(2\pi - \alpha)^2} + \frac{2(1 - \cos \alpha)}{(2\pi - \alpha)^3} \right) + \frac{\pi}{3} \sin \alpha + \cos \alpha - 1 \right] \quad (5.21)$$

Where

$$\alpha = 2 \cos^{-1} \left( -\frac{h_s}{r} \right) \quad \text{for } -1 \leq \left( \frac{h_s}{r} \right) \leq 1 \quad (5.22)$$

Figure 5.15 shows the estimated values for idealized drag and slam coefficients based on eq. (5.21).

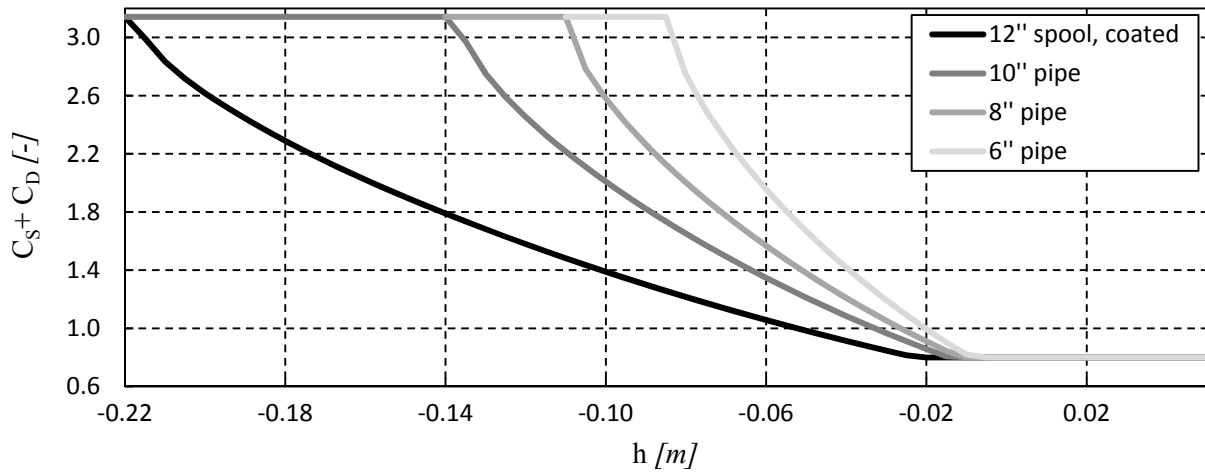


Figure 5.15:  $C_s+C_D$  versus submergence level,  $h$  for 5 different sized cylinders, based on eq.(5.18), (the equation is applicable for  $-1 < h/r < 1$  and it is assumed that  $0.8 \leq C_s+C_D \leq \pi$ ).

The values given in figure 5.12 are inserted in OrcaFlex for cylinders with different size and submergence level relevant to the still water level. For members defined as lines in OrcaFlex, it is not possible to insert an individual slam coefficient which is why the drag and slam coefficients were combined into one factor.



## 5.4 Dynamic results

After the modeling is finished and the static equilibrium is obtained in OrcaFlex, the structure is analyzed by “running” all necessary dynamic simulations. The goal of the dynamic simulations is to obtain the largest significant wave height that the structure can withstand without exceeding the maximum or minimum loads defined by the acceptance criteria in *section 5.1.1*. The forces on the lifted structure are represented by forces in crane wire and slings making them comparable with forces obtained from Staad.Pro.

The crane wire tension for each load case (sea-state, wave heading and submergence level) is illustrated in graphs where the forces is compared to the *upper limit* and *lower limit* defined in the acceptance criteria in *section 5.1*. The sling forces can be found in *APPENDIX I* given in tables (along with the associated crane wire tension) for each load case. Forces are mainly obtained using a deterministic approach where the structure is exposed to the largest irregular wave in a three hour period, but is compared to forces obtained by different stochastic distributions for the most critical load cases.

The analysis covers sea-states represented by significant wave heights,  $H_s$  between 1.5m and 3.0m where applicable zero up crossing periods,  $T_z$  is en the range given in *eq. (5.9)* (between  $\approx 3.5$ s and 13.0s). The tubular elements are considered as air filled for all simulations due to reasons stated in *section 5.4.2*.

### 5.4.1 Dynamic loads in different wave direction

As stated in *section 5.2.5*, 360 dynamic simulations is needed to do a full dynamic analysis for the structure, (including 3 wave direction, 3 level of submergence, 4 significant wave heights and 10 different zero up crossing periods). The number of simulations can be reduced by obtaining worst case load scenarios (if the structure can withstand the worst load case, it can withstand all lesser loads). To reduce the number of necessary simulations, the worst wave direction is found for a given level submergence height,  $h_B$ , significant wave height,  $H_s$  and zero up crossing period,  $T_z$ . The hydrodynamic coefficients and the values in the graph are given in *APPENDIX H* and *I* respectively.

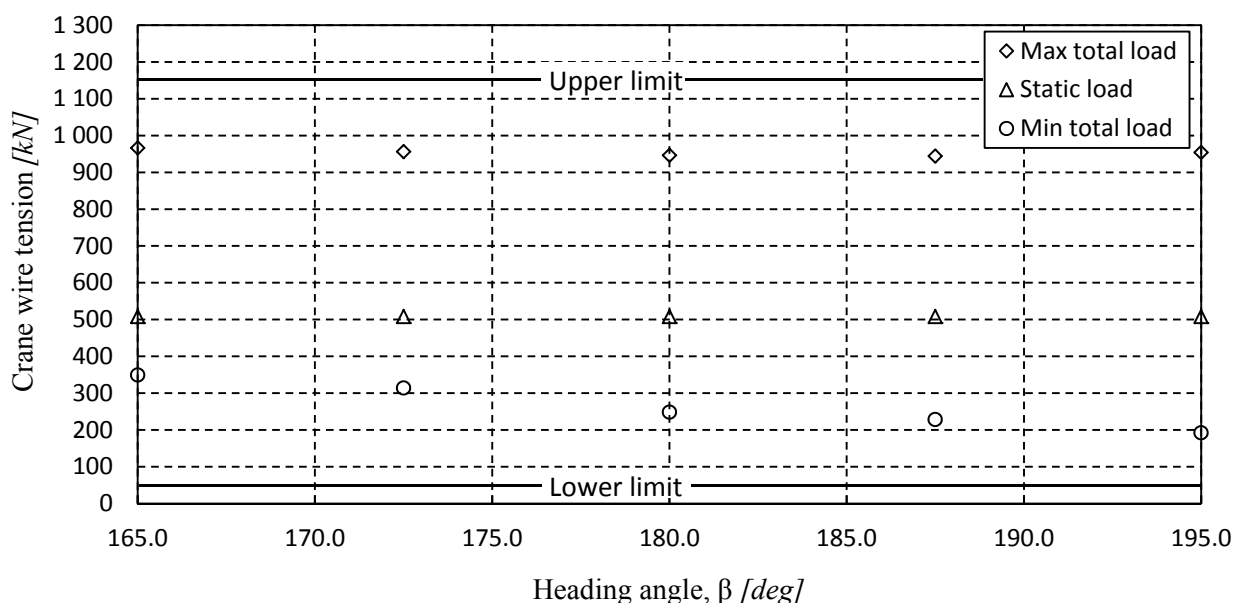


Figure 5.16: Crane wire tension versus heading angle,  $\beta$  for  $H_s=2.0$ m,  $T_z=6.0$ s,  $h_B=1.0$ m.

As illustrated in *figure 5.16* the max total load is pretty much unchanged for all angles, but one can see a clear tendency of increased hydrodynamic loads in minimum total load as the wave heading angle,  $\beta$  is increased to 195 degrees, (see *figure 5.9* for illustration). The waves are approaching the ship from the same direction as where the structure is being lifted making the structure more exposed to the waves. It is also because the structure has a “larger contact area” to waves from that direction due to the shape of the structure in the xy-plane, (see *figure 5.9* for different wave angles). The rest of the dynamic analysis will consider a worst case wave angle of 195 degrees reducing the number of required simulations to 120, (1x3x4x10).

#### 5.4.2 Dynamic loads in different level of submergence

The loads on the structure are highly dependent on the level of submergence of the lifted structure. The vertical equation of motion for lifted structures is given as, (DNV-RP-H103 (2012) 3.2.10.1):

$$\begin{aligned} (M + A_{33})\ddot{\eta} + B_{33}(\dot{\eta} - v_3) + K(\eta - z_{ct}) = \\ (V_S \rho + A_{33})\dot{v}_3 + \frac{1}{2} \rho A_p C_D (v_3 - \dot{\eta})|v_3 - \dot{\eta}| + \frac{1}{2} \rho A_p C_S (\dot{\zeta} - \dot{\eta})^2 \end{aligned} \quad (5.23)$$

Where the meaning of all coefficients is given in *section 2.1.2*. By observing the vertical equation of motion one can see that the following are changing when the structure is lowered down into the ocean:

- Submerged volume,  $V_S$  is increased.
- Stiffness in the crane wire is reduced when the distance,  $L$  between crane wire and lifted object is increased ( $K=EA/L$ ).
- The acceleration and velocity of water particles ( $v_3$  and  $\dot{v}_3$ ) are reduced with increased water depth.
- Contact surface between lifted object and fluid is increased, increasing the contribution from added mass,  $A_{33}$ .
- The interaction between object and fluid is changed with level of submergence. The disturbance is represented by hydrodynamic coefficients for drag, slam and inertia (based on earlier experiments on cylinders) where the slam contribution goes to zero when the object is completely submerged while the drag contribution is increased.

It is assumed that the coefficients for inertia and idealized drag/slam follows the relations illustrated in *figure 5.14* and *figure 5.15* respectively for all cylinders. The total hydrodynamic load is calculated as the sum of forces acting on each tubular element in the structure. The total hydrodynamic forces are obtained by exposing the structure to the largest irregular wave that occurs in a 3 hour period ( $H_{max}$ ) and obtaining the maximum and minimum tensions in the crane wire obtained from OrcaFlex.

The total forces on the lifted structure at different level of submergence is illustrated in *figure 5.18* (and given in *APPENDIX I*) indicated by simulations with 0.2m intervals for different values of  $h_B$ . The structure position relevant to the still water level is illustrated in *figure 5.17*. The “real structure” analyzed in chapter 4 also includes an 8” spool and trawlboard which is not a part of the simplified model with a cross section as illustrated in *figure 5.17*.

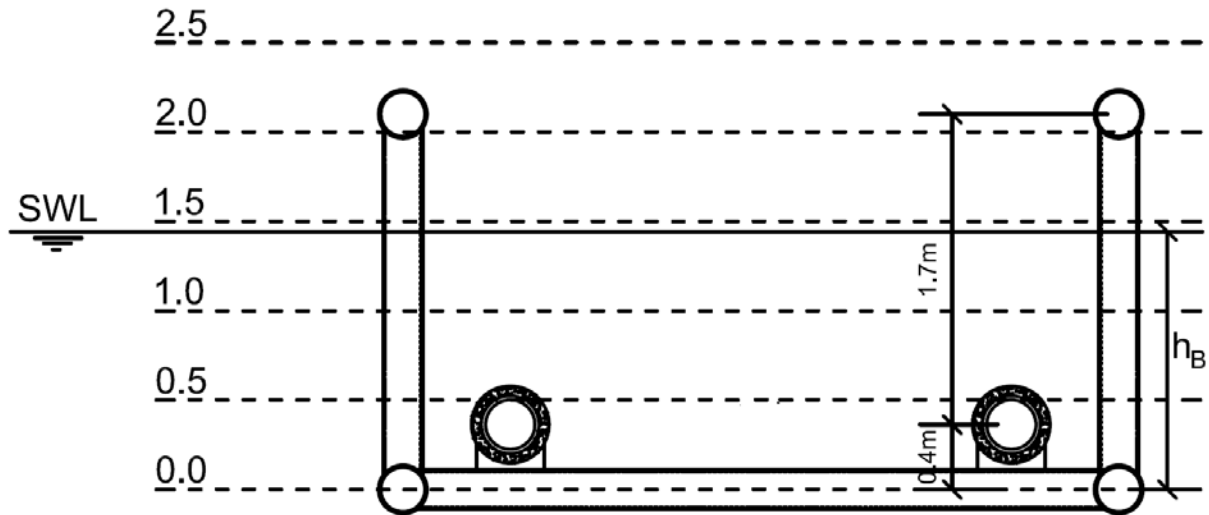


Figure 5.17: Illustration of the lifted structure position relevant to the still water level.

The dynamic simulations are performed for a zero up crossing period,  $T_z=6.0$ seconds (this proves to be the wave period associated with largest forces on the lifted structure in *section 5.4.3* when  $h_B=1.0$ m),  $H_s=2.0$ m and the worst heading angle from *section 5.4.1*. The members are calculated as air filled at all levels of submergence. The forces on the structure is considered in the interval  $h_B=0$  to  $h_B=2.6$  where  $h_B=0$  is the load case when the bottom members in the structure is partly submerged.

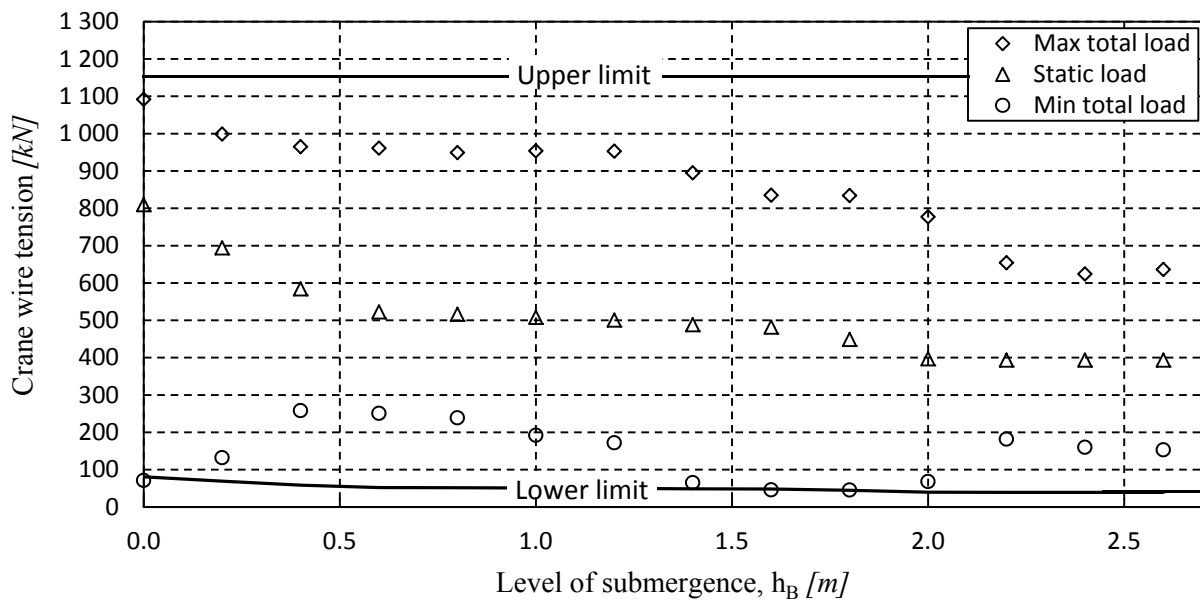


Figure 5.18: Crane wire tension versus level of submergence for  $H_s=2.0$ m,  $T_z=6.0$ s,  $\beta=195$ deg.

When observing the total force in the structure represented by the crane wire tension, one should keep in mind how the forces are obtained in OrcaFlex. As mentioned, the forces are calculated by summing up contribution from all structural parts so that all interaction between members is taken care of by the hydrodynamic coefficients defined for each member, (see *figure 5.14* and *figure 5.15*). The crane wire tension is obtained by a deterministic approach where the structure is subjected to the largest irregular wave in a 3 hour period ( $H_{max}\approx 1.8H_s$ ). When the structure is partly and fully submerged, the members will be flooded increasing the max total load in the crane wire and the max total load will not exceed 1100kN for the given sea-state (even when the structure is flooded at lower depths). The tubular

sections will conservatively be considered as air filled to ensure that the minimum total load doesn't result in slack slings when the structure is deployed.

Since the structure is relative light compared to volume (consisting of mainly air filled tubular sections) the max total load will occur when the structure is not submerged while experiencing vessel motion in form of crane tip motion in upward direction while coefficients for drag+slam and inertia are large. Due to large buoyancy forces the max total load is steadily decreasing with the level of submergence. The members will in truth be flooded during submergence, but the maximum crane wire tension is still considered small compared to the largest forces that the structure is subjected to when the structure is submerged by less than 0.4 meter with respect to the still water level.

The static loads represented by the weight of the structure when the structure is in air, partly submerged and fully submerged as indicated in *figure 5.18* in "flat sea" (no waves). The static load in the crane wire is quickly reduced from 810kN to about 520kN when the 12" spools are fully submerged. Then the static load is pretty stable until the top members of the structure reaches the still water level at  $h_B=2m$ . When fully submerged, the static weight is 394kN which represent the submerged weight of the structure.

From *figure 5.18* one can clearly see two lower peaks in minimum total load in the crane wire. At first impact, the hydrodynamic coefficients for inertia, drag and slam is large exposing the structure to large vertical forces in upward direction. At the same time, the crane tip is moving in downward direction due to vessel motions reducing the tension in the crane wire. The next peak is at a submerged depth,  $h_B=1.6-1.8m$  when the top members of the structure is subjected to slam loads.

Since the structure is composed of tubular elements, the structure is considered relatively light compared to size making the slack wire criteria critical for the design. The members will be flooded in truth be flooded making the minimum crane wire tension at a level of submergence,  $h_B\approx 1.8m$  conservative.

### 5.4.3 Dynamic loads in different sea states

Since the structure passes quickly through the splash zone, it should be sufficient that the structure is analyzed at a mean submerged depth, (Sarkar (2010)). The structure is therefore analyzed at submerged level,  $h_B = 1.0$  since it's not probable (not at all) that the largest wave in a three hour duration will occur at the worst possible level of submergence ( $h_B \leq 0m$ ,  $h_B \approx 1.8m$ ).

The hydrodynamic coefficient used in the analysis is given in *APPENDIX H* and the tension in each wire,  $DAF_{dynamic}$  and slack-sling criteria are given in *APPENDIX I*.

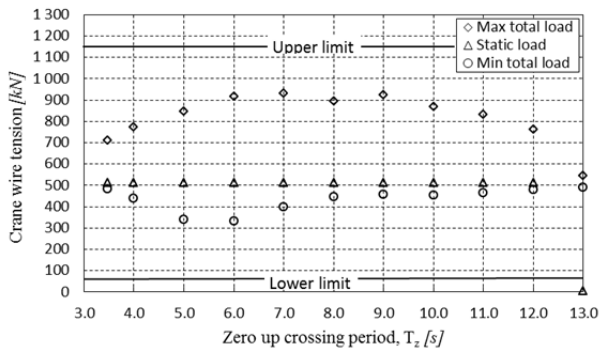


Figure 5.19: Crane wire tension versus zero up crossing period for  $H_S=1.5m$ ,  $h_B=1.0m$  and  $\beta=195^\circ$ .

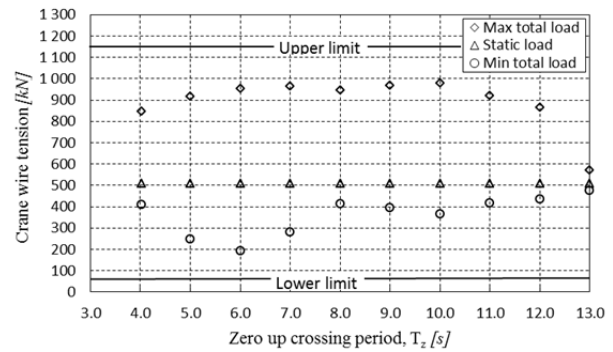


Figure 5.20: Crane wire tension versus zero up crossing period for  $H_S=2.0m$ ,  $h_B=1.0m$  and  $\beta=195^\circ$ .

Extreme values for the crane wire tensions at  $H_S=1.5$  and  $H_S=2.0$  are given in *figure 5.19* and *figure 5.20* respectively. The upper and lower limit is not exceeded for any of the extremes including tension in all slings, (given in *APPENDIX I*). The largest value of  $DAF_{dynamic}$  is 1.1 for the most utilized slings (upper limit=1.2), and the minimum force in all slings is  $0.2 \cdot F_{static.min}$  (lower limit= $0.1 \cdot F_{static.min}$ ), indicating that the structure can be installed in all sea states characterized by  $H_S \leq 2.0$ .

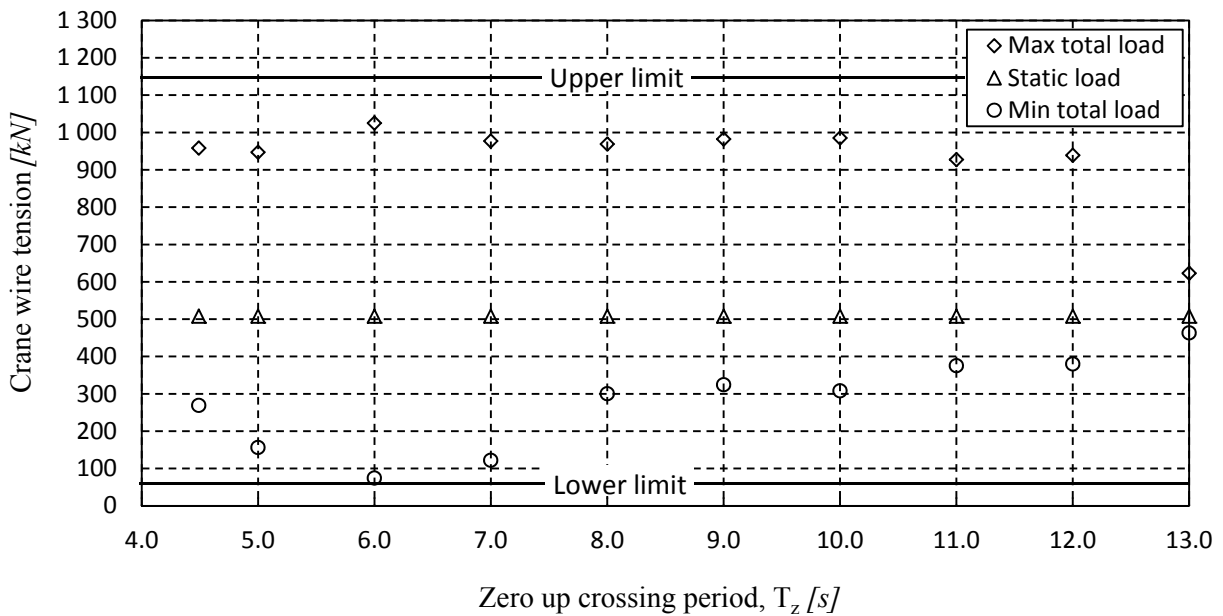


Figure 5.21: Crane wire tension versus zero up crossing period for  $H_S=2.5m$ ,  $h_B=1.0m$  and  $\beta=195^\circ$ .

Extreme values for the crane wire tensions at  $H_S=2.5$  is given in *figure 5.21*. The upper and lower limit is not exceeded for any of the extremes values of the crane tensions. However; some of the slings

experience forces that exceed both upper and lower limit state where four of the six slings is slack at a zero up crossing period,  $T_z=6.0s$ . A conclusion has yet to be made whether or not the structure can withstand loads when installed at a sea state characterized by a significant wave height,  $H_s=2.5m$  since the values are obtained using an extreme condition ( $H_{max}\approx 1.9H_s$ ) rather than the most expected condition for lifting operations in the given sea state.

From *figure 5.19* to *figure 5.21* one can indicate that the largest forces on the structure occurs at a zero-up crossing period,  $T_z=6$  seconds. This can be explained by considering the size of the structure relevant to the wave length. The characteristic length of the structure relevant to the waves can be observed in *figure 5.22* where the characteristic length is approximately 35meter. If one were to consider a solid object with characteristic dimension,  $D_c$  in regular waves, the largest forces on the object would be at a wave length,  $\lambda=2\times D_c$ . If  $D_c > \lambda/2$ , the response would be damped out by the next wave crest, and if  $D_c < \lambda/2$  the object would not experience the full impact of one wave. The same effect should occur for the framework structure indicating that the worst wave length is close to 70m.

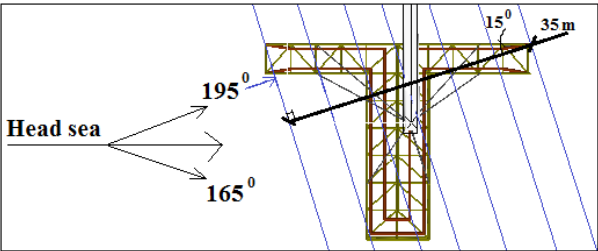


Figure 5.22: Characteristic dimension of the structure relevant to the wave direction,  $\beta$ .

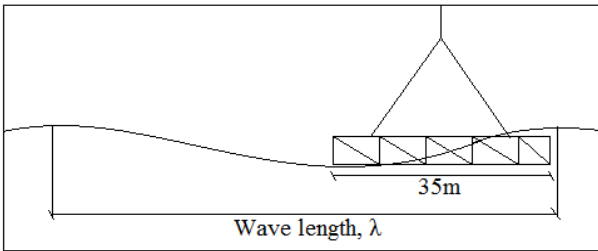


Figure 5.23: Structure (with characteristic dimension) in regular waves with wave length,  $\lambda$ .

The regular wave lengths in deep water with period  $T$  follows the relation in *eq. (5.24)*, (DNV-RP-C205 (2010) table 3-1).

$$\lambda = \frac{gT^2}{2\pi} \tag{5.24}$$

The mean length between zero-up crossings in irregular waves is determined from *eq. (5.24)* where  $T=T_z$ , gives a wave length,  $\lambda=56$ meter for  $T_z=6.0s$ . From *figure 5.22* one can see a lot of open space due to the structural angles so that the average characteristic length should be somewhat less than 35m making the structure resonating with wavelengths of approximately 60 meter.

Vessels RAO (response amplitude operator) indicate which wave periods that give the largest response. The considered vessel has peaks in vertical motion (heave) at  $\approx 7.4s$ , in transverse rotation (roll) at  $\approx 6.5s$  and longitudinal rotation (pitch) at  $\approx 6.3s$  indicating that wave periods close to these peaks gives larger crane tip motions and increasing the tension on the lifted structure.

A significant wave height,  $H_s=3.0m$  will not be considered since the minimum forces in the crane wire exceed the lower limit for  $H_s=2.5m$  in zero up crossing periods in the range;  $5s < T_z < 7s$ .

#### 5.4.4 Limiting sea state using stochastic approaches

Until now, the crane wire tension (and sling forces) has been obtained using a deterministic approach where the largest crane wire tension (and sling tensions) due to the largest irregular wave in a 3 hour period is determined. To obtain more realistic values, stochastic approaches should be used, where the most probable maximum values are obtained. This can be done by performing about 10 random 30min simulations and find average of the maximum values (Sarkar (2010)), or by using distribution functions based on the standard deviation of the load. By assuming that the dynamic loads can be Rayleigh distributed, the most probable largest maximum loads may be found by the Rayleigh distribution function in eq. (5.6), (DNV-RP-H103 (2012) 3.4.3.5).

When the hydrodynamic forces at different level of submergence was determined, a slack crane wire was observed at level of submergence,  $h_B=0m$  and  $h_B=1.8m$  as shown in figure 5.18. A sea state defined by a zero up-crossing period,  $T_Z=6.0s$  and heading angle,  $\beta=195$  for these levels of submergence should represent the worst possible load condition for the lifting operation and will be considered using the Rayleigh distribution to verify if the acceptance criteria is satisfied. The Rayleigh distributed loads, and the extreme values are compared in figure 5.24 for  $h_B=1.8m$ .

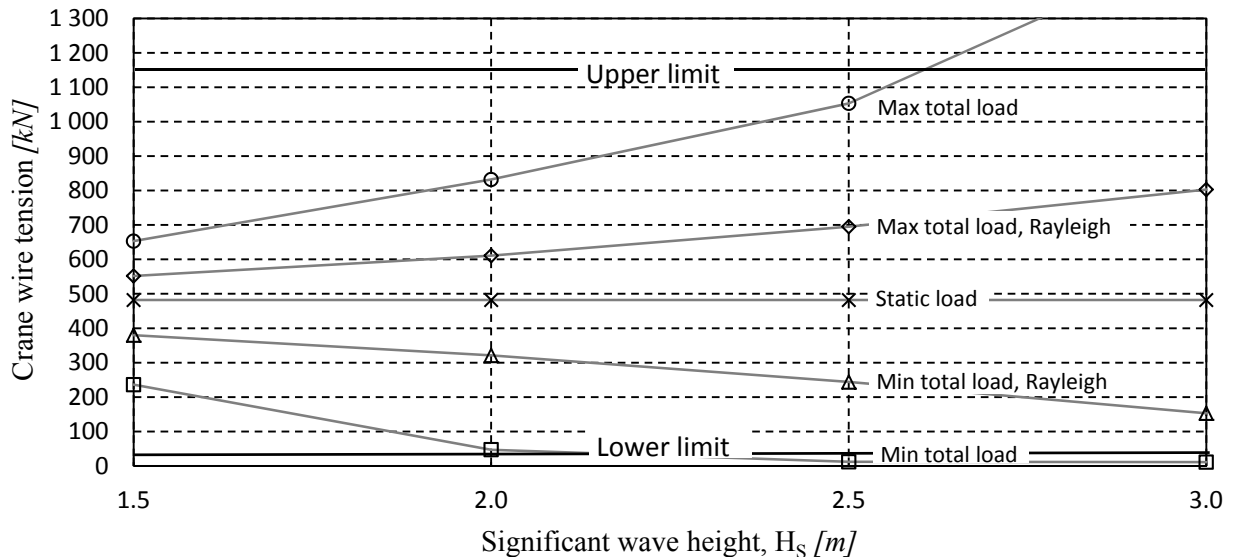


Figure 5.24: Crane wire tension versus significant wave height, for  $T_Z=6.0m$ ,  $h_B=1.8m$  and  $\beta=195.0$ . Rayleigh values are obtained for 30 minutes storm duration.

At  $H_S=2.0m$ , the minimum force in the crane wire due to  $H_{max}$  is close to the lower limit and slack occurs in all slings (given in APPENDIX I) which is not acceptable, but by considering the Rayleigh distribution which is a function of the standard deviation of wire tension,  $\sigma_v$ , time,  $t$  and zero up crossing period,  $T_Z$ , given in eq. (5.6). The structure can be lifted without exceeding the lower or upper limit at  $H_S \leq 3.0m$  for any of the slings considering lifting operations that takes less than 30 minutes.

At  $H_S=2.5m$ , the dynamic loads following the Rayleigh distribution can be increased by a dynamic design factor of 1.8 without exceeding the lower limit of the crane wire tension ( $0.9 \cdot 482 / (482 - 244)$ ) as calculated by eq. (5.25). At  $H_S=3.0$  the dynamic design factor for the lower limit is 1.4 using the Rayleigh distribution.

$$\text{Dynamic design factor} = \frac{0.9 \cdot F_{static}}{R_{max}} \quad (5.25)$$

The dynamic design factor stated in *eq. (5.25)* is used to calculate how much the dynamic force can be increased before the lower design criteria is exceeded when the dynamic loads are obtained using the Rayleigh distribution.

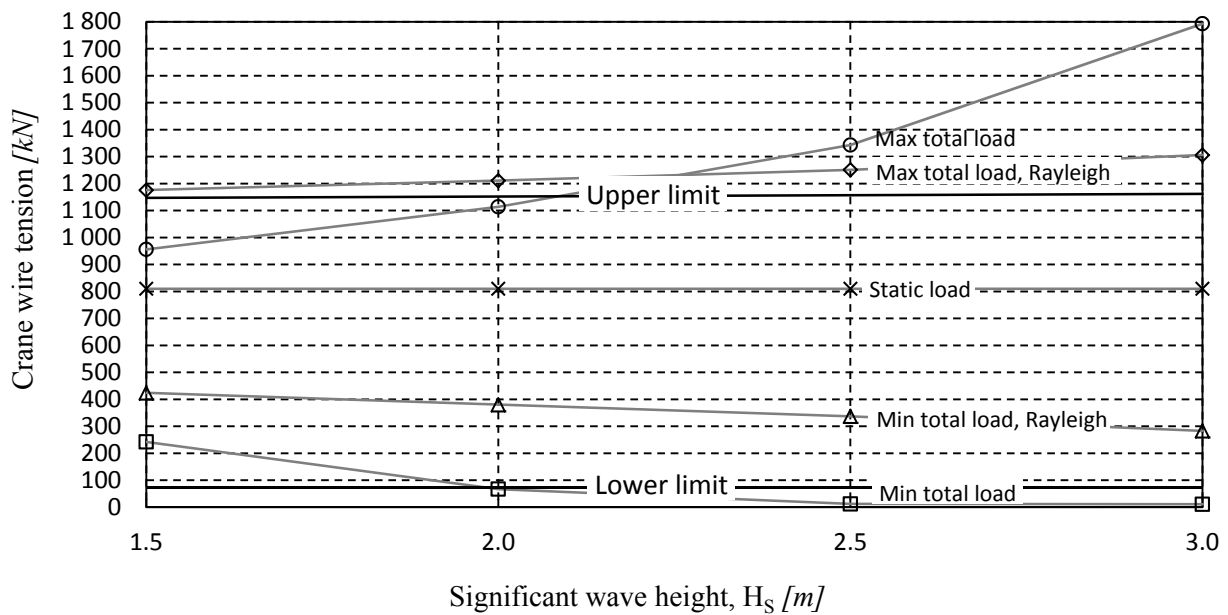


Figure 5.25: Crane wire tension versus significant wave height for  $T_z=6.0\text{m}$ ,  $h_B=0\text{m}$  and  $\beta=195^0$ . Rayleigh values are obtained for 30 minutes storm duration.

When considering the max total loads in slings and crane wire, one can see that the Rayleigh distributed loads are larger than the max total load and exceeds the upper limit at  $H_s=1.5\text{m}$ , when the largest total load due to  $H_{\max}$  is within the accept criteria (upper limit). This is because there are large deviation in forces when the structure is above water resulting in large standard deviation values,  $\sigma_V$  for the 30 minute simulation making the Rayleigh distributed loads less accurate for this load case. If one were to use other distribution functions (e.g. Weibull; threshold=950kN→upper tail load=988kN, Generalized Pareto; threshold=950kN→upper tail load=987kN, at  $H_s=2.0\text{m}$ , in storm duration=30min, (see *figure 5.26* and *figure 5.27*), more realistic values could be obtained.

The minimum total loads are proven to be more accurate for the Rayleigh distribution as one can see by comparing it the Rayleigh distributed crane wire tension to *figure 5.28* where the time history for crane wire tension at  $H_s=2.5\text{m}$  is illustrated for the considered load case. At  $H_s=2.5\text{m}$  the dynamic loads following the Rayleigh distribution can be increased by a dynamic design factor of 1.54 without exceeding the lower limit of the crane wire tension ( $0.9 \cdot 810 / (810 - 337)$ ) as calculated by *eq. (5.25)*. At  $H_s=3.0$  the dynamic design factor for the lower limit is 1.38 using the Rayleigh distribution.

Considering the minimum total load following a Rayleigh distribution, the loads are well within the accept criteria for crane wire and all slings at  $H_s \leq 3.0\text{m}$ , (see *APPENDIX I*).



Figure 5.26 and figure 5.27 illustrate crane wire tensions following the Weibull and Generalized Pareto distribution for  $H_S=2.0\text{m}$  with respect to the time it takes to perform the lifting operation.

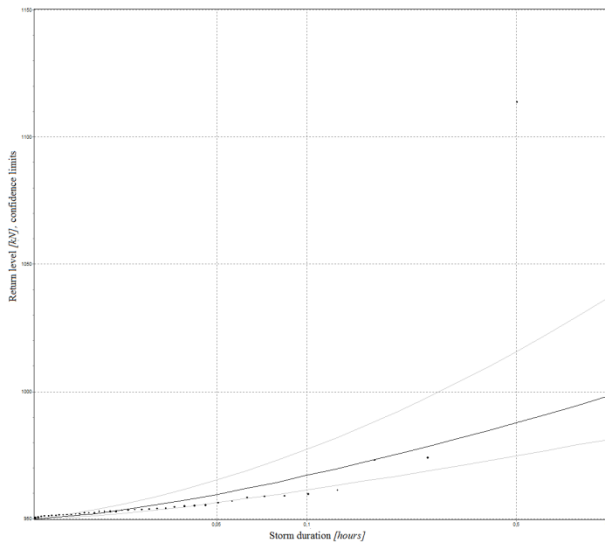


Figure 5.26: Crane wire tension versus storm duration following the Weibull distribution at  $H_S=2.0\text{m}$ .

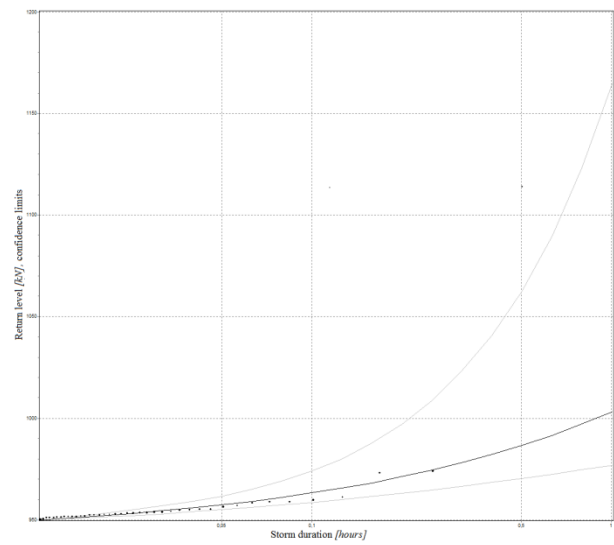


Figure 5.27: Crane wire tension versus storm duration following Generalized Pareto distribution at  $H_S=2.0\text{m}$ .

Figure 5.26 and figure 5.27 are obtained using threshold values of  $950\text{kN}$ , for  $T_Z=6.0\text{m}$ ,  $h_B=0\text{m}$  and  $\beta=195^\circ$ . The black line shows the fitted model, the gray lines indicate upper and lower confidence limits and the dotted values are the extreme values.

Probabilistic loads in the crane wire following the Weibull and Generalized Pareto distribution with respect to storm duration are given in figure 5.26 and figure 5.27 respectively. The threshold parameter indicates which values that should be included in the distributions. After trying a few different threshold values (and observing which value that makes the best fit) a threshold value equal the self-weight of the structure in air ( $950\text{kN}$ ) was used where 41 points (where crane wire tension is larger than  $950\text{kN}$ ) is analyzed for the 30 minute simulation. From the distributions one can see that the most extreme value in a 0.5 hour storm is out of place proving that the largest expected load is not the largest probable load which is within the upper limit when  $H_S=2.0\text{m}$ .

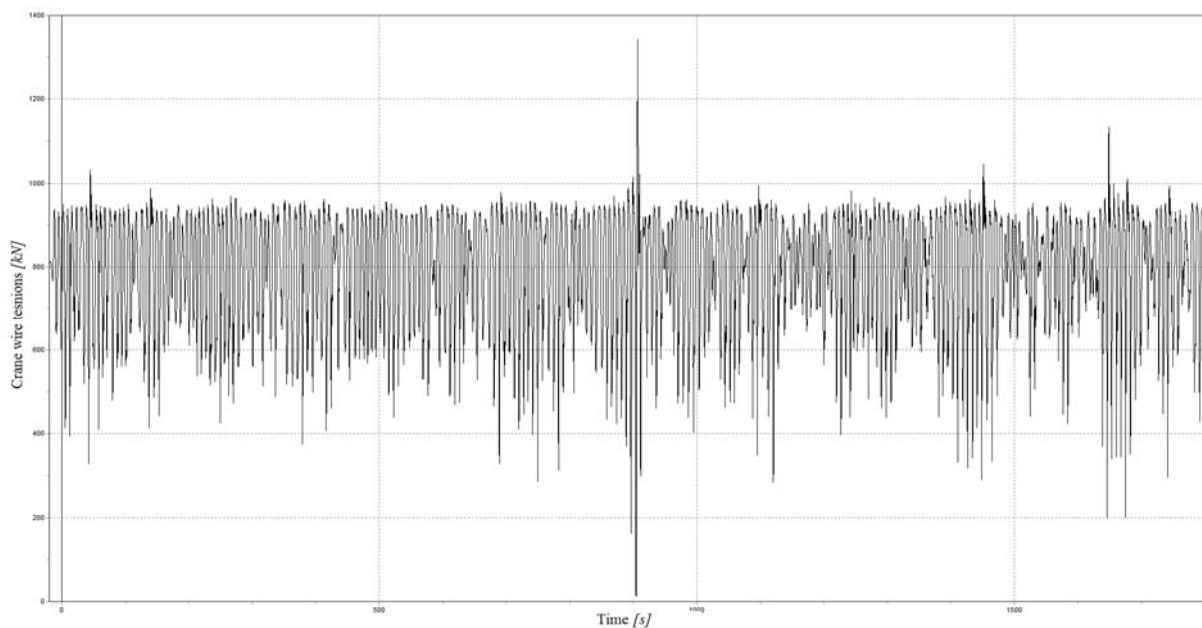


Figure 5.28: Crane wire tension versus time (30min),  $H_S=2.5\text{m}$ ,  $T_Z=6.0\text{m}$ ,  $h_B=0\text{m}$  and  $\beta=195^\circ$ .

From the time history in *figure 5.28* the maximum (and minimum) crane wire tension due to  $H_{\max}$  is clearly out of place and representing unlikely large values. The upper limit is only exceeded two times during the 30 minute interval at this exact level of submergence. In *figure 5.29* the maximum value for total loads are obtained using four different methods for the assumed worst load condition ( $T_z=6.0s$ ,  $h_B=0$ ,  $\beta=195^\circ$ ).

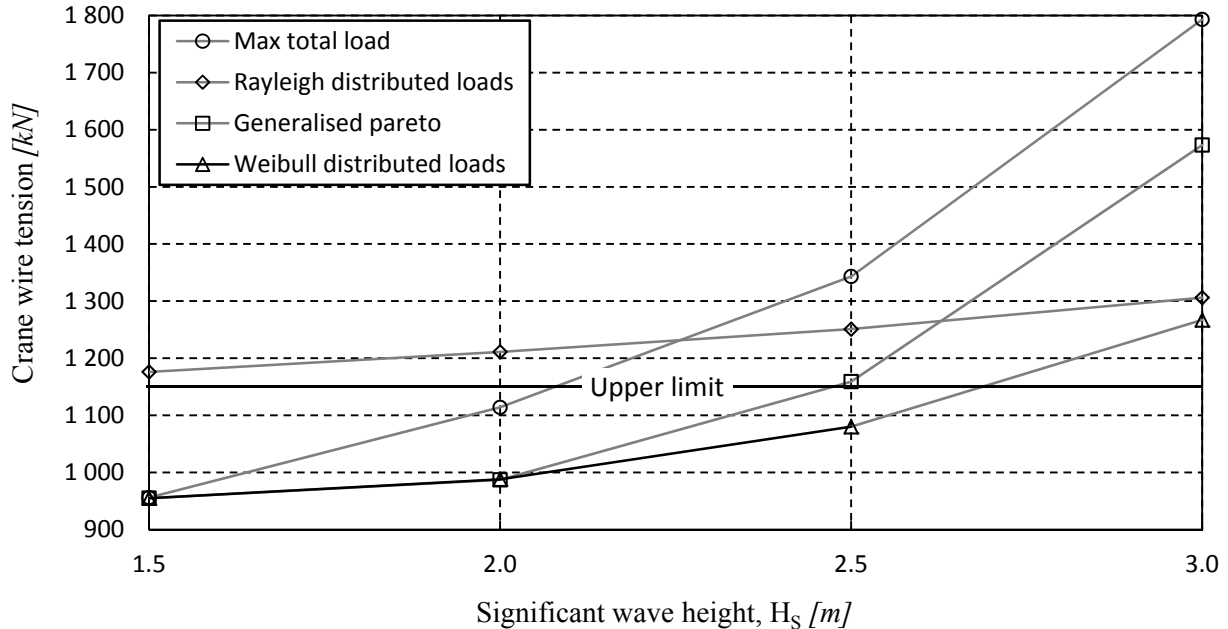


Figure 5.29: Max crane wire tension versus significant wave height for  $T_z=6.0m$ ,  $h_B=0m$  and  $\beta=195^\circ$ , storm duration=30min and threshold=950kN.

The static weight of the structure is 810kN for the given submergence height,  $h_B=0m$  in still water (bottom members are halfway submerged), while the static weight in air is 948kN. At very small waves ( $H_s \leq 1.5m$ ) the total load in the crane wire never exceed the weight of the structure in air even when the structure is subjected to the max irregular wave height,  $H_{\max}$  represented by the “max total load” in *figure 5.28*. Since the Rayleigh distributed loads exceed the max dynamic load one can conclude that the loads don’t fit the Rayleigh model when the structure is located at  $h_B=0$ .

If the dynamic loads fit the Weibull distributed loads, the lift is verified for  $H_s \leq 2.5m$  (the slings does not exceed the limit either as shown in *APPENDIX I*). Keep in mind that the analysis is performed for drag factor which is idealized to the combined drag and slam factor resulting in slam contributions in downward direction. This is a highly conservative way of calculating the max crane wire tension, but the values still indicate that the structure may be lifted in at least  $H_s=2.5m$ .

If one where to reduce the idealized slam coefficient to the drag coefficient ( $C_D+C_S=C_D=0.8$ ) to obtain the maximum crane wire tension (since the slam force only work upwards), the sling and crane wire is obtained using the Weibull distribution at  $H_s=3.0m$  where the max crane wire tension is 1026kN (for  $T_z=6.0s$ ,  $\beta=195^\circ$ ,  $h_B=0m$ , storm duration=30min) which is less than the upper limit which is 1138kN (defined in the acceptance criteria *section 5.1*). The associated dynamic amplification factor,  $DAF_{\text{dynamic}}$  in air is then 1.08 (1026kN/948kN) as calculated by *eq. (5.4)*, which is far from the acceptance criteria of 1.20 ( $DAF_{\text{static}}$ ).

Keep in mind that the values are obtained for installation with a vessel with an infinite stiff crane and no heave compensating effects other than the natural stiffness of the crane wire resulting in conservative hydrodynamic loads on the simplified structure.

## 5.5 Summary, dynamic analysis

The considered structure has been analyzed using a simplified model in OrcaFlex to obtain hydrodynamic loads for different sea states. By using certain assumptions, the simplified model was verified for subsea lifts in sea states characterized by the JONSWAP spectra with significant wave heights,  $H_s \leq 3.0\text{m}$  for all relevant wave periods and wave headings as defined in DNV, (DNV-RP-H103). The static structure was analyzed using a dynamic amplification,  $DAF_{\text{static}}$  in air equal 1.2 defining the upper limit of hydrodynamic loads given in the acceptance criteria from DNV, (*section 5.1.1*). The lower design criteria was also satisfied (slack wire criteria) where the tension in all wires must be larger than 10% of the static loads for all load cases (as obtained for each level of submergence).

The hydrodynamic forces were obtained with hydrodynamic coefficients based on the theory presented in *section 2.3* as illustrated in *section 5.3*. The structural loads were calculated as the combined forces of each individual element. The dynamic coefficients for drag and slam were combined into one factor (as necessary for the modeling in OrcaFlex) giving the slam force the same properties as the drag force. This is a good assumption when obtaining the minimum wire tension due to vertical force in upward direction, but when the maximum force is obtained this is very conservative. When the bottom part of the structure is below the mean water level ( $h_B=0\text{m}$ ) and the structure has not yet been flooded, the structure is considered very light due to air filled tubular sections. The total external force is the sum of inertia, varying buoyancy, slam and drag force. The maximum total load close to the waterline should be considerably lower than those indicated in *figure 5.29* since the slam contribution should be close to zero in downward direction while the varying buoyancy is large for the air filled sections.

Vessel motions play an important part of all subsea lifting operations. The dynamic lifting analysis was performed by assuming that the crane wire tip was fixed following the vessel motion at a chosen position for all simulations (*figure 5.9*), meaning that the stiffness of the crane wire as well as the active heave compensator that the vessel is equipped with is neglected. This is highly conservative and results in increased motions of the lifted structure resulting in larger hydrodynamic loads (inertia, damping, drag and slam) on the structure as indicated in the equation of motion of lifted objects (*eq. (2.3)*). The wave heading (within  $\pm 15^\circ$ ) that gave the largest loads on the lifted structure was waves approaching from the side that the vessel was being lifted. The waves were conservatively designed without spreading, since this would result in increased damping effect and dissipate the structural response (according to test simulations in OrcaFlex with number of wave directions= 3,5 and spreading exponents=6,10) which is increased when the spreading of waves increases.

On the other hand, the model used in the dynamic analysis was designed with less structural mass and volume than the “real” structure”. The estimated projected area is 49% and 32% for the “real” and simplified structure respectively (solid divided by silhouetted area), which is an increase of 53% (*APPENDIX G*). The estimated mass is 1523kN and 935kN for the “real” and simplified structure respectively which is an increase of 61%. By assuming that the hydrodynamic loads is proportional to the largest of projected area or the mass, the *dynamic design factor* or scaling factor (as defined in *eq. (5.25)*) should be larger than 1.6 to ensure that the slack sling criterion is satisfied. If the minimum dynamic sling loads are obtained using the Rayleigh distribution, this is (almost) satisfied for the worst levels of submergence ( $h_B=0\text{m}$  and  $h_B=1.8\text{m}$ ) for  $H_s \leq 2.5\text{m}$  giving a factor of 1.54 when following the Rayleigh distribution.

Since the structure is composed of tubular elements, the structure is considered relatively light compared to size making the slack wire criteria critical for the design. The members will be flooded during submergence, but the maximum crane wire tension is still considered small compared to the largest forces that the structure is designed for.

During subsea lifting operations, the structure will be (relatively) quickly submerged and it is normally sufficient to perform 30 minute simulations while keeping the structure at a constant “mean submerged depth” (Sarkar (2010)). When considering the structure as halfway submerged with respect to the mean water level ( $h_B=1.0\text{m}$ ), the structure could withstand the largest irregular wave in a three hour period ( $H_{\max}\approx 1.9H_S$ ) for sea states characterized by the JONSWAP spectra at  $H_S\leq 2.0\text{m}$ . In case of  $H_S=2.5\text{m}$ , the crane wire was verified according to both upper and lower criteria, but slack was observed in the slings (*APPENDIX I*). Based on *figure 5.28* one can see that the largest response in a three hour period is very large compared to average maximum values in a 30 minute simulation (including the largest wave in a 3h duration) and since it is very unlikely that the structure will be in the splash zone at that one point of time, it’s not necessary that the structure is designed to withstand the max possible load.

By using three different stochastically distributions and comparing them to the maximum crane wire tension for the level of submergence associated largest dynamic loads, the simplified structure was as verified for  $H_S\leq 3.0\text{m}$  and the real structure (by assuming proportional relation between hydrodynamic loads and mass was verified for  $H_S\leq 2.5\text{m}$ ).

### 5.5.1 Further work

The structure is modeled as a simplified framework using the “line function” in OrcaFlex. The “lines” are mainly used for dynamic analysis of flexible risers, pipes and cables which are not exposed to slam forces since they easily penetrate the sea-surface with negligible impact force. In order to account for slam, an idealized drag coefficient was introduced combining the drag and slam coefficient into one coefficient. This is considered conservative since the structure will be subjected to “slam” contributions in both upward and downward direction both during impact and when the wave crest is passing over structural parts. The structure should be compared to results obtained in different marine dynamic program like SIMO which is specially designed for time domain simulation for study of motions of multi-body systems such as the considered operation, (Sintef (2013)).

The motion of the crane tip (the top of the crane wire) was assumed fixed relative to the vessel motion, so that stiffness and active heave compensating effects in the crane is neglected. To obtain more realistic results the crane wire stiffness should be converted to an equivalent crane and crane wire tension and a heave compensator should be taken into the picture.

When the structure is lowered into water, the COG of the lifted object will change resulting in a tilt of the object (approximately 4 meter, ref. *section 4.2.2*). This is not accounted for in the dynamic analysis and will change the force distributions in the slings and should be checked in a dynamic analysis. Additionally, the pendulum motion of the lifted object before hitting the water should be considered by obtaining the resonant motion with respect to structural weight and wire length

## Chapter 6

### CONCLUSION

The primary objective of this thesis has been to examine the subsea lift of a complex framework designed to support three large spools that will be connecting a subsea template and a gas transporting pipeline. The framework also functions as a protection cover that will protect the spools from impact from trawlers and dropped objects after the spools are installed. A static analysis was performed using Staad.Pro to verify the structural integrity of the integrated spool cover according to Eurocode 3. To account for dynamic loads associated with the subsea lift in the static analysis, a dynamic amplification factor (DAF) was introduced to magnify the static loads. A dynamic analysis was necessary to determine maximum allowable limiting sea state in which the structure can be installed safely.

The static analysis reported a maximum utilization ratio of 80% where buckling of members was proven to be the critical failure mode for the most utilized members. The framework structure consist of main members (top and bottom chords) supported by transverse beams and braces supporting the chords. The interaction between members reduces the distance between zero moments in both top and bottom chords reducing the effective buckling length and increasing the maximum load that the structure can withstand. The eight temporary beams (as described in *section 3.3*) where therefore a necessary part of the design since they provided structural stability by reducing the effective buckling length. The structure was checked using a LRFD (load and resistance factor design) approach where the design loads was obtained by multiplying static load (self-weight) with relevant load factors, the SLF and DAF. From the static analysis, limiting sling forces and hook load where obtained and compared to forces obtained from the dynamic analysis performed in OrcaFlex.

According to the dynamic analysis, the structure could be installed in irregular waves characterized by the JONSWAP spectra with significant wave heights equal or less than 2.5 meter (not including uncertainties in weather forecast). The main focus of the dynamic analysis is to ensure that the maximum and minimum sling and crane wire loads are within the acceptance criteria making sure that they are not subjected to slack or larger forces than the structure can withstand which is represented by the DAF defined in the static analysis. The hydrodynamic forces on the lifted object are obtained by finding the sum of contributions from individual structural members with hydrodynamic coefficients representing the magnitude of the dynamic forces in the splash zone. Time domain analysis is performed comparing deterministic and stochastic values to obtain the limiting sea state for different wave headings, wave periods and significant wave heights which characterize the sea state in which the structure will be installed.

# Chapter 7

## REFERENCES

- Bullard E. (2013) *Physical properties of sea water*. National physical laboratory, Kaye & Laby. [[http://www.kayelaby.npl.co.uk/general\\_physics/2\\_7/2\\_7\\_9.html](http://www.kayelaby.npl.co.uk/general_physics/2_7/2_7_9.html), accessed; 15.06.13]
- Bentley (2013) *Structural Analysis & Design Engineering Software*. [<http://www.bentley.com/en-US/Products/STAAD.Pro/>, accessed; 15.06.13]
- Chakrabarti S.K. (2005) *Handbook of offshore engineering, Volume 1*. ISBN: 978-0-08-044568-7. Elsevier. Illinois, USA.
- Cormick, M. E. Mc., Kraemer, D. R. B., Hudson, D. R. B., Noble, W. (2002). *Analysis of the added mass of a barge in restricted water*. U.S. Army corps of Engineers. Washington.
- DOW (2013) DOW Ethylene Glycols, Physical properties, [<http://www.dow.com/ethyleneglycol/about/properties.htm>, accessed; 15.06.13]
- DNV (1996) *Rules for planning and execution of marine operations*, Pt.1 Ch.3. Det Norske Veritas. Høvik, Norge.
- DNV (1996) *Rules for planning and execution of marine operations*, Pt.2 Ch.5. Det Norske Veritas. Høvik, Norge.
- DNV-OS-C101 (2010) *DNV Offshore standard*, Design of offshore steel structures, General. Det Norske Veritas. Høvik, Norge.
- DNV-RP-C205 (2010) *DNV Recommended Practice, Environmental conditions and environmental loads*. Det Norske Veritas. Høvik, Norge.
- DNV-RP-H103 (2011) *DNV Recommended Practice, Modeling and Analysis of Marine Operations*. Det Norske Veritas. Høvik, Norge.
- Eurocode 3 (2005) Design of Steel Structures, Part 1-1: General rules and rules for buildings.*
- Eurocode 3 (2005) Design of Steel Structures, Part 1-8: Design of joints.*
- Elert G. (2013) *Viscosity. The physics hypertextbook*. [<http://physics.info/viscosity>, accessed; 15.06.13]
- Faltinsen, O.M. (1990). *Sea loads on ships and offshore structures*. ISBN: 0-521-37285-2. Cambridge University Press.
- Hosaas A. (2009) Engineering optimization by using the simplified Method for lifting through the splash zone. Subsea 7.
- Kim Y.S. W.B., Hong S.Y, Nam B.W. (2013) *Effects of Passive and Active Heave Compensators on Deepwater Lifting Operation*. Maritime & Ocean Engineering Research Institute, KIOST, Daejon, Korea.
- Kongsberg gruppen (2011), *internal document, Spool design, Feed*.

- NORSOK N-004 (2004) *NORSOK standard, Design of steel structures*. Norwegian Technology Centre. Majorstuen, Norge.
- NORSOK U-001 (2002) *NORSOK standard, Subsea production systems*. Norwegian Technology Centre. Majorstuen, Norge.
- Journée J.M.J. and Massie, W.W. (2001). *Offshore Hydrodynamics. First Edition*. Delft University of technology. The Netherlands.
- Li D.C. (2013). *Lecture notes, mechanics of solids, Chapter 9 Buckling of Columns*. School of Aerospace, Mechanical and Mechatronic Engineering.  
[<http://web.aeromech.usyd.edu.au/AMME2301/Documents/mos/Chapter09.pdf>, accessed; 15.06.13]
- Lovett (2008). *E-learning course, Buckling*.  
[<http://www.ejsong.com/mdme/modules/fea/beams.htm>, accessed; 15.06.13]
- OrcaFlex (2012) *OrcaFlex Manual, Version 9.6a*. Orcina. Cumbria.
- Prasad S. (1994). *Wave impact forces on a horizontal cylinder*. Department of Civil Engineering. The University of British Colombia.
- Rao, S. S. (2011). *Mechanical Vibrations*. ISBN: 13 978-981-06-8712-0. Pearson Education South Asia. Singapore.
- Redaelli tecna (2012) *Hi-Tech wire ropes for hoisting applications*. Redaelli Techa spa Divisione Cordati. Cologno Monzese
- Sarkar, A. and Gudmestad, O. T. (2010) *Splash Zone lifting analysis of subsea structures*. Document nr: OMAE2010-20489. 29<sup>th</sup> International Conference on Ocean, Offshore and Arctic Engineering, Shanghai, China.
- Sarpkaya T. (2010). *Wave forces on offshore structures*. ISBN: 978-0-521-89625-2. Cambridge University Press.
- Sintef (2013) *Software offshore hydrodynamics*. [<http://www.sintef.no/home/MARINTEK/About-MARINTEK/Departments/Offshore-Hydrodynamics/Oil-and-Gas/>, accessed; 15.06.13]
- Statoil (2009) *Compressed way to improve recovery*.  
[<http://www.statoil.com/en/NewsAndMedia/News/2009/Pages/6MayTechnology.aspx>, accessed; 15.06.13]
- Statoil (2012) *Enhanced recovery through subsea compression*.  
[[http://www.statoil.com/en/NewsAndMedia/News/2012/Pages/21May\\_Gullfaks\\_Compression.aspx](http://www.statoil.com/en/NewsAndMedia/News/2012/Pages/21May_Gullfaks_Compression.aspx), accessed; 15.06.13]
- Skandi Acergy (2012) *Skandi Acergy. Subsea 7 datasheet*.  
[[http://www.subsea7.com/content/dam/subsea7/documents/whatwedo/fleet/constructionvertical/Skandi\\_Acergy.pdf](http://www.subsea7.com/content/dam/subsea7/documents/whatwedo/fleet/constructionvertical/Skandi_Acergy.pdf), accessed; 15.06.13]
- Subsea 7 (2011). *Spool Installation Analysis Manual*. Subsea 7 internal document.
- Taylor, J.L. (1930). *Some hydrodynamical inertia coefficients*. Philos. Mag. 9. (161-183).
- Lerner R.G., Trigg G.L (1991). *Encyclopaedia of Physics, second Edition* . ISBN: 3-527-26954-1. VHC Publishers.





# APPENDIX A

## WEIGHT CALCULATIONS

### A.1 Spool weight

Table A.1, Cross sectional properties of spools

Spool size	OD [mm]	wt <sub>spool</sub> [mm]	wt <sub>goose</sub> [mm]	ct <sub>spool</sub> [mm]
12" spools (#1 and #3)	323.8	23.8	31.0	55.0
8" spool (#2)	219.1	15.9	15.9	40.0

Table A.2, Densities of materials

Description	Coefficients	Density [kg/m <sup>3</sup> ]
Density of coating ( <i>assumed weight</i> )	$\rho_{\text{coating}}$	1300
Density of spool content, MEG*	$\rho_{\text{MEG}}$	1115
Density of salt water	$\rho_{\text{sw}}$	1025
Density of super duplex 25%Cr steel	$\rho_{\text{steel}}$	7850

\* Density of MEG at 20<sup>0</sup>C = 1115kg/m<sup>3</sup> (DOW (2013))

The weight contributions for each pipe layer are calculated according to *eq. (A.1)*.

$$W_i = A_i \rho_i g \quad [kN/m] \quad (A.1)$$

Where  $W_i$  is the weigh,  $\rho_i$  is the density and  $A_i$  is the area of “i” as defined in *table A.2*.  $A_i$  is calculated according to *eq. (A.2)*. “g” is the gravity constant,  $g=9.81\text{m/s}^2$ .

$$A_i = \left( OD_i^2 - (OD_i - t_i)^2 \right) \frac{\pi}{4} \quad [m^2] \quad (A.2)$$

Where  $OD_i$  is the outer diameter and  $t_i$  it the thickness of “i”.

Table A.3, Weight of spools and goosenecks in water and air. (Values applied in Staad.Pro)

Spool (number)	Spool pipe [kN/m]	Coating [kN/m]	MEG [kN/m]	Displaced water [kN/m]	Weight in air [kN/m]	Submerged weight [kN/m]
12" spool (#1, #3)	1.73	0.83	0.66	1.49	3.22	1.73
12" gooseneck (#1, #3)	2.20	0.83	0.59	1.49	3.62	2.13
8" spool (#2)	0.78	0.42	0.30	0.71	1.50	0.79
8" gooseneck (#2)	0.78	0.42	0.30	0.71	1.50	0.79

Table A.4, Total weight of spools in water and air. (Values obtained from Staad.Pro)

Spool ( <i>number</i> )	Total weight in air [ <i>Te</i> ]	Total submerged weight [ <i>Te</i> ]
12" spool (#1)	34.69	20.08
8" spool (#2)	17.83	10.57
12" spool (#3)	35.16	20.33
<b>Total weight</b>	<b>87.7</b>	<b>51.0</b>

## A.2 Weight of integrated spool cover

The total weight of the integrated spool cover includes the following:

- Weight of steel members in framework structure.
- Weight of GRP grating protecting the spools from dropped during operation.
- Weight of trapped water during deployment before total submergence.
- Additional weight to account for extra materials needed for connecting the spools to the integrated cover. This includes weight of welds, rigging, paint and polyethylene plates to reduce friction between spools and cover as required for the tie in.
- Additional weight to account for weight of welds, joints and padayes needed to connect the members in the integrated cover, and lifting equipment.

### A.2.1 Weight of steel members

The framework structure is designed with tubular elements with sizes from 6'' to 10'' pipes. The structure will be partly filled with water before submergence, which is accounted for by including 50% trapped water in horizontal members when the structure is in splash zone. Weight of relevant steel members is given in *table A.5*.

Table A.5. Weight of framework sections. (Values applied in Staad.Pro)

Member	OD [ <i>mm</i> ]	wt [ <i>mm</i> ]	Trapped water	Weight trapped water [ <i>kN/m</i> ]	Weight in air [ <i>kN/m</i> ]	Submerged weight [ <i>kN/m</i> ]
10" pipe	273	12.7	50 %	0.24	0.80	0.70
8" pipe	219.1	8.2	50 %	0.16	0.42	0.36
6" pipe	168.3	7.1	50 %	0.09	0.28	0.24
HE240B	NA	NA	0 %	0.00	0.82	0.71

The member weights are accounted for in Staad.Pro by using the self-weight function in *staad.pro*. The members are calculated as waterfilled for submerged members. The weight of steel in water is given in *eq. (A.3)*.

$$W_{submerged} = W_{air} \left( 1 - \frac{\rho_{SW}}{\rho_{steel}} \right) \quad [kN/m] \quad (A.3)$$

Where  $W_{submerged}$  is the submerged weight,  $W_{air}$  is weight in air,  $\rho_{SW}$  is density of salt water and  $\rho_{steel}$  is density of steel.

### A.2.2 Weight of GRP grating

Assumed total weight of GRP is 20kg/m<sup>2</sup> in air and 6kg/m<sup>2</sup> in water. (glassfiber.no (Stangeland GRP))

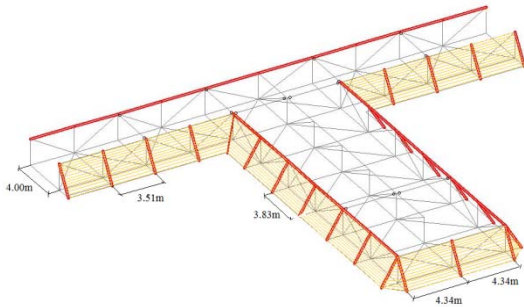


Figure A.1, GRP grating, trawlboards.

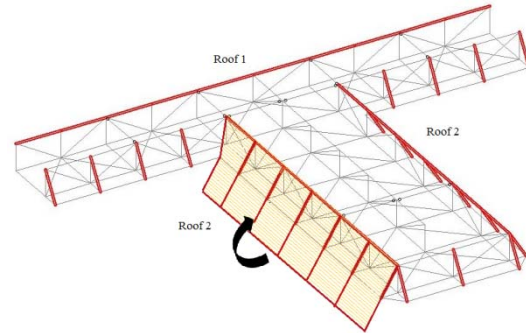


Figure A.2, GRP grating, roof.

$$W_{GRP} \left[ \frac{kN}{m} \right] = W_{GRP} \left[ \frac{kg}{m^2} \right] \cdot g \left[ \frac{m}{s^2} \right] \cdot L_{span} [m] \cdot 10^{-3} \quad (A.4)$$

Where  $W_{GRP}$  is the weight of the GRP grating,  $g$  is the acceleration constant (9.81m/s<sup>2</sup>) and  $L_{span}$  is the relevant span length to calculate applied weight of the GRP grating.

#### GRP grating, trawlboards:

To ensure that the structure doesn't get connected to overpassing trawlgear, GRP grating must be installed along the side of the structure with an angle less than 60 degrees (NORSOK U-001 (2002) 5.3.4). The GRP grating is needed to prevent the "snagloads" from overpassing trawlgear where the grating on the diagonal sides is illustrated in *figure A.1*.

The applied weight used as input in Staad.Pro is calculated according to the span length as calculated in *table A.6*.

#### GRP grating, roof:

To protect the pool after installation from dropped objects and trawlgear after installation, a GRP roof is needed on top of the structure. The GRP roof is attached to the structure as lids during installation hinged at the horizontal lines as in *figure A.2*.

The applied weight used as input in Staad.Pro is calculated according to the span length of each lid as calculated in *table A.6*.

Table A.6. GRP weight. (Values applied in Staad.Pro)

Description	Staad.Pro name	Span length, $L_{span} [m]$	Distributed weight, $W_{GRP.air} [kN/m]$	Distributed weight, $W_{GRP.water} [kN/m]$
GRP grating, trawlboards	_SIDE_TRAWL	3.83	0.75	0.23
GRP grating, roof 1	_TOP_GRP1	4.00	0.78	0.24
GRP grating, roof 2	TOP_GRP2	4.34	0.85	0.26

### A.2.3 Additional weight

To account for extra weight for rigging, paint and connections between spools and integrated cover, additional weight is applied.

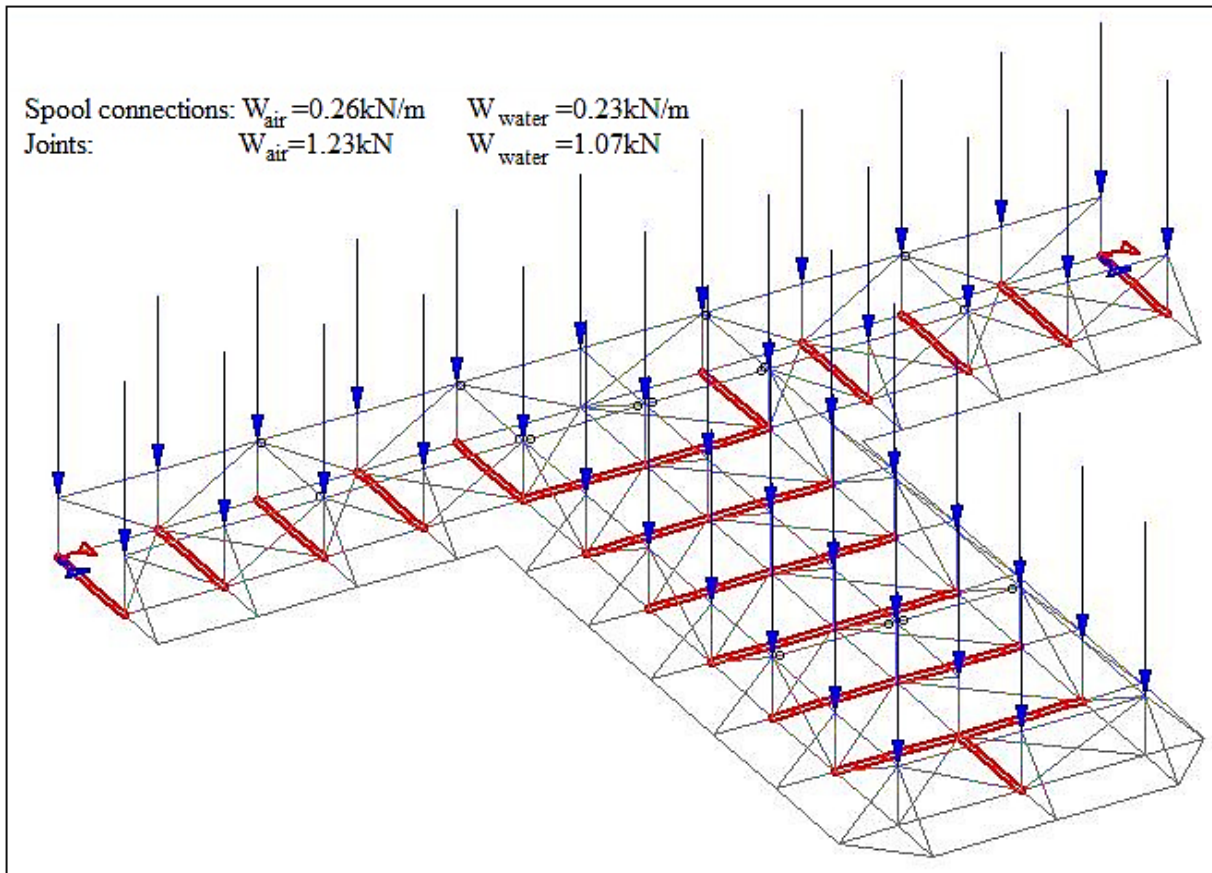


Figure A.3. Additional weight

#### **Additional weight of spool connections:**

The spools will be installed on polyethylene plates located on top of the transverse beams of the structure in order to reduce friction between the spools and the cover as required for the tie-in. In order to account for weight of welds, rigging, paint and the polyethylene plates, additional weight will be applied to the structure and will be evenly distributed on the bottom transverse beams supporting the three spools.

The assumed weight for spool connections are  $2.2T_e$  and are evenly distributed along the red lines illustrated in *figure A.3*. The applied weight in Staad.Pro is given in the same picture for weight in air and in water. The additional weights are assumed the same as steel in water and are calculated according to *eq. (A.4)*.

#### **Additional weight of rigging:**

To account for additional weight of welds, joints and padayes, additional weight of  $5T_e$  is added and distributed over 40 connection points as vertical point loads as illustrated in *figure A.3*. The additional weights are assumed the same as steel in water and are calculated according to *eq. (A.4)*.

### A.3 System weight

The total weight of the system is found by using Staad.Pro. Different weight contributions and total system weight are obtained and illustrated in *table A.7*.

Table A.7. System weight summary

Part	Description	Weight in air [Te]	Submerged weight [Te]
Spools	Weight of steel pipes	42.1	36.6
	Weight of coating	19.9	4.2
	Weight of content (MEG)	15.3	1.2
	Weight of termination heads	10.4	9.0
	Total weight of spools	88	51
Integrated cover	Weight of steel members	48.0	41.8 <sup>(3)</sup>
	GRP weight	11.2	3.4 <sup>(4)</sup>
	Additional weight <sup>(1)</sup>	2.2	2.0 <sup>(3)</sup>
	Additional weight <sup>(2)</sup>	5.0	4.4 <sup>(3)</sup>
	Total weight of cover	66	51
<b>Total static weight of system</b>		<b>154</b>	<b>103</b>

NOTES:

<sup>(1)</sup> Assumed additional weight to account for weight of welds, rigging, paint and polyethylene plates (to reduce friction between spool and cover as required for the tie in. The additional weight is uniformly distributed along the 23 transvers bottom members.

<sup>(2)</sup> Assumed additional weight to account for weight of welds, joints and padayes. The weight is distributed as vertical point loads over 40 joint connections located on top of the structure.

<sup>(3)</sup> Weight of steel members in water is calculated when all members are filled with water so that  $W_{\text{submerged}} = W_{\text{air}} * 0.87$ . Assume that all additional weight has same density as steel.

<sup>(4)</sup>  $W_{\text{grp.submerged}} = W_{\text{grp.air}} * 0.3$



# APPENDIX B

## SENSITIVITY ANALYSIS, SKL-FACTOR:

### B.1 General

The skew load factor is chosen 1.25 for the design according to DNV (DNV (1996) Sec.2.3)). This is applicable for 4 point statically indeterminate lifts with sling length tolerances less than 0.15%. The skew load factor is needed to account for all uncertainties in sling lengths (including displacements in connection points), and may be calculated based on sling fabrication tolerances given in DNV (DNV (1996) Sec.3.1.5).

The skew load factor will be checked by performing a sensitivity analysis in Staad.Pro where the sling lengths are changed by moving the hook node in different directions inside a “hook position envelope” as illustrated in *figure B.1*. The size doesn’t need to be related to the main structure dimensions and is chosen to be 2x2x2 m (considered very large).

The hook position will be moved to the outer points of the rectangular (point 1 to 5) and maximum utilized member and sling forces will be compared to the static load condition when the hook is placed at the center of gravity (point 0).

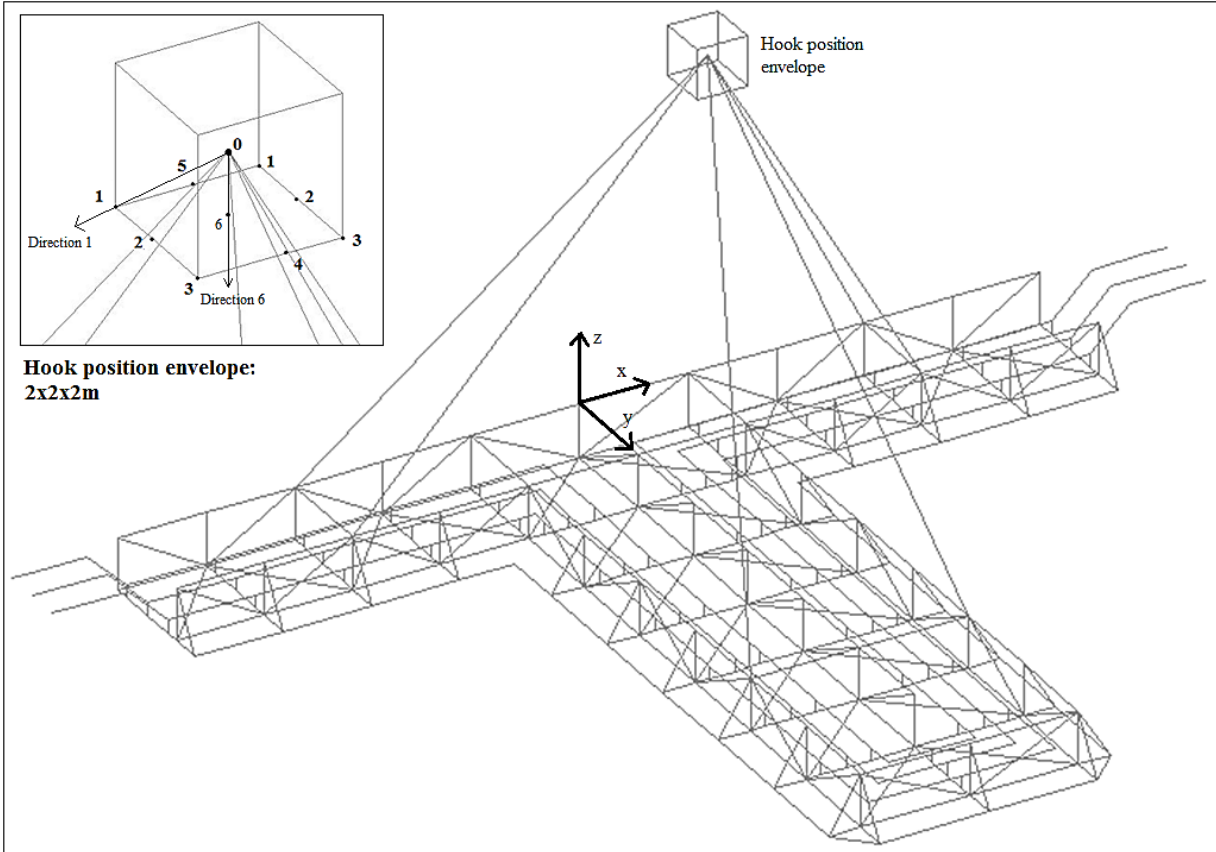


Figure B.1. Hook position envelope

## B.2 Hook position envelope

By moving the hook to the outer nodes of the “hook position envelope” (*figure B.1*). The load distribution in the structure will change as well as the utilization ratios for individual members. The goal of this test is to check how large impact a change in the sling lengths will have on the structure. This is checked by comparing the most utilized beams after the hook-displacement with the utilization ratio of the same members when the structure is stable. The deviation in percent will represent the structural impact of the hook-displacement.

The static load condition in air (load combination 100) is considered when comparing the utilization ratios since this is the basis for all applied load factors.

*Table B.1* shown the utilization ratios for beams with highest loading after the hook node is moved according to the hook-position envelope defined in *figure B.1*. The max deviation between the stable hook position (0) and the relevant hook position is calculated for all positions of the hook node.

Table B.1. Utilization ratios for hook position envelope. (Values obtained from Staad.Pro)

Position	Coordinate ( $\Delta x, \Delta y, \Delta z$ ) [m]	Member number (as defined in Staad.Pro)					
		209	274	250	368	371	503
0	(0, 0, 0)	0.255	0.315	0.258	0.263	0.286	0.274
1	(-1, -1, -1)	<b>0.323</b>	<b>0.401</b>	0.246	0.253	0.291	<b>0.28</b>
2	(-1, 0, -1)	0.286	0.348	0.263	0.281	0.293	0.275
3	(-1, 1, -1)	0.248	0.296	<b>0.28</b>	<b>0.309</b>	<b>0.297</b>	0.271
4	( 0, 1, -1)	0.222	0.274	<b>0.28</b>	0.304	0.289	0.269
5	( 0, -1, -1)	0.297	0.378	0.245	0.249	0.285	0.279
6	( 0, 0, -1)	0.259	0.326	0.262	0.277	0.287	0.274
Max utilization [-]		0.323	0.401	0.280	0.309	0.297	0.280
Max deviation [%]		27%	27%	9%	17%	4%	2%

The interest of the sensitivity test is to see how sensitive the structure is to sudden changes, making member 274 and hook position “1” the critical load case for the analysis (member 209 shows similar increased utilization, but beam 274 has larger utilization ratio and is therefore more critical). The critical beams are illustrated in *figure B.2*. The max deviation is calculated according to the max values obtained from *eq. (B.1)*.

$$\text{Max deviation} = \frac{u_{ij} - u_{0j}}{u_{0j}} \% \quad (B.1)$$

Where  $u_{ij}$  is the utilization ratio for hook-position “i” and member “j”, and  $u_{0j}$  is the utilization ratio for the stable condition and member “j”.



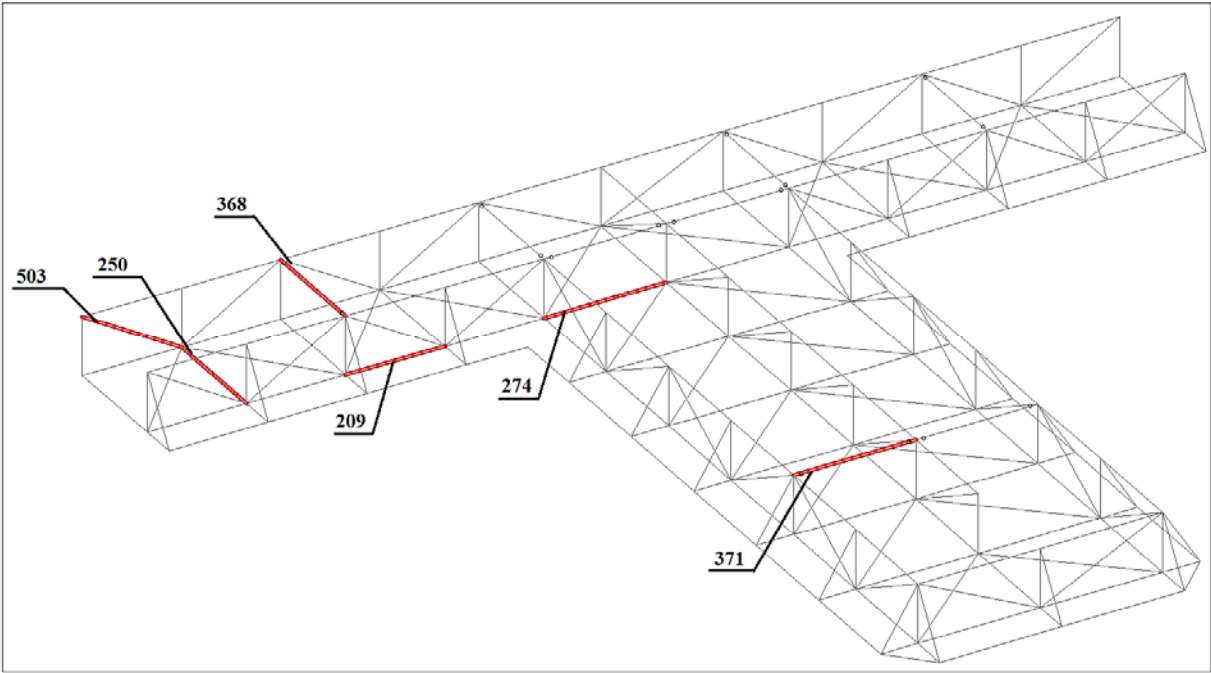


Figure B.2. Critical beams.

### B.3 Sensitivity analysis

From the hook-position envelope it is observed that the highest increase in utilization ratios for the structure happens when the hook is displaced towards point 1 (illustrated in *figure B.1*). The sensitivity analysis is therefore performed for hook position changes in two directions: Movement in, “direction 1” and “direction 6” as they are illustrated in *figure B.1*. “Direction 1” is considered the most “sensitive” direction and “direction 6” is considered to check how the forces in the structure behave when the vertical hook position changes.

Beam 274 is the most utilized members for displacement in “direction 1” and “direction 6” respectively for static lift in air. How the utilization ratios changes relative to the hook displacement are illustrated in *figure B.3*, where *eq. (B.1)* is used to find the deviation.

The skew load factor was chosen 1.25 which means that the structure is designed to tolerate a sling displacement that gives a 25% increase in utilization ratio for the structure (or structural beams). *Figure B.3* illustrates how much the hook position can be moved before this increase is reached for the relevant beams.

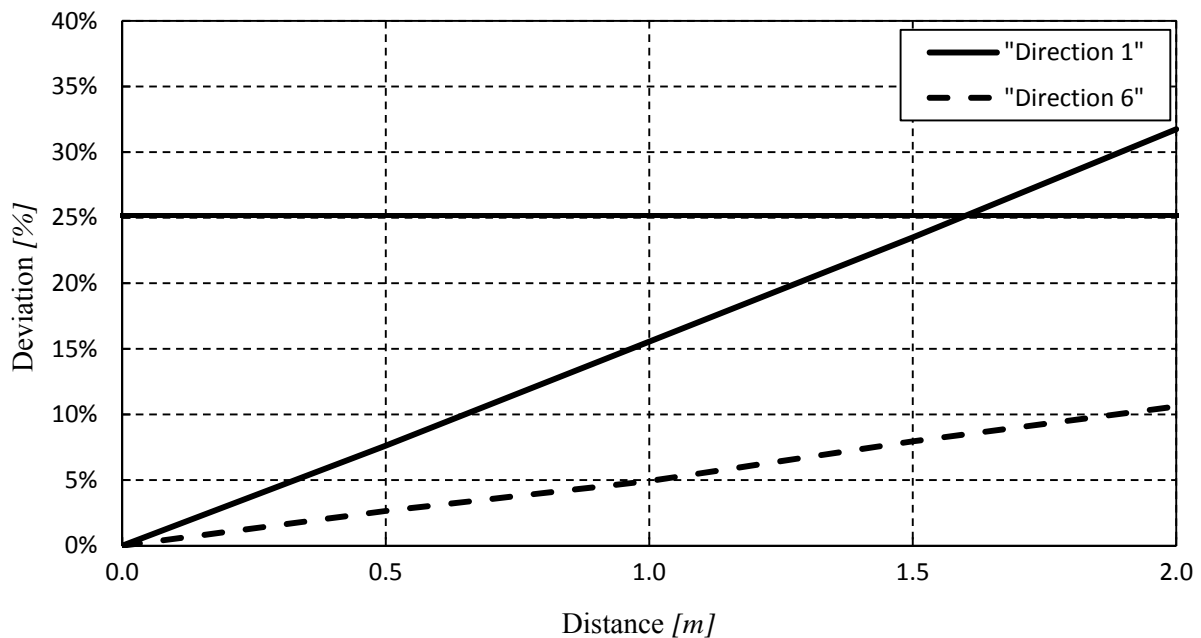
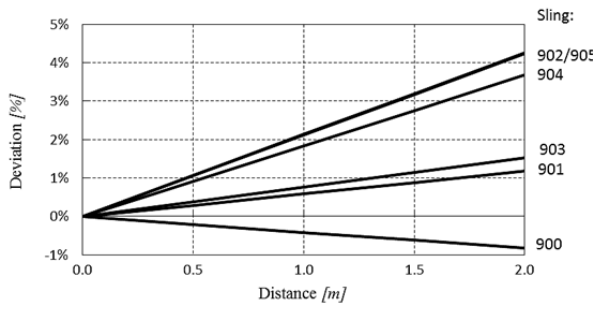
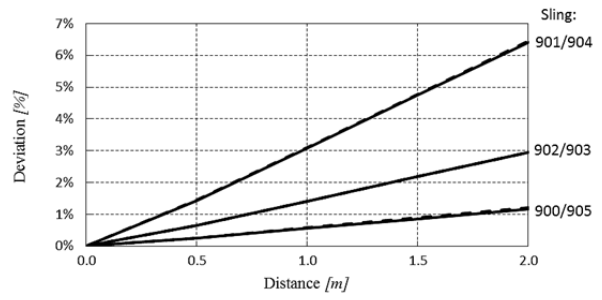


Figure B.3. Change in utilization ratios due to movement of hook-position in “direction 1” and “direction 6”. The directions are illustrated in *figure B.1*.

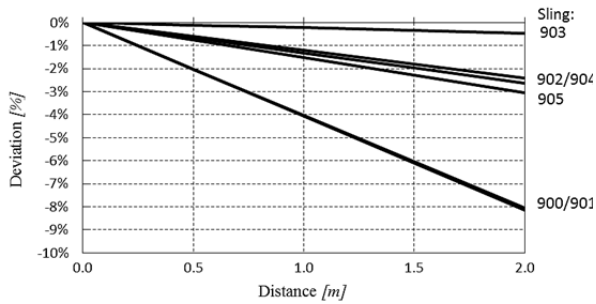
By observing *figure B.3*, one can see that the hook can be displaced by approximately 1.7 meters without reaching the additional load that is accounted for by adding a skew load factor of 1.25 for the structure in the most sensitive direction. The relevant sling elongations are illustrated in *figure B.4*.



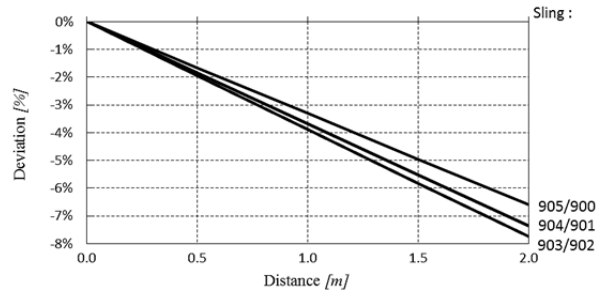
Change in sling loads due to movement of hook-position in “direction 1”.



Change in sling loads due to movement of hook-position in “direction 2”.



Sling elongation due to movement of hook-position in “direction 1”.



Sling elongation due to movement of hook-position in “direction 2”.

Figure B.4. Change in sling loads and sling elongation due to movement of hook-position.

According to DNV (DNV (1996) 3.1.4.2) the maximum tolerated sling elongation is 0.15% which occurs at a displacement less than 0.1m for all slings for all considered load cases. This means that the critical displacement of slings represent a small change in loads in the sling (less than 1%. see *figure B.4*) and a small change in utilization ratio (less than 5%. See *figure B.5*).

The structure is not very sensitive to sling elongations due to the flexibility of the framework and the selected skew load factor of 1.25 is considered very conservative for the design.



# APPENDIX C

## BUCKLING LENGTHS

This appendix is necessary to determine effective buckling lengths for critical main members that is illustrated in *figure C.1*. Be aware that y is pointing upwards and z is pointing in lateral direction due to how the structure is defined in Staad.Pro. This is the opposite as the axes defined in *figure B.1*.

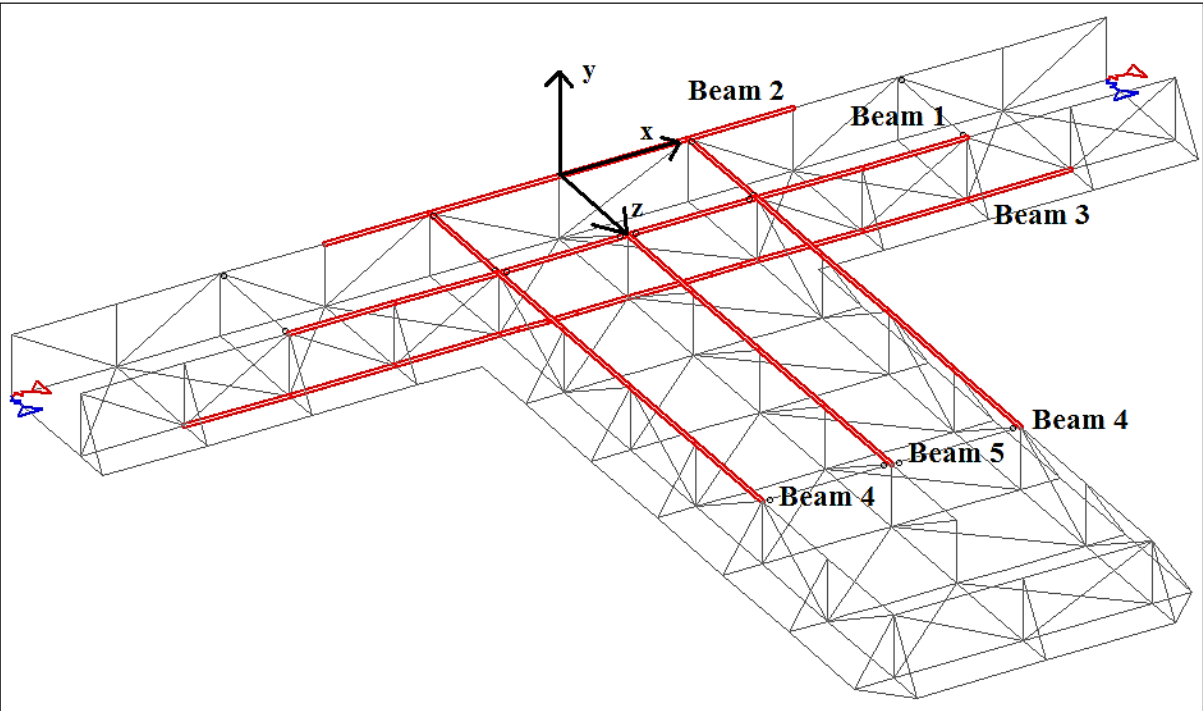


Figure C.1: Main members subjected to buckling.

The moment diagrams in *figure C.2* to *figure C.5* illustrates bending moment diagrams for the main members that are illustrated in *figure C.1*. The maximum zero-moment distance as well as length of compressed part of the members are given in the figures for moment around both z and y axis. These lengths are used for comparison to buckling lengths obtained in *section 4.2.3*.

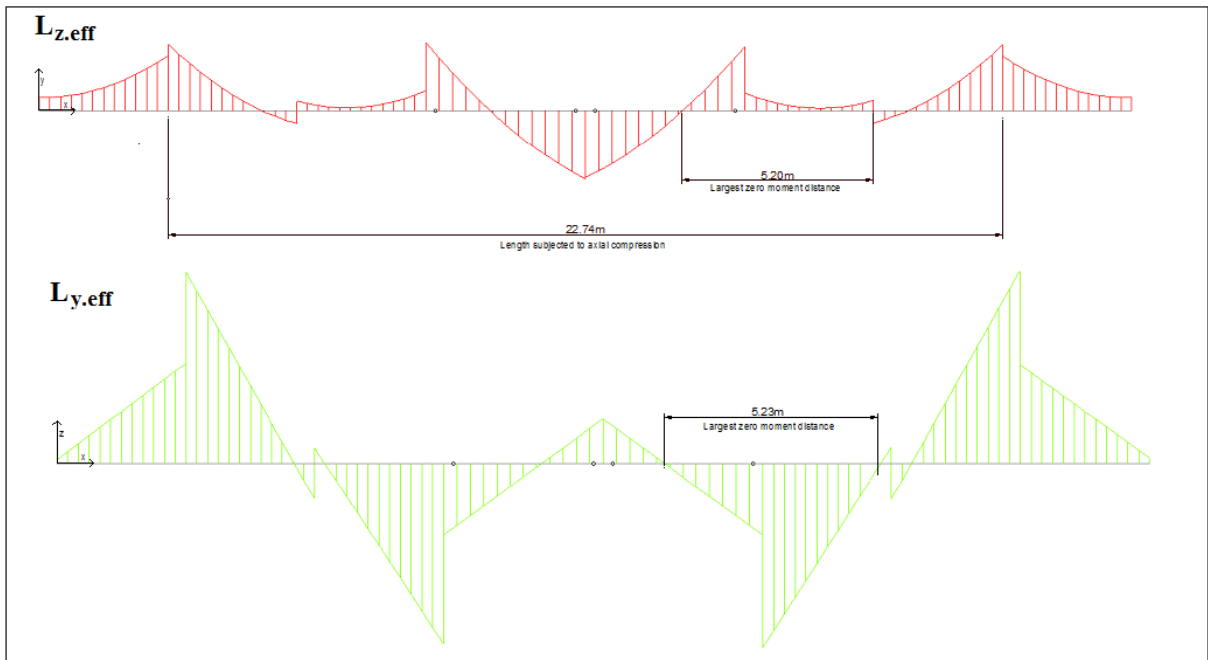


Figure C.2: Bending moment diagrams, "BEAM 1". Bending in both y and z axis, (from Staad.Pro).

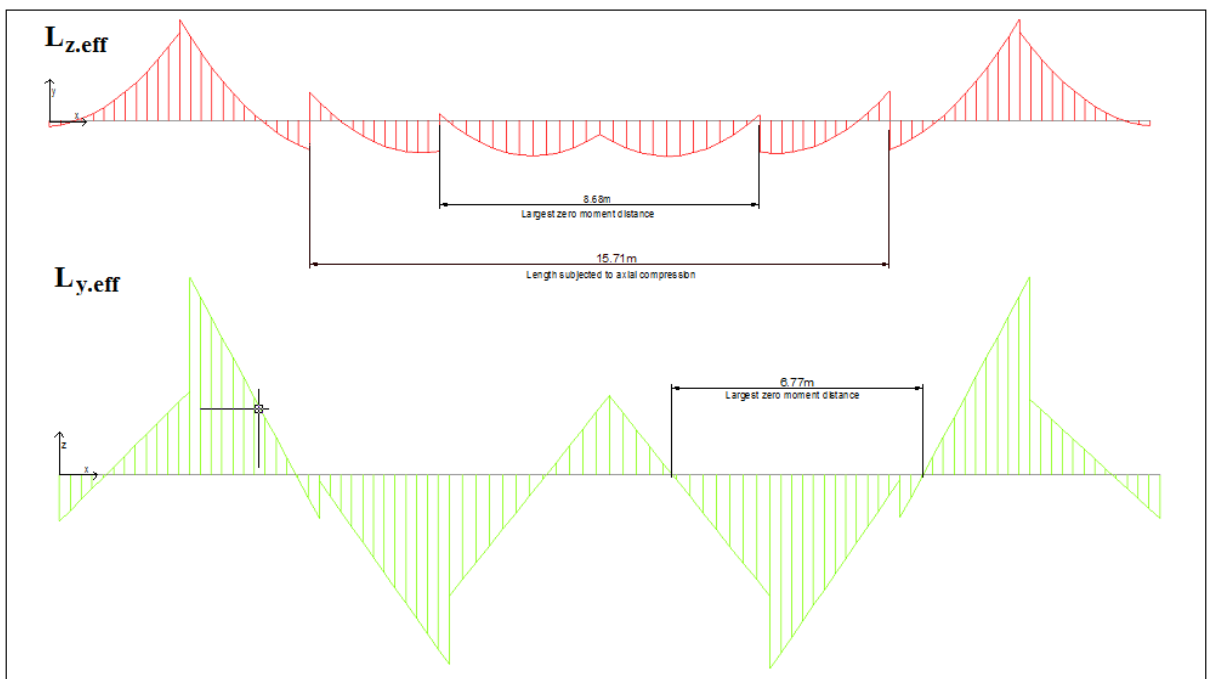


Figure C.3: Bending moment diagrams, "BEAM 2". Bending in both y and z axis, (from Staad.Pro).

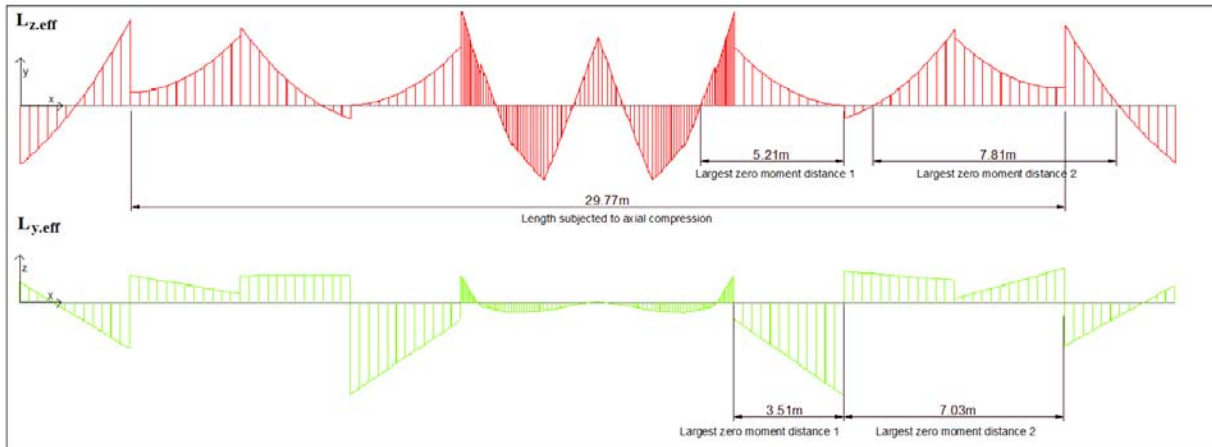


Figure C.4: Bending moment diagrams, “BEAM 3”. Bending in both y and z axis, (from Staad.Pro).”

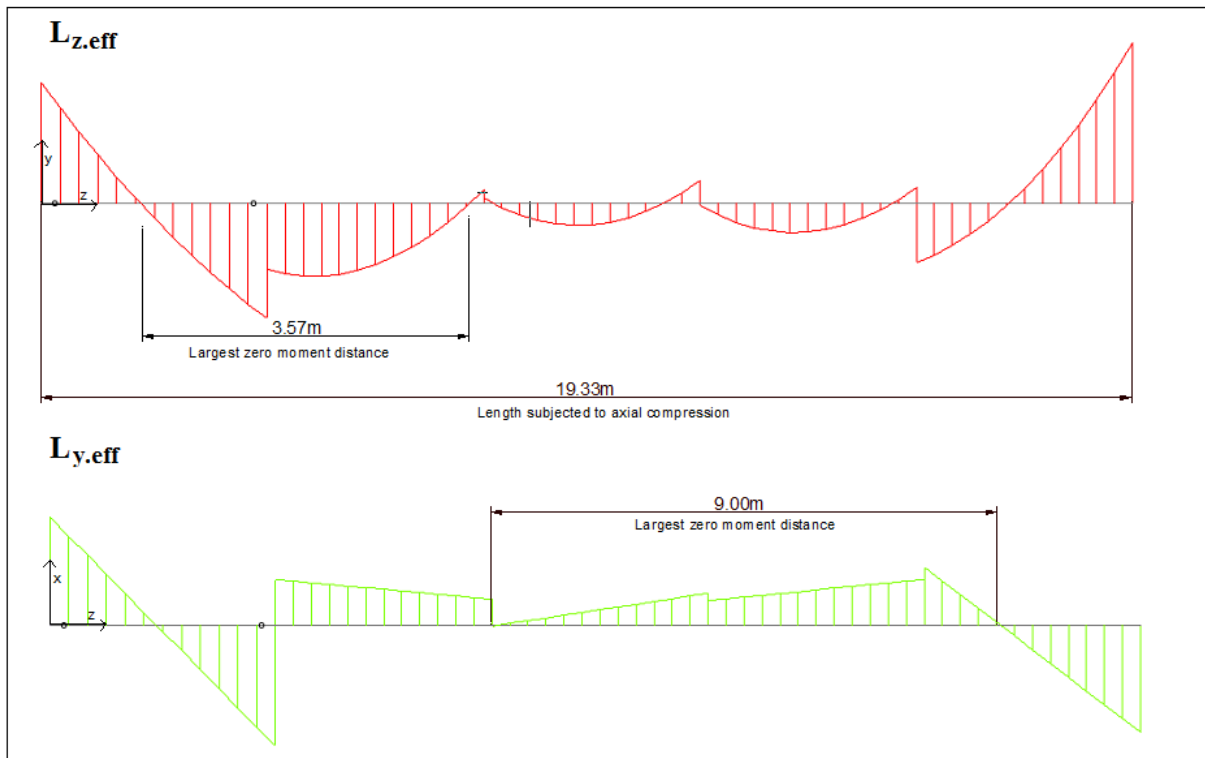


Figure C.5: Bending moment diagrams, “BEAM 4”. Bending in both y and z axis, (from Staad.Pro).





## **APPENDIX D**

### **GLOBAL BUCKLING CHECK OF INTEGRATED SPOOL COVER**

#### **D.1 Introduction**

##### **Scope**

The scope of this calculation is to verify the global buckling capacity of the structure.

##### **Analysis methodology**

The following approach is used to verify the global buckling capacity of the structure.

1. Determine cross sectional properties for the truss
2. Determine the global load picture of the truss
3. Perform a manual buckling capacity check (Euler) according to Eurocode 3

##### **About Mathcad**

The technical calculation software used is MATHCAD 15.0

Calculations are self-explanatory, but the following symbols/expressions may require

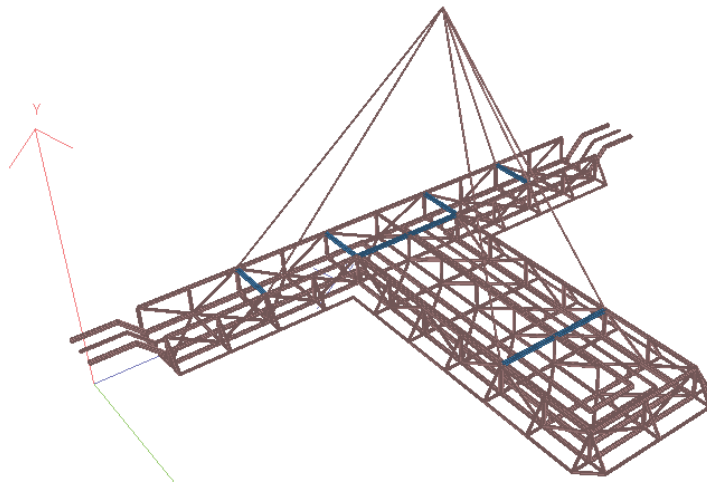
further clarification:

- :=** denotes the definition of a parameter or formula
- =** denotes the recall of a parameter or executes an actual calculation

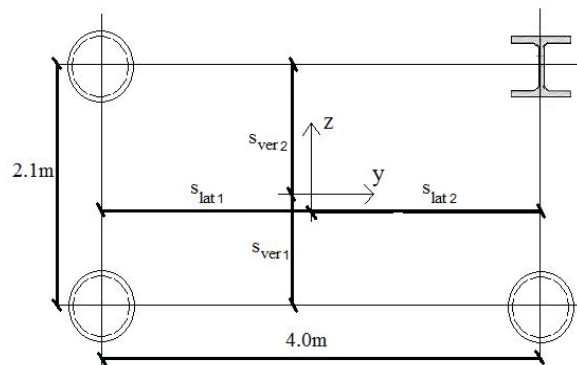
## D.2 Properties of truss "Beam"

The integrated spool cover has been checked for all load combinations using Staad.Pro software. The software is not able to check the global buckling capacity, and the calculation is done manually by considering the framework as a simple beam with equivalent forces found in the Staad.Pro model.

All calculations performed according to eurocode 3, EN-1993-1-1:2005.



Staad.pro model, 3d rendering



Simplified truss beam

\*Considering the cross sectional properties at the weakest cross section where the truss beam connects to the cantilevered part of the integrated spool cover.

## D.2.1 Chord properties

### Pipe properties, 10" pipe:

Outer diameter:		OD := 273mm
Wall thickness:		wt := 20.7mm
Inner diameter:	ID := OD - 2·wt	ID = 231.6·mm
Area:	$A_{x1} := \pi \cdot \frac{(OD^2 - ID^2)}{4}$	$A_{x1} = 1.641 \times 10^4 \text{ mm}^2$
Second moment of inertia:	$I_{y1} := \pi \cdot \frac{(OD^4 - ID^4)}{64}$	$I_{y1} = 1.314 \times 10^8 \text{ mm}^4$
	$I_{z1} := I_{y1}$	$I_{z1} = 1.314 \times 10^8 \text{ mm}^4$

### Sectional properties, HE240B, ref. Stålkatalogen table 1.3

Area:	$A_{x2} := 10.6 \cdot 10^3 \text{ mm}^2$
Second moment of inertia:	$I_{y2} := 112.6 \cdot 10^6 \text{ mm}^4$
	$I_{z2} := 39.2 \cdot 10^6 \text{ mm}^4$

### Chord layout:

Vertical distance between chords:	$z_1 := 2.1\text{m}$
Lateral distance between chords:	$y_1 := 4.0\text{m}$
Number of bottom pipe chords (and "left" pipe chord)	$n_1 := 2$
Number of top pipe chords (and "right" pipe chord)	$n_2 := 1$
Number of top HEB chords (and "right" pipe chord)	$n_3 := 1$

## D.2.2 Calculation of area center of location

Vertical center of area:	$z_e := \frac{(n_2 \cdot A_{x1} + n_3 \cdot A_{x2}) \cdot z_1}{n_1 \cdot A_{x1} + n_2 \cdot A_{x1} + n_3 \cdot A_{x2}}$	$z_e = 0.948 \cdot \text{m}$
Lateral center of area:	$y_e := \frac{(n_2 \cdot A_{x1} + n_3 \cdot A_{x2}) \cdot y_1}{n_1 \cdot A_{x1} + n_2 \cdot A_{x1} + n_3 \cdot A_{x2}}$	$y_e = 1.806 \cdot \text{m}$

### D.2.3 Area

Area:

$$A_x := n_1 \cdot A_{x1} + n_2 \cdot A_{x1} + n_3 \cdot A_{x2} \quad A_x = 5.982 \times 10^4 \text{ mm}^2$$

$$A_y := n_1 \cdot \frac{A_{x1}}{2} + n_2 \cdot \frac{A_{x1}}{2} + n_3 \cdot \frac{A_{x2}}{2} \quad A_y = 2.991 \times 10^4 \text{ mm}^2$$

$$A_z := A_y \quad A_z = 2.991 \times 10^4 \text{ mm}^2$$

### D.2.4 Second moment of area

Bottom chord distance from area center:  $s_{\text{ver.1}} := z_e \quad s_{\text{ver.1}} = 0.948 \cdot m$

Top chord distance from area center:  $s_{\text{ver.2}} := z_1 - z_e \quad s_{\text{ver.2}} = 1.152 \cdot m$

Left chord distance from area center:  $s_{\text{lat.1}} := y_e \quad s_{\text{lat.1}} = 1.806 \cdot m$

Right chord distance from area center:  $s_{\text{lat.2}} := y_1 - y_e \quad s_{\text{lat.2}} = 2.194 \cdot m$

Second moment of area with steiners contribution:

$$I_y := n_1 \cdot (I_{y1} + s_{\text{ver.1}}^2 \cdot A_{x1}) + n_2 \cdot (I_{y1} + s_{\text{ver.2}}^2 \cdot A_{x1}) + n_3 \cdot (I_{y2} + s_{\text{ver.2}}^2 \cdot A_{x2})$$

$$I_y = 6.584 \times 10^{10} \text{ mm}^4$$

$$I_z := n_1 \cdot (I_{z1} + s_{\text{lat.1}}^2 \cdot A_{x1}) + n_2 \cdot (I_{z1} + s_{\text{lat.2}}^2 \cdot A_{x1}) + n_3 \cdot (I_{z2} + s_{\text{lat.2}}^2 \cdot A_{x2})$$

$$I_z = 2.375 \times 10^{11} \text{ mm}^4$$

### D.2.5 Section modulus

Section modulus:

$$W_y := \max\left(\frac{I_y}{s_{\text{ver.2}}}, \frac{I_y}{s_{\text{ver.1}}}\right) \quad W_y = 6.945 \times 10^7 \cdot \text{mm}^3$$

$$W_z := \max\left(\frac{I_z}{s_{\text{lat.2}}}, \frac{I_z}{s_{\text{lat.1}}}\right) \quad W_z = 1.315 \times 10^8 \cdot \text{mm}^3$$

## D.3 Global load picture on truss beam

### D.3.1 Selfweight

Dynamic weight due to load case 115 lift in air from Staad.Pro analysis

$$\text{Beam 1, main beam} \quad Q_1 := \frac{1685 \text{ kN}}{36.8 \text{ m}} \quad Q_1 = 45.788 \cdot \frac{\text{kN}}{\text{m}}$$

$$\text{Beam 2} \quad Q_2 := \frac{1962 \text{ kN}}{25.08 \text{ m}} \quad Q_2 = 78.23 \cdot \frac{\text{kN}}{\text{m}}$$

$$\text{Beam 3, gooseneck/termin.*} \quad Q_3 := \frac{208 \text{ kN}}{4.6 \text{ m}} \quad Q_3 = 45.217 \cdot \frac{\text{kN}}{\text{m}}$$

\*The beam 3 load case includes all weight from the spool part that stick out from the integrated spool cover (pipe section, termination head, coating, etc.).

### D.3.2 Hook and padeye coordinates

$$\text{Hook coordinates:} \quad x_{\text{hook}} := 23\text{m} \quad y_{\text{hook}} := 5.48\text{m} \quad z_{\text{hook}} := 20\text{m}$$

$$\text{Sling coordinates:} \quad x_{900} := 11.63\text{m} \quad y_{900} := -3.4\text{m} \quad z_{900} := 1.6\text{m}$$

$$x_{901} := 11.63\text{m} \quad y_{901} := 0.6\text{m} \quad z_{901} := 1.6\text{m}$$

$$x_{902} := 18.66\text{m} \quad y_{902} := 15.93\text{m} \quad z_{902} := 1.6\text{m}$$

Due to structure symmetry, the loads in sling 905, 904 and 903 will be equal the loads in sling 900, 901 and 902 respectively

### D.3.3 Sling force

Dynamic sling loads due to load case 115 lift in air from Staad.Pro analysis

$$\text{Sling forces:} \quad \begin{pmatrix} \text{Sling900} \\ \text{Sling901} \\ \text{Sling902} \end{pmatrix} \quad F_{\text{sling}} := \begin{pmatrix} 517 \\ 1022 \\ 907 \end{pmatrix} \text{ kN}$$

### D.3.4 Sling angles

Vertical angles:

$$\phi_{\text{sling}} := \begin{bmatrix} \text{atan} \left[ \frac{z_{\text{hook}} - z_{900}}{\sqrt{(y_{\text{hook}} - y_{900})^2 + (x_{\text{hook}} - x_{900})^2}} \right] \\ \text{atan} \left[ \frac{z_{\text{hook}} - z_{901}}{\sqrt{(y_{\text{hook}} - y_{901})^2 + (x_{\text{hook}} - x_{901})^2}} \right] \\ \text{atan} \left[ \frac{z_{\text{hook}} - z_{902}}{\sqrt{(y_{\text{hook}} - y_{902})^2 + (x_{\text{hook}} - x_{902})^2}} \right] \end{bmatrix}$$

$$\begin{pmatrix} \text{Sling900} \\ \text{Sling901} \\ \text{Sling902} \end{pmatrix} \quad \phi_{\text{sling}} = \begin{pmatrix} 0.906 \\ 0.979 \\ 1.019 \end{pmatrix} \text{ rad}$$

\*The vertical angles are given by the geometrical relation  $\phi_{1\text{sling}}$  and is measured from the global horizontal plane, xy. (Where z is the vertical direction)

$$\phi_{1\text{sling}} := \arctan \left( \frac{z}{y^2 + x^2} \right)$$

Horizontal angles:

$$\beta_{\text{sling}} := \begin{pmatrix} \text{atan} \left( \frac{x_{\text{hook}} - x_{900}}{y_{\text{hook}} - y_{900}} \right) \\ \text{atan} \left( \frac{x_{\text{hook}} - x_{901}}{y_{\text{hook}} - y_{901}} \right) \\ \text{atan} \left( \frac{x_{\text{hook}} - x_{902}}{y_{\text{hook}} - y_{902}} \right) + \pi \end{pmatrix}$$

$$\begin{pmatrix} \text{Sling900} \\ \text{Sling901} \\ \text{Sling902} \end{pmatrix} \quad \beta_{\text{sling}} = \begin{pmatrix} 0.908 \\ 1.165 \\ 2.748 \end{pmatrix} \text{ rad}$$

\*The horizontal angles are given by the geometrical relation  $\beta_{1\text{sling}}$  and is measured from the global vertical plane, zy. (Where z is the vertical direction).

$$\beta_{1\text{sling}} \equiv \arctan \left( \frac{x}{y} \right)$$

### D.3.5 Force components in connection points

$$\text{Horizontal force components} \quad F_h := \begin{pmatrix} F_{\text{sling}_0} \cdot \cos(\phi_{\text{sling}_0}) \\ F_{\text{sling}_1} \cdot \cos(\phi_{\text{sling}_1}) \\ F_{\text{sling}_2} \cdot \cos(\phi_{\text{sling}_2}) \end{pmatrix} \quad F_h = \begin{pmatrix} 318.998 \\ 570.292 \\ 475.122 \end{pmatrix} \cdot \text{kN}$$

$$\text{Vertical force components} \quad F_z := \begin{pmatrix} \left[ (F_{\text{sling}_0})^2 - (F_{h_0})^2 \right]^{0.5} \\ \left[ (F_{\text{sling}_1})^2 - (F_{h_1})^2 \right]^{0.5} \\ \left[ (F_{\text{sling}_2})^2 - (F_{h_2})^2 \right]^{0.5} \end{pmatrix} \quad F_z = \begin{pmatrix} 406.853 \\ 848.086 \\ 772.598 \end{pmatrix} \cdot \text{kN}$$

$$\text{Force in global x-direction} \quad F_x := \begin{pmatrix} F_{h_0} \cdot \sin(\beta_{\text{sling}_0}) \\ F_{h_1} \cdot \sin(\beta_{\text{sling}_1}) \\ F_{h_2} \cdot \sin(\beta_{\text{sling}_2}) \end{pmatrix} \quad F_x = \begin{pmatrix} 251.408 \\ 524.062 \\ 182.232 \end{pmatrix} \cdot \text{kN}$$

$$\text{Force in global y-direction} \quad F_y := \begin{pmatrix} F_{h_0} \cdot \cos(\beta_{\text{sling}_0}) \\ F_{h_1} \cdot \cos(\beta_{\text{sling}_1}) \\ F_{h_2} \cdot \cos(\beta_{\text{sling}_2}) \end{pmatrix} \quad F_y = \begin{pmatrix} 196.351 \\ 224.927 \\ -438.785 \end{pmatrix} \cdot \text{kN}$$

### D.3.6 Eccentric moments

Eccentric distance from connection points to truss neutral axis for main beam

$$\text{Eccentric moments about transvers axis:} \quad M_y := F_{x_0} \cdot s_{\text{ver}.2} + F_{x_1} \cdot s_{\text{ver}.2} \quad M_y = 893.288 \cdot \text{kN} \cdot \text{m}$$

$$\text{Eccentric moments about vertical axis:} \quad M_z := F_{x_0} \cdot s_{\text{lat}.1} - F_{x_1} \cdot s_{\text{lat}.2} \quad M_z = -695.867 \cdot \text{kN} \cdot \text{m}$$

$$\text{Eccentric (torsional) moments about lateral axis:} \quad M_x := (-F_{z_1} \cdot s_{\text{lat}.2} + F_{z_0} \cdot s_{\text{lat}.1}) + (F_{y_1} \cdot s_{\text{lat}.2} + F_{y_0} \cdot s_{\text{lat}.1})$$

\*All loads are based on the dynamic load case 115, lift in air from Staad.Pro where the total applied load factors are  $\gamma_{d,\text{spool}}=2.35$  and  $\gamma_{d,\text{cover}}=2.66$  for spool and cover respectively.

## D.4 Forces applied in Staad.Pro beam model

### D.4.1 Distributed load

$$Q_1 = 45.788 \cdot \frac{\text{kN}}{\text{m}}$$

$$Q_2 = 78.23 \cdot \frac{\text{kN}}{\text{m}}$$

$$Q_3 = 45.217 \cdot \frac{\text{kN}}{\text{m}}$$

### D.4.2 Point loads

$$F_1 := F_{y_0} + F_{y_1}$$

$$F_1 = 421.278 \cdot \text{kN}$$

$$F_2 := -F_{y_2}$$

$$F_2 = 438.785 \cdot \text{kN}$$

Deviation between  $F_1$  and  $F_2$

$$\text{dev}_1 := \frac{(F_2 - F_1) \cdot 100}{F_2}$$

$$\text{dev}_1 = 3.99 \%$$

\*The deviation should be 0

### D.4.3 Eccentric moments

$$M_y = 893.288 \cdot \text{kN} \cdot \text{m}$$

$$M_z = -695.867 \cdot \text{kN} \cdot \text{m}$$

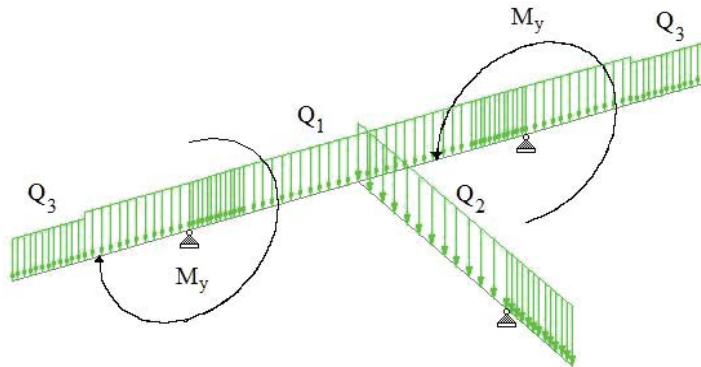
$$M_x = -278.014 \cdot \text{kN} \cdot \text{m}$$

All forces applied in the simplified Staad model is illustrated on the next page.



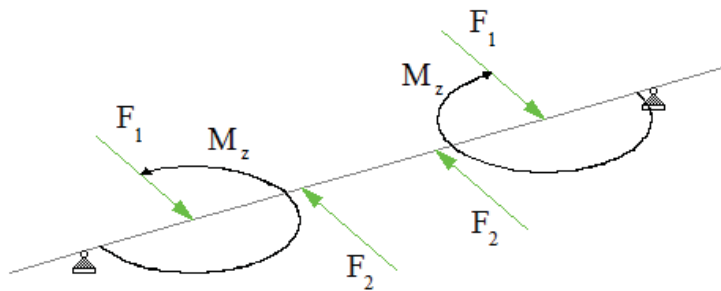
#### D.4.4 Vertical loading

The lifting points are modelled as pinned connections. The calculated eccentricity moments are applied to account for the distance between sling connection points and this simplified truss "beam" which follows the centerline of the integrated spool cover. The values of the applied loads are shown in the previous page.



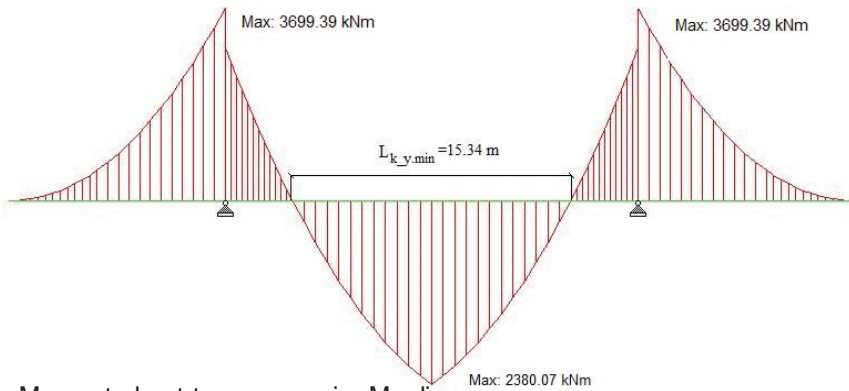
Staad model to create moment about transverse axis and vertical shear force diagram

The calculated longitudinal components are applied at the same position as the sling connection points, and the additional eccentricity is taken into account by applying the moments,  $M_z$ . The values of the applied loads are shown in the previous page.

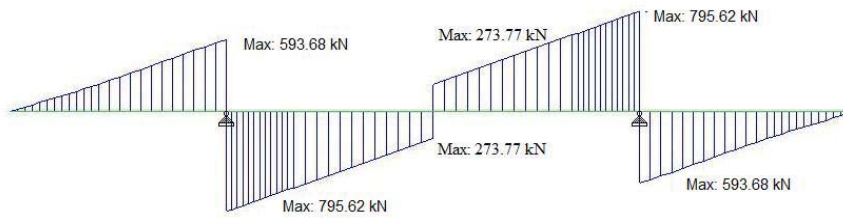


Staad model to create moment about lateral axis and transvers shear force diagram

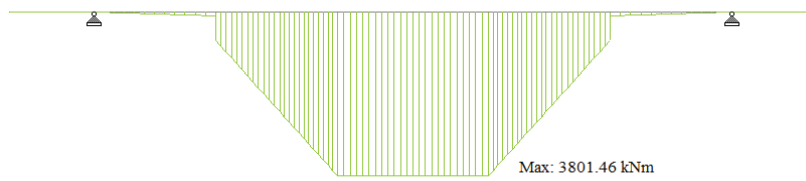
### D.4.5 Force diagrams



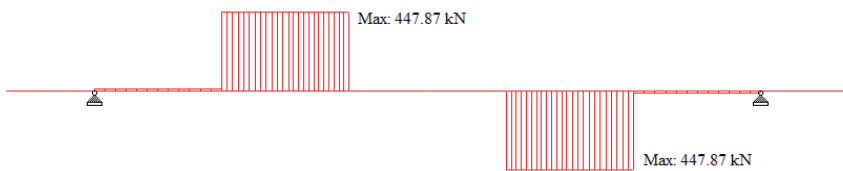
Moment about transvers axis,  $M_y$  diagram



Vertical shear force,  $V_z$  diagram



Moment about vertical axis,  $M_z$  diagram



Transvers shear force,  $V_y$  diagram

\*The maximum loads illustrated in the moment and shear diagrams are used for the buckling analysis

## D.5 Global Buckling check with hand calculations

Length of member:  $L := 22.74\text{m}$

The length is the total physical length of the member subjected to buckling, which is equal the distance between the sling connection points.

### D.5.1 Material

Yield strength:  $f_y := 355\text{N}\cdot\text{mm}^{-2}$

Youngs modulus:  $E := 210000\text{N}\cdot\text{mm}^{-2}$

Poissons ratio:  $\nu := 0.3$

Material factor:  $\gamma_{m1} := 1.15$

Shear modulus:  $G := \frac{E \cdot (1 + \nu)}{2}$   $G = 1.365 \times 10^5 \cdot \text{N}\cdot\text{mm}^{-2}$

### D.5.2 Buckling length

Effectiv length factor, about bending axis  $\beta_y := 0.7$   $\beta_z := 1.0$

### D.5.3 Load input from from Staad.Pro model

Highest axial force:  $N_{Ed} := F_{x_0} + F_{x_1}$   $N_{Ed} = 775.471 \cdot \text{kN}$

Highest transverse shear force:  $V_{Ed_y} := 448\text{kN}$

Highest vertical shear force:  $V_{Ed_z} := 796\text{kN}$

Highest moment about transverse axis:  $M_{Ed_y} := 3699\text{kN}\cdot\text{m}$

Highest moment about vertical axis:  $M_{Ed_z} := 3801\text{kN}\cdot\text{m}$

Highest moment about lateral axis:  $M_{Ed_x} := -2 \cdot M_x$   $M_{Ed_x} = 556.028 \cdot \text{kN}\cdot\text{m}$

\*Note that loads used as input for this buckling check should be max loads found along entire member for the considered load case.

### D.5.4 Calculation of cross sectional class

10" Pipe:

Yield ratio,  
ref. Table 5.2:

$$\varepsilon := \sqrt{\frac{235 \text{ N} \cdot \text{mm}^{-2}}{f_y}} \quad \varepsilon = 0.814$$

Section class, chords,  
ref. Table 5.2:

$$\text{Class}_c := \begin{cases} \text{"1"} & \text{if } 0 < \frac{\text{OD}}{\text{wt}} \leq 50\varepsilon^2 \\ \text{"2"} & \text{if } 50\varepsilon^2 < \frac{\text{OD}}{\text{wt}} \leq 70\varepsilon^2 \\ \text{"3"} & \text{if } 70\varepsilon^2 < \frac{\text{OD}}{\text{wt}} \leq 90\varepsilon^2 \\ \text{"FAIL"} & \text{otherwise} \end{cases}$$

$$\text{Class}_c = \text{"1"}$$

HE220B is class 1

### D.5.5 Calculation of cross sectional properties

Cross sectional area:  $A := A_x$   $A = 5.982 \times 10^4 \cdot \text{mm}^2$

Total shear area,  
ref. 6.2.6(3):  $A_v := A \cdot \frac{2}{\pi}$   $A_v = 3.808 \times 10^4 \text{ mm}^2$

Second moment of area  
about vertical axis:  $I_z = 2.375 \times 10^{11} \text{ mm}^4$

Second moment of area  
about transverse axis:  $I_y = 6.584 \times 10^{10} \text{ mm}^4$

Elastic section modulus  
about vertical axis:  $W_z = 1.315 \times 10^8 \cdot \text{mm}^3$

Elastic section modulus  
about transverse axis:  $W_y = 6.945 \times 10^7 \cdot \text{mm}^3$

Plastic section modulus  
about vertical axis:  $W_{pl_z} := W_z$

Plastic section modulus  
about transverse axis:  $W_{pl_y} := W_y$

\*Choosing plastic section modulus equal the elastic section modulus is considered ver conservative.

## D.5.6 Buckling of column

Equivalent form factor	$\alpha := 0.49$	Ref. Table 6.1 and Table 6.2 - Buckling curve a (0.21) for hot formed pipe - Buckling curve c (0.49) for cold formed pipe
------------------------	------------------	---

### Calculation of buckling stress, ref. 6.3.1

Effective length:	$L_{k_y} := L \cdot \beta_y$	$L_{k_y} = 15.918 \cdot \text{m}$
	$L_{k_z} := L \cdot \beta_z$	$L_{k_z} = 22.74 \cdot \text{m}$
Euler stress:	$N_{cr_y} := \frac{\pi^2 E \cdot I_y}{L_{k_y}^2}$	$N_{cr_y} = 5.385 \times 10^5 \cdot \text{kN}$
	$N_{cr_z} := \frac{\pi^2 E \cdot I_z}{L_{k_z}^2}$	$N_{cr_z} = 9.518 \times 10^5 \cdot \text{kN}$
Relative Slenderness, ref. eq. (6.50):	$\lambda_{rel_y} := \sqrt{A \cdot \frac{f_y}{N_{cr_y}}}$	$\lambda_{rel_y} = 0.199$
	$\lambda_{rel_z} := \sqrt{A \cdot \frac{f_y}{N_{cr_z}}}$	$\lambda_{rel_z} = 0.149$

\*Ref. 6.3.1.2(4): If the one of the two following requirements are satisfied, the buckling effects may be ignored

$$\begin{array}{l}
 \text{check}_y := \left\{ \begin{array}{l} \text{"No buckling"} \quad \text{if } \frac{N_{Ed}}{N_{cr_y}} \leq 0.04 \\ \text{"No buckling"} \quad \text{if } \lambda_{rel_y} \leq 0.2 \\ \text{"Perform buckling check"} \quad \text{otherwise} \end{array} \right. \quad \text{check}_y = \text{"No buckling"} \\
 \text{check}_z := \left\{ \begin{array}{l} \text{"No buckling"} \quad \text{if } \frac{N_{Ed}}{N_{cr_z}} \leq 0.04 \\ \text{"No buckling"} \quad \text{if } \lambda_{rel_z} \leq 0.2 \\ \text{"Perform buckling check"} \quad \text{otherwise} \end{array} \right. \quad \text{check}_z = \text{"No buckling"}
 \end{array}$$

\*The standard buckling checks will be checked according to procedures regardless.

Ref. 6.3.1.2:

$$\phi_y := 0.5 \left[ 1 + \alpha \cdot (\lambda_{\text{rel}_y} - 0.2) + \lambda_{\text{rel}_y}^2 \right] \quad \phi_y = 0.519$$

$$\phi_z := 0.5 \left[ 1 + \alpha \cdot (\lambda_{\text{rel}_z} - 0.2) + \lambda_{\text{rel}_z}^2 \right] \quad \phi_z = 0.499$$

Buckling factor,  
ref. eq. (6.49):

$$\chi_y := \frac{1}{\phi_y + \sqrt{\phi_y^2 - \lambda_{\text{rel}_y}^2}} \quad \chi_y = 1.001$$

$$\chi_z := \frac{1}{\phi_z + \sqrt{\phi_z^2 - \lambda_{\text{rel}_z}^2}} \quad \chi_z = 1.026$$

## D.6 Capacity calculations

### D.6.1 Axial capacity

#### Compression of members, ref.6.2.4

Cross-section axial capacity,  
ref. eq. (6.10):

$$N_{c.Rd} := \frac{A \cdot f_y}{\gamma_{m1}} \quad N_{c.Rd} = 1.847 \times 10^4 \cdot \text{kN}$$

Design axial load:

$$N_{Ed} = 775.471 \cdot \text{kN}$$

Cross-sectional axial utilization,  
ref. eq. (6.9)

$$n := \frac{N_{Ed}}{N_{c.Rd}} \quad n = 0.042$$

#### Buckling stress, ref.6.3.1.1

Axial buckling capacity,  
ref. eq. (6.47):

$$N_{b.Rdy} := \frac{\chi_y \cdot A \cdot f_y}{\gamma_{m1}} \quad N_{b.Rdy} = 1.848 \times 10^4 \cdot \text{kN}$$

$$N_{b.Rdz} := \chi_z \cdot A \cdot \frac{f_y}{\gamma_{m1}} \quad N_{b.Rdz} = 1.895 \times 10^4 \cdot \text{kN}$$

Cross-sectional axial utilization,  
ref. eq. (6.9)

$$n_y := \frac{N_{Ed}}{N_{b.Rdy}} \quad n_y = 0.042$$

$$n_z := \frac{N_{Ed}}{N_{b.Rdz}} \quad n_z = 0.041$$

$$n_{\max} := \max(n_y, n_z) \quad n_{\max} = 0.042$$

## D.6.2 Shear capacity

### Shear capacity of members, ref.6.2.6

Shear capacity,  
ref. eq. (6.18):

$$V_{c.Rd} := \frac{A_v \cdot f_y}{\gamma_{m1} \cdot \sqrt{3}} \quad V_{c.Rd} = 6.788 \times 10^3 \cdot \text{kN}$$

Design shear force:

$$V_{Ed_y} = 448 \cdot \text{kN}$$

$$V_{Ed_z} = 796 \cdot \text{kN}$$

Shear utilization,  
ref. eq. (6.17)

$$v_y := \frac{V_{Ed_y}}{V_{c.Rd}} \quad v_y = 0.066$$

$$v_z := \frac{V_{Ed_z}}{V_{c.Rd}} \quad v_z = 0.117$$

$$v_{\max} := \max(v_y, v_z) \quad v_{\max} = 0.117$$

## D.6.3 Bending capacity

### Pure bending capacity of members, ref.6.2.5

Pure bending capacity,  
ref. eq. (6.13):

$$M_{c.Rd_y} := \frac{W_{pl_y} \cdot f_y}{\gamma_{m1}} \quad M_{c.Rd_y} = 2.144 \times 10^4 \cdot \text{kN}\cdot\text{m}$$

$$M_{c.Rd_z} := \frac{W_{pl_z} \cdot f_y}{\gamma_{m1}} \quad M_{c.Rd_z} = 4.059 \times 10^4 \cdot \text{kN}\cdot\text{m}$$

Design moments:

$$M_{Ed_y} = 3.699 \times 10^3 \cdot \text{kN}\cdot\text{m}$$

$$M_{Ed_z} = 3.801 \times 10^3 \cdot \text{kN}\cdot\text{m}$$

Pure bending utilization,  
ref. eq. (6.12)

$$m_y := \frac{M_{Ed_y}}{M_{c.Rd_y}} \quad m_y = 0.173$$

$$m_z := \frac{M_{Ed_z}}{M_{c.Rd_z}} \quad m_z = 0.094$$

$$m_{\max} := \max(m_y, m_z) \quad m_{\max} = 0.173$$



### Bending and axial force capacity, ref.6.2.5

Plastic axial capacity,  
ref. eq. (6.6)

$$N_{pl.Rd} := N_{c.Rd} \quad N_{pl.Rd} = 1.847 \times 10^4 \cdot \text{kN}$$

Plastic moment capacity,  
ref. eq. (6.13)

$$M_{pl.Rd_y} := M_{c.Rd_y} \quad M_{pl.Rd_y} = 2.144 \times 10^4 \cdot \text{kN}\cdot\text{m}$$

$$M_{pl.Rd_z} := M_{c.Rd_z} \quad M_{pl.Rd_z} = 4.059 \times 10^4 \cdot \text{kN}\cdot\text{m}$$

Reduced plastic moment capacity,  
ref. eq. (6.32)

$$M_{N.Rd_y} := M_{pl.Rd_y} \cdot \left[ 1 - \left( \frac{N_{Ed}}{N_{pl.Rd}} \right) \right]$$

$$M_{N.Rd_y} = 2.054 \times 10^4 \cdot \text{kN}\cdot\text{m}$$

$$M_{N.Rd_z} := M_{pl.Rd_z} \cdot \left[ 1 - \left( \frac{N_{Ed}}{N_{pl.Rd}} \right) \right]$$

$$M_{N.Rd_z} = 3.889 \times 10^4 \cdot \text{kN}\cdot\text{m}$$

Constants,\*  
ref. 6.2.9.1(6):

$$\alpha_M := 1 \quad \beta_M := 1$$

Bending and axial utilization,  
ref. eq. (6.41):

$$mn_{\max} := \left( \frac{M_{Ed_y}}{M_{N.Rd_y}} \right)^{\alpha_M} + \left( \frac{M_{Ed_z}}{M_{N.Rd_z}} \right)^{\beta_M}$$

$$mn_{\max} = 0.278$$

\*Constants for determining the bending and axial capacity is set to 1 which is conservative

### Bending, shear and axial force capacity, ref.6.2.10

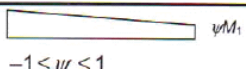
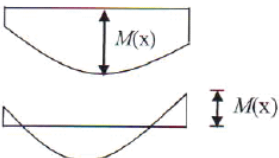


\*Ref 6.2.10(2) If design shear load  $V_{Ed}$  is less than 50% of the shear plastic capacity,  $V_{pl.Rd}$ , reduction due to shear is neglected

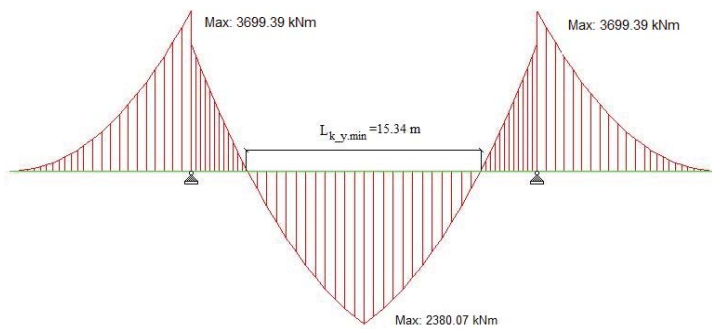
$$\text{check}_V := \begin{cases} \text{"No shear reduction"} & \text{if } \frac{V_{Ed_y}}{V_{c.Rd}} \leq 0.5 \\ \text{"Account for shear"} & \text{otherwise} \end{cases}$$

$$\text{check}_V = \text{"No shear reduction"}$$

Finding  $k_{yy}$ ,  $k_{zz}$ ,  $k_{zy}$  and  $k_{yz}$  using Method 1 for interaction factors, ref. Appendix A

Tabell A.2 – Ekvivalente momentfaktorer,  $C_{mi,0}$

Momentdiagram	$C_{mi,0}$
 <p><math>M_1</math> <math>\psi M_1</math> <math>-1 \leq \psi \leq 1</math></p>	$C_{mi,0} = 0,79 + 0,21\psi_1 + 0,36(\psi_1 - 0,33) \frac{N_{Ed}}{N_{cr,i}}$
 <p><math>M(x)</math> <math>M(x)</math></p>	$C_{mi,0} = 1 + \left( \frac{\pi^2 EI_x  \delta_x }{L^2  M_{1,Ed}(x) } - 1 \right) \frac{N_{Ed}}{N_{cr,i}}$ <p><math>M_{1,Ed}(x)</math> er største første ordens moment av <math>M_{y,Ed}</math> og <math>M_{z,Ed}</math> <math> \delta_x </math> er største forskyvning langs staven</p>
	$C_{mi,0} = 1 - 0,18 \frac{N_{Ed}}{N_{cr,i}}$
	$C_{mi,0} = 1 + 0,03 \frac{N_{Ed}}{N_{cr,i}}$

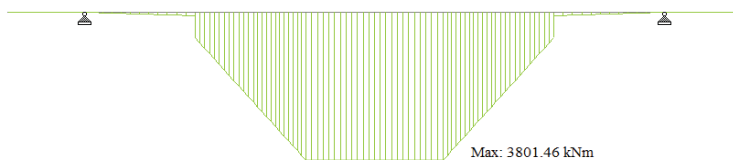


\*Largest deflection is found from the original staad model where the largest displacement values along the considered beam is inserted in the interaction formula

$$\delta_y := 41.4\text{mm}$$

$$C_{my,0} := 1 + \frac{\pi^2 \cdot E \cdot I_y \cdot \delta_y}{L^2 \cdot M_{Ed,y}} \cdot \frac{N_{Ed}}{N_{c,Rd}}$$

$$C_{my,0} = 1.124$$



$$\delta_z := 21.2\text{mm}$$

$$C_{mz,0} := 1 + \frac{\pi^2 \cdot E \cdot I_z \cdot \delta_z}{L^2 \cdot M_{Ed,z}} \cdot \frac{N_{Ed}}{N_{c,Rd}}$$

$$C_{mz,0} = 1.223$$

**Values from. table 6.7**

$$N_{Rk} := f_y \cdot A \quad N_{Rk} = 2.124 \times 10^4 \cdot \text{kN}$$

$$M_{y1} := f_y \cdot W_{pl_y} \quad M_{y1} = 2.465 \times 10^4 \cdot \text{kN} \cdot \text{m}$$

$$M_{z1} := f_y \cdot W_{pl_z} \quad M_{z1} = 4.668 \times 10^4 \cdot \text{kN} \cdot \text{m}$$

$$\Delta M_{Ed_y} := 0$$

$$\Delta M_{Ed_z} := 0$$

Torsional buckling factor,  
ref. 6.3.3(4):

$$\chi_{LT} := 1$$

Assume no torsional buckling

**Values from Table A.2:**

$$W_{el_y} := W_y$$

$$W_{el_z} := W_z$$

$$\epsilon_y := \frac{M_{Ed_y} \cdot A}{N_{Ed} \cdot W_{el_y}} \quad \epsilon_y = 4.109$$

$$\epsilon_z := \frac{M_{Ed_z} \cdot A}{N_{Ed} \cdot W_{el_z}} \quad \epsilon_z = 2.23$$

Relative slenderness for lateral  
torsional buckling due to uniform  
bending is 0  $\lambda_{rel0} := 0$

Constant set to 1.0

$$C_1 := 1$$

Axial capacity:

$$N_{cr_y} = 5.385 \times 10^5 \cdot \text{kN}$$

$$N_{cr_z} = 9.518 \times 10^5 \cdot \text{kN}$$

$$N_{cr_T} := A \cdot G$$

$$N_{cr_T} = 8.166 \times 10^6 \cdot \text{kN}$$

Moment capacity:

$$M_{Rk_y} := f_y \cdot W_y$$

$$M_{Rk_y} = 2.465 \times 10^4 \cdot \text{kN} \cdot \text{m}$$

$$M_{Rk_z} := f_y \cdot W_z$$

$$M_{Rk_z} = 4.668 \times 10^4 \cdot \text{kN} \cdot \text{m}$$

Equivalent factors:  $\lambda_{rel0} \leq 1.02 \cdot \sqrt{C_1} \cdot \sqrt[4]{\left(1 - \frac{N_{Ed}}{N_{cr_z}}\right) \cdot \left(1 - \frac{N_{Ed}}{N_{cr_T}}\right)} = 0.2$  ok

$C_{my} := C_{my,0}$   $C_{my} = 1.124$

$C_{mz} := C_{mz,0}$   $C_{mz} = 1.223$

$C_{mLT} := 1$   $C_{mLT} = 1$

Additional factors:

$\mu_y := \frac{1 - \frac{N_{Ed}}{N_{cr_y}}}{1 - \chi_y \cdot \frac{N_{Ed}}{N_{cr_y}}}$   $\mu_z := \frac{1 - \frac{N_{Ed}}{N_{cr_z}}}{1 - \chi_y \cdot \frac{N_{Ed}}{N_{cr_z}}}$

$w_y := \begin{cases} \frac{W_{pl_y}}{W_{el_y}} & \text{if } \frac{W_{pl_y}}{W_{el_y}} \leq 1.5 \\ \text{"FAIL"} & \text{otherwise} \end{cases}$   $w_y = 1$

$w_z := \begin{cases} \frac{W_{pl_z}}{W_{el_z}} & \text{if } \frac{W_{pl_z}}{W_{el_z}} \leq 1.5 \\ \text{"FAIL"} & \text{otherwise} \end{cases}$   $w_z = 1$

\*Conservative choice from earlier

$n_{pl} := \frac{N_{Ed}}{\frac{N_{Rk}}{\gamma_{m1}}}$   $n_{pl} = 0.042$

$\lambda_{max} := \max(\lambda_{rel_y}, \lambda_{rel_z})$   $\lambda_{max} = 0.199$

$I_T := 0$  \*Very conservative

$a_{LT} := \begin{cases} 1 - \frac{I_T}{I_y} & \text{if } 1 - \frac{I_T}{I_y} \geq 0 \\ \text{"FAIL"} & \text{otherwise} \end{cases}$   $a_{LT} = 1$

since  $\lambda_{rel0}=0 \rightarrow$

$b_{LT} := 0$   $c_{LT} := 0$   $d_{LT} := 0$   $e_{LT} := 0$

$$C_{yy} := \max \left[ 1 + (w_y - 1) \left[ \left( 2 - \frac{1.6}{w_y} C_{my}^2 \cdot \lambda_{\max} - \frac{1.6}{w_y} C_{my}^2 \cdot \lambda_{\max}^2 \right) n_{pl} - b_{LT} \right], \frac{W_{el_y}}{W_{pl_y}} \right]$$

$$C_{yy} = 1$$

$$C_{yz} := \max \left[ 1 + (w_z - 1) \left[ \left( 2 - 14 \cdot C_{mz}^2 \cdot \frac{\lambda_{\max}^2}{w_z^5} \right) n_{pl} - c_{LT} \right], 0.6 \cdot \sqrt{\frac{w_z}{w_y}} \cdot \frac{W_{el_z}}{W_{pl_z}} \right]$$

$$C_{yz} = 1$$

$$C_{zy} := \max \left[ 1 + (w_y - 1) \left[ \left( 2 - 14 \cdot C_{my}^2 \cdot \frac{\lambda_{\max}^2}{w_y^5} \right) n_{pl} - c_{LT} \right], 0.6 \cdot \sqrt{\frac{w_y}{w_z}} \cdot \frac{W_{el_y}}{W_{pl_y}} \right]$$

$$C_{zy} = 1$$

$$C_{zz} := \max \left[ 1 + (w_z - 1) \left[ \left( 2 - \frac{1.6}{w_z} C_{mz}^2 \cdot \lambda_{\max} - \frac{1.6}{w_z} C_{mz}^2 \cdot \lambda_{\max}^2 \right) n_{pl} - b_{LT} \right], \frac{W_{el_z}}{W_{pl_z}} \right]$$

$$C_{zz} = 1$$

\*All factors equal 1 due to conservative choice where the plastic section modulus was set equal the elastic section modulus.

**Interaction factors for section class 1, Method 1, ref. Table A.1**

$$k_{yy} := C_{my} \cdot C_{mLT} \cdot \frac{\mu_y}{1 - \frac{N_{Ed}}{N_{cr_y}}} \cdot \frac{1}{C_{yy}} \quad k_{yy} = 1.126$$

$$k_{yz} := C_{mz} \cdot \frac{\mu_y}{1 - \frac{N_{Ed}}{N_{cr_z}}} \cdot \frac{1}{C_{yz}} \cdot 0.6 \cdot \sqrt{\frac{w_z}{w_y}} \quad k_{yz} = 0.734$$

$$k_{zy} := C_{my} \cdot C_{mLT} \cdot \frac{\mu_z}{1 - \frac{N_{Ed}}{N_{cr_y}}} \cdot \frac{1}{C_{zy}} \cdot 0.6 \cdot \sqrt{\frac{w_y}{w_z}} \quad k_{zy} = 0.734$$

$$k_{zz} := C_{mz} \cdot \frac{\mu_z}{1 - \frac{N_{Ed}}{N_{cr_z}}} \cdot \frac{1}{C_{zz}} \quad k_{zz} = 1.224$$

**Combined axial and compression force, ref. 6.3.3(4):**

$$mc_y := \frac{N_{Ed}}{\chi_y \cdot \frac{N_{Rk}}{\gamma_{m1}}} + k_{yy} \cdot \frac{M_{Ed_y} + \Delta M_{Ed_y}}{\chi_{LT} \cdot \frac{M_{Rk_y}}{\gamma_{m1}}} + k_{yz} \cdot \frac{M_{Ed_z} + \Delta M_{Ed_z}}{\chi_{LT} \cdot \frac{M_{Rk_z}}{\gamma_{m1}}} = 0.305$$

$$mc_z := \frac{N_{Ed}}{\chi_z \cdot \frac{N_{Rk}}{\gamma_{m1}}} + k_{zy} \cdot \frac{M_{Ed_y} + \Delta M_{Ed_y}}{\chi_{LT} \cdot \frac{M_{Rk_y}}{\gamma_{m1}}} + k_{zz} \cdot \frac{M_{Ed_z} + \Delta M_{Ed_z}}{\chi_{LT} \cdot \frac{M_{Rk_z}}{\gamma_{m1}}} = 0.272$$

$$mc_{max} := \max(mc_y, mc_z) \quad mc_{max} = 0.305$$

\*Max utilization is 0.29 due to combined axial and compression force.

**D.7 Max utilization EC3**

$$Utilization_{max} := \max(n_{max}, v_{max}, m_{max}, mn_{max}, mc_{max})$$

$$Utilization_{max} = 0.305$$

# APPENDIX E

## ILLUSTRATIONS FROM STAAD.PRO

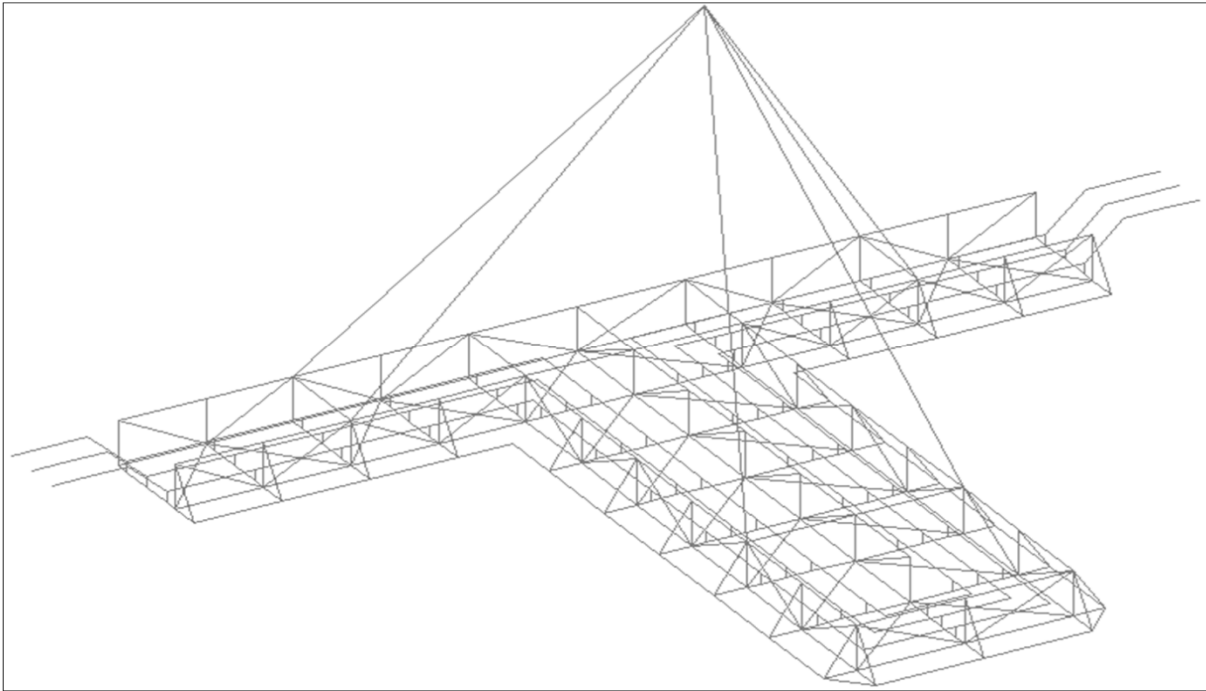


Figure E.1: Staad.Pro model after defining the geometry of the structure

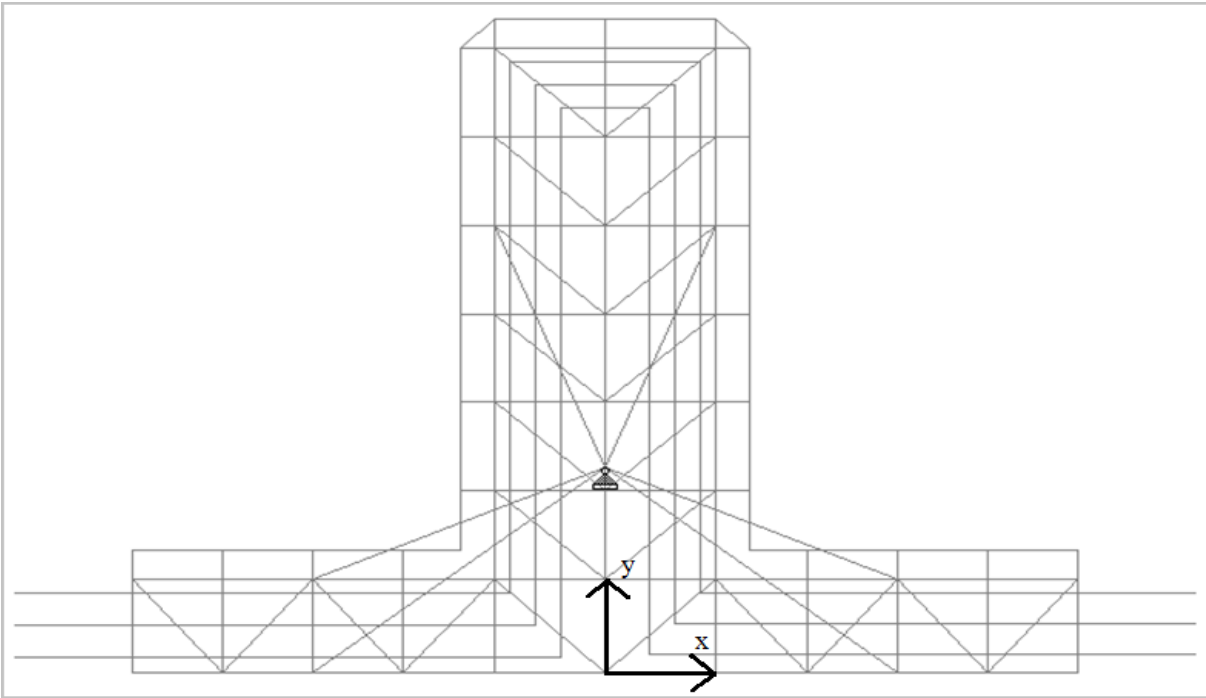


Figure E.2: Staad.Pro model, xy plane





# APPENDIX F

## DOMINATING WAVE FORCE REGIMES

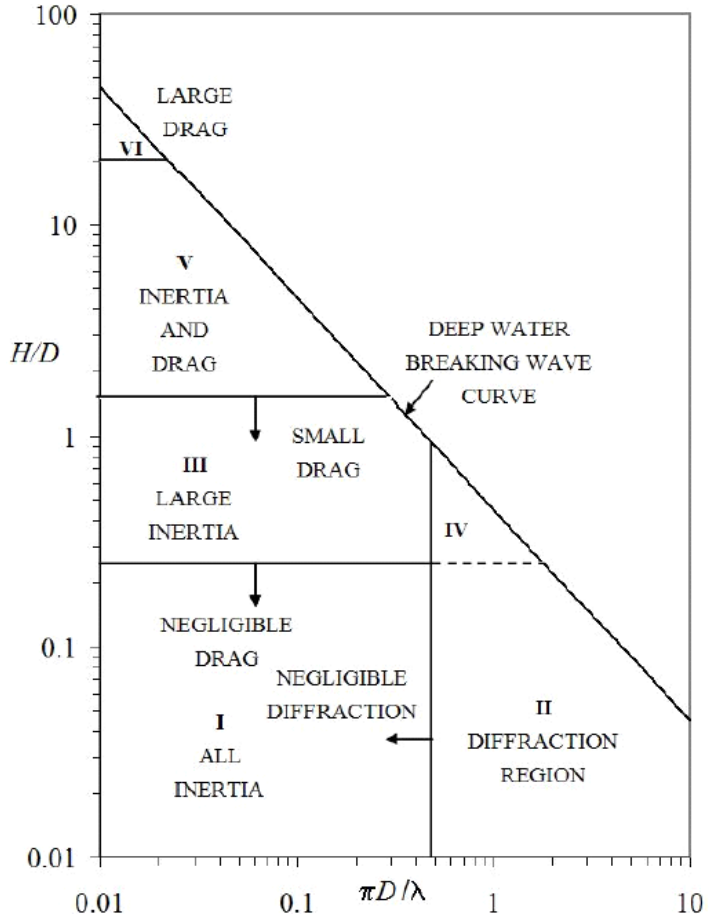


Figure F.1: Different wave force regimes, where H is wave height, D is characteristic dimension and λ is wave length, (DNV-RP-H103 (2012) figure 2-3).

Table F.1: Dominating wave force regimes for largest and smallest cylinder

$H_s$	$H/D_{12''\text{spool}}$	$\pi D_{12''\text{spool}}/\lambda(T_{z,\min})$	$H/D_{6''\text{pipe}}$	$\pi D_{6''\text{pipe}}/\lambda(T_{z,\min})$
1.5	3.5	0.07	8.9	0.03
2	4.6	0.05	11.9	0.02
2.5	5.8	0.04	14.9	0.02
3	6.9	0.04	17.8	0.01
Dominating force:	Both inertia and drag		Both inertia and drag	

Where:  $T_{z,\min} = 8.9 \sqrt{H_s/g}$ ,  $T_{z,\max} = 13$  Ref: DNV-RP-H103 (2012) 4.3.2.1 (0.1)



## APPENDIX G

### SOLID HORIZONTAL PROJECTED AREA

The forces on the “real structure” is be obtained with a scale factor that is obtained assuming that the hydrodynamic forces are proportional to the largest relative increase in mass or solid projected area with respect to the simplified model. The assumption is appropriate since the simplified model has the same structural properties as the “real structure” with less structural members.

Projected area in the horizontal plane versus silhouetted area is calculated in *table G.1* and *table G.2* for the “real structure” and simplified model respectively.

Table G.1: Calculated solid area versus total silhouetted area of the “real structure”.

Description	Length of members [m]	Number	Diameter [m]	Total length [m]	Area [m <sup>2</sup> ]
12" spool excluding gooseneck	82.80	2	0.434	165.6	71.8
8" spool excluding goosenecks	82.80	1	0.299	82.8	24.8
Bottom main (10" section)	127.60	1	0.273	127.6	34.8
Bottom transvers beams (8" tubular sections)	4.00	6	0.219	24.0	5.3
	4.34	6	0.219	26.0	5.7
Bottom transvers beams (10" tubular sections)	4.00	2	0.273	8.0	2.2
	4.34	6	0.273	26.0	7.1
Bottom brace (6" tubular sections)	5.32	6	0.168	31.9	5.4
	5.90	2	0.168	11.8	2.0
	5.79	12	0.168	69.5	11.7
Bottom brace (8" section)	5.32	2	0.219	10.6	2.3
Bottom trawl (6" tubular sections)	1.32	23	0.168	30.4	5.1
	85.44	1	0.168	85.4	14.4
Total area of members					193
Total silhouetted area					456
Projected area in percent					42 %
Area grp grating					65
Grp grating in percent (assuming 50% fill rate)					7 %
Projected area in percent including assumed Grp grating					49 %

Table G.2: Calculated solid area versus total silhouetted area of the “simplified structure”.

Description	Length of members [m]	Number	Diameter [m]	Total length [m]	Area [m <sup>2</sup> ]
12" spool excluding gooseneck	82.80	2	0.434	165.6	71.8
8" spool excluding goosenecks	82.80	0	0.299	0.0	0.0
Bottom main (10" section)	127.60	1	0.273	127.6	34.8
Bottom transvers beams (8" tubular sections)	4.00	6	0.219	24.0	5.3
	4.34	6	0.219	26.0	5.7
Bottom transvers beams (10" tubular sections)	4.00	2	0.273	8.0	2.2
	4.34	6	0.273	26.0	7.1
Bottom brace (6" tubular sections)	5.32	6	0.168	31.9	5.4
	5.90	2	0.168	11.8	2.0
	5.79	12	0.168	69.5	11.7
Bottom brace (8" section)	5.32	0	0.219	0.0	0.0
Bottom trawl (6" tubular sections)	1.32	0	0.168	0.0	0.0
	85.44	0	0.168	0.0	0.0
Total area of members					146
Total silhouetted area					456
Projected area in percent					32 %
Area grp grating					0
Grp grating in percent (assuming 50% fill rate)					0 %
Projected area in percent including assumed Grp grating					32 %

# APPENDIX H

## HYDRODYNAMIC COEFFICIENTS

Hydrodynamic coefficients based on the discussion in *chapter 2* is calculated for the considered cylinders in this appendix.

### H.1 $K_C$ and $R_e$ – numbers for considered cylinders

Keulegan Carpenter number and Reynolds number for various cylinders is given in this section and is part of the determination of the hydrodynamic coefficients applied in OrcaFlex.

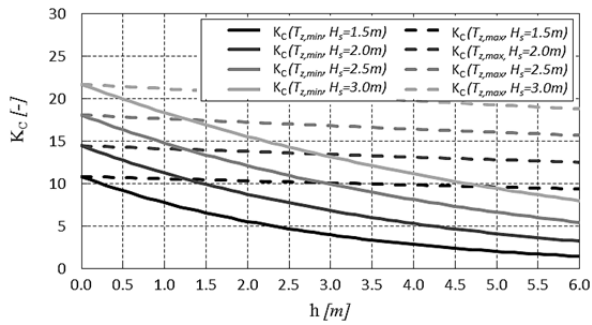


Figure H.1:  $K_C$  versus level of submergence for cylinders with diameter,  $D=0.434m$

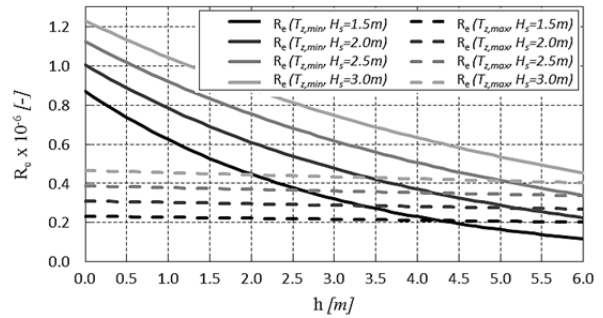


Figure H.2:  $R_e$  versus level of submergence for cylinders with diameter,  $D=0.434m$

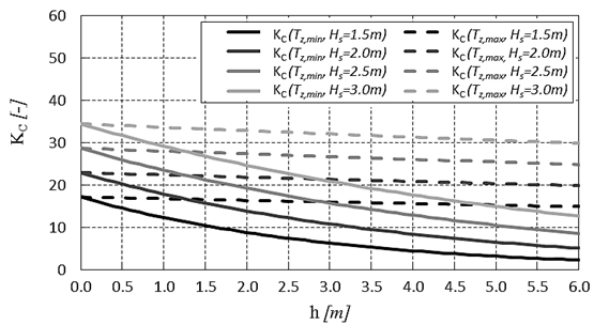


Figure H.3:  $K_C$  versus level of submergence for cylinders with diameter,  $D=0.273m$

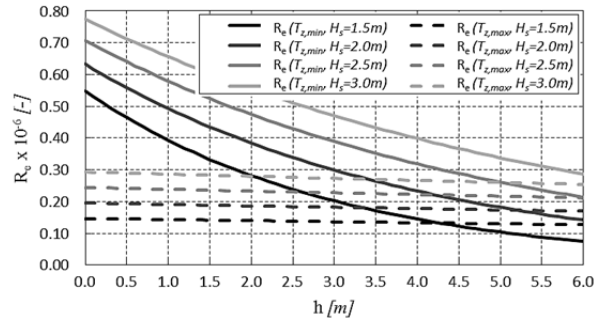


Figure H.4:  $R_e$  versus level of submergence for cylinders with diameter,  $D=0.273m$

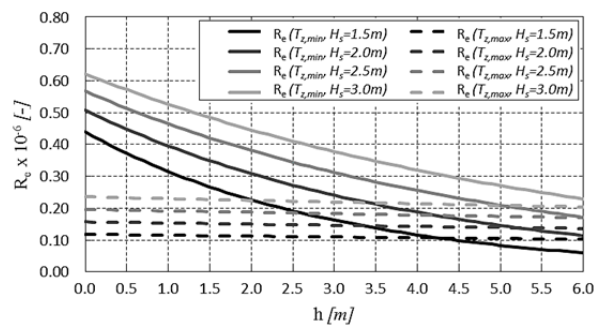
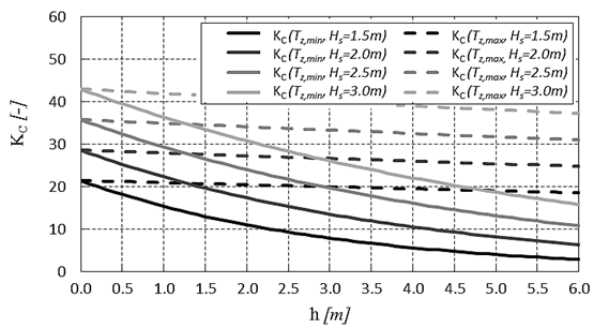


Figure H.5:  $K_C$  versus level of submergence for cylinders with diameter,  $D=0.219\text{m}$

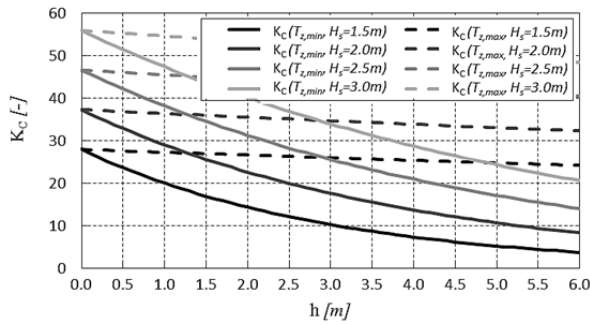


Figure H.6:  $R_e$  versus level of submergence for cylinders with diameter,  $D=0.219\text{m}$

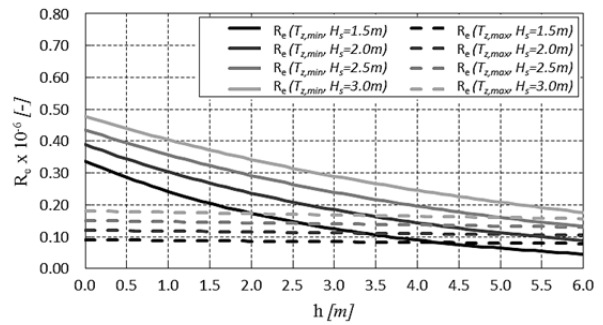


Figure H.7:  $K_C$  versus level of submergence for cylinders with diameter,  $D=0.168\text{m}$

Figure H.8:  $R_e$  versus level of submergence for cylinders with diameter,  $D=0.168\text{m}$

Where:  $T_{z,\min} = 8.9\sqrt{\frac{H_s}{g}}, T_{z,\max} = 13$  Ref: DNV-RP-H103 (2012) 4.3.2.1 (0.1)

## H.2 Hydrodynamic coefficients

Estimated hydrodynamic coefficients for all structural members (cylinders) are given for various level of submergence. The superscripts defines the location of the cylinder where “h.b” is horizontal bottom, “v” is vertical, “d” is the diagonal (vertical) braces and “h.t” represents the horizontal members located on top of the structure.

Table H.1: Hydrodynamic coefficients for all members at submerged height,  $h_B=0.0\text{m}$ .

Description	Diameter [m]	Location, h [m]	$C_A$ [-]	$C_M$ [-]	$C_S+C_D$ [-]
10" pipe <sup>(h.b)</sup>	0.273	0.00	2.0	3.0	0.8
8" pipe <sup>(h.b)</sup>	0.219	0.00	2.0	3.0	0.8
6" pipe <sup>(h.b)</sup>	0.168	0.00	2.0	3.0	0.8
10" pipe <sup>(v)</sup>	0.273	-2.10 to 0.00	2.0	3.0	0.8
8" pipe <sup>(v)</sup>	0.219	-2.10 to 0.00	2.0	3.0	0.8
6" pipe <sup>(v)</sup>	0.168	-2.10 to 0.00	2.0	3.0	0.8
12" spool	0.434	-0.36	2.0	3.0	3.1
8" pipe <sup>(d)</sup>	0.219	-2.10 to 0.00	2.0	3.0	3.1
6" pipe <sup>(d)</sup>	0.168	-2.10 to 0.00	2.0	3.0	3.1
10" pipe <sup>(h.t)</sup>	0.273	-2.10	2.0	3.0	3.1
8" pipe <sup>(h.t)</sup>	0.219	-2.10	2.0	3.0	3.1

Table H.2: Hydrodynamic coefficients for all members at submerged height,  $h_B=1.0m$ .

Description	Diameter [m]	Location, h [m]	$C_A$ [-]	$C_M$ [-]	$C_S+C_D$ [-]
10" pipe <sup>(h.b)</sup>	0.273	1.00	1.0	2.0	0.8
8" pipe <sup>(h.b)</sup>	0.219	1.00	1.0	2.0	0.8
6" pipe <sup>(h.b)</sup>	0.168	1.00	1.0	2.0	0.8
10" pipe <sup>(v)</sup>	0.273	-1.10 to 1.00	1.0	2.0	0.8
8" pipe <sup>(v)</sup>	0.219	-1.10 to 1.00	1.0	2.0	0.8
6" pipe <sup>(v)</sup>	0.168	-1.10 to 1.00	1.0	2.0	0.8
12" spool	0.434	0.64	1.1	2.1	0.8
8" pipe <sup>(d)</sup>	0.219	-1.10 to 1.00	2.0	3.0	3.1
6" pipe <sup>(d)</sup>	0.168	-1.10 to 1.00	2.0	3.0	3.1
10" pipe <sup>(h.t)</sup>	0.273	-1.10	2.0	3.0	3.1
8" pipe <sup>(h.t)</sup>	0.219	-1.10	2.0	3.0	3.1

Table H.3: Hydrodynamic coefficients for all members at submerged height,  $h_B=1.8m$ .

Description	Diameter [m]	Location, h [m]	$C_A$ [-]	$C_M$ [-]	$C_S+C_D$ [-]
10" pipe <sup>(h.b)</sup>	0.273	1.80	1.0	2.0	0.8
8" pipe <sup>(h.b)</sup>	0.219	1.80	1.0	2.0	0.8
6" pipe <sup>(h.b)</sup>	0.168	1.80	1.0	2.0	0.8
10" pipe <sup>(v)</sup>	0.273	-0.30 to 1.80	1.0	2.0	0.8
8" pipe <sup>(v)</sup>	0.219	-0.30 to 1.80	1.0	2.0	0.8
6" pipe <sup>(v)</sup>	0.168	-0.30 to 1.80	1.0	2.0	0.8
12" spool	0.434	1.44	1.0	2.0	0.8
8" pipe <sup>(d)</sup>	0.219	-0.30 to 1.80	2.0	3.0	3.1
6" pipe <sup>(d)</sup>	0.168	-0.30 to 1.80	2.0	3.0	3.1
10" pipe <sup>(h.t)</sup>	0.273	-0.30	2.0	3.0	3.1
8" pipe <sup>(h.t)</sup>	0.219	-0.30	2.0	3.0	3.1





# APPENDIX I

## ORCAFLEX RESULTS

The OrcaFlex results that is plotted and discussed in *chapter 5* is given under proper titles in tables in this APPENDIX.

### I.1 Dynamic loads in different wave direction, $\beta$

Table I.1: Crane wire tension versus heading angle for  $H_s=2\text{m}$ ,  $T_z=6\text{s}$ ,  $h_B=1.0\text{m}$ , (from OrcaFlex)

Heading direction, $\beta$ [-]	Zero up crossing period, $T_z$ [s]	Crane wire tension [kN]		
		Max	Min	Static
165	6.0	966	349	508.2
172.5	6.0	956	314	508.2
180	6.0	946	248	508.2
187.5	6.0	944	228	508.2
195	6.0	954.0	192	508.2

### I.2 Dynamic loads at different level of submergence, $h_B$

Table I.2: Crane wire tension versus level of submergence for  $H_s=2\text{m}$ ,  $\beta=195\text{deg}$ ,  $T_z=6\text{s}$ , (from OrcaFlex).

Level of submergence, $h_B$ [m]	Crane wire tension [kN]		
	Max	Min	Static
-0.2	1281	12	927.5
0.0	1092	71	809.7
0.2	999.0	132.0	694.2
0.4	965.0	258.0	584.5
0.6	961.0	251.0	522.4
0.8	949.0	239.0	516.0
1.0	954.0	192.0	508.2
1.2	953.0	172.0	500.8
1.4	895.0	65.0	488.2
1.6	835.0	46.0	481.8
1.8	834.0	45.3	449.0
2.0	777.0	68.0	396.9
2.2	654.0	182.0	393.5
2.4	624.0	160.0	393.5
2.6	636.0	153.0	393.5

### I.3 Dynamic loads in different sea states

Table I.3: Crane wire and sling tension versus zero up crossing period for  $H_s=1.5\text{m}$ ,  $h_B=1.0\text{m}$  and  $\beta=195$ .

$H_s$ [m]	$T_z$ [s]	Crane wire tension [kN]		Sling 900 tension [kN]		Sling 901 tension [kN]		Sling 902 tension [kN]		Sling 903 tension [kN]		Sling 904 tension [kN]		Sling 905 tension [kN]	
		max.	min.	max.	min.	max.	min.	max.	min.	max.	min.	max.	min.	max.	min.
Staad.Pro		1269		207		240		319		319		240		207	
$F_{\text{static}}$		948	508.2	151	77.3	176	95.3	234	123	234	123	176	95.3	151	77.3
1.5	3.48	707	483	118	66	136	81	188	107	204	85	142	85	120	69
	4.0	770	439	128	56	137	76	204	91	213	82	134	89	125	70
	5.0	845	341	144	43	160	56	221	59	224	67	155	69	142	55
	6.0	915	333	153	42	173	57	239	67	240	74	175	68	154	55
	7.0	927	397	151	55	170	70	243	86	238	88	183	80	157	66
	8.0	893	445	138	64	157	76	236	92	229	100	160	78	140	63
	9.0	920	456	150	70	172	87	243	93	242	93	167	82	146	65
	10.0	865	453	142	67	164	85	229	85	229	88	157	86	134	70
	11.0	828	464	128	70	146	89	223	88	227	88	154	85	133	68
	12.0	760	481	117	69	136	91	209	101	209	102	133	91	115	69
13.0	543	490	128	70	83	73	100	91	139	112	138	111	99	91	
<b>Extremes</b>		<b>927</b>	<b>333</b>	<b>153</b>	<b>42</b>	<b>173</b>	<b>56</b>	<b>243</b>	<b>59</b>	<b>242</b>	<b>67</b>	<b>183</b>	<b>68</b>	<b>157</b>	<b>55</b>
Slack slings		0.66		0.54		0.59		0.48		0.54		0.71		0.71	
$DAF_{\text{conv}}$		0.98		1.01		0.98		1.04		1.03		1.04		1.04	

Table I.4: Crane wire and sling tension versus zero up crossing period for  $H_s=2.0\text{m}$ ,  $h_B=1.0\text{m}$  and  $\beta=195$ .

$H_s$ [m]	$T_z$ [s]	Crane wire tension [kN]		Sling 900 tension [kN]		Sling 901 tension [kN]		Sling 902 tension [kN]		Sling 903 tension [kN]		Sling 904 tension [kN]		Sling 905 tension [kN]	
		max.	min.	max.	min.	max.	min.	max.	min.	max.	min.	max.	min.	max.	min.
Staad.Pro		1269		207		240		319		319		240		207	
$F_{\text{static}}$		948	508.2	151	77.3	176	95.3	234	123	234	123	176	95.3	151	77.3
2.0	4.02	848	409	151	40	171	64	220	77	242	55	157	89	147	71
	5.0	916	249	158	23	174	40	239	42	248	40	186	63	171	51
	6.0	954	192	161	17	186	35	242	34	243	33	186	53	163	27
	7.0	964	282	164	35	185	50	250	52	244	54	186	71	163	49
	8.0	946	413	155	55	176	72	246	87	241	90	184	74	162	60
	9.0	970	394	167	63	187	78	253	72	252	70	185	78	165	63
	10.0	978	366	168	59	190	76	248	57	249	56	180	80	161	64
	11.0	920	416	151	68	169	82	240	61	238	67	183	84	160	68
	12.0	864	435	140	70	160	89	241	74	239	79	166	86	149	69
	13.0	571	475	88	69	103	89	148	98	146	98	103	85	86	67
<b>Extremes</b>		<b>978</b>	<b>192</b>	<b>168</b>	<b>17</b>	<b>190</b>	<b>35</b>	<b>253</b>	<b>34</b>	<b>252</b>	<b>33</b>	<b>186</b>	<b>53</b>	<b>171</b>	<b>27</b>
Slack slings		0.38		0.22		0.37		0.28		0.27		0.56		0.35	
$DAF_{\text{conv}}$		1.03		1.11		1.08		1.08		1.08		1.06		1.13	

Table I.5: Crane wire and sling tension versus zero up crossing period for  $H_s=2.5\text{m}$ ,  $h_B=1.0\text{m}$  and  $\beta=195$ .

$H_s$ [m]	$T_z$ [s]	Crane wire tension [kN]		Sling 900 tension [kN]		Sling 901 tension [kN]		Sling 902 tension [kN]		Sling 903 tension [kN]		Sling 904 tension [kN]		Sling 905 tension [kN]	
		max.	min.	max.	min.	max.	min.	max.	min.	max.	min.	max.	min.	max.	min.
Staad.Pro		1269		207		240		319		319		240		207	
$F_{\text{static}}$		948	508.2	151	77.3	176	95.3	234	123	234	123	176	95.3	151	77.3
2.5	4.49	958	269	195	17	210	46	260	47	299	25	191	71	174	54
	5.0	947	156	189	3	206	28	240	25	285	15	209	61	184	27
	6.0	1025	74	176	1	205	14	296	1	313	1	201	26	171	2
	7.0	977	122	166	5	191	25	265	15	281	12	189	44	164	16
	8.0	969	300	158	38	186	56	254	66	244	60	187	71	165	50
	9.0	982	324	167	52	188	64	251	54	251	49	185	75	163	61
	10.0	985	308	174	54	196	64	255	44	253	41	184	68	163	55
	11.0	927	375	154	68	176	82	237	44	235	51	182	83	161	69
	12.0	939	380	154	69	177	77	247	50	245	59	186	80	162	66
	13.0	623	463	104	67	119	89	163	96	157	98	115	83	102	66
<b>Extremes</b>		<b>1025</b>	<b>74</b>	<b>195</b>	<b>1</b>	<b>210</b>	<b>14</b>	<b>296</b>	<b>1</b>	<b>313</b>	<b>1</b>	<b>209</b>	<b>26</b>	<b>184</b>	<b>2</b>
Sling criteria		0.15		0.01		0.15		0.01		0.01		0.27		0.03	
$DAF_{\text{conv}}$		1.08		1.29		1.19		1.26		1.34		1.19		1.22	

## I.4 Limiting sea state using Rayleigh distribution

Table I.6: Crane wire tension versus significant wave height for  $T_z=6.0\text{m}$ ,  $h_B=1.8\text{m}$  and  $\beta=195$ . Rayleigh values are obtained for 30 minutes duration.

$H_s$ [m]	Description	Crane wire tension [kN]		Sling 900 tension [kN]		Sling 901 tension [kN]		Sling 902 tension [kN]		Sling 903 tension [kN]		Sling 904 tension [kN]		Sling 905 tension [kN]	
		max.	min.	max.	min.	max.	min.	max.	min.	max.	min.	max.	min.	max.	min.
$F_{\text{static}}$		948	482	151	73	176	90	234	117	234	117	176	90	151	73
1.5	$R_{\text{max}} \pm F_{\text{static}}$	552	380	84	56	103	71	140	86	143	83	108	66	88	52
	<b>Slack sling</b>		<b>0.79</b>		<b>0.77</b>		<b>0.79</b>		<b>0.74</b>		<b>0.71</b>		<b>0.73</b>		<b>0.71</b>
	$F_{\text{total}}$	653	236	106	24	127	43	180	57	177	43	116	60	98	36
Slack sling		0.62		0.43		0.61		0.66		0.52		0.91		0.69	
2.0	$R_{\text{max}} \pm F_{\text{static}}$	611	321	93	47	112	62	159	67	160	66	119	55	99	41
	<b>Slack sling</b>		<b>0.67</b>		<b>0.64</b>		<b>0.69</b>		<b>0.57</b>		<b>0.56</b>		<b>0.61</b>		<b>0.56</b>
	$F_{\text{total}}$	832	47	137	1	163	8	236	9	232	1	165	20	150	1
Slack sling		0.12		0.02		0.11		0.10		0.01		0.30		0.02	
2.5	$R_{\text{max}} \pm F_{\text{static}}$	695	244	107	35	126	49	183	45	184	44	135	40	115	26
	<b>Slack sling</b>		<b>0.51</b>		<b>0.48</b>		<b>0.54</b>		<b>0.38</b>		<b>0.38</b>		<b>0.44</b>		<b>0.36</b>
	$F_{\text{total}}$	1053	12	179	1	213	1	313	1	302	1	207	1	181	1
Slack sling		0.03		0.02		0.01		0.01		0.01		0.02		0.02	
3.0	$R_{\text{max}} \pm F_{\text{static}}$	803	153	126	19	145	34	215	18	212	19	156	21	136	8
	<b>Slack sling</b>		<b>0.32</b>		<b>0.26</b>		<b>0.38</b>		<b>0.15</b>		<b>0.16</b>		<b>0.23</b>		<b>0.11</b>
	$F_{\text{total}}$	1516	11	189	1	288	1	388	1	402	1	392	1	373	1
Slack sling		0.03		0.02		0.01		0.01		0.01		0.02		0.02	

Table I.7: Crane wire tension versus significant wave height for  $T_z=6.0m$ ,  $h_B=0m$  and  $\beta=195$ . Rayleigh values are obtained for 30 minutes duration.

$H_s$ [m]	Description	Crane wire tension [kN]		Sling 900 tension [kN]		Sling 901 tension [kN]		Sling 902 tension [kN]		Sling 903 tension [kN]		Sling 904 tension [kN]		Sling 905 tension [kN]	
		max.	min.	max.	min.	max.	min.	max.	min.	max.	min.	max.	min.	max.	min.
$F_{static}$		948	810	151	128	176	149	234	200	234	200	176	149	151	128
1.5	$R_{max} \pm F_{static}$	1176	424	194	62	219	81	307	93	308	90	222	78	174	62
	$DAF_{conv}$	<b>1.24</b>		<b>1.28</b>		<b>1.24</b>		<b>1.31</b>		<b>1.32</b>		<b>1.26</b>		<b>1.15</b>	
	<b>Slack sling</b>		<b>0.88</b>		<b>0.85</b>		<b>0.90</b>		<b>0.79</b>		<b>0.77</b>		<b>0.87</b>		<b>0.85</b>
	$F_{total}$	956	242	165	21	190	40	247	51	257	50	186	68	160	40
	$DAF_{conv}$	1.01		1.09		1.08		1.06		1.10		1.06		1.06	
	<b>Slack sling</b>		0.64		0.38		0.56		0.59		0.60		1.03		0.77
2.0	$R_{max} \pm F_{static}$	1211	380	202	52	227	71	318	78	320	76	227	72	199	56
	$DAF_{conv}$	<b>1.28</b>		<b>1.34</b>		<b>1.29</b>		<b>1.36</b>		<b>1.37</b>		<b>1.29</b>		<b>1.32</b>	
	<b>Slack sling</b>		<b>0.79</b>		<b>0.71</b>		<b>0.79</b>		<b>0.67</b>		<b>0.65</b>		<b>0.80</b>		<b>0.77</b>
	$F_{total}$	1114	67	177	1	202	14	303	14	329	4	199	27	171	1
	$DAF_{conv}$	1.18		1.17		1.15		1.29		1.41		1.13		1.13	
	<b>Slack sling</b>		0.18		0.02		0.20		0.16		0.05		0.41		0.02
2.5	$R_{max} \pm F_{static}$	1251	337	212	41	238	59	331	64	333	62	233	67	205	50
	$DAF_{conv}$	<b>1.32</b>		<b>1.40</b>		<b>1.35</b>		<b>1.41</b>		<b>1.42</b>		<b>1.32</b>		<b>1.36</b>	
	<b>Slack sling</b>		<b>0.70</b>		<b>0.56</b>		<b>0.66</b>		<b>0.55</b>		<b>0.53</b>		<b>0.74</b>		<b>0.68</b>
	$F_{total}$	1343	12	239	1	265	1	382	1	425	1	235	1	196	1
	$DAF_{conv}$	1.42		1.58		1.51		1.63		1.82		1.34		1.30	
	<b>Slack sling</b>		0.03		0.02		0.01		0.01		0.01		0.02		0.02
3.0	$R_{max} \pm F_{static}$	1306	283	225	28	251	46	347	48	351	44	242	59	214	41
	$DAF_{conv}$	<b>1.38</b>		<b>1.49</b>		<b>1.43</b>		<b>1.48</b>		<b>1.50</b>		<b>1.38</b>		<b>1.42</b>	
	<b>Slack sling</b>		<b>0.59</b>		<b>0.38</b>		<b>0.51</b>		<b>0.41</b>		<b>0.38</b>		<b>0.66</b>		<b>0.56</b>
	$F_{total}$	1793	11	350	1	364	1	509	1	565	1	409	1	383	1
	$DAF_{conv}$	1.89		2.32		2.07		2.18		2.41		2.32		2.54	
	<b>Slack sling</b>		0.03		0.02		0.01		0.01		0.01		0.02		0.02

Table I.8: Max crane wire tension versus significant wave height for  $T_z=6.0m$ ,  $h_B=0m$  and  $\beta=195^\circ$ , storm duration=30min and threshold=950kN.

$H_s [m]$	Mode/method used to obtain maximum crane wire tension	Threshold [kN]	Storm duration [h]	Crane wire tension [kN]	$DAF_{conv} [-]$
	Static load, $F_{static}$			948	
1.5	Total load, $F_{total}$	n/a	n/a	956	1.0
	Rayleigh distribution	n/a	0.5	1176	1.2
	Weibull distribution	950	0.5	955	1.0
	Generalised Pareto	950	0.5	955	1.0
2.0	Total load, $F_{total}$	n/a	n/a	1114	1.2
	Rayleigh distribution	n/a	0.5	1211	1.3
	Weibull distribution	950	0.5	988	1.0
	Generalised Pareto	950	0.5	987	1.0
2.5	Total load, $F_{total}$	n/a	n/a	1343	1.4
	Rayleigh distribution	n/a	0.5	1251	1.3
	Weibull distribution	950	0.5	1080	1.1
	Generalised Pareto	950	0.5	1159	1.2
3.0	Total load, $F_{total}$	n/a	n/a	1793	1.9
	Rayleigh distribution	n/a	0.5	1306	1.4
	Weibull distribution	950	0.5	1267	1.3
	Generalised Pareto	950	0.5	1573	1.7



**APPENDIX J**

**OUTPUT FILE FROM**  
**STAAD.PRO ANALYSIS**

```

*****
*
*          STAAD.Pro V8i SELECTseries3          *
*          Version  20.07.08.20                 *
*          Proprietary Program of              *
*          Bentley Systems, Inc.               *
*          Date=    JUN 10, 2013               *
*          Time=    12:45:17                   *
*
*          USER ID: Subsea 7                   *
*****

```

```

1. STAAD SPACE
INPUT FILE: Integrated spool cover.STD
2. START JOB INFORMATION
3. JOB NAME GULLFAKS SUBSEA COMPRESSION PROJECT
4. JOB CLIENT STATOIL
5. ENGINEER DATE 07-MAR-13
6. *****
7. *REFERENCES *
8. *****
9. * /1/ DNV (1996) RULES FOR PLANNING AND EXECUTION OF MARINE OPERATION PT.2CH.5*
10. * /2/ EC3 EN 1993-1-1-2005 EUROCODE 3 *
11. *****
12. JOB COMMENT ANALYSIS ACCORDING TO DNV (1996)
13. JOB COMMENT - DAF IN AIR =1.20
14. JOB COMMENT - DAF IN WATER =1.60
15. JOB COMMENT - SKEW LOAD FACTOR, SKL =1.25
16. JOB COMMENT - WEIGHT INACCURACY FACTOR =1.05
17. JOB COMMENT - COG INACCURACY FACTOR =1.05
18. JOB COMMENT - LOAD FACTOR =1.30
19. JOB COMMENT - CONSEQUENCE FACTOR, SPOOL =1.00
20. JOB COMMENT - CONSEQUENCE FACTOR, INTEGRATED COVER =1.30
21. JOB COMMENT CODE CHECK ACCORDING TO EUROCODE 3, 1993-1-1-2005
22. JOB COMMENT - MATERIAL FACTOR =1.15
23. JOB COMMENT - SPOOL YIELD LIMIT =374MPA
24. JOB COMMENT - INTEGRATED COVER YIELD LIMIT =355MPA
25. END JOB INFORMATION
26. INPUT WIDTH 79
27. *****
28. *NODE NUMBERING *
29. *****
30. * 001-199 - SPOOL NODES *
31. * 200-299 - INTEGRATED COVER NODES *
32. * 999 - HOOK NODE (COG) *
33. *****
34. *MEMBER NUMBERING *
35. *****
36. * 001-199 - SPOOL MEMBERS *
37. * 200-699 - INTEGRATED COVER MEMBERS *
38. * 800-899 - RIGGING MEMBERS *
39. * 900-999 - SLING MEMBERS *
40. *****

```



## 41. UNIT METER KN

## 42. JOINT COORDINATES

43. 1 -14.885 0.5 3.4; 2 -11.37 0.5 3.4; 3 -7.855 0.5 3.4; 4 -4.34 0.5 3.4  
44. 5 -3.74 0.5 3.4; 6 -3.74 0.5 4; 7 -3.74 0.5 7.8333; 8 -3.74 0.5 11.6667  
45. 9 -3.74 0.5 15.5; 10 -3.74 0.5 19.3333; 11 -3.74 0.5 23.1667  
46. 12 -3.74 0.5 26.4; 13 0 0.5 26.4; 14 3.74 0.5 26.4; 15 3.74 0.5 23.1667  
47. 16 3.74 0.5 19.3333; 17 3.74 0.5 15.5; 18 3.74 0.5 11.6667; 19 3.74 0.5 7.8333  
48. 20 3.74 0.5 4; 21 3.74 0.5 3.4; 22 4.34 0.5 3.4; 23 7.855 0.5 3.4  
49. 24 11.37 0.5 3.4; 25 14.885 0.5 3.4; 26 -14.885 0.5 0.6; 27 -11.37 0.5 0.6  
50. 28 -7.855 0.5 0.6; 29 -4.34 0.5 0.6; 30 -1.74 0.5 0.6; 31 -1.74 0.5 4  
51. 32 -1.74 0.5 7.8333; 33 -1.74 0.5 11.6667; 34 -1.74 0.5 15.5  
52. 35 -1.74 0.5 19.3333; 36 -1.74 0.5 23.1667; 37 -1.74 0.5 24.4; 38 0 0.5 24.4  
53. 39 1.74 0.5 24.4; 40 1.74 0.5 23.1667; 41 1.74 0.5 19.3333; 42 1.74 0.5 15.5  
54. 43 1.74 0.5 11.6667; 44 1.74 0.5 7.8333; 45 1.74 0.5 4; 46 1.74 0.5 0.756  
55. 47 4.34 0.5 0.756; 48 7.855 0.5 0.756; 49 11.37 0.5 0.756; 50 14.885 0.5 0.756  
56. 51 -23 2.1 3.4; 52 -20 2.1 3.4; 53 -18.4 0.5 3.4; 54 -16.4 0.5 3.4  
57. 55 16.4 0.5 3.4; 56 18.4 0.5 3.4; 57 20 2.1 3.4; 58 23 2.1 3.4; 59 -23 2.1 0.6  
58. 60 -20 2.1 0.6; 61 -18.4 0.5 0.6; 62 -16.4 0.5 0.6; 63 16.4 0.5 0.756  
59. 64 18.4 0.5 0.756; 65 20 2.1 0.756; 66 23 2.1 0.756; 67 -14.885 0.5 2  
60. 68 -11.37 0.5 2; 69 -7.855 0.5 2; 70 -4.34 0.5 2; 71 -2.74 0.5 2  
61. 72 -2.74 0.5 4; 73 -2.74 0.5 7.8333; 74 -2.74 0.5 11.6667; 75 -2.74 0.5 15.5  
62. 76 -2.74 0.5 19.3333; 77 -2.74 0.5 23.1667; 78 -2.74 0.5 25.4; 79 0 0.5 25.4  
63. 80 2.74 0.5 25.4; 81 2.74 0.5 23.1667; 82 2.74 0.5 19.3333; 83 2.74 0.5 15.5  
64. 84 2.74 0.5 11.6667; 85 2.74 0.5 7.8333; 86 2.74 0.5 4; 87 2.74 0.5 2.078  
65. 88 4.34 0.5 2.078; 89 7.855 0.5 2.078; 90 11.37 0.5 2.078; 91 14.885 0.5 2.078  
66. 92 -23 2.1 2; 93 -20 2.1 2; 94 -18.4 0.5 2; 95 -16.4 0.5 2; 96 16.4 0.5 2.078  
67. 97 18.4 0.5 2.078; 98 20 2.1 2.078; 99 23 2.1 2.078; 100 -21.975 2.1 3.4  
68. 101 21.975 2.1 3.4; 102 -21.975 2.1 0.6; 103 21.975 2.1 0.756  
69. 104 -21.975 2.1 2; 105 21.975 2.1 2.078; 200 -18.4 0 0; 201 -18.4 0 4  
70. 202 -14.885 0 0; 203 -14.885 0 4; 204 -11.37 0 0; 205 -11.37 0 4  
71. 206 -7.855 0 0; 207 -7.855 0 4; 208 -4.34 0 0; 209 -4.34 0 4  
72. 210 -4.34 0 7.8333; 211 -4.34 0 11.6667; 212 -4.34 0 15.5; 213 -4.34 0 19.3333  
73. 214 -4.34 0 23.1667; 215 -4.34 0 27; 216 0 0 0; 217 0 0 4; 218 0 0 7.8333  
74. 219 0 0 11.6667; 220 0 0 15.5; 221 0 0 19.3333; 222 0 0 23.1667; 223 0 0 27  
75. 224 4.34 0 0; 225 4.34 0 4; 226 4.34 0 7.8333; 227 4.34 0 11.6667  
76. 228 4.34 0 15.5; 229 4.34 0 19.3333; 230 4.34 0 23.1667; 231 4.34 0 27  
77. 232 7.855 0 0; 233 7.855 0 4; 234 11.37 0 0; 235 11.37 0 4; 236 14.885 0 0  
78. 237 14.885 0 4; 238 18.4 0 0; 239 18.4 0 4; 240 -18.4 0 0.6; 241 -18.4 0 2  
79. 242 -18.4 0 3.4; 243 0 0 24.4; 244 0 0 25.4; 245 0 0 26.4; 246 18.4 0 0.756  
80. 247 18.4 0 2.078; 248 18.4 0 3.4; 249 -14.885 0 0.6; 250 -14.885 0 2  
81. 251 -14.885 0 3.4; 252 -11.37 0 0.6; 253 -11.37 0 2; 254 -11.37 0 3.4  
82. 255 -7.855 0 0.6; 256 -7.855 0 2; 257 -7.855 0 3.4; 258 -4.34 0 0.6  
83. 259 -4.34 0 2; 260 -4.34 0 3.4; 261 -3.74 0 4; 262 -3.74 0 7.8333  
84. 263 -3.74 0 11.6667; 264 -3.74 0 15.5; 265 -3.74 0 19.3333  
85. 266 -3.74 0 23.1667; 267 -2.74 0 4; 268 -2.74 0 7.8333; 269 -2.74 0 11.6667  
86. 270 -2.74 0 15.5; 271 -2.74 0 19.3333; 272 -2.74 0 23.1667; 273 -1.74 0 4  
87. 274 -1.74 0 7.8333; 275 -1.74 0 11.6667; 276 -1.74 0 15.5; 277 -1.74 0 19.3333  
88. 278 -1.74 0 23.1667; 279 1.74 0 4; 280 1.74 0 7.8333; 281 1.74 0 11.6667  
89. 282 1.74 0 15.5; 283 1.74 0 19.3333; 284 1.74 0 23.1667; 285 2.74 0 4  
90. 286 2.74 0 7.8333; 287 2.74 0 11.6667; 288 2.74 0 15.5; 289 2.74 0 19.3333  
91. 290 2.74 0 23.1667; 291 3.74 0 4; 292 3.74 0 7.8333; 293 3.74 0 11.6667  
92. 294 3.74 0 15.5; 295 3.74 0 19.3333; 296 3.74 0 23.1667; 297 4.34 0 0.756  
93. 298 4.34 0 2.078; 299 4.34 0 3.4; 300 7.855 0 0.756; 301 7.855 0 2.078  
94. 302 7.855 0 3.4; 303 11.37 0 0.756; 304 11.37 0 2.078; 305 11.37 0 3.4  
95. 306 14.885 0 0.756; 307 14.885 0 2.078; 308 14.885 0 3.4; 309 -18.4 2.1 0  
96. 310 -18.4 2.1 4; 311 -14.885 2.1 0; 312 -14.885 2.1 4; 313 -11.37 2.1 0

97. 314 -11.37 2.1 4; 315 -7.855 2.1 0; 316 -7.855 2.1 4; 317 -4.34 2.1 0  
 98. 318 -4.34 2.1 4; 319 -4.34 2.1 7.8333; 320 -4.34 2.1 11.6667  
 99. 321 -4.34 2.1 15.5; 322 -4.34 2.1 19.3333; 323 -4.34 2.1 23.1667  
 100. 324 -4.34 2.1 27; 325 0 2.1 0; 326 0 2.1 4; 327 0 2.1 7.8333  
 101. 328 0 2.1 11.6667; 329 0 2.1 15.5; 330 0 2.1 19.3333; 331 0 2.1 23.1667  
 102. 332 0 2.1 27; 333 4.34 2.1 0; 334 4.34 2.1 4; 335 4.34 2.1 7.8333  
 103. 336 4.34 2.1 11.6667; 337 4.34 2.1 15.5; 338 4.34 2.1 19.3333  
 104. 339 4.34 2.1 23.1667; 340 4.34 2.1 27; 341 7.855 2.1 0; 342 7.855 2.1 4  
 105. 343 11.37 2.1 0; 344 11.37 2.1 4; 345 14.885 2.1 0; 346 14.885 2.1 4  
 106. 347 18.4 2.1 0; 348 18.4 2.1 4; 349 -18.4 0 5.32; 350 -14.885 0 5.32  
 107. 351 -11.37 0 5.32; 352 -7.855 0 5.32; 353 -5.66 0 5.32; 354 -5.66 0 7.8333  
 108. 355 -5.66 0 11.6667; 356 -5.66 0 15.5; 357 -5.66 0 19.3333  
 109. 358 -5.66 0 23.1667; 359 -5.66 0 27; 361 -4.34 0 28.32; 362 0 0 28.32  
 110. 363 4.34 0 28.32; 364 5.66 0 5.32; 365 5.66 0 7.8333; 366 5.66 0 11.6667  
 111. 367 5.66 0 15.5; 368 5.66 0 19.3333; 369 5.66 0 23.1667; 370 5.66 0 27  
 112. 372 7.855 0 5.32; 373 11.37 0 5.32; 374 14.885 0 5.32; 375 18.4 0 5.32  
 113. 999 0 20.5 8.843  
 114. \*\*\*\*\*  
 115. MEMBER INCIDENCES  
 116. 1 54 1; 2 1 2; 3 2 3; 4 3 4; 5 4 5; 6 5 6; 7 6 7; 8 7 8; 9 8 9; 10 9 10  
 117. 11 10 11; 12 11 12; 13 12 13; 14 13 14; 15 14 15; 16 15 16; 17 16 17; 18 17 18  
 118. 19 18 19; 20 19 20; 21 20 21; 22 21 22; 23 22 23; 24 23 24; 25 24 25; 26 25 55  
 119. 27 62 26; 28 26 27; 29 27 28; 30 28 29; 31 29 30; 32 30 31; 33 31 32; 34 32 33  
 120. 35 33 34; 36 34 35; 37 35 36; 38 36 37; 39 37 38; 40 38 39; 41 39 40; 42 40 41  
 121. 43 41 42; 44 42 43; 45 43 44; 46 44 45; 47 45 46; 48 46 47; 49 47 48; 50 48 49  
 122. 51 49 50; 52 50 63; 53 102 60; 54 100 52; 55 60 61; 56 52 53; 57 61 62  
 123. 58 53 54; 59 63 64; 60 55 56; 61 64 65; 62 56 57; 63 65 103; 64 57 101  
 124. 65 51 100; 66 59 102; 67 101 58; 68 103 66; 69 95 67; 70 67 68; 71 68 69  
 125. 72 69 70; 73 70 71; 74 71 72; 75 72 73; 76 73 74; 77 74 75; 78 75 76; 79 76 77  
 126. 80 77 78; 81 78 79; 82 79 80; 83 80 81; 84 81 82; 85 82 83; 86 83 84; 87 84 85  
 127. 88 85 86; 89 86 87; 90 87 88; 91 88 89; 92 89 90; 93 90 91; 94 91 96  
 128. 95 104 93; 96 93 94; 97 94 95; 98 96 97; 99 97 98; 100 98 105; 101 92 104  
 129. 102 105 99; 200 200 240; 201 240 241; 202 241 242; 203 242 201; 204 202 200  
 130. 205 201 203; 206 204 202; 207 203 205; 208 206 204; 209 205 207; 210 208 206  
 131. 211 207 209; 212 209 210; 213 210 211; 214 211 212; 215 212 213; 216 213 214  
 132. 217 214 215; 218 216 208; 219 215 223; 220 224 216; 221 223 231; 222 226 225  
 133. 223 227 226; 224 228 227; 225 229 228; 226 230 229; 227 231 230; 228 232 224  
 134. 229 225 233; 230 234 232; 231 233 235; 232 236 234; 233 235 237; 234 238 236  
 135. 235 237 239; 236 246 238; 237 247 246; 238 248 247; 239 239 248; 240 216 217  
 136. 241 217 218; 242 218 219; 243 219 220; 244 220 221; 245 221 222; 246 222 243  
 137. 247 243 244; 248 244 245; 249 245 223; 250 202 249; 251 206 255; 252 208 258  
 138. 253 224 297; 254 232 300; 255 236 306; 256 249 250; 257 255 256; 258 258 259  
 139. 259 297 298; 260 300 301; 261 306 307; 262 250 251; 263 256 257; 264 259 260  
 140. 265 298 299; 266 301 302; 267 307 308; 268 251 203; 269 257 207; 270 260 209  
 141. 271 299 225; 272 302 233; 273 308 237; 274 209 261; 275 261 267; 276 267 273  
 142. 277 273 217; 278 217 279; 279 279 285; 280 285 291; 281 291 225; 282 210 262  
 143. 283 262 268; 284 268 274; 285 274 218; 286 218 280; 287 280 286; 288 286 292  
 144. 289 292 226; 290 211 263; 291 263 269; 292 269 275; 293 275 219; 294 219 281  
 145. 295 281 287; 296 287 293; 297 293 227; 298 213 265; 299 265 271; 300 271 277  
 146. 301 277 221; 302 221 283; 303 283 289; 304 289 295; 305 295 229; 306 212 264  
 147. 307 264 270; 308 270 276; 309 276 220; 310 220 282; 311 282 288; 312 288 294  
 148. 313 294 228; 314 204 252; 315 252 253; 316 253 254; 317 254 205; 318 214 266  
 149. 319 266 272; 320 272 278; 321 278 222; 322 222 284; 323 284 290; 324 290 296  
 150. 325 296 230; 326 234 303; 327 303 304; 328 304 305; 329 305 235; 330 311 309  
 151. 331 310 312; 332 313 311; 333 312 314; 334 315 313; 335 314 316; 336 317 315  
 152. 337 316 318; 338 318 319; 339 319 320; 340 320 321; 341 321 322; 342 322 323

STAAD SPACE

-- PAGE NO. 4

153. 343 323 324; 344 325 317; 345 324 332; 346 333 325; 347 332 340; 348 335 334  
154. 349 336 335; 350 337 336; 351 338 337; 352 339 338; 353 340 339; 354 341 333  
155. 355 334 342; 356 343 341; 357 342 344; 358 345 343; 359 344 346; 360 347 345  
156. 361 346 348; 362 325 326; 363 326 327; 364 327 328; 365 328 329; 366 329 330  
157. 367 330 331; 368 313 314; 369 317 318; 370 318 326; 371 322 330; 372 326 334  
158. 373 330 338; 374 333 334; 375 343 344; 391 201 202; 392 202 205; 393 205 206  
159. 394 209 216; 395 210 217; 396 218 211; 397 212 219; 398 220 213; 399 214 221  
160. 400 222 215; 401 216 225; 402 226 217; 403 218 227; 404 228 219; 405 220 229  
161. 406 230 221; 407 222 231; 408 232 235; 409 235 236; 410 236 239; 411 206 209  
162. 412 225 232; 457 200 309; 458 201 310; 459 202 311; 460 203 312; 461 206 315  
163. 462 207 316; 463 208 317; 464 209 318; 465 210 319; 466 211 320; 467 212 321  
164. 468 214 323; 469 215 324; 470 216 325; 471 223 332; 472 224 333; 473 225 334  
165. 474 226 335; 475 227 336; 476 228 337; 477 230 339; 478 231 340; 479 232 341  
166. 480 233 342; 481 236 345; 482 237 346; 483 238 347; 484 239 348; 485 204 313  
167. 486 205 314; 487 213 322; 488 229 338; 489 234 343; 490 235 344; 491 217 326  
168. 492 218 327; 493 219 328; 494 220 329; 495 221 330; 496 222 331; 497 216 326  
169. 498 217 327; 499 218 328; 500 219 329; 501 220 330; 502 221 331; 503 309 202  
170. 504 203 310; 505 313 202; 506 313 206; 507 317 206; 508 207 318; 509 210 318  
171. 510 210 320; 511 212 320; 512 212 322; 513 214 322; 514 214 324; 515 317 216  
172. 516 223 324; 517 333 216; 518 223 340; 519 334 226; 520 336 226; 521 336 228  
173. 522 338 228; 523 338 230; 524 340 230; 525 333 232; 526 233 334; 527 343 232  
174. 528 343 236; 529 347 236; 530 237 348; 531 203 314; 532 207 314; 533 233 344  
175. 534 237 344; 600 201 349; 601 349 350; 602 203 350; 603 350 351; 604 205 351  
176. 605 351 352; 606 207 352; 607 352 353; 608 353 354; 609 354 355; 610 355 356  
177. 611 356 357; 612 357 358; 613 358 359; 614 354 210; 615 355 211; 616 356 212  
178. 617 357 213; 618 358 214; 619 359 215; 620 359 361; 621 215 361; 622 361 362  
179. 623 223 362; 624 362 363; 625 231 363; 626 226 365; 627 227 366; 628 228 367  
180. 629 229 368; 630 230 369; 631 231 370; 632 363 370; 633 365 364; 634 366 365  
181. 635 367 366; 636 368 367; 637 369 368; 638 370 369; 639 364 372; 640 233 372  
182. 641 372 373; 642 235 373; 643 373 374; 644 237 374; 645 374 375; 646 375 239  
183. 647 349 310; 648 350 312; 649 351 314; 650 352 316; 651 354 319; 652 355 320  
184. 653 356 321; 654 357 322; 655 358 323; 656 359 324; 657 361 324; 658 362 332  
185. 659 363 340; 660 365 335; 661 366 336; 662 367 337; 663 368 338; 664 369 339  
186. 665 370 340; 666 372 342; 667 373 344; 668 374 346; 669 375 348; 800 240 61  
187. 801 241 94; 802 242 53; 803 249 26; 804 250 67; 805 251 1; 806 252 27  
188. 807 253 68; 808 254 2; 809 255 28; 810 256 69; 811 257 3; 812 258 29  
189. 813 259 70; 814 260 4; 815 261 6; 816 262 7; 817 263 8; 818 264 9; 819 265 10  
190. 820 266 11; 821 267 72; 822 268 73; 823 269 74; 824 270 75; 825 271 76  
191. 826 272 77; 827 273 31; 828 274 32; 829 275 33; 830 276 34; 831 277 35  
192. 832 278 36; 833 243 38; 834 244 79; 835 245 13; 836 279 45; 837 280 44  
193. 838 281 43; 839 282 42; 840 283 41; 841 284 40; 842 285 86; 843 286 85  
194. 844 287 84; 845 288 83; 846 289 82; 847 290 81; 848 291 20; 849 292 19  
195. 850 293 18; 851 294 17; 852 295 16; 853 296 15; 854 297 47; 855 298 88  
196. 856 299 22; 857 300 48; 858 301 89; 859 302 23; 860 303 49; 861 304 90  
197. 862 305 24; 863 306 50; 864 307 91; 865 308 25; 866 246 64; 867 247 97  
198. 868 248 56; 900 313 999; 901 314 999; 902 322 999; 903 338 999; 904 344 999  
199. 905 343 999  
200. \*  
201. \*  
202. \*  
203. \*  
204. \*  
205. \*  
206. \*  
207. \*  
208. \*

```

209. *****
210. *DESCRIPTION OF GROUPS *
211. *****
212. *SPOOLS *
213. * -"12''SPOOL"          DEFINES 12''SPOOLS (SPOOL #1 AND #3) *
214. * -"12''GOOSENECK"      DEFINES 12'' GOOSENECKS (SPOOL #1 AND #3) *
215. * -"8''SPOOL"           DEFINES 8''SPOOL (SPOOL #2) *
216. * -"8''GOOSENECK"       DEFINES 8''GOOSENECK (SPOOL #2) *
217. *INTEGRATED SPOOL COVER *
218. * -"BOTTOM MAIN"        BOTTOM MAIN FRAME (CHORD) MEMBERS *
219. * -"BOTTOM TRANSVER"    BOTTOM TRANSVERSE MEMBERS SUPPORTING THE THREE SPOOLS *
220. * -"BOTTOM STRESSED"    BOTTOM TRANSVERSE MEMBERS WITH INCREASED CROSS SECTIONS *
221. * -"BOTTOM BRACE"       DEFINES THE BOTTOM DIAGONAL MEMBERS *
222. * -"TOP MAIN"           DEFINES THE TOP MAIN FRAME (CHORD) MEMBERS *
223. * -"VERTICAL"           VERTICAL BEAMS CONNECTING TOP AND BOTTOM MAIN FRAMES *
224. * -"VERTICAL STRESSED"  VERTICAL MEMBERS WITH INCREASED CROSS SECTIONS *
225. * -"MID VERTICAL"       CONNECTING THE TOP AND BOTTOM MID LINES *
226. * -"SIDE BRACE"         DEFINES ALL BRACE MEMBERS IN VERTICAL DIRECTION *
227. * -"STRESSED BRACES"   BRACES WITH INCREASED CROSS SECTIONS *
228. * -"BOTTOM TRAWL"       DEFINES BOTTOM MEMBERS OF THE TRAWL BOARDS *
229. * -"SIDE TRAWL"         DEFINES DIAGONAL MEMBERS OF TRAWL BOARDS *
230. * -"TOP TRANSVER"      TEMPORARY HEB BEAMS SUPPORTING THE STRUCTURE *
231. *RIGGING *
232. * -"CONNECTIONS"        DEFINES MEMBERS CONNECTING THE SPOOLS WITH THE COVER *
233. * -"SLINGS"            DEFINES THE SLING MEMBERS *
234. *MAIN PARTS *
235. * -"SPOOLS"            DEFINES ALL SPOOL MEMBERS *
236. * -"SPREADER"          DEFINES ALL MEMBERS IN INTEGRATED SPOOL COVER *
237. * -"RIGGING"          SLINGS AND MEMBERS CONNECTING SPOOLS WITH THE COVER *
238. *LOAD COMBINATION 16 *
239. * -"LOAD CASE 13"      ALL BOTTOM MEMBERS IN COVER AND IS NEEDED TO SEPERATE *
240. *                      MEMBERS FOR PARTLY SUBMERGED LOAD COMBINATION *
241. * -"LOAD CASE 14"      ALL MEMBERS NOT ACCOUNTED FOR IN "LOAD CASE 13" TO *
242. *                      SEPERATE MEMBERS FOR PARTLY SUBMERGED LOAD COMBINATION *
243. *GRP *
244. * -"TOP GRP1"          MEMBERS SUPPORTING GRP-COVER WHERE THE SPAN IS 4.00M *
245. * -"TOP GRP2"          MEMBERS SUPPORTING GRP-COVER WHERE THE SPAN IS 4.34M *
246. *MEMBERS SUBJECTED TO BUCKLING *
247. * -"BUCKLE TRANS Z"   BOTTOM TRANSVERS MEMBERS PARALLELL TO Z-AXIS SUBJECTED *
248. *                      TO COMPRESSIVE AXIAL LOAD *
249. * -"BUCKLE TRANS X"   BOTMOM TRANSVERS MEMBERS PARALLELL TO X-AXIS SUBJECTED *
250. *                      TO COMPRESSIVE AXIAL LOAD *
251. * -"BEAM 1-5"         MEMBER AS DEFINED IN SECTION 4.1.7 *
252. *ADDITIONAL GROUPS *
253. * -"SPOOL1"           SPOOL #1 TO OBTAIN TOTAL LOAD OF INDIVIDUAL SPOOLS *
254. * -"GOOSE1"           GOOSENECK #1 TO OBTAIN TOTAL LOAD OF INDIVIDUAL SPOOLS *
255. * -"SPOOL3"           SPOOL #3 TO OBTAIN TOTAL LOAD OF INDIVIDUAL SPOOLS *
256. * -"GOOSE3"           GOOSENECK #3 TO OBTAIN TOTAL LOAD OF INDIVIDUAL SPOOLS *
257. *NODE GROUPS *
258. * -"TERMINATION"      JOINTS WHERE WEIGHT OF TERMINATION HEADS ARE APPLIED *
259. * -"HOOK"             THE HOOK (COG) NODE *
260. * -"STIFFENERS"       THE NODES FOR WEAK STIFFENERS TO AVOID SINGULARITIES *
261. * -"JOINTS"           TO APPLY ADDITIONAL WEIGHT FROM WELDS, PADEYES, ETC *
262. *****
263. *
264. *

```

```
265. *****
266. START GROUP DEFINITION
267. MEMBER
268. *SPOOLS*****
269. _12''SPOOL 1 TO 52
270. _12''GOOSENECK 53 TO 68
271. _8''SPOOL 69 TO 94
272. _8''GOOSENECK 95 TO 102
273. *INTEGRATED SPOOL COVER*****
274. _BOTTOM_MAIN 200 TO 239
275. _BOTTOM_TRANSVER 250 TO 297
276. _BOTTOM_STRESSED 298 TO 329
277. _BOTTOM_BRACE 391 TO 410
278. _TOP_MAIN 330 TO 361
279. _VERTICAL 457 TO 484
280. _VERTICAL_STRESSED 485 TO 490
281. _MID_VERTICAL 491 TO 502
282. _MID_LINE 240 TO 249 362 TO 367
283. _SIDE_BRACE 503 TO 530
284. _STRESSED_BRACE 411 412 531 TO 534
285. _BOTTOM_TRAWL 600 TO 646
286. _SIDE_TRAWL 647 TO 669
287. _TOP_TRANSVER 368 TO 375
288. *RIGGING*****
289. _CONNECTIONS 800 TO 868
290. _SLINGS 900 TO 905
291. *MAIN PARTS*****
292. _SPOOLS 1 TO 102
293. _SPREADER 200 TO 375 391 TO 412 457 TO 534 600 TO 669
294. _RIGGING 800 TO 868 901 TO 905
295. *LOAD COMBINATION 116*****
296. _LOAD_CASE_13 200 TO 329 391 TO 412 600 TO 646
297. _LOAD_CASE_14 330 TO 375 457 TO 534 647 TO 669
298. *GRP*****
299. _TOP_GRP1 338 TO 343 348 TO 353
300. _TOP_GRP2 330 332 334 336 344 346 354 356 358 360
301. *MEMBERS SUBJECTED TO BUCKLING*****
302. _BUCKLE_TRANS_Z 314 TO 317 326 TO 329
303. _BUCKLE_TRANS_X 282 TO 297
304. _BEAM1 335 337 355 357 370 372
305. _BEAM2 336 344 346 354
306. _BEAM4 338 TO 341 348 TO 351 369 374
307. _BEAM5 363 TO 366
308. _BEAM3_2 207 209 231 233
309. _BEAM3_1 211 229 274 TO 281
310. *ADDITIONAL GROUPS*****
311. _SPOOL1 1 TO 26
312. _GOOSE1 54 56 58 60 62 64 65 67
313. _SPOOL3 27 TO 52
314. _GOOSE3 53 55 57 59 61 63 66 68
315. *****
316. JOINT
317. _TERMINATION 100 TO 105
318. _STIFFENERS 200 238
319. _JOINTS 309 TO 348
320. END GROUP DEFINITION
```

```

321. *****
322. *MATERIALS *
323. *****
324. * -"SPOOLS" MATERIAL: 25% SUPER DUPLEX STEEL *
325. * E=200GPA, DENSITY=7820KG/M3, V=0.3, ALPHA=1.73X10E-6 *
326. * -"INTEGRATED COVER" MATERIAL: STEEL *
327. * E=205GPA, DENSITY=7850KG/M3, V=0.3 ALPHA=1.73X10E-6 *
328. * -"WIRE ROPE" MATERIAL: WIRE STEEL *
329. * E=110GPA, DENSITY=NA V=0.3 *
330. *****
331. *STEEL PROPERTIES*****
332. DEFINE MATERIAL START
333. ISOTROPIC STEEL
334. E 2.05E+008
335. POISSON 0.3
336. DENSITY 78.5
337. ALPHA 1.73E-005
338. DAMP 0.03
339. *25%CR STEEL PROPERTIES*****
340. ISOTROPIC 25%CR_STEEL
341. E 2E+008
342. POISSON 0.3
343. DENSITY 78.2
344. ALPHA 1.73E-005
345. DAMP 0.03
346. *WIRE PROPERTIES*****
347. ISOTROPIC WIRE
348. E 1.01E+008
349. POISSON 0.3
350. DENSITY 1E-006
351. END DEFINE MATERIAL
352. *****
353. CONSTANTS
354. MATERIAL STEEL MEMB _SPREADER
355. MATERIAL STEEL MEMB _SPOOLS
356. MATERIAL STEEL MEMB _CONNECTIONS
357. MATERIAL WIRE MEMB _SLINGS
358. *****
359. *CROSS SECTIONAL PROPERTIES *
360. *****
361. *SPOOLS *
362. * -"12''SPOOL" OD=323.9MM, WT=23.8MM, ID=276.2MM (WITHOUT COATING) *
363. * -"12''GOOSENECK" OD=323.9MM, WT=31.0MM, ID=261.9MM (WITHOUT COATING) *
364. * -"8''SPOOL" OD=219.1MM, WT=15.9MM, ID=187.3MM (WITHOUT COATING) *
365. * -"12''GOOSENECK" OD=219.1MM, WT=15.9MM, ID=187.3MM (WITHOUT COATING) *
366. *INTEGRATED COVER *
367. * -MAIN MEMBERS IN COVER DESIGNED AS 10'', 8'' AND 6'' TUBULAR SECTIONS *
368. * ACCORDING TO RELEVANT JOINT CONSIDERATIONS AND STRESSES IN RESPECTIVE BEAMS*
369. * -"10'' TUBULAR SEC." OD=273.0MM WT=12.7MM, ID=247.6MM *
370. * -"8'' TUBULAR SEC." OD=219.1MM WT= 8.2MM, ID=202.7MM *
371. * -"6'' TUBULAR SEC." OD=168.3MM WT= 7.1MM, ID=154.1MM *
372. * -THE TEMPORARY BEAMS IS DESIGNED AS HE220B BEAMS *
373. *RIGGING *
374. * -"CONNECTIONS" SECTIONAL PROP. IS N.A. -SAME PROPERTIES AS SPREADER *
375. * -"SLINGS 52MM *
376. *****

```

```

377. MEMBER PROPERTY EUROPEAN
378. *SPOOLS*****
379. _12''SPOOL TABLE ST PIPE OD 0.3238 ID 0.2762
380. _8''SPOOL TABLE ST PIPE OD 0.2191 ID 0.1873
381. _12''GOOSENECK TABLE ST PIPE OD 0.3238 ID 0.2618
382. _8''GOOSENECK TABLE ST PIPE OD 0.2191 ID 0.1873
383. *INTEGRATED COVER*****
384. _BOTTOM_MAIN TABLE ST PIPE OD 0.273 ID 0.2476
385. _BOTTOM_TRANSVER TABLE ST PIPE OD 0.2191 ID 0.2027
386. _BOTTOM_STRESSED TABLE ST PIPE OD 0.273 ID 0.2476
387. _BOTTOM_BRACE TABLE ST PIPE OD 0.1683 ID 0.1541
388. _TOP_MAIN TABLE ST PIPE OD 0.273 ID 0.2476
389. _VERTICAL TABLE ST PIPE OD 0.2191 ID 0.2027
390. _VERTICAL_STRESSED TABLE ST PIPE OD 0.273 ID 0.2476
391. _MID_VERTICAL TABLE ST PIPE OD 0.1683 ID 0.1541
392. _MID_LINE TABLE ST PIPE OD 0.2191 ID 0.2027
393. _SIDE_BRACE TABLE ST PIPE OD 0.1683 ID 0.1541
394. _STRESSED_BRACE TABLE ST PIPE OD 0.273 ID 0.2476
395. _BOTTOM_TRAWL TABLE ST PIPE OD 0.1683 ID 0.1541
396. _SIDE_TRAWL TABLE ST PIPE OD 0.1683 ID 0.1541
397. _TOP_TRANSVER TABLE ST HE240B
398. *RIGGING*****
399. _CONNECTIONS TABLE ST PIPE OD 0.1 ID 0.001
400. _SLINGS TABLE ST PIPE OD 0.052 ID 1E-011
401. *****
402. *SUPPORTS *
403. *****
404. * -HOOK THE HOOK NODE IS DEFINED AS PINNED CONNECTION PREVENTING *
405. * MOTION IN X, Y AND Z DIRECTION *
406. * -STIFFENERS WEAK SPRINGS WITH NEGLIGIBLE PROPERTIES ON EACH SIDE OF THE *
407. * SPOOL TO PREVENT SINGULARITIES *
408. *****
409. SUPPORTS
410. 999 PINNED
411. _STIFFENERS FIXED BUT FY MX MY MZ KFX 1 KFZ 1
412. *200 FIXED
413. *****
414. *MEMBER RELEASE *
415. *****
416. * -SLINGS THE SLINGS WHICH ARE CONNECTED TO PADAYES SHOULD WILL NOT *
417. * TRANSFER MOMENTS. ALL MOMENTS ARE RELEASED (MX, MY, MZ) AT *
418. * THE PADEYE (START), THE SLINGS ARE ALREADY RELEASED AT THE *
419. * HOOK POINT (PINNED SUPPORT). *
420. * -CONNECTIONS THE CONNECTION BETWEEN SPOOL AND SPOOL COVER IS TO ENSURE *
421. * THAT THE FORCES TRANSLATED TO THE SPREADER ARE ONLY THE *
422. * VERTICAL FORCES. THEREFORE THE MEMBERS ARE RELEASED FOR ALL *
423. * MOMENTS (MX, MY, MZ) AND TRANSVERS FORCES (LOCAL DIRECTION *
424. * FY AND FX). THE CONNECTION POINTS AT EACH END (800-803 + *
425. * 836-838) ARE NOT RELEASED FOR SHEAR FORCES IN ORDER FOR *
426. * THE SPOOLS TO BE ATTACHED TO THE SPREADER IN HORIZONTAL *
427. * DIRECTION. THE HORIZONTAL STRESSES IN THOSE BEAMS SHOULD *
428. * BE CLOSE TO ZERO (SHOULD BE CHECKED). *
429. * -TEMPORARY BEAMS THE TEMPORARY HEB BEAMS IS DESIGNED TO NOT TRANSFER MOMENT *
430. * AROUND THE LOCAL X-AXIS OF THE BEAMS AND IS THEREFORE *
431. * RELEASED AT START AND END (MX). *
432. *****

```

```

433. MEMBER RELEASE
434. _SLINGS START MX MY MZ
435. _CONNECTIONS END MX MY MZ
436. 803 865 END FY FZ
437. _TOP_TRANSVER START MX
438. _TOP_TRANSVER END MX
439. *****
440. *PRIMARY LOAD CASES *
441. ***** *
442. *REFER TO APPENDIX A FOR DETAILED WEIGHT CALCULATIONS *
443. *SPOOLS *
444. * -"12''SPOOL"          WEIGHT IN AIR: 3.22KN/M    WEIGHT IN WATER: 1.73KN/M *
445. * -"12''GOOSENECK"      WEIGHT IN AIR: 3.63KN/M    WEIGHT IN WATER: 2.14KN/M *
446. * -"8''SPOOL"           WEIGHT IN AIR: 1.50KN/M    WEIGHT IN WATER: 0.79KN/M *
447. * -"12''GOOSENECK"      WEIGHT IN AIR: 1.50KN/M    WEIGHT IN WATER: 0.79KN/M *
448. * -"TERMINATION"        WEIGHT IN AIR: 16.92KN     WEIGHT IN WATER: 14.72KN/M *
449. *          NOTE: SAME WEIGHT APPLIED FOR ALL TERMINATION HEADS *
450. *INTEGRATED SPOOL COVER *
451. * -WEIGHT OF MEMBERS    WEIGHT IN AIR: SELFWEIGHT  WEIGHT IN WATER: SELFW.*0.87*
452. *          NOTE1: WEIGHT OF MEMBERS IN WATER IS CALCULATED WHEN *
453. *          ALL MEMBERS ARE WATERFILLED (0.87=1-DENSITYWATER/STEEL)*
454. *          NOTE2: THE WEIGHT OF ALL MEMBERS IS INCLUDED WHEN USING*
455. *          THE SELFWEIGHT COMMAND. IRRELEVANT MEMBERS ARE GIVEN *
456. *          NEGLIGIBLE WEIGHT. *
457. * -WEIGHT OF GRP        WEIGHT IN AIR: 20KG/M3     WEIGHT IN WATER: 6KG/M3 *
458. *          NOTE: CONSIDERING DESIGN WHERE GRP COVER IS DESIGNED AS*
459. *          OPEN LIDS DURING THE LIFT AND THE GRP WEIGHT IS FOUND *
460. *          BY MULTIPLYING WEIGHT WITH RELEVANT SPAN. (WEIGHT OF *
461. *          GRP IN WATER IS 0.3 * WEIGHT IN AIR). *
462. * -"TOP GRP1"           WEIGHT IN AIR: 0.78KN/M    WEIGHT IN WATER: 0.23KN/M *
463. * -"TOP GRP2"           WEIGHT IN AIR: 0.85KN/M    WEIGHT IN WATER: 0.26KN/M *
464. * -"SIDE TRAWL"         WEIGHT IN AIR: 0.75KN/M    WEIGHT IN WATER: 0.23KN/M *
465. * -TRAPPED WATER        ASSUME THAT STEEL MEMBERS ABOVE WATER CAN BE FILLED *
466. *          50% BEFORE DEPLOYMENT (CONSERVATIVE). *
467. * -SPOOLS               ALREADY FILLED WITH MEG, NO TRAPPED WATER *
468. * -10''PIPE (273MM)     WEIGHT OF TRAPPED WATER: 0.24KN/M *
469. * - 8''PIPE (219MM)     WEIGHT OF TRAPPED WATER: 0.16KN/M *
470. * - 6''PIPE (168MM)     WEIGHT OF TRAPPED WATER: 0.09KN/M *
471. *ADDITIONAL WEIGHT *
472. * -SPOOL CONNECTION     TO ACCOUNT FOR WEIGHT OF WELDS, RIGGING, PAINT AND *
473. *          POLYETHYLENE (ON TOP OF BOTTOM TRANSVERS BEAMS) TO *
474. *          REDUCE FRICTION BETWEEN SPOOL AND COVER AS REQUIRED FOR*
475. *          THE TIE-IN, ADDITIONAL WEIGHT OF 2.2TE IS ADDED AND *
476. *          DISTRIBUTED OVER THE "BOTTOM TRANSVERS" BEAMS. *
477. *          NOTE: WEIGHT IN WATER IS THE WEIGHT OF STEEL IN WATER: *
478. *          WEIGHT IN WATER=0.87 * WEIGHT IN AIR. *
479. * -"BOTTOM TRANSVE"     WEIGHT IN AIR: 0.26KN/M    WEIGHT IN WATER: 0.23KN/M *
480. * -"BOTTOM STRESSE"     WEIGHT IN AIR: 0.26KN/M    WEIGHT IN WATER: 0.23KN/M *
481. * -RIGGING              TO ACCOUNT FOR WEIGHT OF ADDITIONAL WEIGHT FOR WELDS, *
482. *          JOINTS AND PADAYES, ADDITIONAL WEIGHT OF 5TE IS ADDED *
483. *          AND DISTRIBUTED OVER 40 CONNECTION POINTS AS VERTICAL *
484. *          POINT LOADS. (5TE/40=125KG=1.23KN) *
485. *          NOTE: WEIGHT IN WATER IS THE WEIGHT OF STEEL IN WATER: *
486. *          WEIGHT IN WATER=0.87 X WEIGHT IN AIR. *
487. * -"JOINTS"             WEIGHT IN AIR: 1.23KN     WEIGHT IN WATER: 1.07KN *
488. *****

```



```

489. *****
490. *LOAD 11 WEIGHT OF SPOOLS IN AIR *
491. *****
492. *-MASS OF SPOOLS IN AIR INCLUDING: *
493. * -STEEL PIPE *
494. * -COATING *
495. * -MEG *
496. * -TERMINATION HEADS *
497. *-NOTE: *
498. * -SPOOL WEIGHT GIVEN IN LINE 443 TO 447 *
499. *****
500. LOAD 11 WEIGHT OF SPOOLS IN AIR
501. MEMBER LOAD
502. *SPOOL WEIGHT IN AIR*****
503. _12''SPOOL UNI GY -3.22
504. _8''SPOOL UNI GY -1.5
505. _12''GOOSENECK UNI GY -3.63
506. _8''GOOSENECK UNI GY -1.5
507. JOINT LOAD
508. *TERMINATION HEADS IN AIR*****
509. _TERMINATION FY -16.925
510. *****
511. *LOAD 12 WEIGHT OF INTEGRATED COVER IN AIR *
512. *****
513. *-MASS OF INTEGRATED COVER IN AIR INCLUDING: *
514. * -STEEL MEMBERS *
515. * -GRP COVER *
516. * -ADDITIONAL WEIGHT FOR SPOOL CONNECTIONS *
517. * -ADDITIONAL WEIGHT FOR RIGGING *
518. *-NOTE: *
519. * -SELFWEIGHT OF ALL MEMBERS IS INCLUDED TO AVOID WARNENGS*
520. * IN STAAD.PRO. *
521. * -GRP WEIGHT GIVEN IN LINE 462 TO 464 *
522. * -ADDITIONAL WEIGHT, SPOOL CONNECTION, LINE 473 AND 474 *
523. * -ADDITIONAL WEIGHT, RIGGING ("JOINT"), GIVEN IN LINE 481*
524. *****
525. LOAD 12 WEIGHT OF INTEGRATED COVER IN AIR
526. *WEIGHT OF STEEL MEMBERS IN AIR*****
527. SELFWEIGHT Y -1 _SPREADER
528. SELFWEIGHT Y -1E-010 _CONNECTIONS
529. SELFWEIGHT Y -1E-010 _SLINGS
530. SELFWEIGHT Y -1E-010 _SPOOLS
531. MEMBER LOAD
532. *GRP WEIGHT*****
533. _TOP_GRP1 UNI GY -0.78
534. _TOP_GRP2 UNI GY -0.85
535. _SIDE_TRAWL UNI GY -0.75
536. *ADDITIONAL WEIGHT, SPOOL CONNECTION*****
537. _BOTTOM_TRANSVER UNI GY -0.26
538. _BOTTOM_STRESSED UNI GY -0.26
539. JOINT LOAD
540. *ADDITIONAL WEIGHT, RIGGING*****
541. _JOINTS FY -1.23
542. *****
543. *LOAD 13 PARTLY SUBMERGED COVER, SUBMERGED PART *
544. *****

```

```

545. *-MASS OF INTEGRATED COVER SUBMERGED PART IN WATER INCLUDING:      *
546. *           -WATERFILLED STEEL MEMBERS IN WATER. (INCLUDED MEMBERS  *
547. *           ARE THE BOTTOM HORIZONTAL MEMBERS)                       *
548. *           -ADDITIONAL WEIGHT FOR SPOOL CONNECTIONS                 *
549. *-NOTE:                                                                *
550. *           -SELFWEIGHT OF ALL MEMBERS IS INCLUDED TO AVOID WARNENGS*
551. *           IN STAAD.PRO. (0.87* SELFWEIGHT FOR STEEL)              *
552. *           -ADDITIONAL WEIGHT, SPOOL CONNECTION, LINE 473 AND 474   *
553. *****
554. LOAD 13 SPREADER PARTLY SUBMERGED, SUBMERGED PART
555. *WATERFILLED STEEL MEMBERS IN WATER*****
556. SELFWEIGHT Y -0.8693 _LOAD_CASE_13
557. SELFWEIGHT Y -1E-010 _LOAD_CASE_14
558. SELFWEIGHT Y -1E-010 _CONNECTIONS
559. SELFWEIGHT Y -1E-010 _SLINGS
560. SELFWEIGHT Y -1E-010 _SPOOLS
561. MEMBER LOAD
562. *ADDITIONAL WEIGHT, SPOOL CONNECTION*****
563. _BOTTOM_TRANSVER UNI GY -0.23
564. _BOTTOM_STRESSED UNI GY -0.23
565. *****
566. *LOAD 14 PARTLY SUBMERGED COVER, PART IN AIR                          *
567. *****
568. *-MASS OF INTEGRATED COVER, PART IN AIR INCLUDING:                    *
569. *           -STEEL MEMBERS ABOVE WATERLINE IN AIR. (ALL MEMBERS     *
570. *           NOT INCLUDED IN LOAD CASE 13)                             *
571. *           -GRP COVER                                                *
572. *           -50% TRAPPED WATER IN STEEL MEMBERS                      *
573. *           -ADDITIONAL WEIGHT FOR RIGGING                            *
574. *-NOTE:                                                                *
575. *           -SELFWEIGHT OF ALL MEMBERS IS INCLUDED TO AVOID WARNENGS*
576. *           IN STAAD.PRO.                                              *
577. *           -WEIGHT OF TRAPPED WATER GIVEN IN LINE 468 TO 470        *
578. *           -GRP WEIGHT GIVEN IN LINE 462 TO 464                      *
579. *           -ADDITIONAL WEIGHT, RIGGING ("JOINT"), GIVEN IN LINE 481*
580. *****
581. LOAD 14 PARTLY SUBMERGED COVER, PART IN AIR
582. *WEIGHT OF STEEL MEMBERS IN AIR*****
583. SELFWEIGHT Y -1 _LOAD_CASE_14
584. SELFWEIGHT Y -1E-010 _LOAD_CASE_13
585. SELFWEIGHT Y -1E-010 _CONNECTIONS
586. SELFWEIGHT Y -1E-010 _SLINGS
587. SELFWEIGHT Y -1E-010 _SPOOLS
588. MEMBER LOAD
589. *GRP WEIGHT*****
590. _TOP_GRP1 UNI GY -0.78
591. _TOP_GRP2 UNI GY -0.85
592. _SIDE_TRAWL UNI GY -0.75
593. *TRAPPED WATER IN STEEL MEMBERS*****
594. _TOP_MAIN UNI GY -0.242
595. _MID_LINE UNI GY -0.162
596. _SIDE_BRACE UNI GY -0.094
597. _SIDE_TRAWL UNI GY -0.094
598. JOINT LOAD
599. *ADDITIONAL WEIGHT, RIGGING*****
600. _JOINTS FY -1.23

```

```

601. *****
602. *LOAD 15 TRAPPED WATER IN SPOOL *
603. *****
604. *-THE SPOOLS ARE FILLED WITH MEG. ->NO TRAPPED WATER IN SPOOLS *
605. *****
606. LOAD 15 TRAPPED WATER IN SPOOL
607. MEMBER LOAD
608. *TRAPPED WATER IN SPOOL*****
609. _12''SPOOL UNI GY 0
610. _8''SPOOL UNI GY 0
611. _12''GOOSENECK UNI GY 0
612. _8''GOOSENECK UNI GY 0
613. *****
614. *LOAD 16 TRAPPED WATER IN INTEGRATED COVER *
615. *****
616. *-MASS OF TRAPPED WATER IN STEEL MEMBERS. *
617. *-NOTE: *
618. * -WEIGHT OF TRAPPED WATER GIVEN IN LINE 468 TO 470 *
619. *****
620. LOAD 16 TRAPPED WATER IN INTEGRATED COVER
621. MEMBER LOAD
622. *TRAPPED WATER IN INTEGRATED COVER*****
623. _BOTTOM_MAIN UNI GY -0.242
624. _BOTTOM_TRANSVER UNI GY -0.162
625. _BOTTOM_STRESSED UNI GY -0.242
626. _BOTTOM_BRACE UNI GY -0.094
627. _TOP_MAIN UNI GY -0.242
628. _VERTICAL UNI GY -0.162
629. _VERTICAL_STRESSED UNI GY -0.242
630. _MID_VERTICAL UNI GY -0.094
631. _MID_LINE UNI GY -0.162
632. _SIDE_BRACE UNI GY -0.094
633. _BOTTOM_TRAWL UNI GY -0.094
634. _SIDE_TRAWL UNI GY -0.094
635. *****
636. *****
637. *LOAD 21 WEIGHT OF SPOOLS IN WATER *
638. *****
639. *-MASS OF SPOOLS IN WATER INCLUDING: *
640. * -STEEL PIPE *
641. * -COATING *
642. * -MEG *
643. * -TERMINATION HEADS *
644. *-NOTE: *
645. * -SPOOL WEIGHT GIVEN IN LINE 443 TO 447 *
646. *****
647. LOAD 21 WEIGHT OF SPOOLS IN WATER
648. MEMBER LOAD
649. *SPOOL WEIGHT IN WATER*****
650. _12''SPOOL UNI GY -1.73
651. _8''SPOOL UNI GY -0.79
652. _12''GOOSENECK UNI GY -2.14
653. _8''GOOSENECK UNI GY -0.79
654. JOINT LOAD
655. *WEIGHT OF TERMINATION HEADS IN WATER*****
656. _TERMINATION FY -14.715
    
```

```

657. *****
658. *LOAD 22 WEIGHT OF INTEGRATED COVER IN WATER *
659. *****
660. *-MASS OF INTEGRATED COVER IN WATER INCLUDING: *
661. * -WATERFILLED STEEL MEMBERS IN WATER *
662. * -GRP COVER *
663. * -ADDITIONAL WEIGHT FOR SPOOL CONNECTIONS *
664. * -ADDITIONAL WEIGHT FOR RIGGING *
665. *-NOTE: *
666. * -SELFWEIGHT OF ALL MEMBERS IS INCLUDED TO AVOID WARNENGS*
667. * IN STAAD.PRO. (0.87* SELFWEIGHT FOR STEEL) *
668. * -GRP WEIGHT GIVEN IN LINE 462 TO 464 *
669. * -ADDITIONAL WEIGHT, SPOOL CONNECTION, LINE 473 AND 474 *
670. * -ADDITIONAL WEIGHT, RIGGING ("JOINT"), GIVEN IN LINE 481*
671. *****
672. LOAD 22 WEIGHT OF INTEGRATED COVER IN WATER
673. *WEIGHT OF STEEL MEMBERS IN WATER*****
674. SELFWEIGHT Y -0.8693 _SPREADER
675. SELFWEIGHT Y -1E-010 _CONNECTIONS
676. SELFWEIGHT Y -1E-010 _SLINGS
677. SELFWEIGHT Y -1E-010 _SPOOLS
678. MEMBER LOAD
679. *GRP WEIGHT*****
680. _TOP_GRP1 UNI GY -0.23
681. _TOP_GRP2 UNI GY -0.26
682. _SIDE_TRAWL UNI GY -0.23
683. *ADDITIONAL WEIGHT, SPOOL CONNECTION*****
684. _BOTTOM_TRANSVER UNI GY -0.23
685. _BOTTOM_STRESSED UNI GY -0.23
686. JOINT LOAD
687. *ADDITIONAL WEIGHT, RIGGING*****
688. _JOINTS FY -1.07
689. *****
690. *LOAD COMBINATIONS *
691. *****
692. *****
693. *100 - STATIC WEIGHT OF SYSTEM IN AIR *
694. * | DESCRIPTION | SPOOL | INTEGRATED COVER *
695. *-----*
696. * | TOTAL FACTOR | 1.00 | 1.00 *
697. *****
698. *101 - STATIC WEIGHT OF SYSTEM IN WATER *
699. * | DESCRIPTION | SPOOL | INTEGRATED COVER *
700. *-----*
701. * | TOTAL FACTOR | 1.00 | 1.00 *
702. *****
703. *115 - LIFT IN SPLASH ZONE, STRUCTURAL DESIGN *
704. * | DESCRIPTION | SPOOL | INTEGRATED COVER *
705. *-----*
706. * | LOAD FACTOR | 1.30 | 1.30 *
707. * | CONSEQUENSE FACTOR | 1.00 | 1.30 *
708. * | WEIGHT INACCURACY FACTOR | 1.05 | 1.05 *
709. * | COG INACCURACY FACTOR | 1.05 | 1.05 *
710. * | SKEW LOAD FACTOR | 1.25 | 1.25 *
711. * | DYNAMIC AMPLIFICATION | 1.20 | 1.20 *
712. * | TOTAL FACTOR | 2.15 | 2.79 *

```

```

713. *****
714. *116 - PARTLY SUBMERGED, STRUCTURAL DESIGN *
715. * | DESCRIPTION | SPOOL | INTEGRATED COVER *
716. * | | | WATER AIR *
717. *-----*
718. * | LOAD FACTOR | 1.30 | 1.30 1.30 *
719. * | CONSEQUENSE FACTOR | 1.00 | 1.30 1.30 *
720. * | WEIGHT INACCURACY FACTOR | 1.05 | 1.05 1.05 *
721. * | COG INACCURACY FACTOR | 1.05 | 1.05 1.05 *
722. * | SKEW LOAD FACTOR | 1.25 | 1.25 1.25 *
723. * | DYNAMIC AMPLIFICATION | 1.60 | 1.60 1.20 *
724. * | TOTAL FACTOR | 2.87 | 3.73 2.79 *
725. *****
726. *117 - LIFT IN WATER, STRUCTURAL DESIGN *
727. * | DESCRIPTION | SPOOL | INTEGRATED COVER *
728. *-----*
729. * | LOAD FACTOR | 1.30 | 1.30 *
730. * | CONSEQUENSE FACTOR | 1.00 | 1.30 *
731. * | WEIGHT INACCURACY FACTOR | 1.05 | 1.05 *
732. * | COG INACCURACY FACTOR | 1.05 | 1.05 *
733. * | SKEW LOAD FACTOR | 1.25 | 1.25 *
734. * | DYNAMIC AMPLIFICATION | 1.60 | 1.60 *
735. * | TOTAL FACTOR | 2.87 | 3.73 *
736. *****
737. *
738. *****
739. *NOTE: LOAD COMBINATION 125 TO 127 IS NESCESSARY FOR PERFORMING *
740. * THE RIGGING DESIGN (SLINGS, WIRES) SINCE DESIGN FACTORS FOR *
741. * THOSE ARE CHOSEN SEPARATELY *
742. *****
743. *125 - LIFT IN SPLASH ZONE, RIGGING DESIGN (DYNAMIC SLING LOADS) *
744. * | DESCRIPTION | SPOOL | INTEGRATED COVER *
745. *-----*
746. * | WEIGHT INACCURACY FACTOR | 1.05 | 1.05 *
747. * | COG INACCURACY FACTOR | 1.05 | 1.05 *
748. * | SKEW LOAD FACTOR | 1.25 | 1.25 *
749. * | DYNAMIC AMPLIFICATION | 1.20 | 1.20 *
750. * | TOTAL FACTOR | 1.65 | 1.65 *
751. *****
752. *126 - PARTLY SUBMERGED, RIGGING DESIGN (DYNAMIC SLING LOADS) *
753. * | DESCRIPTION | SPOOL | INTEGRATED COVER *
754. * | | | WATER AIR *
755. *-----*
756. * | WEIGHT INACCURACY FACTOR | 1.05 | 1.05 1.05 *
757. * | COG INACCURACY FACTOR | 1.05 | 1.05 1.05 *
758. * | SKEW LOAD FACTOR | 1.25 | 1.25 1.25 *
759. * | DYNAMIC AMPLIFICATION | 1.60 | 1.60 1.20 *
760. * | TOTAL FACTOR | 2.21 | 2.21 1.65 *
761. *****
762. *127 - LIFT IN WATER, RIGGING DESIGN (DYNMAMIC SLING LOADS) *
763. * | DESCRIPTION | SPOOL | INTEGRATED COVER *
764. *-----*
765. * | WEIGHT INACCURACY FACTOR | 1.05 | 1.05 *
766. * | COG INACCURACY FACTOR | 1.05 | 1.05 *
767. * | SKEW LOAD FACTOR | 1.25 | 1.25 *
768. * | DYNAMIC AMPLIFICATION | 1.60 | 1.60 *
    
```

```

769. *      | TOTAL FACTOR          | 2.21      | 2.21      *
770. *****
771. LOAD COMB 100 STATIC WEIGHT IN AIR
772. 11 1.0 12 1.0
773. LOAD COMB 101 STATIC WEIGHT IN WATER
774. 21 1.0 22 1.0
775. LOAD COMB 115 LIFT IN SPLASH ZONE, STRUCTURAL DESIGN
776. 11 2.15 15 2.15 12 2.79 16 2.79
777. LOAD COMB 116 PARTLY SUBMERGED, STRUCTURAL DESIGN
778. 21 2.87 13 3.73 14 2.79
779. LOAD COMB 117 LIFT IN WATER, STRUCTURAL DESIGN
780. 21 2.87 22 3.73
781. LOAD COMB 125 LIFT IN SPLASH ZONE, RIGGING DESIGN
782. 11 1.65 15 1.65 12 1.65 16 1.65
783. LOAD COMB 126 PARTLY SUBMERGED, RIGGING DESIGN
784. 21 2.21 13 2.21 14 1.65
785. LOAD COMB 127 LIFT IN WATER, RIGGING DESIGN
786. 21 2.21 22 2.21
787. *****
788. PERFORM ANALYSIS
    
```

P R O B L E M   S T A T I S T I C S

-----

NUMBER OF JOINTS/MEMBER+ELEMENTS/SUPPORTS = 280/ 523/ 3

SOLVER USED IS THE OUT-OF-CORE BASIC SOLVER

ORIGINAL/FINAL BAND-WIDTH= 189/ 47/ 285 DOF  
TOTAL PRIMARY LOAD CASES = 8, TOTAL DEGREES OF FREEDOM = 1677  
SIZE OF STIFFNESS MATRIX = 478 DOUBLE KILO-WORDS  
REQRD/AVAIL. DISK SPACE = 18.2/ 1134.0 MB

```

789. *****
790. *CODE CHECK ACCORDING TO EN 1993-1-1:2005 *
791. *****
792. *      - ALL LOAD COMBINATIONS ARE CHECKED ACCORDING TO THE CODE *
793. *      - MATERIAL FACTOR IS 1.15 FOR ALL MEMBERS *
794. *      - YIELD STRESS OF SPOOL MEMBERS IS 374MPA *
795. *      - YIELD STRESS OF INTEGRATED COVER MEMBERS IS 355MPA *
796. *****
797. PARAMETER 1
798. CODE EN 1993-1-1:2005
799. *MATERIAL FACTORS FOR SPOOL AND SPREADER*****
800. GM0 1.15 MEMB _SPOOLS
801. GM0 1.15 MEMB _SPREADER
802. GM1 1.15 MEMB _SPOOLS
803. GM1 1.15 MEMB _SPREADER
804. *YIELD STRESS FOR SPOOL AND SPREADER MEMBERS*****
805. PY 374000 MEMB _SPOOLS
    
```

```

806. PY 355000 MEMB _SPREADER
807. PY 1E+007 MEMB _SLINGS
808. *****
809. *BUCKLING LENGTHS *
810. *****
811. *NOTE: *
812. * - STAAD.PRO DESIGN CHECK ACCORDING TO EC3, PERFORMS A BUCKLING CHECK *
813. * FOR EACH ELEMENT BASED ON THE EFFECTIVE BUCKLING LENGTH (LENGTH *
814. * BETWEEN ZERO MOMENT POINTS) FOR ALL ELEMENTS. *
815. * - MEMBERS CONNECTED AS FIXED CONNECTIONS HAS A EFFECTIVE LENGTH 0.7 *
816. * TIMES THE LENGTH OF THE MEMBER (K-FACTOR=0.7). *
817. * - IF NOTHING IS DEFINED THE EFFECTIVE LENGTH = LENGTH OF MEMBERS *
818. * - MEMBERS SUBJECTED TO AXIAL COMPRESSION IS SUBJECTED TO BUCKLING *
819. *BUCKLING OF THE STRUCTURE *
820. * - BOTTOM TRANSVERS: TRUE LENGTHS OF BEAMS ARE 4.00M AND 4.34M, WITH *
821. * RELEVANT BUCKLING FACTOR 0.7 DUE TO FIXED *
822. * CONNECTIONG. *
823. * - MAIN MEMBERS: TOP AND BOTTOM CHORDS SUBJECTED TO AXIAL *
824. * COMPRESSION IS CHECKED FOR BUCKLING. THE EFFECTIVE*
825. * LENGHT IS THE LENGTH BETWEEN ZERO MOMENT POINTS. *
826. * REFER TO MOMENT DIAGRAMS, (APPENDIX C,SECTION 4.2)*
827. * BUCKLING LENGHT THAN THE OTHER MEMBERS. *
828. * - OTHER MEMBERS: BUCKLING FACTORS NOT DEFINED. SINCE THE LENGTH OF *
829. * THE MEMBERS ARE THE TRUE MEMBER LENGTH. STAAD.PRO *
830. * DEFINES THE BUCKLING LENGHT AS 1.0L (CONSERVATIVE)*
831. *MEMBER LENGTH, L: *
832. * -BOTTOM TRANSVERS Z LY=LZ=4.00M (BEAMS PARALELL TO Z-AXIS) *
833. * -BOTTOM TRANSVERS X LY=LZ=4.34M (BEAMS PARALELL TO X-AXIS) *
834. * -MAIN CHORDS DEFINED IN "SECTION 4.2.3" *
835. * -OTHER BEAMS MEMBER LENGTH (DEFAULT VALUE) *
836. *BUCKLING FACTORS, K: *
837. * -BOTTOM TRANSVERS Z KY=KZ=0.7 (BEAMS PARALELL TO Z-AXIS) *
838. * -BOTTOM TRANSVERS X KY=KZ=0.7 (BEAMS PARALELL TO X-AXIS) *
839. * -MAIN CHORDS DEFINED IN "SECTION 4.2.3" *
840. * -OTHER BEAMS KY=KZ=1.0 (DEFAULT VALUE) *
841. *TRUE MEMBER LENGTH: (L*K) *
842. * -MAIN CHORDS LY= 7.8M, LZ= 8.7M *
843. * -BOTTOM CRITICAL LY=16.0M, LZ=15.3M *
844. *****
845. *****
846. *BUCKLING LENGTHS *
847. *****
848. *MEMBER LENGTH, L*****
849. LY 4 MEMB _BUCKLE_TRANS_Z
850. LY 4.34 MEMB _BUCKLE_TRANS_X
851. LZ 4 MEMB _BUCKLE_TRANS_Z
852. LZ 4.34 MEMB _BUCKLE_TRANS_X
853. *TOP AND BOTTOM CHORDS:
854. LY 15.71 MEMB _BEAM2
855. LZ 15.71 MEMB _BEAM2
856. LY 19.33 MEMB _BEAM4
857. LZ 19.33 MEMB _BEAM4
858. LY 15.33 MEMB _BEAM5
859. LZ 15.33 MEMB _BEAM5
860. *BUCKLING FACTOR, K*****
861. KY 0.7 MEMB _BUCKLE_TRANS_Z

```

STAAD SPACE

-- PAGE NO. 17

```
862. KY 0.7 MEMB _BUCKLE_TRANS_X
863. KZ 0.7 MEMB _BUCKLE_TRANS_Z
864. KZ 0.7 MEMB _BUCKLE_TRANS_X
865. *TOP AND BOTTOM CHORDS:
866. KY 0.8 MEMB _BEAM2
867. KZ 0.8 MEMB _BEAM2
868. KY 0.8 MEMB _BEAM4
869. KZ 0.8 MEMB _BEAM4
870. KY 0.65 MEMB _BEAM5
871. KZ 0.65 MEMB _BEAM5
872. *EFFECTIV LENGTHS, LE*****
873. *BASED ON MOMENT DIAGRAMS, WHERE BUCKLING LENGTH = ZERO MOMENT LENGTH      *
874. *****
875. LY 5.23 MEMB _BEAM1
876. LZ 5.2 MEMB _BEAM1
877. LY 3.51 MEMB _BEAM3_1
878. LZ 5.21 MEMB _BEAM3_1
879. LY 7.03 MEMB _BEAM3_2
880. LZ 7.81 MEMB _BEAM3_2
881. *****
882. BEAM 1 ALL
883. TRACK 0 ALL
884. CHECK CODE ALL
```

```
STAAD.PRO CODE CHECKING - EN 1993-1-1:2005
*****
NATIONAL ANNEX - NOT USED
```

PROGRAM CODE REVISION V1.9 BS\_EC3\_2005/1